THE UNIVERSITY *of* EDINBURGH

The function of the forkhead gene *fd3F* in *Drosophila* chordotonal neuron differentiation

Fay Newton

A thesis presented for the degree of Ph.D.

University of Edinburgh

2012

Abstract

Drosophila chordotonal (Ch) organs are internal stretch receptors required for coordination, balance and hearing. The outer dendritic segment of the Ch neuron is a compartmentalised motile cilium, a feature that is exclusive to this neuron subtype. Ch organs are specified early in development by expression of the proneural gene *atonal* in the proneural cluster and sense organ precursors (SOPs) (Jarman *et al.*, 1993). However little is known about how chordotonal SOP specification is linked to differentiation of Ch organs. *fd3F* encodes a forkhead transcription factor which has been identified as a potential downstream target of *atonal* in microarray experiments (Cachero *et al.*, 2011). I have shown that *fd3F* is exclusively expressed in Ch neurons and their precursors in *Drosophila* embryos and Ch SOPs in larval imaginal discs. I have also generated an *fd3F* deletion mutant by imprecise excision of a P element. Mutant adults and larvae exhibit impaired coordination characteristic of Ch neuron defects and a similar phenotype was observed in *fd3F* RNAi lines. *fd3F* mutant Ch neurons do not show gross morphological defects, however the tips of the Ch neuron cilia appear swollen when analysed by electron microscopy and there is also some mis-localisation of proteins within the cilia.

I have identified several Ch-specific genes that show strongly reduced mRNA expression in *fd3F* mutant embryos compared with wild type and could therefore be downstream targets of *fd3F*. These include a number of genes known to be essential for Ch neuron function such as transient receptor potential (TRP) ion channels, dyneins required for motility of the Ch neuron cilium and components of the

retrograde transport machinery that may be required for protein localisation within the cilium. In addition several uncharacterised genes were identified as *fd3F* targets and these genes may therefore also be important for Ch neuron function. I have shown that *fd3F* directly regulates two of these genes, *nanchung* and *inactive* using GFP enhancer constructs and gel retardation assays. I therefore hypothesise that *fd3F* is an important component of the gene regulatory network that links *atonal* expression in SOPs to differentiation of Ch organs. In particular *fd3F* regulates genes required specifically for Ch neuron function and enhances expression of retrograde transport genes that may be required to ensure correct distribution of proteins within the compartmentalised Ch neuron cilium.

Declaration

I declare that this thesis has been composed by me and that the work presented within it is my own unless otherwise stated in the text. This work has not been submitted for any other degree or qualification.

Fay Newton

January 2012

Acknowledgements

I would like to thank my supervisor Andrew Jarman for his guidance and encouragement over the last four years. I feel I have benefited hugely from his experience and, most importantly, he has given me the freedom to plan my own experiments and the confidence and inspiration to pursue my own research interests in the future.

I would also like to thank past and present lab members: Lynn Powell, Petra zur Lage, Lina Ma, Ian Simpson, Giuseppe Gallone, Daniel Moore, Kasia Styczynska, Sadie Kemp, Pan Filis and Sebastian Cachero for making working in this lab such an enjoyable experience. The lab has a wonderful atmosphere and I feel I have been very lucky to work here. I especially thank Petra zur Lage and Lynn Powell whose knowledge, experience and support has been invaluable throughout my PhD. Thanks also go to members of the neighbouring Armstrong and Pennetta labs (past and present) for support, advice and cake.

This work was funded by a studentship from the BBSRC. I am grateful for their generous financial support.

Finally, I would like to thank my parents, Keith and Alison, for their continued encouragement and for helping me to keep my sense of humour.

Publications from this thesis

Cachero S, Simpson TI, zur Lage P, Ma L, Newton FG, Holohan EE, Armstrong JD, Jarman AP. (2011). The gene regulatory cascade linking proneural specification with differentiation in *Drosophila* sensory neurons. *PLoS Biology* 9.

Newton FG, zur Lage PI, Karak S, Moore DJ, Göpfert MC, Jarman AP. (2012). A Forkhead transcription factor, Fd3F, cooperates with Rfx to regulate a cell-type specific programme for mechanosensory cilia specialisation.

(Submitted to *Developmental Cell*, in revision).

Contents

Abbreviations

Ac	Achaete
Ato	Atonal
bHLH	basic helix-loop-helix
btv	beethoven
cato	cousin of atonal
Ch	chordotonal organ
CNS	central nervous system
Da	Daughterless
Dhc	Dynein heavy chain
elav	embryonic lethal abnormal vision
ES	external sense organ
fd3F	forkhead domain 3F
FOX	forkhead box
GAL	galactosidase
GFP	Green Fluorescent Protein
Hh	Hedgehog pathway
iav	inactive
IFT	intraflagellar transport
IFT-A	IFT complex A
IFT-B	IFT complex B
JO	Johnston's organ
LIC	light intermediate chain
md	multidendritic neuron
nan	nanchung
nompC	no mechanoreceptor potentials C
OrR	Oregon R
PCD	primary ciliary dyskinesia
PKD	polycystic kidney disease
PNC	Proneural cluster
PNS	peripheral nervous system
rempA	reduced mechanoreceptor potentials A
Rfx	Regulatory factor X
robo3	Roundabout 3
RT-PCR	Reverse transcription PCR
Sca	scabrous
Sc	Scute
Shh	Sonic hedgehog pathway
SOP	Sense Organ Precursor
TEM	Transmission electron microscopy
tilB	touch insensitive larva B
TPR	Tetratrichopeptide repeat
TRP	Transient receptor potential channel
UAS	Upstream Activating Sequence
Wnt	wingless pathway
YFP	Yellow Fluorescent Protein

1

General Introduction

All multicellular organisms begin life as a single cell. During development this cell divides repeatedly to produce the complex variety of cell types that make up a fully functioning organism. The final identities of the different cell types are determined through a series of precisely ordered patterning events in the developing embryo and are ultimately controlled by the genes expressed in different cells. The challenge of developmental biology is therefore to understand how these genes are regulated in different cell types. Many aspects of early development are well known. For example, early patterning events are controlled by gradients of long range signalling molecules called morphogens and the level of morphogen a cell is exposed to affects the genes expressed in that cell. Later events are also controlled by uneven distribution of proteins during cell division (asymmetric division) and inhibitory signals from neighbouring cells (lateral inhibition). However the precise regulation of genes required to achieve the specific morphological and physiological features of particular cell types is less well understood.

Drosophila melanogaster has been used for decades as a model organism to study the genetics of animal development. Like other insects *Drosophila* undergoes two distinct developmental events; embryogenesis that results in formation of the larva

and metamorphosis, the radical remodelling of the body that occurs inside the pupa to produce the adult fly. Interestingly many of the genes required for body patterning and organogenesis during metamorphosis are identical to those that regulate embryogenesis. *Drosophila* embryogenesis can be divided into 17 stages and, like other insects, it begins with a series of nuclear divisions generating a large multinucleate cell or syncytium.

The initial embryonic patterning originates from asymmetric distribution of mRNAs inside the egg and signals from the follicle cells around it. This results in morphogen gradients that determine the basic body plan: head versus rear, dorsal versus ventral and endoderm, mesoderm and ectoderm layers. Different morphogen gradients in different parts of the embryo progressively subdivide it into a series of repeating segments. The identity of each segment is conferred by expression of different genes known as homeotic selector genes. These genes encode homeodomain transcription factors that interact with other gene regulatory proteins and modulate their actions so as to give each segment its characteristic features. Most of these early patterning genes are highly conserved across all multicellular animals. About halfway through embryogenesis cells become specified as the precursors of particular organs and tissues. These cells and their progeny differentiate into particular cell types during the second half of embryogenesis. Much of the recent and current research in developmental biology has focused on understanding the regulation of genes required for differentiation of specific cell types.

1.1 The *Drosophila* peripheral nervous system

The ability to sense the environment is vital to all organisms and in *Drosophila* as in other multicellular animals this requires a variety of sensory neurons with different specialised functions. The development of *Drosophila* sensory organs is a useful model for understanding neural development and also for understanding the regulatory pathways that lead from initial cell specification to differentiation. The *Drosophila* larval peripheral nervous system (PNS) is a well-defined system, there is a relatively small number of neurons in each larval segment (for example there are 43 sensory neurons in each abdominal hemisegment) and these neurons are arranged in a defined pattern (figure 1.01). Individual neurons can therefore be easily identified making it relatively simple to study the effect of genetic manipulation on particular neuron subtypes. Many of the genes involved in *Drosophila* neural specification are conserved in vertebrates.

The *Drosophila* PNS consists of photoreceptors, type I sensory organs and type II multidendritic neurons. The type I sensory organs can be further divided into external mechanosensory/ chemosensory bristles, olfactory sensilla and internal stretch receptors (chordotonal organs). The type I neurons have a single dendrite based on a modified cilium and are associated with several different accessory cells to make up the sensory organ. In contrast type II neurons have multiple dendrites and generally have no associated accessory cells. Each of these sensory organs arises from an individual precursor cell, which is committed to a neural fate early in development.

The individual characteristics of each subtype are acquired through expression of specific genes during differentiation.

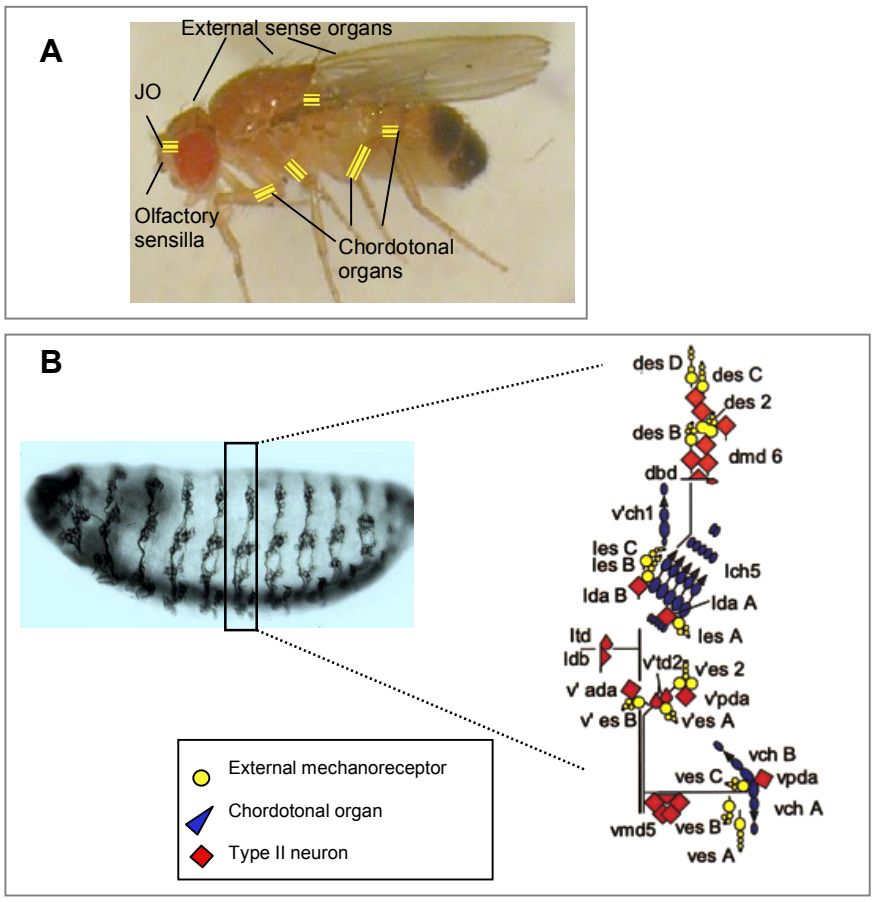

Figure 1.01: The Drosophila PNS. A) Approximate location of a selection of adult sensory organs. JO = Johnston's Organ. B) Sensory neurons in a late stage embryo stained with MAb-22C10 (left) the arrangement of neurons in one hemisegment is shown schematically on the right (from Brewster & Bodmer, 1995).

The regulation of sense organ precursor (SOP) cell specification and the structural and molecular features of different types of sensory neuron have been well characterised. However much less is known about the later stages of sensory neuron differentiation, both in terms of the gene regulatory networks acting immediately

downstream of the genes that determine sensory organ cell fate, and how and when the terminal differentiation genes are regulated. My work is concerned with understanding the regulation of chordotonal neuron differentiation as a model for regulation of neuron subtype specialisation. This will therefore be the main focus of this introductory chapter, however the structural features of some of the other sensory organ subtypes are also described briefly below.

1.1.1 Multidendritic neurons

Each larval hemisegment contains 15 multidendritic (md) neurons. These can be divided into four subclasses (I-IV) depending on the shape and complexity of their dendritic arbours with class I being the simplest and class IV the most complicated and expansive (Grueber *et al.,* 2003; Sugimura *et al*., 2003). The different shapes of the dendritic arbours produced by the different subclasses are regulated by the transcription factors expressed in the post-mitotic neurons (Crozatier & Vincent, 2008; Grueber & Jan, 2003; Kim *et al*., 2006; Li *et al*., 2004). For example the complex branching of class IV md neurons requires expression Collier along with moderate levels of Cut, while expression of high levels of Cut results in md neurons with unbranched dendritic spikes (Crozatier & Vincent, 2008; Grueber & Jan, 2003). The transcription factor Abrupt is required to limit branching in the simplest md neuron subclasses (Li *et al.,* 2004). Class IV md neurons are required for nociception and thermosensation (Hwang *et al*., 2007; Liu *et al*., 2003), while the dorsal bipolar dendrite (dbd) and class I md neurons are involved in the proprioceptive feedback required to coordinate larval muscle contractions (Hughes & Thomas, 2007).

1.1.2 External sensory (ES) organs

The ES organs are composed of an external bristles or sensilla connected to type I sensory neurons (reviewed in Kernan, 2007). Purely mechanosensory bristles (macrochaetae and microchaetae) have closed bristle shafts, and each shaft is innervated at its base by a single neuron. Most of these bristles are thought to function as tactile receptors however some smaller bristles at the leg joints may provide proprioceptive feedback. Mechanosensory campaniform sensilla are located on the adult wing, haltere and limb joints and respond to local deformations of the cuticle, such as bending due to wing movements during flight (Dickinson, 1990). Apart from the bristle shaft being replaced by a cuticular dome, campaniform sensilla are structurally similar to other sensory bristles. Chemosensory bristles are located on the mouthparts, legs, and wings are innervated by multiple neurons including a single mechanosensory neuron that contacts the bristle base, along with several chemosensory neurons. The third category of ES organs are the olfactory sensilla located on the third antennal segment and mouthparts. These are innervated by multiple chemosensory neurons but do not have a mechanosensory neuron.

ES neurons associate with three support cells: the sheath (thecogen), socket (tormogen) and the shaft cell (trichogen) that forms the bristle (figure 1.02A). All four cells are derived from the same SOP (reviewed in Jan & Jan, 1993). The outer segment of the mechanosensory ES neuron dendrite is a modified cilium. The distal portion of the cilium contains tightly packed microtubules (tubular bundle) embedded in an electron dense matrix and this portion of the cilium is connected to the bristle via an extracellular matrix structure produced by the sheath cell, which is

known as the dendritic sheath. In contrast, chemosensory neurons have long cilia that extend into the porous bristle shaft and the neurons of olfactory sensilla have branched dendrites (reviewed in Kernan, 2007). The membranes of chemosensory neuron dendrites contain gustatory or olfactory receptor proteins that bind molecules that defuse into the bristle shaft. Binding particular odorant or gustatory molecules results in ion channel opening and depolarisation of the neuron. In the case of mechanosensory bristles, movement of the bristle is transmitted directly to the neuron cilium via the dendritic sheath resulting in ion channel opening (Kernan, 2007). The cation channel encoded by *no mechanoreceptor potentials C* (*nompC*) is essential for this mechanotransduction (Walker *et al*., 2000). The support cells secrete a high K^+, low Ca^{2+} endolymph that surrounds the neuron dendrite (Grünert & Gnatzy, 1987) and the opening of cation channels in response to movement of the neuron cilium therefore causes an influx of K^+ resulting in depolarisation of the neuron.

1.1.3 Chordotonal organs

Chordotonal (Ch) organs (figure 1.02B) are internal stretch receptors. In *Drosophila* they are required for coordination (Kernan *et al*., 1994), balance and hearing (Eberl *et al*., 2000). Like ES neurons, the outer segment of the Ch neuron dendrite is a modified cilium. However, in contrast to ES neuron cilia, Ch cilia have a regular axonemal structure and a protein dense inclusion known as the ciliary dilation that separates the cilium into two structurally and functionally distinct compartments (Eberl *et al*., 2000). The tip of the Ch neuron cilium is connected to the cap cell by

the extracellular dendritic cap (equivalent to the ES dendritic sheath) and the cap cell itself is in contact with the epithelium. Stretching of the Ch organ is transmitted to the ciliated dendrite of the sensory neuron, which is held by the rigid scolopale cell. This is thought to cause opening of mechanically gated cation channels such as NompC in the neuron dendrite, eventually resulting in an influx of K^+ from the surrounding endolymph and depolarisation of the neuron. The structural tension of the Ch organs is essential to their function and the cytoskeletal protein DmEB1 is thought to play an important role in maintaining structural integrity (Elliott *et al*., 2005). DmEB1 is expressed at high levels at the anterior end of the cap cell and the ligament cell (which are in contact with the body walls), and also in the scolopale cells. *DmEB1* mutants show disrupted alignment of Ch neuron dendrites and exhibit coordination defects (Elliott *et al*., 2005).

The Johnston's Organ (JO) in the second antennal segment is required for hearing and gravitaxis in *Drosophila*. These are large clusters of 227 individual Ch organs (scolopidia) (Kamikouchi *et al*., 2006) with 2-3 neurons per scolopale unit (Todi *et al*., 2004). The JO has been shown to produce sound evoked potentials in electrophysiology experiments (Eberl *et al*., 2000). It is thought that the JO scolopidia are deformed in response to movement of the joint between the second and third antennal segments (which vibrate in response to sound) and this results in ion channel opening in the neuron dendrites (Todi *et al*., 2004). Several ion channels involved in mechanotransduction in JO neurons have been identified, although the precise gating mechanism is not well understood. The JO can also generate movement in the antenna (Göpfert & Robert, 2003) and this may help to improve

auditory sensitivity and broaden the range of frequencies that can be detected. The JO could also be considered analogous to the mammalian cochlear amplifier (Boekhoff-Falk, 2005). The hair cells of the cochlea are required for auditory transduction in vertebrates. These cells have a number of protruding stereocilia that are deflected by sound vibrations. In addition to amplifying the auditory inputs the vertebrate cochlea can produce active oscillations to regulate amplification. As with the active vibrations generated by the JO neurons, this increases hearing sensitivity and allows detection of very faint sounds (Robles & Ruggero, 2001).

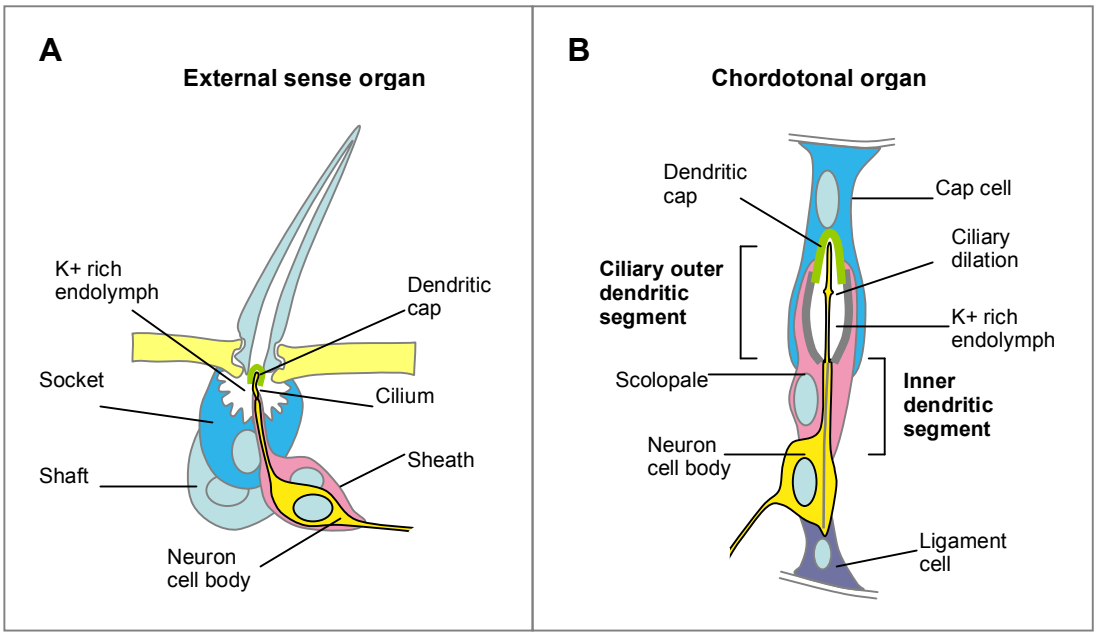

Figure 1.02: Type I sensory organs. The approximate arrangement of the neuron and accessory cells in A) mechanosensory bristles and B) chordotonal organs (Jarman, 2002).

1.2 Specification and differentiation of the *Drosophila* PNS

Drosophila neurogenesis begins at embryonic stage 9 and is complete by stage 16. By stage 9 (approximately 3h 40min after fertilisation at 25^{o}C) anterior-posterior patterning of the embryo is already established along with the endoderm, mesoderm

and ectoderm layers. The polarity and identity of each of the embryonic segments has also been determined. During stage 9 the precursor cells of the PNS arise from groups of ectodermal cells within each of the thoracic and abdominal segments of the embryo. The earliest SOPs (such as the those of the thoracic dch3 Ch organs and the three most posterior scolopidia of the lch5 Ch cluster) appear during stage 10. Later SOPs such as those of the two anterior scolopidia of the lch5 cluster appear during stage 11 (Campos-Ortega & Hartenstein, 1997).

1.2.1 Sense organ precursors are specified by expression of proneural genes

It has been well established in both *Drosophila* and vertebrate models that a small number of genes encoding basic helix-loop-helix (bHLH) transcription factors are necessary and sufficient to initiate development of neural lineages (reviewed in Bertrand *et al*., 2002). In *Drosophila* these genes include *achaete*, *scute*, *lethal of scute*, *atonal* and *amos*. In the developing embryo these 'proneural genes' are expressed in groups of ectodermal cells known as proneural clusters (PNCs) (Cabrera *et al*., 1987; Alonso & Cabrera, 1988). *achaete* (*ac*) and *scute* (*sc*) are required for specification of external sensory organ lineages (Jimenez *et al*., 1990; Ruiz-Gomez & Ghysen, 1993) while *atonal* (*ato*) specifies Ch organs (Jarman *et al*., 1993; Jarman *et al*., 1995), a subset of olfactory sensilla (sensilla coeloconica) (Gupta and Rodrigues, 1997) and the R8 photoreceptors in the developing eye (Jarman *et al*., 1994). *Amos* is required for development of the remaining subsets of olfactory sense organs (Goulding *et al*., 2000; zur Lage *et al*., 2003) and some larval md neurons (Huang *et al*., 2000; zur Lage *et al*., 2003).

The PNC is an equivalence group; all the cells within the cluster have the potential to become SOPs by virtue of proneural gene expression. One cell from each PNC is specified to become the SOP via the Notch signalling pathway (Cabrera *et al*., 1987). Expression of proneural genes in the PNC leads to expression of the transmembrane ligand Delta (Dl) in these cells, which activates the transmembrane Notch (N) receptor on surrounding cells. This activation results in cleavage of N releasing its intracellular domain. The intracellular domain can then enter the nucleus and activate expression of target genes (figure 1.03). This is an inhibitory signal that discourages cells from becoming SOPs. However, as development continues proneural gene expression is reinforced in three or four PNC cells and is eventually highly up-regulated in just one cell in the cluster, which will become the SOP. This cell increases expression of Dl and therefore more strongly inhibits proneural expression in the surrounding cells (reviewed in Artavanis-Tsakonas *et al*., 1999). The result of this lateral inhibition process is the up-regulation of proneural genes in the SOP and down-regulation in the rest of the PNC.

However the exact mechanism that decides which cell in the cluster will become the SOP is not well understood. One suggestion is that N-Dl signalling is modulated by the cell adhesion protein Echinoid (Ed), although the mechanism is still unclear. Ed may either enhance Dl function in the future SOP or cause Dl to be down-regulated in cells which are not to become SOPs (Rawlins *et al*., 2003). Members of the *bearded* family of genes have recently been shown to inhibit the Notch-Dl interaction and, since these genes are up-regulated in the non-SOP PNC cells, it is possible that this also forms part of the feedback loop that underlies lateral inhibition

(Chanet *et al*., 2009). It is also thought that the Notch and EGFR pathways may act antagonistically to ensure correct patterning during sense organ development (Culi *et al.*, 2001). Recent studies in developing *Drosophila* eye imaginal discs have suggested a role for *split ends* (*spen*) in modulating these two pathways (Doroquez *et al.*, 2007). Again the exact mechanism for this modulation remains unclear.

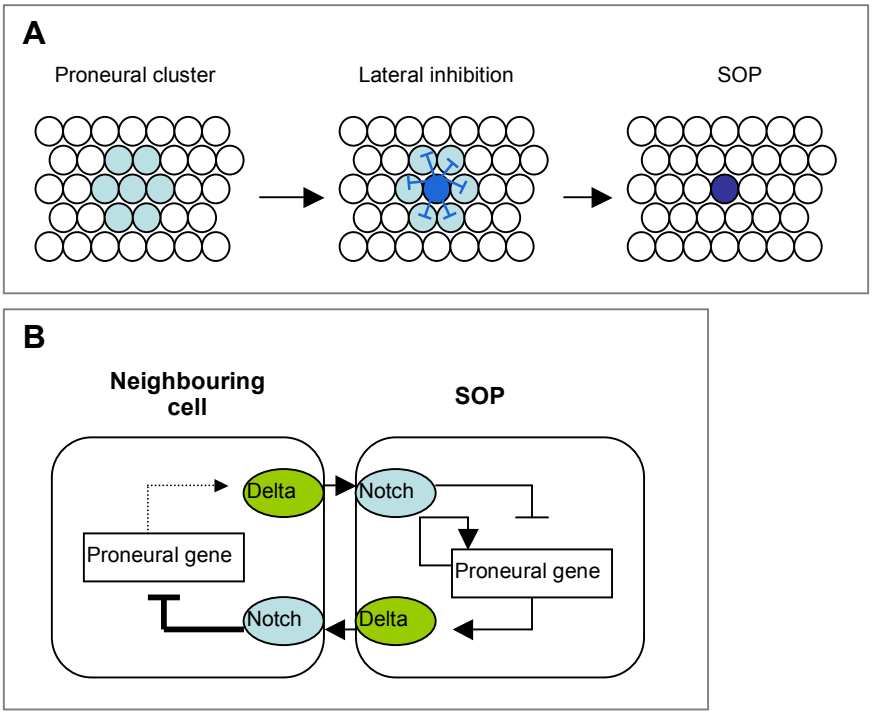

Figure 1.03: SOP selection by lateral inhibition. A) Proneural genes are initially expressed at low levels in the PNC (light blue circles). Proneural expression is up-regulated in the cell destined to become the SOP (darker blue circle) and this results in inhibition of proneural expression in neighbouring cells. B) Simplified schematic of the Notch pathway. Proneural expression induces expression of Delta, which binds to Notch on adjacent cells resulting in inhibition of proneural gene expression. As one cell becomes selected as the SOP proneural gene expression in this cell is increased by autoregulation and inhibition of Notch signalling. This results in higher levels of Delta expression and consequently increased Notch signalling and decreased proneural expression in adjacent cells.

Proneural gene expression can be divided into two different temporal phases: initial expression in the PNC and the retained high expression in the selected SOP

following lateral inhibition. The first phase of expression is regulated by *hedgehog*, *hairy*, *hairless*, *extramacrochaete* and *charlatan* (Moscoso del Prado & Garcia-Bellido, 1984; Orenic *et al*., 1993; Skeath & Carroll, 1991; Yamasaki *et al*., 2011) as well as upstream genes that determine segmental patterning. The second phase is thought to be due to autoregulation (van Doren *et al*., 1992; Martinez *et al*., 1993; Gibert *et al*., 2003). In the case of *ac/ sc* and *ato* these two phases of expression are regulated by separate enhancers (Rodriguez *et al*., 1990; Sun *et al*., 1998). Notch and EGFR can also inhibit and enhance autoregulation via binding sites in these enhancers (Culi *et al*., 2001; zur Lage *et al*., 2004). However *amos* expression does not seem to depend on autoregulation through a separate enhancer (Holohan *et al*., 2006).

The capacity of proneural genes to produce sensory organs depends on the location and timing of their expression (Jarman *et al*., 1993; Rodriguez *et al*., 1990). The effect of proneural gene expression is also context dependent, for example *ato* directs formation of photoreceptors in the developing eye but Ch organs when expressed in other locations (Jarman *et al*., 1994; Jarman *et al*., 1995). However mis-expression of proneural genes within these context and temporal constraints has been shown to result in formation of ectopic sensory organs (Campuzano *et al*., 1986; Jarman & Ahmed, 1998). This shows that proneural gene expression is not only sufficient for SOP formation but also shows that they control the subtype specificity of neural differentiation.

The proneural proteins are able to form heterodimers with the bHLH protein Daughterless (Da) (Jarman *et al*., 1993; Brown *et al*., 1996). These heterodimers

regulate gene expression in the SOP by binding to E-boxes, which have the core sequence CANNTG, via the basic regions of the bHLH domain (Chien *et al*., 1996). Proneural proteins can also form heterodimers with an HLH protein encoded by *extramacrochaetae* (*emc*) that lacks the basic DNA binding domain. High levels of Emc therefore inhibit proneural function by sequestering the proneural proteins in inactive heterodimers (Van Doren *et al*., 1991; Cabrera *et al*., 1994). Ato-Da heterodimers have been shown to bind to E-boxes with a different sequence from that used by Sc-Da heterodimers (Powell *et al*., 2004). Ato-Da heterodimers bind to the consensus sequence: 5'-A(A/T)**CA**(G/T) G**TG**(G/T)- 3' (where letters in bold represent the core E box sequence) while Sc-Da heterodimers bind to 5'-G**CA**G(C/G)**TG**(G/T)-3'. The zinc finger transcription factor Senseless (Sens) acts as a cofactor that may contribute to proneural specificity. Sens has two activities; it binds to DNA sequences upstream of E-boxes and can also enhance the function of Sc-Da and Ato-Da on their cognate E-boxes (Powell *et al*., 2008).

The basic region of the bHLH domain is important for DNA binding specificity. This has been demonstrated using a chimeric protein where the basic domain of Sc is replaced with that of Ato. Expression of this chimera can induce ectopic Ch organs and is sufficient to rescue the *ato*-null mutant phenotype (Chien *et al*., 1996). An exception to this is the structural basis of the different specification properties of Ato and Amos. The basic domains of these two proneural proteins differ only by a single amino acid and the Amos bHLH domain can substitute for that of Ato to regulate Ato-specific functions (Maung & Jarman, 2007). The specificity of Ato relative to

Amos is therefore dependent on the non-bHLH portion of the Ato protein, which may be required for context dependent cofactor binding.

1.2.2 SOPs divide and differentiate to form cells of specific sensory organs

Inhibition of Notch is thought to trigger the switch from symmetric proliferative division to asymmetric differentiative division. For example in the optic lobe expression of the proneural gene *lethal of scute* in the neuroepithelium downregulates Notch and this triggers the transition from symmetrically dividing neuroepithelial cells to asymmetrically dividing neuroblasts (Eggar *et al*., 2010). In the developing PNS, the SOPs undergo precisely regulated asymmetric cell divisions (Orgogozo *et al*., 2001) and the resulting daughter cells differentiate to form the specific neuronal and glial cell types that make up a particular sensory organ (figure 1.04). In the case of Ch organs, for example, the daughter cells of the SOP (PIIa and PIIb) divide at different times. PIIb divides first giving rise to PIIIb and the precursor of the ligament cell. PIII then divides producing two cells that will then differentiate to form the neuron and the scolopale cell. PIIa divides later than PIIb producing the precursor of the cap cell and an ectodermal cell. Multidendritic (md) neurons are derived from three sources, one group from external sensory organ lineages, a second set from the chordotonal lineage and a third set is unrelated to sensory organs (Brewster & Bodmer, 1995).

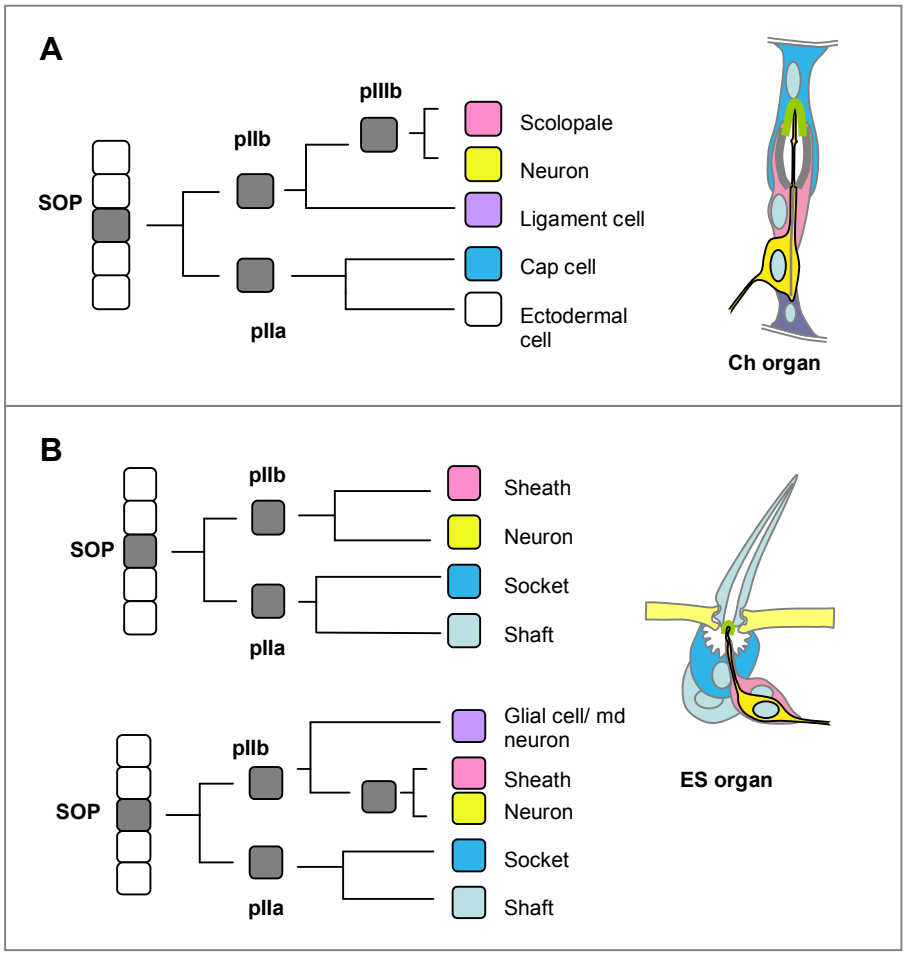

Figure 1.04: Differentiation of sensory organ cells from the SOP. A) In chordotonal organ development SOPs delaminate from the epidermis and become attached to the basal surface of the ectoderm. The SOP divides asymmetrically to produce pIIa and pIIb. pIIb divides first giving rise to pIIIb and the ligament cell. pIIIb then divides to produce the neuron and socolpale. B) In larval ES organs the neuron and sheath are derived from pIIb and the socket and shaft are derived from pIIa (Brewster & Bodmer, 1995). In the adult ES lineage pIIb divides earlier giving rise to pIIIb and a glial cell (Gho et al., 1999). In some md/ es lineages this cell differentiates to form an md neuron (Orgogozo et al., 2001).

The gene *numb* is required to regulate proper differentiation of the cells derived from these lineages. In *numb* mutants neural precursors differentiate into support cells (Uemura *et al*., 1989; Brewster & Bodmer, 1995) and asymmetric segregation of

Numb in SOPs and their daughter cells has been shown to be essential for cell fate determination (Bhalerao et al., 2005). The Numb protein segregates into one of the SOP daughter cells where it negatively regulates Notch signalling to specify pIIb cell fate. Numb has been shown to form a complex with the transmembrane protein Sanpodo *in vivo* (O'Connor-Giles & Skeath, 2003) and it is thought that Numb acts by inducing endocytosis of Sanpodo in the pIIb cell (Hutterer & Knoblich, 2005). It has therefore been suggested that plasma membrane-localised Sanpodo is responsible for Notch activation in pIIa cells (O'Connor-Giles & Skeath, 2003; Hutterer & Knoblich, 2005). Endocytic recycling of the Notch ligand Delta is required for proper specification of neural cell fate and the exocyst complex protein Sec15 is thought to mediate this endocytic recyling (Jefar-Nejad *et al*., 2005). Sec15 mutants have extra ES neurons at the expense of support cells (Jefar-Nejad *et al*., 2005).

In the adult bristle lineage Notch signalling has been found to inhibit glial cell fate through negative regulation of *glial cells missing* (*gcm*), a gene required for glial cell fate (Van de Bor & Giangrande, 2001). However in the embryonic dbd sensory lineage Notch is specifically activated in one of the daughter cells and is required for *gcm* expression and glial fate (Umesono *et al*., 2002). The effect of Notch signalling on cell fate determination is therefore highly context dependent.

1.2.3 Regulatory targets of proneural genes

Many genes identified as direct regulatory targets of proneural genes are involved in very early steps of neurogenesis such as SOP selection, for example *Bearded*, *Enhancer of split* (*E(spl)*) genes and *scabrous* (Singson et al., 1994). Another direct

target of proneural genes is *cut*, a homeobox gene specifically expressed in ES organ precursors and required for ES organ fate (Bodmer *et al*., 1987). Expression of *cut* is induced by Ac/Sc and repressed by Ato (Blochlinger *et al*., 1991; Jarman & Ahmed, 1998) and the presence or absence of Cut controls the commitment of SOPs to ES or Ch fate. Neural differentiation requires cell cycle exit and, in the developing eye, proneural proteins promote cell cycle exit by directly inducing expression of cdk inhibitors such as Dacapo (Sukhanova *et al*., 2007). Other genes involved in regulating cell cycle exit include the bHLH genes *deadpan*, *asense* and *cousin of atonal* (*cato*) (Wallace *et al*., 2000; zur Lage & Jarman, 2010). Cato is thought to control the number of cell divisions in the neuronal branch of the Ch lineage and has been shown to be regulated directly by both Amos and Ato in different sensory lineages (zur Lage & Jarman, 2010).

However the majority of proneural protein target genes are unknown and many of the known targets involved in the early stages of neurogenesis are not exclusive to one neuron subtype. The different proneural genes must also direct differentiation of subtype-specific features responsible for the particular structure and physiology of a sensory organ. Understanding the genetic regulation of these later stages of the neurogenic pathway is therefore an important goal.

1.2.4 Chordotonal organs are specified by expression of *atonal*

The role of *ato* in regulating Ch organ differentiation has been well established. Ch organs are missing in *atonal* mutant embryos and larvae (Jarman et al., 1993; Jarman et al., 1995) and ectopic sense organs of this class are induced when *ato* is

misexpressed (Jarman & Ahmed, 1998). *Ato* is therefore both necessary and sufficient for controlling Ch organ differentiation. Expression of *Atoh1* (*Math1)*, the vertebrate homologue of *ato*, in *ato* mutant flies has been shown to fully rescue the mutant phenotype as did expression of *ato* in *Atoh1* null mice showing that these two proteins not only share high sequence similarity but are also functionally interchangeable (Wang *et al*., 2002). Interestingly *Atoh1* is required for forming the non-neuronal inner ear hair cells (Bermingham *et al*., 1999; Zheng & Gao, 2000) providing further evidence of a link between the *Drosophila* auditory Johnston's organ and the mammalian cochlea.

Unlike external sensory bristles individual Ch organ scolopidia normally aggregate into organised clusters. In the larva these clusters contain a maximum of five scolopidia (lch5) and this clustering is thought to be achieved during SOP selection by a two-step process. First one SOP is selected through ato function and Notch-Delta signalling. Subsequent SOPs are then recruited by this priming SOP from the surrounding non-committed cells through EGFR signalling (Okabe & Okano, 1997; zur Lage *et al*., 1997). This signalling is directly activated by *ato* function in the primary SOP. Moreover, in the recruited SOPs, EGFR activation stimulates *ato* autoregulation. This is achieved by Ato-Da and Pointed (a target of EGFR) binding to adjacent sites in the *ato* autoregulatory enhancer (zur Lage *et al*., 2004). In the case of the most dorsally located *ato*-expressing SOP (the P cell) the EGFR signalling induces recruitment of oenocytes rather than Ch SOPs (Elstob *et al*., 2001). Oenocytes are hepatocyte-like secretory cells located as clusters of about six cells in the same lateral position as the lch5 cluster. They are derived from the embryonic ectoderm of the abdominal segments A1-A7 (Hartenstein *et al*., 1992).

Cells in dorsal regions of the ectoderm express the transcription factor Spalt, which is thought to bias cellular response to the EGFR ligand Spitz in favour of oenocyte fate (Elstob *et al*., 2001; Rusten *et al*., 2001). EGFR mediated recruitment by the dorsal SOP therefore recruits oenocytes, whereas in lateral regions of the ectoderm where Spalt is not expressed EGFR signalling results in recruitment of further Ch SOPs (reviewed in Gould *et al*., 2001).

In adult Ch organs the situation is more complicated due to the much larger clusters. For example the adult femoral Ch organ is composed of a cluster of about 70-80 scolopidia. Such large clusters are thought to be formed by reiterative recruitment of SOPs rather than a two-step process (zur Lage & Jarman, 1999). In this case recruited SOPs go on to recruit further ectodermal cells. Notch signalling is slightly reduced in the SOP due to EGFR signalling, which allows the surrounding cells to remain competent. Direct signalling via EGFR also recruits further SOPs and both Notch and EGFR signalling may be regulated by Ato.

While most SOPs are born in their final location (so that little cell migration is needed) the lateral lch5 chordotonal organ cluster SOPs form in a dorsal position. In order to reach their lateral position the daughter cells of the SOP must rotate approximately 145^{o} to achieve the correct polarity and then migrate ventrally to their final position (Salzberg *et al*., 1994). Similarly the v'ch SOP forms in a ventral position and the daughter cells must migrate dorsally. Such migration only occurs in the abdominal segments. The exact mechanism for this migration is still unclear, however it has been suggested that the transcription factor ventral veinless (vvl) may

play a role in regulating the ventral stretching of lch5 into the correct position (Inbal *et al*., 2003). In *vvl* mutants the lch5 Ch organs fail to rotate and develop in the dorsal position, although cell fates within the chordotonal organ are determined correctly.

Other important aspects of Ch neuron structure and physiology will be discussed in detail in later chapters. However, for *ato* expression to be sufficient to induce Ch differentiation, it must initiate a gene regulatory network that controls differentiation of Ch-specific features. As with neural differentiation in other species this is poorly understood. Recent work in this area has therefore focused on identifying regulatory targets of proneural genes and understanding the roles of these targets in neural specialisation.

1.2.5 Recent studies identifying downstream targets of proneural genes

Several recent studies in *Drosophila* and vertebrate models have analysed the expression profiles of cells expressing particular proneural genes as a means of identifying direct regulatory targets of proneural genes. One of the earliest of these (Reeves & Posokony, 2005) used an *E(spl)m4*-GFP reporter construct to label proneural clusters (PNC) and SOPs in *Drosophila* wing imaginal discs. The PNCs and SOPs were then separated by fluorescence activated cell sorting (FACS) and the expression profiles of GFP^+ and GFP^- cells were compared in a microarray experiment. This approach identified 204 PNC enriched genes, predicted to be downstream targets of Ac/ Sc. 27 of these genes were shown to be expressed in the appropriate Ac/ Sc PNC specific pattern by *in situ* hybridisation. These included several genes already known to be Ac/ Sc targets as well as some novel targets

including transcription factors, receptors and signalling molecules, microtubule associated proteins and some genes of unknown function. It is possible that at least some of these genes are required for ES-specific differentiation. However, since this study is mainly concerned with the expression profile of PNC cells (rather than SOPs), many may have a more general role in SOP selection and cell division.

In a more recent study Bassem Hassan and colleagues used microarray experiments to compare the expression profiles of developing eye discs when Ato is mutated or over-expressed (Aerts *et al*., 2010). This identified 451 potential downstream targets of Ato in R8 precursors. Aerts et al. also developed a computational method, *cis*TargetX, which predicts regulatory targets through integrating gene expression data with conserved clusters of regulatory motifs (in this case *ato*-type E-boxes) in the upstream regions of these genes. When this was used to analyse the microarray data it identified 74 potential direct targets of Ato in developing photoreceptors and 20 of these were validated using *in vivo* enhancer-reporter constructs. These genes include some previously known Ato targets such as *sens* and *dacapo* as well as a number of new targets. Many of the new target genes are known to be involved in neural differentiation and retinal specification. These results were compared to publicly available microarray data sets obtained for genetic perturbations of other transcription factors required for retinal differentiation such as Eyeless, Sens, Suppressor of Hairless, Rough and Glass. This study therefore provides information about the gene regulatory network that controls the early stages of retinal differentiation.

Similar studies have been carried out in mouse and *Xenopus*. For example, downstream targets of Mash1 and Ngn2 in mouse telencephelon have been identified by microarray experiments (Gohlke *et al*., 2008). The expression patterns of genes found to be differentially expressed following genetic perturbation of *Mash1* or *Ngn2* in the telencephelon were confirmed by *in situ* hybridisation. Many of these genes were found to have conserved E-boxes in nearby non-coding regions. Further bioinformatic analysis of the predicted enhancers of these target genes identified binding sites for other known regulators of neurogenesis. This study therefore provides information about the relationship between Mash1 and Ngn2 and other regulators such as POU transcription factors and transcriptional regulators acting downstream of Wnt signalling during neural specification.

Another study identified potential direct downstream targets of the *ato*-related proneural genes *neuroD* and *Ngnr1* in *Xenopus* (Seo *et al*., 2007). In these experiments the proneural proteins were expressed as fusions with the human glucocorticoid receptor (GR) hormone binding domain in explants of multipotent ectodermal tissue. Following addition of the GR ligand DEX neuroD-GR and Ngnr1-GR are rapidly transported to the nucleus and activate gene expression. The expression profiles of DEX-treated versus untreated samples were compared in a microarray experiment. This approach identifies only genes that are differentially expressed 2.5h after DEX treatment and, since the experiments were also carried out in the presence of a translational inhibitor, it prevents expression of indirect secondary targets. These experiments therefore identified genes that are likely to be direct targets of neuroD or Ngnr1. These results were validated using qRT-PCR.

Analysis of the enhancers of validated targets identified minimal enhancer signatures recognised by neuroD and Ngnr1 during regulation of genes involved in neural differentiation. Interestingly this study did not identify genes that are known to be regulated by neuroD in the developing pancreas. This suggests that neuroD regulates neuronal and non-neuronal differentiation genes through different enhancer motifs.

The experiments described above have been useful for identifying novel direct targets of proneural genes, however there is still little known about how transient expression of proneural genes is linked to regulation of the later differentiation events that lead to neural specialisation. A recent microarray study in the Jarman lab (Cachero *et al*., 2011) has attempted to address this. Embryonic *ato*-expressing cells were labelled using an *ato*-GFP reporter and separated by FACS. In contrast to the other studies described the expression profile of *ato*-expressing cells was compared to that of cells that do not express *ato* at three different time points. The results therefore provide a temporal expression profile of *ato*-dependent cells and provide some insight into the regulatory cascade acting downstream of Ato. This study identified both potential direct targets of Ato and novel Ch-specific genes expressed later during differentiation. These results will be described in more detail in chapter 2.

Many of the direct regulatory targets of proneural genes identified so far in both *Drosophila* and vertebrates encode transcription factors and it is likely that these regulate expression of genes required for neuron subtype-specific features. Identifying the regulatory targets of these transcription factors and their role in

neuron subtype specialisation is the logical next step towards understanding how proneural genes control differentiation of specific neuron subtypes.

1.3 Aims of this thesis

My work focuses on identifying genes which act downstream of *ato* to direct Ch neuron specialisation in *Drosophila*. The recent Jarman lab microarray study (Cachero *et al*., 2011) has identified a number of genes that are enriched in *ato*-expressing cells, many of which may be direct regulatory targets of Ato. I selected one of these genes, *fd3F*, that encodes a previously uncharacterised forkhead transcription factor for further study. The aim of this thesis is to determine the role of *fd3F* in *Drosophila* Ch neuron differentiation through analysis of the effect of fd3F deficiency on Ch neuron morphology and adult proprioceptive behaviour and also by identifying genes that are directly regulated by fd3F.

2

Preliminary Experiments to Identify fd3F as an Intermediate Regulator of Chordotonal Neuron Differentiation

2.1 Introduction

2.1.1 Understanding differentiation of sensory neuron subtypes

The development of *Drosophila* sensory organs is a useful model for understanding neural development and also for understanding the regulatory pathways that lead from initial cell specification to differentiation. Nervous systems require a variety of subtly different neuron subtypes that are specialised for different functions. These specialisations may include differences in dendrite morphology or expression of a particular ion channel. While it is known that these neuron subtypes are specified early in development by expression of different proneural genes in sense organ precursor cells (SOPs) much less is known about how proneural genes direct events occurring later during differentiation. For example *Drosophila* chordotonal (Ch) neurons are specified by expression of *atonal* (*ato*) in SOPs (Jarman *et al*., 1993; Jarman *et al*., 1995). However, as with other proneural genes, the direct downstream targets of *ato* and the gene regulatory network that directs chordotonal organ development are not well known. Recent work in this area has therefore focused on trying to identify these downstream targets.

Expression of *ato* is switched off shortly after the first SOP division and many of the Ch-specific genes required for differentiation are not expressed until much later. Therefore it is expected that *ato* regulates intermediate transcription factors and these in turn regulate expression of the later differentiation genes. *Drosophila regulatory factor X* (*Rfx*) encodes one possible intermediate transcription factor. Rfx is a homologue of *C. elegans* daf-19 and human RFX1, 2 and 3 all of which are required for normal morphogenesis of ciliated cells. In *Drosophila* Rfx is required for development of ciliated sensory neurons and sperm (Dubruille *et al*., 2002). Expression of *Rfx* is directly regulated by *ato* in Ch neurons (Cachero *et al*., 2011) and many genes required later during differentiation, for example genes required for formation of the Ch neuron cilium, are predicted to be direct targets of Rfx (Laurençon *et al*., 2007).

However Rfx is also expressed in developing external sensory (ES) neurons at low levels and is not Ch-specific until the latest stages of embryogenesis. Many genes required later in Ch organ differentiation are exclusively expressed in Ch neurons and are likely to be expressed earlier than this so cannot be exclusively regulated by Rfx. Such genes must therefore be at least partially regulated by Ch-specific transcription factors. Identification and characterisation of these transcription factors is therefore an important goal for understanding differentiation of specific neuron subtypes.

2.1.2 Identification of fd3F as a potential intermediate regulator of Ch neuron differentiation

2.1.2.1 Microarray experiments to identify genes acting downstream of *atonal*

Microarray experiments to compare the gene expression profiles of *ato* expressing cells with cells that do not express *ato* (*ato*$^-$ cells) at three different time points during embryogenesis (Cachero *et al*., 2011) have identified a number of potential direct targets of *ato*. Ato-expressing cells were labelled using an *ato*-GFP enhancer construct and the embryos were then dissociated and the GFP$^+$ and GFP$^-$ cells were separated by fluorescence activated cell sorting. RNA from the two cell types was used to probe Affymetrix *Drosophila* microarray chips to identify differentially expressed genes (Sir Henry Wellcome Functional Genomics Facility, Glasgow, UK). The three time points used (t1-t3) correspond to the first three hours of neurogenesis. Ato expression overlaps maximally with t1, so the genes enriched in *ato*-GFP$^+$ cells at this time point should include direct targets of *ato*. The later time points represent the subsequent stages of development (SOP division and early differentiation). Even at t3, however, many known differentiation genes were not found to be differentially expressed, for example, *futsch* and two genes encoding subunits of a Ch-specific transient receptor potential (TRP) channel, *nanchung* and *inactive*. This confirms that these differentiation genes are not expressed until the very latest stages of Ch neuron differentiation and so cannot be regulated by ato directly.

This study was expanded by similar microarray experiments comparing genes expressed in cells expressing *cousin of atonal* (*cato*) and cells that do not express

cato (*cato*$^{-}$ cells) at four time points (Petra zur Lage, unpublished). *cato* encodes a bHLH transcription factor that is closely related to *ato* and has roles in maintaining SOP identity and control of cell division (Goulding *et al.*, 2000; zur Lage & Jarman 2010). *cato* is expressed in the developing PNS during the stages between SOP selection and terminal differentiation although it is not confined to chordotonal organs at later stages. While the earlier *cato* time points overlap with the later *ato* data, time points t3 and t4 provide information about chordotonal gene expression during the later stages of differentiation (for example *nanchung* was found to be differentially expressed at *cato* t4).

Differentially expressed genes at each of the different time points were ranked according to fold change. Unsurprisingly many of the most highly ranked genes at t1 are known to be involved in neural development including *spineless*, *twin of eyeless*, *cato*, *couch potato*, *ato*, *Rfx* and *senseless*. Gene ontology (GO) analysis of the data showed that the most highly represented GO terms for genes enriched at t1 were 'SOP cell fate determination' and 'components of the notch signalling pathway' confirming that t1 represents the SOP selection stage. t2 represents the cell division stage and, as expected, genes involved in DNA replication were over-represented at this stage. At t3 however, there is a large increase in genes associated with cell differentiation processes such as cilium assembly and sensory perception of sound. The expression patterns of 43 of these genes were examined by mRNA *in situ* hybridisation and in at least 90% of cases their expression overlapped with *ato*-dependent cell lineages with the majority expressing in Ch cells. These data therefore

describe a temporal gene expression profile for the events occurring downstream of *ato* expression that lead to Ch organ differentiation.

In order to link the expression profiles of developing Ch cells to *ato* function a further microarray experiment was carried out to compare the expression profiles of *ato*-GFP expression cells from ato^{1} mutant embryos to wild type embryos at t1 (Cachero *et al*., 2011). From these experiments 50 genes were identified that are ≥2-fold differentially expressed in wild type *ato*-GFP^{+} cells (compared with GFP^{-} cells) but not in mutant GFP^{+} cells (compared with mutant GFP^{-} cells). 11 of these genes were also found to show more than 2-fold difference between the fold changes observed in the wild type and mutant embryos (table 2.1). These 11 genes are therefore good candidates to be direct regulatory targets of *ato*.

Gene	Function	Wt fc	Mut fc	Wt/Mut
cato	Transcription factor	16.95	1.77	9.56
dila	Cilium assembly	11.07	1.79	6.20
unc	Cilium assembly	9.90	1.91	5.20
Rfx	Transcription factor	9.76	1.75	5.59
ImpL3	Lactate dehydrogenase, glycolysis	7.22	1.40	5.15
CG9095	Cell adhesion	5.71	1.77	3.23
fd3F	Transcription factor	5.55	1.76	3.15
CG30427	Oxidoreductase, phagocytosis	4.40	1.52	2.89
nervy	Axon guidance, dendrite morphogenesis	4.22	1.94	2.17
CG6129	Stability of ciliary rootlet	4.13	1.72	2.40
CG41452	Cell adhesion	3.52	1.72	2.05

Table 2.1: Potential *ato* targets based on genes differentially represented in Wt versus *ato*-mutant cells. These 11 genes show more than 2-fold difference between the fold changes (fc) observed in Wt and mutant GFP^{+} cells (versus GFP^{-} cells). These include transcription factors, genes required for formation of the Ch neuron dendrite and cilium and genes predicted to encode cell adhesion molecules that could be involved in formation of the dendritic cap. The functions given for *CG30427* and *ImpL3* are those described in the adult or predicted from sequence similarity although the reason for these genes being enriched in Ch SOPs in the embryo is unclear.

Three of these genes encode transcription factors: *Rfx*, *cato* and a previously uncharacterised forkhead factor, *forkhead domain 3F* (*fd3F*, CG12632). It is therefore possible that *fd3F* encodes a novel intermediate regulator of Ch organ differentiation.

2.1.2.2 *fd3F* is a potential downstream target of *atonal*

The forkhead family genes encode a highly conserved group of transcription factors with a DNA binding domain similar to that first identified in the *Drosophila* Forkhead (Fkh) protein (Weigel *et al*., 1989). Currently there are more than 2000 known forkhead family members identified in 108 species of animals and fungi, although none have been identified in plants. Most of these proteins can be classed as belonging to one of the 19 identified subfamilies (A-S) and the majority of these are now referred to as FOX (forkhead box) followed by a letter to denote their subfamily. *fd3F* was originally identified as encoding a forkhead transcription factor by a search of the *Drosophila* genome for forkhead domain genes (Hacker *et al*., 1992; Lee & Frasch, 2004). The amino acid sequence of the fd3F forkhead domain closely resembles that of other *Drosophila* forkhead factors and the human and mouse FOX proteins (figure 2.01). However, *fd3F* is not closely related to any of the FOX gene subfamilies (Lee & Frasch, 2004) and nothing else is known about its function, although other forkhead genes are known to play important roles in neurogenesis.

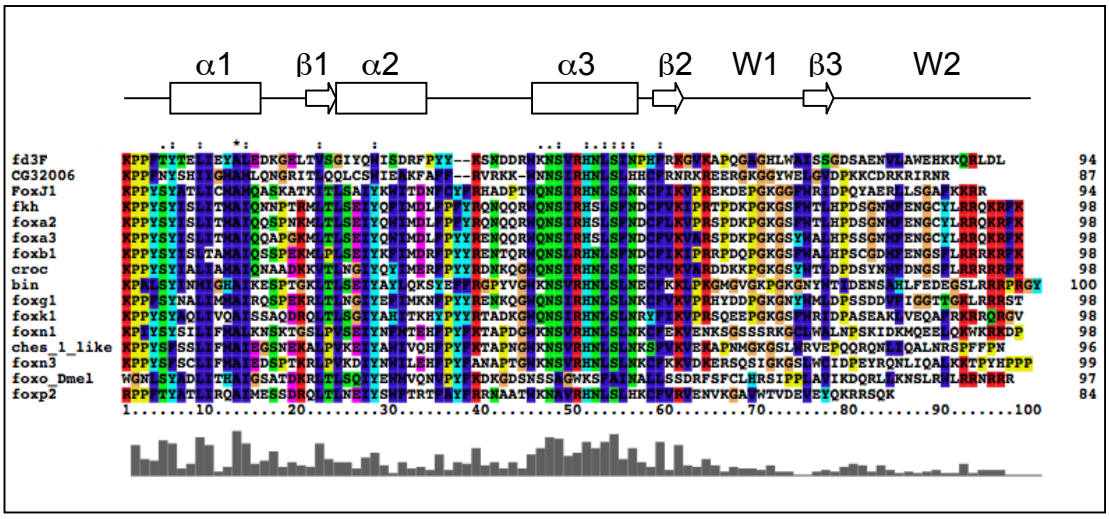

Figure 2.01: Alignment of forkhead domains in *Drosophila* and mouse proteins. The sequence of the fd3F forkhead domain was aligned to forkhead domains from six other *Drosophila* forkhead proteins (CG32006, Fkh, Croc, Bin, Ches-1-like and FoxO) and nine mouse proteins (foxJ1, foxA2, foxA3, foxB1, foxG1, foxN1, foxN3 and foxP2) using ClustalX. The approximate position of the forkhead domain structural features is shown above the alignment. Comparison of these secondary structure features to the alignment shows highest conservation in the 3rd helix (α3) and lowest conservation in the wings (W1 and W2).

Since *fd3F* is highly enriched across all time points in the *ato* microarray data we would expect it to be expressed in Ch cells and to have a role in regulating Ch organ differentiation. The expression pattern of *fd3F* has been described (Lee & Frasch, 2004) and was found to be restricted to Ch cells from stage 12 onwards, however the transcripts were uniformly distributed throughout the embryo prior to stage 12. This contradicts the *ato* microarray data since *fd3F* expression was strongly enriched in *ato*-GFP^{+} cells even at t1 (which corresponds to embryonic stages 10-11). *fd3F* has also been identified in an RNAi screen (Parrish *et al.*, 2005) as being required for morphogenesis of larval multidendritic neurons, although the expression pattern of *fd3F* was not analysed in this study. Again this contradicts the *in situ* results of Lee

& Frasch since no *fd3F* expression was found in multidendritic neurons. The first aim of my project was therefore to analyse *fd3F* function via expression pattern and genetic analysis.

2.1.3 Forkhead factors have important roles in development and human disease

2.1.3.1 Forkhead domain structure and mechanism of transcriptional regulation

The forkhead domain is composed of three α-helices and three β-sheets connected by two loops. These loops or 'wings' fold around the helices in a butterfly shape and this domain is therefore sometimes referred to as a winged helix (figure 2.01). The 3D structure of this domain complexed to DNA was first resolved by X-ray crystallography for FOXA3 (HNF3γ) (Clark *et al*., 1993) and since then several other forkhead domains have been found to have similar crystal structures. Forkhead factors are thought to bind to DNA via helix3 (α3) of this domain, which acts as a recognition helix and makes sequence specific contacts with the major groove (reviewed in Gajiwala & Burley, 2000). This helix has been shown to be essential for DNA binding and is, unsurprisingly, the most highly conserved part of the domain across all forkhead proteins (Lee & Frasch 2004; Wijchers *et al*., 2006) including fd3F (figure 2.01). Both the wings and the region between α2 and α3 are also able to interact with bases in the minor groove of DNA, however these regions are much less well conserved than any of the helices or β-sheets. It is thought that these regions

modulate the binding affinity and specificity of the domain allowing different forkhead proteins to regulate different target genes (Cirillo & Zaret, 2007).

Forkhead factors are able to activate or repress gene expression by binding to sequences matching the consensus 5'-(G/A)(T/C)(C/A)AA(C/T)A-3' in the enhancers of target genes. This sequence was identified by *in vitro* binding site selection experiments for various different forkhead domain genes and comparison of known forkhead domain binding sites (Pierrou *et al*., 1994; Kaufmann *et al*., 1995; Perez-Sanchez, 2000; Biggs & Cavenee, 2001). While most forkhead factors bind to DNA as monomers some, such as FOXK1 and several FOXP family members are able to form homodimers (Stroud *et al*., 2006; Li *et al*., 2004; Tsai *et al*., 2006) and others can form heterodimers, for example FoxO3a and FoxG1 form a dimer to regulate the growth inhibitor *p21Cip1* (Seoane *et al*., 2004). Forkhead proteins can also interact with other proteins that are not transcription factors including co-activators and co-repressors. For instance, Foxk1 is able to repress transcription of specific target genes by recruiting a co-repressor complex that includes histone deacetylases and chromatin remodelling factors resulting in increased chromatin compaction at specific loci (Yang *et al*., 2000).

In addition to the conventional mode of gene regulation some FOX proteins have recently been found to regulate gene expression by affecting chromatin structure directly. The basis of this is thought to be the similarity between the forkhead domain and the winged helix structures of histones H1 and H5. For example FOXA1 can activate transcription from the albumin enhancer by binding to nucleosomal core

histones, replacing the H1 and H5 linker histones, and opening the chromatin structure (Shim *et al*., 1998). FOXA binding also causes the DNA to bend, which widens the minor groove and helps to relieve chromatin compaction (Cirillo *et al*., 1998). Similarly FOXI1, FOXE1 and FOXO1 have all been found to be able to bind to condensed nucleosomes and activate transcription by reducing chromatin compaction (Yan *et al*., 2006; Cuesta *et al*., 2007; Hatta *et al*., 2009).

Forkhead gene activity can also be modulated by a number of post-translational modifications. For example acetylation of lysine residues within the forkhead domain is thought to decrease the transcriptional activity of mouse FoxO proteins by reducing their affinity for binding sites in target DNA (Matsuzaki *et al*., 2005). Phosphorylation of serine, threonine and tyrosine residues has also been reported and the most extensively studied example of this is FoxO protein phosphorylation by PKB. PKB phosphorylates FoxO family members in response to insulin-like growth factors and this modification stops FoxO proteins from entering the nucleus and therefore prevents them from functioning as transcription factors (Biggs *et al*., 1999). FOXO transcription factors can also undergo arginine methylation (Yamagata *et al*., 2008) and both FOXO4 and FoxM1 have been reported to O-GlcNAcetylation of serine or threonine residues (Ho *et al*., 2010; Caldwell *et al*., 2010). In addition some FOXO proteins can also be regulated by ubiquitination (van der Horst *et al*., 2006; Matsuzaki *et al*., 2003).

2.1.3.2 Forkhead factors regulate key biological processes

Many forkhead factors are known to play key roles in embryonic development and FOX genes have been linked to human genetic diseases including cleft lip and palate, congenital alopecia, premature ovarian failure, T-cell immunodeficiency, mental retardation and language impairment (reviewed in Lehmann *et al*., 2003). The forkhead factors studied so far in *Drosophila* have all been found to have important roles in embryogenesis. For example, Fkh (a homologue of the foxA subfamily) is required for specification of structures at the extreme anterior and posterior of the developing embryo and for salivary gland morphogenesis (Myat & Andrew, 2000). *Crocodile* (*croc*, *foxC*) is needed for development of head structures (Hacker et al., 1995) and *biniou* (*bin*, *foxF*) regulates differentiation of visceral mesoderm into gut musculature (Zaffran *et al*., 2001). Forkhead factors are often expressed in a tissue specific manner and are involved in regulating differentiation of particular cell types. Since fd3F is expected to be expressed in Ch organs and their precursors in *Drosophila*, the roles of forkhead proteins in neurogenesis and formation of motile cilia are of particular interest and will be discussed further in the next section.

Forkhead factors are also known to play key roles in biological processes in adult organisms. In fact many forkhead proteins required for cell fate determination and morphogenesis during development also perform important functions in the adult. For example FoxO, FoxA and FoxC family proteins have been implicated in regulation of metabolic processes such as insulin signalling, glucose homeostasis and fat metabolism (Accili *et al*., 2004; Shen *et al*., 2001; Cederberg *et al*., 2001). In addition to insulin signalling, FOX proteins can also act as effectors in several other

signalling pathways including the Hedgehog pathway, MAP kinase pathway, TGF-β cascade and Wnt/ β-catenin pathway (reviewed in Carlsson & Mahlapuu, 2002; Hu *et al*., 2010). Forkhead factors are also implicated in regulation of the immune system particularly in the prevention of autoimmunity. FoxP3 is required for the function of regulatory T-cells, which are required to control T-cell reactivity (Hori *et al*., 2003), and FoxJ1 may have a role in regulating release of T-cells into the periphery (Srivatsan & Peng, 2005). Both these processes are necessary to prevent autoimmunity.

Many of the forkhead factors required during embryonic development have roles in regulation of the cell cycle, proliferation, differentiation and apoptosis and these functions are often retained in the adult. Deregulation or mutation of forkhead factors has therefore been implicated in both cancer and ageing. Several human FOX proteins are now suspected to act as either oncogenes or tumour suppressors (reviewed in Myatt & Lam, 2007) and FOXM1 and FOXO subfamily members have been associated with regulation of longevity and cell survival (Laoukili *et al*., 2007; Gilley *et al*., 2003; Nakamura *et al*., 2000). In particular FOXO3a variants have been linked to ovarian ageing and premature ovarian failure (Gallardo *et al*., 2008).

2.1.3.3 Forkhead genes and neurogenesis

Although *fd3F* is not closely related to other forkhead genes in *Drosophila* or other species many forkhead genes have been associated with neurogenesis. Some are directly involved in regulating cell fate determination and differentiation of specific neuron subtypes while others have more general roles in regulating cell cycle

kinetics and cell survival. Examples of these more general regulators include FoxG1 and FoxO family members. FoxG1 is important for determining ventral cell fate within the mouse telencephalon (Martynoga *et al*., 2005). FoxG1 is thought to be involved in regulating cell cycle kinetics in this region, ensuring that neural progenitor cells are produced in the correct numbers at the appropriate time. FoxO1, 3 and 4 have been shown to act cooperatively to regulate neural stem cell homeostasis in mammalian brains (Paik *et al*., 2009). In particular FoxO proteins negatively regulate cell cycle exit as well as regulating lineage-specific genes in committed neural progenitors that are required to control their proliferation. In *Drosophila* FoxO has been reported to promote neuroblast survival in the mushroom bodies, the centre for learning and memory in the fly brain (Seigrist *et al*., 2010).

FoxA1 and FoxA2 have been shown to regulate differentiation of midbrain dopaminergic (mDA) neurons (Ferri *et al*., 2007). In this study *Foxa1* and *Foxa2* single and double mouse mutants were used to show that FoxA1/2 play different roles at different stages of mDA neuron development. FoxA1/2 regulate specification of mDA progenitors via regulation of *Ngn2*, they then regulate *Nurr1* and *Engrailed 1* during early differentiation and markers of mature mDA neurons during late differentiation. Higher levels of FoxA1/2 are required to regulate the later differentiation stages than for regulation of cell fate specification.

Another example of a forkhead factor with a role in differentiation of specific neuron subsets is FOXP2. A point mutation in *FOXP2* has been identified in a family with a severe speech and language disorder (Lai *et al*., 2001). This disorder characterised by

inability to coordinate the movements required for speech rather than impaired memory or comprehension. In mouse and human brains FOXP2 is expressed in the developing cerebellum and motor cortex and is thought to regulate development of the neural circuitry required for these complex movements (MacDermot *et al*., 2005).

2.1.3.4 FoxJ1 regulates genes required for formation of motile cilia

One striking morphological feature of Ch neurons is the structure of the neuron dendrite. The outer dendritic segment is a modified cilium and ciliogenesis is therefore an important process in Ch neuron differentiation. It is therefore interesting that forkhead proteins have been linked to regulation of ciliogenesis in other species. In *C. elegans*, for example, the forkhead transcription factor FKH-2 is required for differentiation of ciliated AWB chemosensory neurons (Mukhopadhyay *et al*., 2007). Ch neuron cilia have been found to be motile and this ciliary motility is essential for Ch neuron function (Göpfert & Robert, 2003). FoxJ1 has been identified as a key regulator of motile cilia formation in *Xenopus*, zebrafish and mice (Stubbs *et al*., 2008;Yu *et al*., 2008; Jacquet *et al*., 2009).

In vertebrates motile cilia are predominantly required for fluid movement and are therefore found on cell types such as those lining of the airways of the lungs, oviducts and kidneys. In humans, defects in formation of motile cilia results in disorders such as primary ciliary dyskinesia (PCD). PCD is characterised by immotile cilia and sperm flagella, resulting in severely reduced ability to clear mucus from the lungs and male infertility. Rotary beating of motile cilia is also required for directional fluid flow over the developing embryonic node, which is required to

produce correct left-right asymmetry of internal organs. Individuals with PCD therefore also show defects in this left-right patterning. Similar patterning defects have also been observed in *FoxJ1* null mice (Brody *et al*., 2000) and node cilia required for left-right patterning in both *Xenopus* and zebrafish were found to be missing or severely shortened in FoxJ1 morphants (Stubbs *et al*., 2008).

Mutation of *foxj1a* in zebrafish also results in loss of motile cilia in other tissues such as pronephric ducts and ectopic expression of *foxj1a* is sufficient to allow development of motile-like cilia (Yu *et al*., 2008). In mice FoxJ1 is expressed in a range of cell types that have motile cilia (Lim *et al*., 1997; Hackett *et al*., 1999) and *foxj1* mutant mice show a severe depletion of motile cilia in a number of different tissues (Brody *et al*., 2000). In particular differentiation of ependymal cells in the mouse CNS, which require motile cilia for their function, has been shown to be dependent on FoxJ1 (Jacquet *et al*., 2009). FoxJ1 has been show to directly regulate expression of genes required for the structure and function of motile cilia. These include axonemal dyneins and *centrin2*, a gene that may be involved in basal body docking at the cell surface prior to ciliogenesis (Stubbs *et al*., 2008;Yu *et al*., 2008; Jacquet *et al*., 2009).

FoxJ1 is therefore a highly important regulator of motile cilia differentiation in vertebrates, however so far no equivalent gene has been identified in *Drosophila*. *FoxJ1* does not show any strong homology to *fd3F* and appears to be most closely related to *fd68A* (FoxK), *bin* and the *sloppy paired* genes (*slp1* and *slp2*) in *Drosophila* (Lee & Frasch, 2004). However none of these genes are expressed in

ciliated cell types. *fd68A* is expressed in the CNS only (Lee & Frasch, 2004), *bin* is required for mesoderm differentiation and salivary gland morphogenesis (Zaffran *et al*., 2001; Vining *et al*., 2005) and *slp1* and *slp2* are involved primarily in regulating segmental identity and heart formation (Grossniklaus *et al*., 1994; Park *et al*., 1996). These forkhead factors have therefore evolved completely different functions from FoxJ1. Sequence analysis therefore suggests that fd3F will have a different function in Ch neurons compared with FoxJ1, despite being expressed in cells with motile cilia.

2.2 Results

2.2.1 *fd3F* encodes a forkhead transcription factor with enriched expression in *ato*-expressing cells

fd3F is located at position 3F2 on the X chromosome (X: 3698218 – 3704546) and encodes a 360 amino acid protein. According to the current annotation (FlyBase update May 2011) the open reading frame spans four exons with exons 1 and 2 divided by a 5kb intron (figure 2.02A). The forkhead domain is located close to the N-terminus of the protein (encoded by exon1 and the start of exon2) however no other obvious functional domains have been identified elsewhere in the protein. The majority of the *fd3F* open reading frame (ORF) is conserved across many *Drosophila* species, however the most notable exception to this is the ATG start codon, which is actually poorly conserved (figure 2.02B). In at least three species (*D. yakuba*, *D. persimilis* and *D. mojavensis*) the region sharing homology with the upstream gene *CG32779* is included in the same ORF as the predicted *fd3F* orthologue. The function of *CG32779* in *D. melanogaster* is not known and it may be worth considering whether *CG32779* does form part of the *fd3F* ORF. This possibility will be discussed in detail in chapter 5.

In the *ato* and *cato* microarray data (Cachero *et al*., 2011) *fd3F* was highly ranked across all time points (table 2.2). The high ranking of *fd3F* at *ato* t1 combined with its relatively high enrichment in wild type *ato*-GFP compared with *ato*-GFP cells form *ato1*

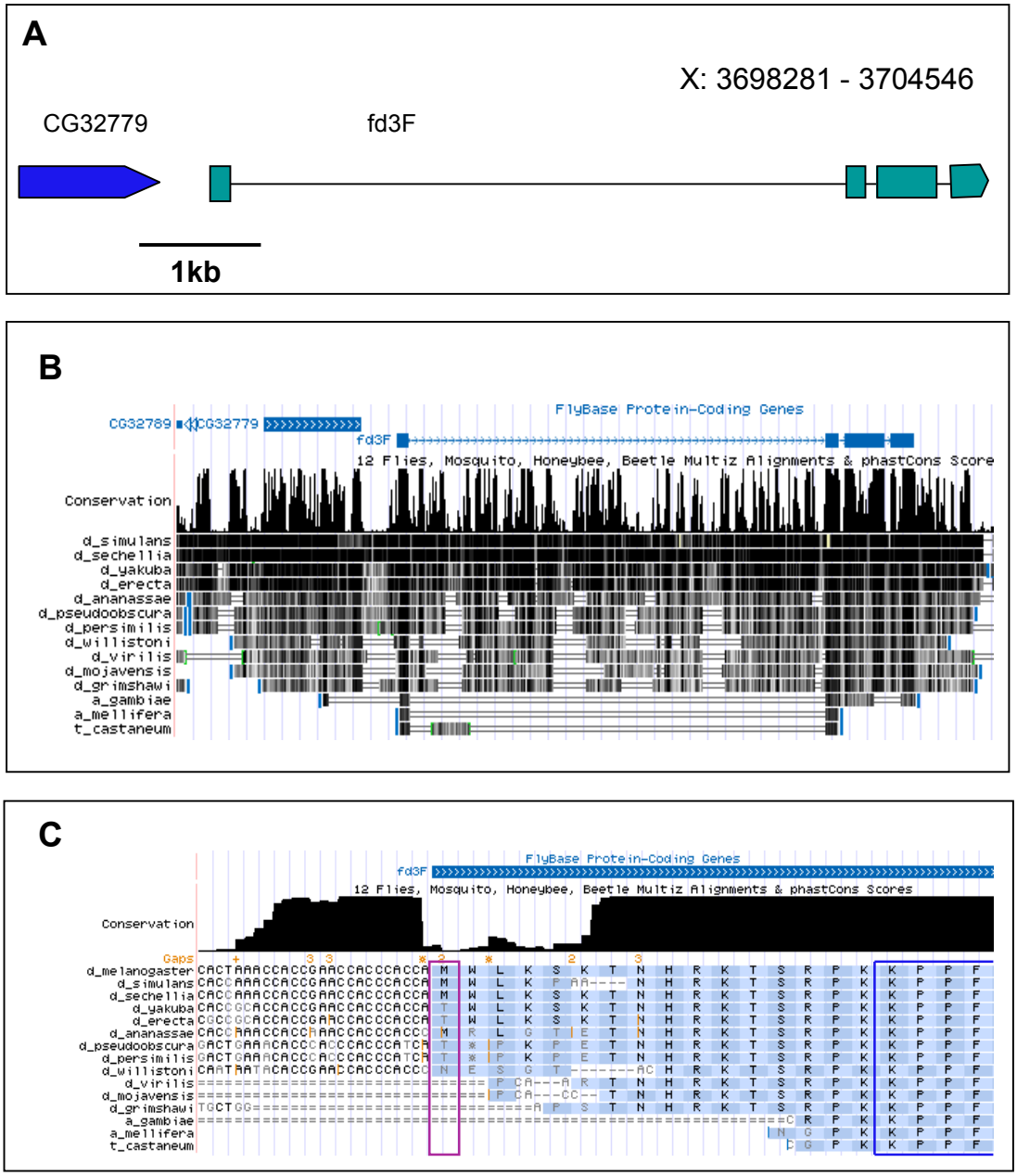

Figure 2.02: A) Map of the fd3F gene. B) Alignment of the fd3F gene region with homologous regions in 12 Drosophila species plus mosquito, honeybee and beetle species (UCSC Genome Browser). The fd3F exon sequences are highly conserved. C) Close up of the first predicted exon of fd3F showing the lack of conservation of the methionine start codon (magenta box). The blue box indicates the start of the forkhead domain.

mutant embryos (3-fold enrichment, ranked 44th) suggest that early *fd3F* expression coincides with *ato* expression and that *fd3F* could be directly regulated by *ato*. The increased enrichment of *fd3F* at *ato* t3 and *cato* t2 and t3 coincides with increased enrichment of genes expected to be required for Ch neuron structure and function. These include a number of genes with roles in ciliogenesis such as *nompB* (homologue of IFT-88), *CG15161* (IFT-46), *oseg6* and *beethoven* as well as genes required for ciliary motility (such as *Dhc62B* and *tilB*), cell adhesion (*Cad96Cb* and *nompA*) and ion channel regulation (*tipE*). It is therefore likely that fd3F is required to regulate expression of at least some of these genes.

Timepoint	Embryonic stage	Fold change	Rank
ato t1	10	5.55	24
ato t2	11	5.44	24
ato t3	12	19.7	3
cato t2	11-12	35.8	2
cato t3	12-13	27.0	3
cato t4	14-15	19.6	10
ato t1 vs *ato*^{1} mut	10	3.0	44

Table 2.2: Enrichment of *fd3F* in *ato* and *cato* expressing cells in microarray experiments. The fold change (ratio of expression in Ch cells versus the rest of the embryo) is shown for each time point along with the ranking of this fold change relative to that of other Ch-enriched genes at this time point. Embryonic developmental stages (as described by Campos-Ortega & Hartenstein, 1997) corresponding to each time point are shown. The fold change and rank of *fd3F* enrichment in wild type Ch cells at *ato* t1 versus *ato*^{1} mutant Ch cells at t1 is also shown.

2.2.2 *fd3F* expression pattern

2.2.2.1 *fd3F* is expressed throughout neurogenesis in *Drosophila* embryos

Due to the conflict between the in situ pattern observed by Lee and Frasch and the *ato* microarray data (Cachero *et al*., 2011) I have used RNA *in situ* hybridisation to characterise the expression pattern of *fd3F* (figure 2.03A-C). I have used a DIG-labelled RNA probe that hybridises to 1.1kb of the *fd3F* mRNA (from the start of exon 2 to the end of exon 4). *fd3F* is expressed in the embryo from late stage 10, about 5 hours after the start of embryogenesis. At this stage expression is restricted to one cell in each abdominal segment. This is likely to be the P cell, the precursor for the lch5 chordotonal organs and the earliest *ato*-expressing SOP (Ghysen & O'Kane, 1989; Jarman *et al*., 1993). Contrary to the observations of Lee and Frasch, there was no uniform *fd3F* expression observed before this stage. To confirm that *fd3F* expression overlaps with ato in the P cells I repeated the *in situ* and combined it with anti-atonal immunostaining (figure 2.03D). Atonal protein is expressed in a cluster of cells in each abdominal segment at stage 11 and its expression ceases by stage 12. The results show overlap between *fd3F* mRNA expression and atonal protein in one cell in each of these clusters (likely to be the P cell) in stage 11 embryos. This agrees with the *ato* microarray data and confirms that *fd3F* expression is early enough to coincide with *ato* expression.

By stage 12, about 7 hours into embryogenesis, *fd3F* is expressed in a small cluster of cells in each segment of the embryo that could correspond to later *ato*-expressing SOPs (figure 2.03B). In late stage embryos, *fd3F* expression appears to be specific to

chordotonal organs (as judged by the location of the expression, figure 2.03C) again supporting *fd3F* being a target of *ato*. However, no expression is seen in multidendritic neurons or their precursors and this contradicts results obtained previously by Parrish *et al.*, which suggested that *fd3F* knockdown by RNAi causes defects in multidendritic neuron morphology. This result from the Parrish study may therefore be an artefact of the RNAi screen.

Antibodies were raised in rabbits against a peptide from the C-terminal end of fd3F (NH_2-NLNYFGYNPGSDIVAC-COOH). This peptide was synthesised, covalently attached to a carrier protein and injected into two rabbits by CovalAb. Serum from one of these rabbits was found to be positive for anti-fd3F antibody by immunohistochemistry. RbAb-fd3F exclusively labels the nuclei of Ch cells in the embryo confirming that fd3F protein is expressed in the same Ch specific pattern seen with in situ hybridisation (figure 2.03E & F). fd3F protein is expressed in Ch SOPs from stage 11, although this expression is quite weak until after stage 13. To determine in which cells of the chordotonal organs *fd3F* is expressed I used RbAb-fd3F combined with MAb-22C10 antibody staining, which marks all PNS neurons in late stage embryos (figure 2.03F). In later stage embryos fd3F expression is restricted to the nuclei of Ch neurons. I therefore concluded that *fd3F* is specifically expressed in chordotonal neurons in stage 14 and later embryos.

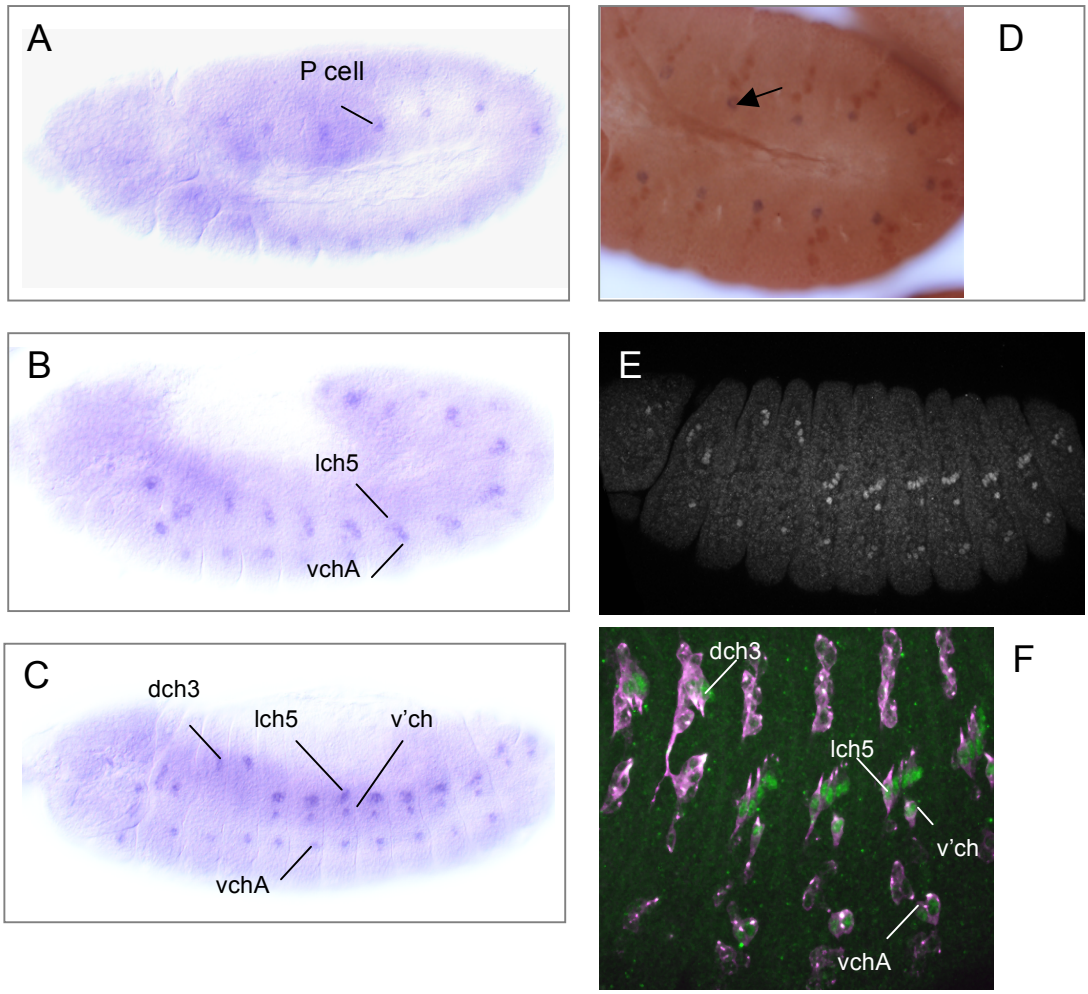

Figure 2.03: *fd3F* expression in *Drosophila* embryos. A- C RNA *in situ* in A) stage 11 embryo, expression is seen in one cell in each abdominal segment, B) Stage 12 embryo and C) stage 14 embryo at this stage expression is Ch-specific, in abdominal segments *fd3F* is expressed in the lateral chordotonal neurons (lch5 and v'ch) and the ventral chordotonal neurons (vchAB) and in thoracic segments t2 and t3 *fd3F* is expressed in vch and the dorsal chordotonal neurons (dch3). D) *fd3F* RNA *in situ* (blue) in stage 11 embryo co-stained with RbAb-ato (brown). Arrow indicates overlap of fd3F and ato expression in the P cell. E) RbAb-fd3F labels Ch neurons in late stage embryos. F) Late stage embryo labelled with RbAb-fd3F (green) Mab-22C10 (magenta) showing fd3F expression is specific to Ch neurons.

2.2.2.2 *fd3F* is expressed in Ch SOPs in larval imaginal discs

To compare the expression patterns of *ato* and *fd3F* during larval development stages I have used both RNA *in situ* hybridisation and immunostaining in imaginal discs from third instar larvae (figure 2.04). In the mesothoracic leg discs *fd3F* expression appears to match that of *ato*. *Ato* is expressed in the PNC and SOPs that specify precursors of the femoral chordotonal organ and in the femur-tibia joint (Jarman *et al*., 1993). *fd3F* staining appears in both these regions, however there are slight differences in the position of the staining which could be due to *fd3F* only being expressed in SOPs while *ato* is also expressed in the PNC. Once the femoral Ch SOP cells form they migrate away from the PNC at the epithelium, forming a stalk two cells wide. The stalk curls back on itself as the SOPs mature and the SOPs are therefore seen at a slightly different position and focal plane from the PNC (zur Lage & Jarman, 1999). *Ato* is expressed in the PNC and throughout the stalk while *fd3F* expression is restricted to the mature SOPs.

In eye-antennal discs *ato* is expressed in the morphogenetic furrow in the eye and the precursors and pro-neural cluster of the Johnston's organ (JO) in the antenna. Fd3F is expressed in the JO precursor cells in antennal discs, however this expression appears later than the ato expression and even in late third instar and pre-pupal discs fd3F appears in only a subset of JO cells (these may be the earliest ato-expressing SOPs) (figure 2.04H). This may mean that *fd3F* expression begins only at the end of larval development suggesting it may be required to switch on genes needed during the late stages of adult Ch neuron differentiation during morphogenesis.

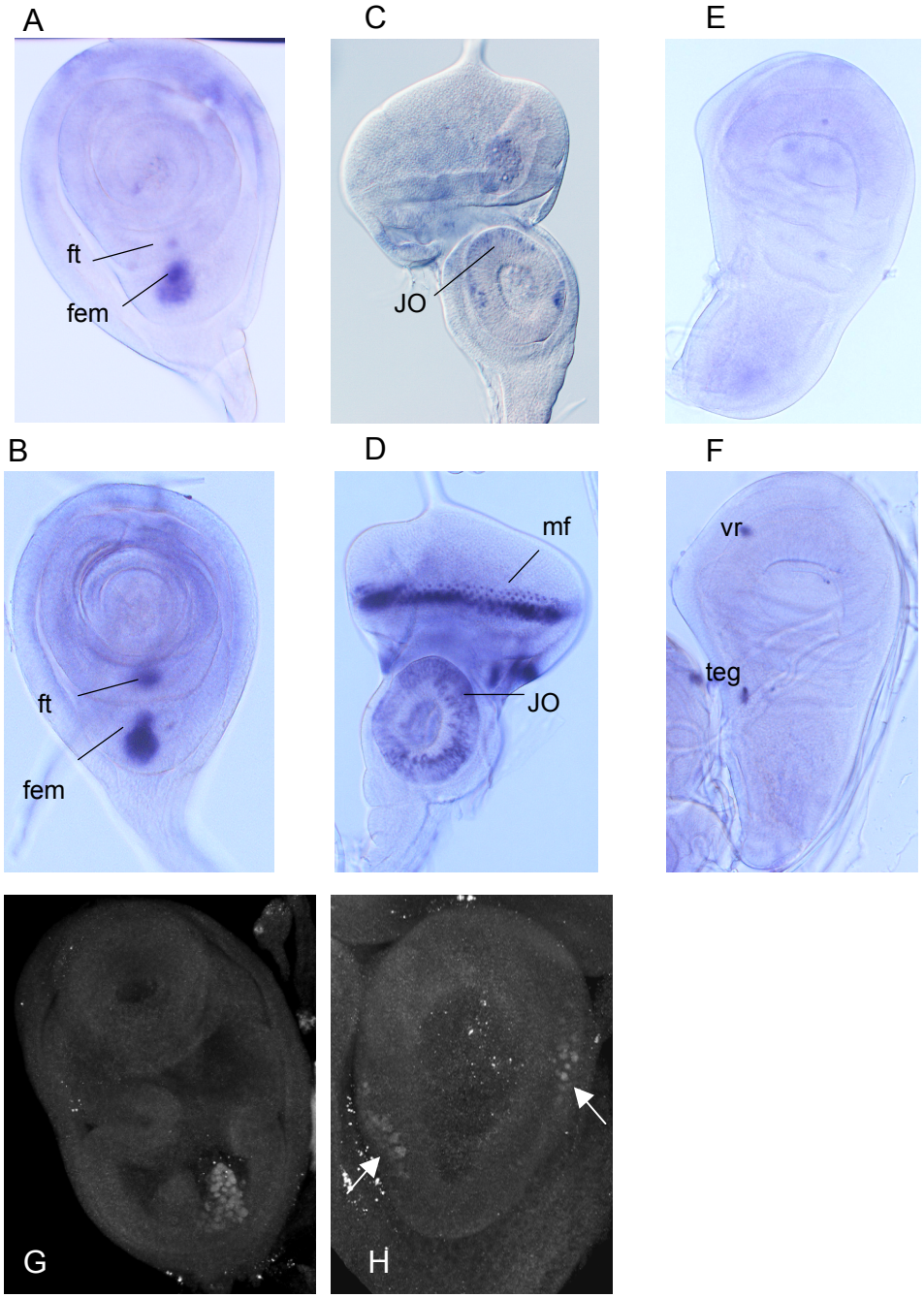

Figure 2.04: fd3F expression in imaginal discs. A-F RNA in situ, A, C &E show fd3F mRNA expression; ato expression is shown for comparison in B, D & E. A &B mesothoracic leg disc, C & D eye-antennal disc, E & F wing disc. Abbreviations are: fem (femoral Ch SOPs), ft (femor-tibia joint), mf (morphogenetic furrow), JO (Johnston's organ), vr (ventral radius), teg (tegula). G & H: RbAb-fd3F staining in leg (G) and eye-antennal discs (H). Arrows indicate JO SOPs in antenna.

In contrast to *ato* expression there is no *fd3F* expression seen in the eye disc. However this is consistent with the embryonic expression pattern since no expression is seen in the Bolwigs organ (larval eye). This suggests *fd3F* is specifically involved in the development of chordotonal organs and not in the *ato* directed development of R8 photoreceptors in the eye. If *fd3F* does turn out to be directly regulated by ato this raises the question of how *fd3F* expression is prevented in the developing eye disc.

In wing discs *ato* is expressed in precursors of the ventral radius chordotonal organs (VR) and the tegula. *fd3F* expression would be expected in the VR however I did not see any mRNA or protein expression in this region even in pre-pupal discs. This may be because, unlike *ato*, *fd3F* is only expressed in SOPs and not the whole PNC so it is difficult to see staining in a much smaller number of cells. It may also be that, as in JO SOPs, fd3F is not expressed until very late so it may not be possible to find expression at this stage. If this is the case it is perhaps not surprising that no staining was seen in the tegula since these SOPs develop later than the VR SOPs. Alternatively it is possible that fd3F is not required for wing Ch neuron development. If fd3F plays this role in other Ch cells this would mean that ato would have to direct Ch differentiation in the wing via a different regulatory pathway.

2.2.2.3 *ato*^{1} mutant embryos and larvae do not express *fd3F*

In *ato*^{1} mutant embryos and imaginal discs *fd3F* expression is completely abolished (figure 2.05). Since theses mutants lack *ato*-expressing SOPs this suggests that *fd3F* expression is restricted to *ato* dependent cell lineages. Although some P cells do form in *ato* mutants (Jarman *et al*., 1995) the fact that *fd3F* expression is lost despite

this strongly suggests that it could be a direct target of *ato*. Taken together the expression pattern data support the hypothesis that *fd3F* is a target of *ato* and that its function may be to regulate genes required specifically for chordotonal neuron development and differentiation.

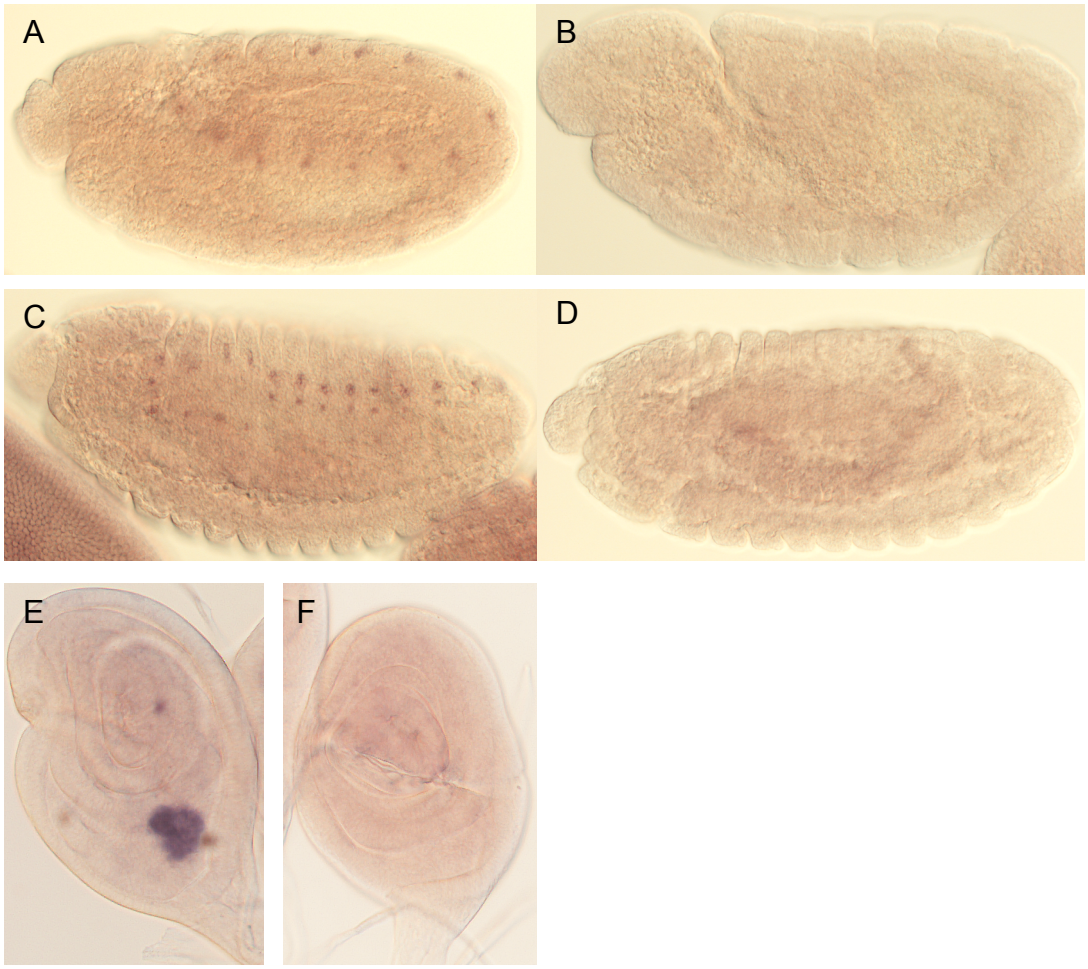

Figure 2.05: *fd3F* expression is absent in *ato1* mutant embryos. *fd3F* RNA *in situ* in *ato*^{1} mutant embryos (B & D) and wild type controls (A & C). A & B stage 11 embryos, C & D stage 15. *fd3F* mRNA is completely absent in *ato*^{1} mutant embryos. E & F *fd3F* RNA *in situ* in mesothoracic leg discs from wild type (E) and *ato*^{1} (F) third instar larvae showing *fd3F* expression is also missing in *ato*^{1} leg discs.

2.2.3 fd3F knockdown by RNAi

The most obvious way to study *fd3F* function is to examine the effect of an *fd3F* deficiency mutation on behaviour and Ch neuron differentiation. Chapter 3 describes the generation of this mutant by imprecise excision of a P element, however as this was quite a long process I used RNAi as a means of knocking down *fd3F* expression in the meantime. The results are described below, however, while this gave some indication of the type of phenotype expected to result from fd3F knockdown, the RNAi phenotype was subsequently found to be different from that observed in the loss-of-function mutant allele of *fd3F.* This suggests that many of the observed effects of the RNAi are probably due to off-target effects.

2.2.3.1 fd3F knockdown results in proprioception defects in adults and larvae

The phenotypes of two *fd3F* RNAi lines (37745 and 37746) from the Vienna *Drosophila* RNAi Centre were analysed. These lines contain a short fragment of the *fd3F* gene cloned as an inverted repeat under control of the UAS enhancer (Dietzl *et al*., 2007). These lines were crossed to several different Gal4 lines including *ato*-Gal4, which allows expression of the dsRNA specifically in *ato* expressing cells; *scabrous* (*sca)*-Gal4, which drives dsRNA expression in all SOPs in the PNS and *hairy*-Gal4, as *hairy* is a pair rule gene this allows more general expression in alternate segments of the embryo. RNA *in situ* hybridisation was used to check whether this knockdown was effective, however no reduction in *fd3F* transcript was observed. This may be due to the probe binding to the dsRNA. This seems likely

since *fd3F* transcript was detected in ES as well as Ch cells when the ds*fd3F* expression was driven by *sca*-Gal4.

The *sca*$^{109\text{-}68}$-Gal4/ CyO line was used to drive expression of ds*fd3F* during larval development in order to analyse the effect of *fd3F* knockdown on adult flies. RNAi knockdown at 25^{o}C resulted in a mildly uncoordinated phenotype for line 37746 and no obvious phenotype in line 37745. However when the flies were raised at 29^{o}C the RNAi knockdown in line 37746 was adult lethal, while ds*fd3F*(37745)/ *sca*$^{109\text{-}68}$-Gal4 flies displayed severe proprioception defects similar to those seen in *ato*^{1} mutants. These defects were not seen in ds*fd3f*/ CyO progeny or wild type controls. This suggests firstly that these phenotypes are due to expression of ds*fd3F* since RNAi phenotypes would be expected to become more severe at 29^{o}C as the UAS-Gal4 system is more efficient at this temperature than at 25^{o}C. Secondly, the RNAi knockdown is stronger in the 37746 line, however there may also be more off-target effects in this line particularly at 29^{o}C since Ch organ defects alone would not be expected to cause lethality (*ato*^{1} mutants are viable despite lacking Ch organs). ds*fd3F*(37745)/ *sca*$^{109\text{-}68}$-Gal4 flies had difficulty walking and righting themselves and were unable to fly, however unlike *ato*^{1} mutants the RNAi knockdown flies held their wings erect at all times. It seems unlikely that this effect is due to fd3F knockdown, particularly since no fd3F expression was observed in wing imaginal discs, and may therefore indicate some off-target effects of the RNAi knockdown.

I used a larval crawling assay to examine the effect of fd3F RNAi knockdown on larval proprioception. Individual larvae were allowed to crawl for two minutes on a

plain agarose plate and their paths were traced onto the lid. The lids were then photographed and the path lengths were measured using ImageJ. Both ds*fd3F*(37745)/ *sca*-gal4 and *sca*-gal4; ds*fd3F*(37746) larvae raised at 29^{o}C crawled significantly shorter distances than *sca*-Gal4/+ controls (by *t* test, p = 1.4 x 10^{-8} and p = 1 x 10^{-13} respectively). There was also a significant difference between the two RNAi lines (p = 0.008), which corresponds to the more severe adult phenotype seen in the 37746 line (figure 2.06). This suggests that *fd3F* knockdown results in coordination defects in larvae as well as adults.

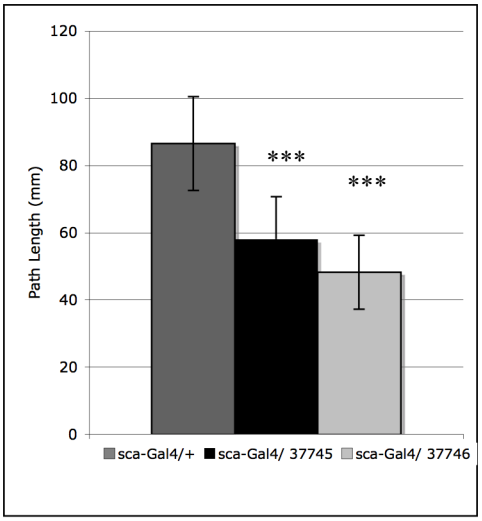

Figure 2.06: Larval Crawling Analysis
Mean path length (mm) crawled by individual larvae on plain agarose plate in 2min. sca-Gal4/+ n = 33, sca-Gal4/ dsfd3F(37745) n = 31, sca-Gal4; dsfd3F(37746) n = 34.
*** Highly significant (p< 0.001 by *t* test)
Error bars = standard deviation.

2.2.3.2 Effect of *fd3F* RNAi on Ch neuron morphology

Since *fd3F* expression is Ch-specific and the severe proprioception defects observed in adults and larvae are characteristic of Ch neuron defects, we would expect that *fd3F* knockdown would have some effect on Ch neuron morphology. Therefore ds*fd3F*/ *sca*-gal4 embryos were stained with MAb-22C10 and RbAb-HRP to look for any morphological defects in chordotonal neurons in these lines. 22C10 detects futsch, a microtubule binding protein expressed throughout the PNS in late stage embryos (Roos *et al*., 2000; Hummel *et al*., 2000). The horseradish peroxidase

(HRP) antibody was originally raised against a plant glycoprotein, however it has since been found to label both PNS and CNS neurons in *Drosophila* and it is thought to recognise a carbohydrate epitope on the cell membranes of these neurons (Katz *et al*., 1988).

Late stage embryos raised at 29^{o}C had a few missing Ch neurons and some of the remaining were slightly deformed (for example with elongated dendrites) (figure 2.07) although other Ch neurons formed normally. This phenotype was also observed when ds*fd3F* was expressed with *ato*-Gal4 and *hairy*-gal4 for both the 37745 and 37746 lines and occurred in about 30% of embryos. It is interesting that only some Ch neurons are affected and this partial phenotype could be due to incomplete knockdown of fd3F in these RNAi lines, in which case we would expect an *fd3F* mutant phenotype to be more severe. However it is also possible that these effects are caused by off-target effects of the RNAi. Interestingly in cases where a neuron was missing I often observed small cell fragments close to where the neuron should be located (figure 2.07G & H). Another possibility would therefore be that the neurons start to form as normal but then degenerate and the fragments could be the remains of the cell following apoptosis.

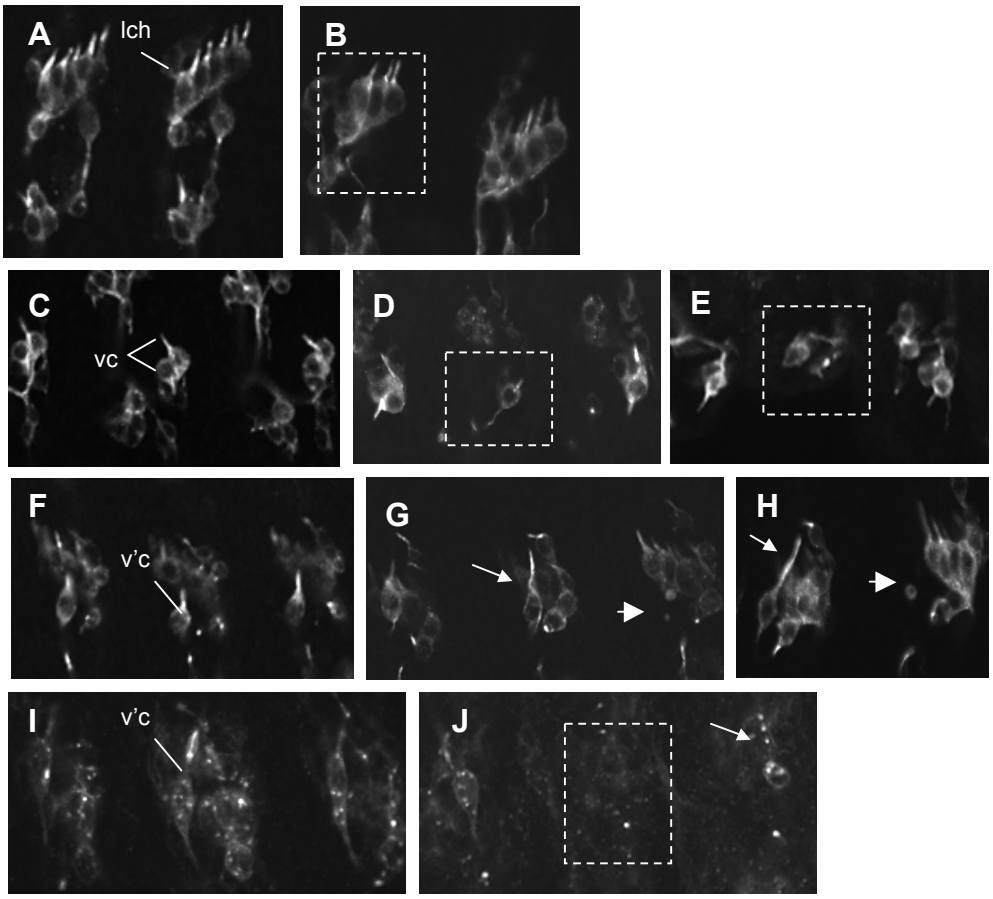

Figure 2.07: Effect of fd3F RNAi knockdown on Ch neuron morphology. A-H Late stage embryos stained with MAb-22C10. A & B show the lateral group of five Ch neurons (lch5) in two abdominal segments in wild type (A) and sca-Gal4/ UAS-dsfd3F(37745) (B). One lch cluster in B has only 3 Ch neurons (dashed box). C, D & E show the ventral pair of Ch neurons (vchA & vchB) in three abdominal segments in wild type (C), sca-Gal4/ UAS-dsfd3F(37745) (D) and ato-Gal4/ UAS-dsfd3F(37745) (E). vch neurons are missing in both D and E (dashed boxes). F, G and H show the lateral v'ch neurons in abdominal segments in wild type (F), sca-Gal4/ UAS-dsfd3F(37745) (G) and sca-Gal4; UAS-dsfd3F(37746) (H). In both G and H one v'ch neuron is missing, although cell fragments can be seen close to its expected position (arrow heads). The adjacent v'ch neurons have elongated dendrites (arrows). I & J v'ch neurons stained with RbAb-HRP in wild type (I) and sca-Gal4/ UAS-dsfd3F(37745) embryos (J). Again one v'ch neuron is missing (dashed box) and there appears to be blebbing of the adjacent neuron dendrite membrane (arrow).

The effect appears to be Ch-specific even when dsfd3F is expressed throughout the PNS since I did not observe any missing or deformed ES neurons. To check whether the phenotype was specific to the neuron rather than the whole Ch organ ds*fd3F*/ *sca*-Gal4 embryos were co-labelled with MAb-22C10 and RbAb-couch potato. Couch potato (Cpo) is an RNA-binding domain protein expressed in the nucleus of all PNS SOPs and their daughter cells (Bellen *et al*., 1992) RbAb-Cpo therefore labels both neurons and accessory cells in late embryos. In all cases where a Ch neuron was absent the corresponding accessory cells were still present (figure 2.08) suggesting that fd3F RNAi knockdown specifically affects Ch neurons.

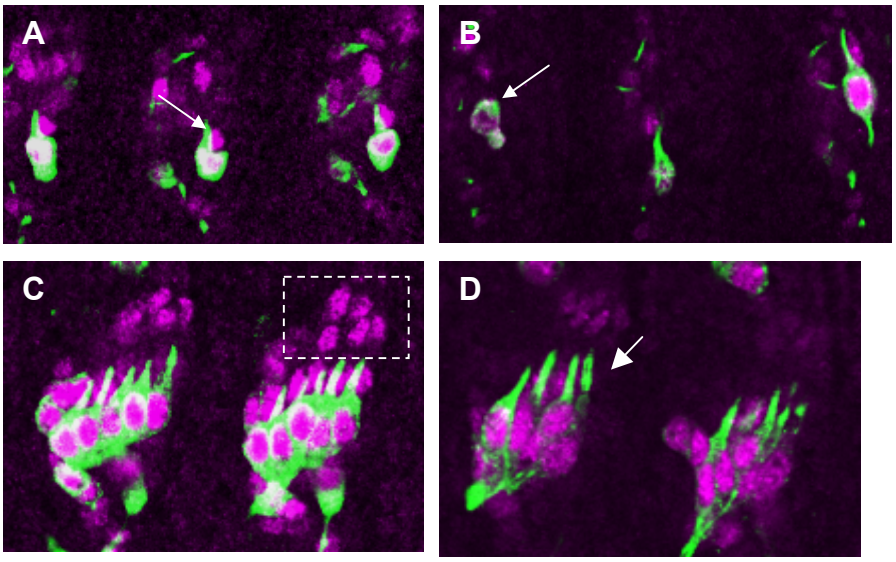

Figure 2.08: fd3F knockdown affects Ch neurons but not accessory cells. Late stage embryos stained with MAb-22C10 (green) and RbAb-cpo (magenta). A & B show v'ch neurons in three abdominal segments, RbAb-cpo stains the nucleus of the neuron and the scolopale cell (arrow) in each segment in wild type (A). In sca-Gal4/ UAS-dsfd3F(37745) (B) one v'ch neuron is missing, however the scolpale cell is still present (arrow). C & D show the lateral lch5 neurons in two abdominal segments. In each cluster in wild type embryos (C) RbAb-cpo labels the neurons, scolopale cells and cap cells (dashed box). In sca-Gal4; UAS-dsfd3F(37745) embryos (D) one lch5 neuron is missing (arrow), however all five cap cells can still be seen.

2.3 Discussion

2.3.1 *fd3F* expression is Ch-specific and ato-dependent although its regulation remains unclear

I have shown that *fd3F* expression is restricted to *ato*-dependent cell lineages in both embryos and larvae. The onset of *fd3F* expression coincides with ato expression in SOPs making fd3F a possible direct regulatory target of ato. A possible enhancer for *fd3F* has been identified within its 5kb intron (Petra zur Lage). A 1.5kb fragment of this intron allows GFP expression in Ch cells in embryos and Ch SOPs in imaginal discs in enhancer-GFP lines corresponding to the fd3F expression pattern (Cachero *et al*., 2011; Petra zur Lage, unpublished). This region contains three conserved *ato*-type E-boxes (Powell *et al*., 2004), however so far none of these sites have been found to be necessary for expression from this enhancer. One explanation for this would be that *fd3F* is not regulated by ato directly, however if this is the case then it is not clear how *fd3F* is regulated. There is no loss of *fd3F* expression in *Rfx* mutant embryos (Petra zur Lage, unpublished) meaning that Rfx cannot be a direct regulator of *fd3F* and so far no other Ch-specific transcription factors have been identified. The other possibility would be that ato regulates *fd3F* via other E-box sites within this region that may not conform to the *ato*-type consensus.

In embryos *fd3F* expression persists until long after *ato* expression has ceased, again it is not clear how this continued expression is regulated although the predicted enhancer region contains several conserved forkhead factor binding sites so this later expression may be due to self regulation. Alternatively the fd3F transcripts may be

stable enough to persist in Ch cells throughout neurogenesis without need for more transcript to be synthesised, although this seems unlikely since in the later stages fd3F expression is restricted to the neuron and not the accessory cells that arise from the same lineage. The fact that fd3F expression is maintained throughout neurogenesis makes it an ideal candidate to be regulating some of the later expressing Ch-specific genes.

Another interesting question regarding the regulation of *fd3F* is that although *fd3F* expression is *ato*-dependent it is not expressed in all *ato*-expressing cells. In addition to Ch SOPs ato is also expressed in the precursors of the R8 photoreceptors in the eye as well as a subset of olfactory neurons. However *fd3F* expression in both embryos and larval imaginal discs appears to be exclusive to Ch neurons and their precursors so if *fd3F* is a direct target of *ato* it would be interesting to determine how its expression is repressed in these other cell types. There may be cell-type-specific repressors expressed in these cells that either compete for the regulatory sites in the *fd3F* enhancer or bind to nearby sites and recruit co-repressors such as chromatin remodelling complexes and histone deacetylases or block co-activator binding. In vertebrates bHLH-orange (bHLH-O) proteins related to *Drosophila* Hairy and Enhancer of Split act as transcriptional repressors and compete with bHLH proteins for binding sites in the enhancers of target genes (Fisher & Caudy, 1998; Kageyama *et al*., 2000). It is possible that bHLH-O proteins function in a similar way in *Drosophila*, however bHLH-O proteins usually function as part of the notch pathway in vertebrates, leading to more general repression of differentiation i.e. all ato target genes would be affected by this type of repression, not just fd3F. Therefore it is more

likely that, if *fd3F* is directly regulated by ato, cell-type-specific repressors would bind to adjacent sites in the *fd3F* enhancer rather than competing for E-box sites. It is also unclear how and why *fd3F* expression is prevented in adult Ch SOPs in wing discs. Unless *fd3F* is not switched on until just before formation of the pupa (and therefore not detected by immunostaining in pre-pupal discs) the late differentiation genes of wing Ch neurons must be regulated by an alternative transcription factor.

2.3.2 Knockdown of fd3F affects Ch neuron function

The effects of *fd3F* knockdown by RNAi suggest that *fd3F* may have an important role in regulating Ch neuron differentiation. Knockdown in both larvae and adult flies results in coordination defects similar to those observed in ato^{1} mutants and some Ch neurons in late stage embryos appear to be missing or deformed. However the adult flies also showed defects such as constantly holding the wings erect that are not normally associated with defective Ch neurons. This suggests that there could be off-target effects of the RNAi and the phenotype may therefore be more severe than that of a true *fd3F* mutant. For this reason it is necessary to be cautious when interpreting the effect of *fd3F* knockdown on Ch neuron morphology.

The most striking effect of *fd3F* RNAi knockdown was the loss of some Ch neurons in late stage embryos. Often, although not always, I observed cell fragments in place of the missing neurons and it is possible that these are the remains of the neurons following apoptosis. If this is the case then *fd3F* may be required to regulate

expression of anti-apoptotic factors. Several forkhead genes are known to have roles in cell survival in other species. For example in mammals FoxO family members have been reported to regulate transcription of both pro- and anti-apoptotic genes under different conditions (Gilley *et al*., 2003; Nakamura *et al*., 2000). Under stressful conditions FoxO proteins up-regulate expression of antioxidant enzymes and the DNA repair gene *GADD45a* to protect against oxidative stress and promote cell survival (Kops *et al*., 2002; Tran *et al*., 2002).

It is unclear why only a few cells in each embryo are affected, although some of the elongated dendrites showed blebbing of the membrane around the dendrite when labelled with RbAb-HRP and this could be an early sign of apoptosis in these cells. These effects do at least appear to be Ch specific, there was no effect on ES cells even when ds*fd3F* expression was driven in all PNS neurons. The Ch accessory cells were still present even in cases where the neuron was missing, since these cells arise form the same cell lineage as the neuron this suggests that the defects and/ or cell death are due to a failure in neural differentiation rather than loss of Ch SOPs. However the labelling method used is not sufficient to show whether there are any morphological defects in the accessory cells.

Taken together with the expression pattern data, these results do seem to indicate that *fd3F* is necessary for differentiation of functional Ch neurons. However we cannot rule out the possibility that these defects are partly due to off-target effects of the RNAi and that fd3F knockdown may be causing a more subtle phenotype which, combined with the off-target effects, results in Ch neurons being more severely

affected. Therefore in order to determine precisely how fd3F regulates this process it is necessary to analyse an *fd3F* deficiency mutant and this will be the subject of the next chapter.

3

Generation and Characterisation of an *fd3F* Deficiency Mutant

3.1 Introduction

3.1.1 Differentiation of Ch neurons

Based on the expression pattern of fd3F and the effect of RNAi knockdown it seems likely that fd3F regulates genes required specifically for Ch neuron differentiation. Mutation of *fd3F* would therefore be expected to have an effect on Ch neuron morphology or physiology or both. This chapter will concentrate mainly on the morphological features of Ch neurons and how they are affected in *fd3F* mutants. There are two major features of Ch neurons that are unique to their subtype: firstly the position where the axons terminate and form synaptic connections with the CNS, and secondly the structure of the dendrite. Some of these features are described in detail in this introduction.

3.1.1.1 Ch neuron axon guidance during embryogenesis

During development the growing axons of different types of PNS neurons must terminate and branch at specific positions in order to form appropriate synaptic connections with CNS neurons. This is dependent on the neuron responding to specific guidance signals. In *Drosophila* different subsets of sensory neurons terminate at different dorso-ventral and medio-lateral positions in the region of the

ventral nerve cord (Merritt & Whitington, 1995). The position of these terminal axon branches is determined by the particular combination of receptors expressed in the axon growth cone and their response to signalling molecules expressed in the neuropile.

The dorso-ventral position is determined by the response of Plexin A and Plexin B receptors on the axons of sensory neurons to gradients of the repellent signalling molecules Semaphorin 1a (Sema 1a) and Semaphorin 2a (Sema 2a) (Zlatic *et al*., 2009). Motor neuron axons terminate in the most dorsal layer of the neuropile while Ch neuron axons terminate more ventrally and class IV multidendritic (md) neurons terminate in the most ventral layer (figure 3.01; Merritt & Whitington, 1995). Experiments by Zlatic *et al.* showed that different combinations of semaphorins are expressed in different dorso-ventral layers of the neuropile and that different neuron subtypes express different combinations of Plexin A and Plexin B in their axon growth cones. Plexin A responds to high levels of Sema 1a and excludes axons form the first (most dorsal) and third layers of the neuropile, while Plexin B responds to Sema 2a and therefore excludes axons from the central layers of the neuropile.

The medio-lateral positions of terminal axon branches are determined by a gradient of the midline repellent signal Slit, which is detected by guidance receptors of the Roundabout (Robo) family (Kidd *et al*., 1998). Ch neurons terminate their axons further from the midline than dorsal bipolar dendritic (dbd) or class IV md neurons (figure 3.01) (Merritt & Whitington, 1995). These different neurons subtypes express different Robo receptors that respond differently to the Slit signal and this dictates

the position of the axon terminals (Simpson *et al.*, 2000; Zlatic *et al.*, 2003). For example Robo3 is the Ch-specific Slit receptor and is required to terminate Ch axon growth at the correct medio-lateral position (Zlatic *et al.*, 2003). Expression of *robo3* is ato-dependent (Zlatic *et al.*, 2003) although it is not expressed until the very late stages of embryogenesis and therefore would be expected to be regulated by an *ato*-dependent intermediate transcription factor such as fd3F. One way in which fd3F could regulate Ch neuron differentiation might therefore be to control the medio-lateral position where the axons terminate through transcriptional regulation of *robo3*.

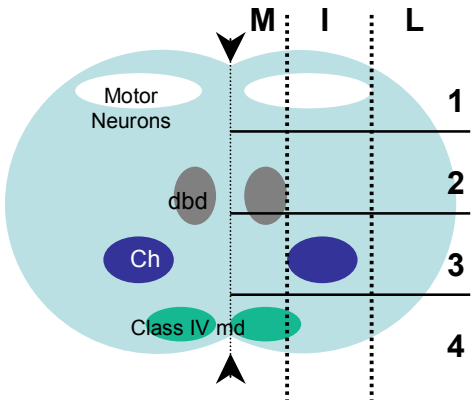

Figure 3.01: Different neuron classes project to different dorso-ventral and medio-lateral positions in the neuropile. Transverse section of an embryonic neuropile, dorsal at the top. dbd = dorsal bipolar dendritic neurons, Ch = chordotonal neurons, arrows indicate the midline. The approximate positions of the medio-lateral domains M (medial), I (intermediate) and L (lateral) and droso-ventral layers (1-4) are indicated. Adapted from Zlatic et al., 2009.

3.1.1.2 Structure of the Ch neuron dendrite

The outer segment of the Ch neuron dendrite is a modified cilium and Ch neurons are one of only three ciliated cell types in *Drosophila*, the other two being ES neurons and sperm. Mutations that result in loss or disruption of Ch neuron cilia cause severe coordination defects and loss of sound evoked potentials, implying that cilia are essential for Ch neuron function (Eberl *et al.*, 2000; Dubruille *et al.*, 2002;

Caldwell *et al*., 2003; Han *et al*., 2003). In *Drosophila* both sperm flagella and Ch neuron cilia are motile (Bressac *et al*., 1991; Göpfert & Robert, 2003), while ES neuron cilia are thought to be non-motile. Motility of Ch neuron cilia is known to be essential for their function (Göpfert & Robert, 2003) however Ch cilia have structural features that make them distinct from classic motile cilia. Firstly they lack a central microtubule pair present in the majority of motile cilia and secondly Ch cilia are divided into two compartments (proximal and distal) with only the proximal segment being motile. These two compartments are separated by the ciliary dilation, a paracrystalline inclusion that appears as an electron dense lattice in transmission electron microscopy (Eberl *et al*., 2000). Different subsets of ion channels localise to either the proximal or distal ciliary compartments (Kim *et al*., 2003; Gong *et al*., 2004; Lee *et al*., 2010) and the integrity of the ciliary dilation is essential for maintaining this segregation (Lee *et al*., 2008).

ES cilia are shorter than Ch cilia, they are not compartmentalised, lack the ciliary dilation and are non-motile. Understanding how ciliogenesis is regulated to produce functionally and structurally distinct cilia on Ch and ES neuron subtypes is therefore essential to understanding how these two neuron subtypes differentiate. If fd3F has a role in Ch-specific differentiation it seems reasonable to expect that some of the genes regulated by fd3F will encode structural or functional components of the Ch cilium or the machinery required for cilium assembly.

3.1.2 Functions and structure of cilia

Cilia and flagella are hair-like structures that protrude from the apical cell surface and perform a variety of functions in both unicellular and multicellular organisms. Cilia can be broadly classified into two categories, motile cilia and immotile (primary) cilia. The term 'flagella' is often used to describe long motile cilia on the surface of unicellular organisms and sperm although there is no strict structural distinction between cilia and flagella. Much of our understanding of ciliary structure and assembly comes from early work on the biflagellated green alga *Chlamydomanas* (Ringo, 1967; Johnson & Porter, 1968; McVittie 1972; Witman *et al*., 1978; Luck, 1984; Kozminski *et al*., 1993) although many of the proteins involved are highly conserved across all organisms with ciliated cells. In invertebrates such as *C. elegans*, *Drosophila* and other insects, cilia are found only on differentiated cells and are restricted to specific cell types such as sensory neurons and sperm. In contrast almost all vertebrate cell types are ciliated at some point during their life cycle.

3.1.2.1 Functions of vertebrate cilia and their association with human diseases

The main role of motile cilia in vertebrates is thought to be fluid movement. In particular fluid movement by motile cilia in the vertebrate embryonic node is widely accepted as the origin of left-right patterning in the developing embryo. Coordinated directional ciliary beating generates a leftward flow of extra-embryonic fluid over the node during gastrulation and this results in asymmetric signalling at the node through distribution of extracellular morphogens (McGrath *et al*., 2003; Tabin & Vogan,

2003). Cilia of the respiratory tract are required for clearance of mucus from the lungs, which is extremely important both for respiratory clearance and to prevent colonisation by pathogens (Satir & Sleigh, 1990). Motile cilia are also known to have a role in fluid movement in other tissues such as the kidney and oviduct. In zebrafish ciliary beat frequency has been found to increase in response to obstruction or injury of the kidney (Hellman *et al*., 2010). This is thought to be regulated by increased expression of *foxj1a* and consequently increased expression of tektins and axonemal dyneins required for motility. Similar adjustments in beat frequency have also been observed in the mouse oviduct and cilia of ependymal cells in the brain (Andrade *et al.*, 2005; O'Callaghan *et al*., 2008). These mechanosensory functions of motile cilia are thought to be dependent on the presence of transient receptor potential (TRP) Ca^{2+} ion channels, particularly TRPV4 and TRPP2 (Teilmann *et al*., 2005; Lorenzo *et al*., 2008). The fact that such an autoregulatory pathway exists to regulate ciliary beat frequency highlights the importance of motile cilia in fluid clearance.

Non-motile cilia have an important role in sensing extracellular signals such as morphogens, growth factors and hormones. Recent research has also established a role for vertebrate primary cilia and the ciliary assembly machinery in several developmental signalling pathways including canonical Wnt signalling (Corbit *et al*., 2008), non-canonical Wnt signalling such as the planar cell polarity pathway (Gerdes *et al*., 2007; Jonassen *et al*., 2008; Jones *et al*., 2008) and Hedgehog (Hh) signalling (Huangfu *et al*., 2003; Haycraft *et al*., 2005; Tran *et al*., 2008; Cortellino *et al*., 2009). In *Drosophila* these signalling pathways occur independently from cilium assembly due to the absence of primary cilia during *Drosophila* development.

Vertebrate cilia are also required for visual, auditory and olfactory senses. The light detecting outer segments of vertebrate photoreceptor cells are cilia and the cilia of mammalian olfactory sensory neurons are necessary for detecting odorants. In mammals sound is detected by hair cells of the inner ear. Auditory signal transduction in these hair cells involves coordinated bending of stereocilia on the cell surface. Although these stereocilia are not true cilia (they are composed of actin cytoskeletal fibres rather than tubulin) they depend on the presence of a single cilium, the kinocilium, on the cell surface during development. The kinocilium is thought to play an important role in defining the polarity of the stereocilia within the cochlea (the stereocilia bend towards where the kinocilium used to be) and is therefore important for differentiation of functional hair cells (Hudspeth & Corey, 1977).

Given the number of important functions of vertebrate cilia and their almost ubiquitous distribution it is not surprising that ciliary defects have been linked to a variety of different human diseases. These diseases are collectively known as ciliopathies and have a number of overlapping symptoms such as inversion of internal organs, retinal degeneration, kidney cysts and mental retardation. Many of these disorders are thought to be due to abnormal Hh and/ or Wnt signalling resulting from loss of cilia (reviewed in Logan *et al*., 2011). One of the best studied is polycystic kidney disease (PKD). In PKD ciliary defects in the renal epithelium lead to uncontrolled cell proliferation and kidney cyst formation (reviewed in Chapin & Caplan, 2010). Bardet-Biedl syndrome (BBS) is another disease affecting multiple

organs with symptoms including polydactyly, retinal degeneration, obesity, kidney disease and mental retardation (Katsanis, 2004). So far eight genes associated with BBS have been identified at eight different loci (Mykytyn *et al*., 2002; Ansley *et al*., 2003; Li *et al*., 2004) and all are thought to be required for formation of functional cilia. As mentioned in the previous chapter primary ciliary dyskinesia (PCD) is a condition associated with a lack of motile cilia. The clinical features of PCD are, unsurprisingly, due to effects on processes in which ciliary motility is essential. For instance, inability to clear mucus from the lungs, male infertility and also a reduction in female fertility due to loss of motile cilia in the oviduct.

3.1.2.2 Axonemal structures of motile and non-motile cilia

The core structure of the primary cilium is a ring of nine parallel microtubule doublets (called the axoneme) surrounded by the cytoplasmic membrane. The microtubule doublets themselves are polymers of α- and β-tubulin associated with tektins for added stability (Steffen & Linck, 1988). The majority of motile cilia have two extra microtubules at the centre of the axoneme, known as the central pair (figure 3.02A). The outer microtubule doublets contact this central pair via the radial spokes. The radial spokes are composed of a thin stalk connected to the outer microtubule doublets and a globular head that contacts the central pair. The interaction between the spoke heads and the central pair is transient and the spokes detach and re-attach as the axomene bends during ciliary beating (Warner & Satir, 1974). This configuration is often described as a '9+2' arrangement and is the configuration found in the common ciliated eukaryotic ancestor. The central pair is thought to have been lost in immotile (9+0) cilia. There are exceptions to this

however. Both *Drosophila* Ch neuron cilia and zebrafish ependymal cell cilia, for example, are motile despite having a 9+0 axonemal configuration (Göpfert & Robert 2003; Kramer-Zucker *et al*., 2005).

Another feature of motile cilia is the dynein arms. Dyneins are microtubule associated motor proteins that use ATP hydrolysis to drive movement towards the minus ends of microtubules (usually towards the cell body). Dyneins fall into only two main subclasses: axonemal dyneins required for ciliary beating and cytoplasmic dyneins that drive intracellular transport. The cytoplasmic dyneins will be discussed further in section 3.1.3 below. The dynein arms are complexes of axonemal dynein proteins composed of up to three heavy chains (HC) that contain the motor domain associated with several intermediate chains (IC), and light chains (LC). The HCs are related to the AAA+ ATPases (Neuwald *et al*., 1999) and each HC head has six ATPase domains that are conserved from algae to vertebrates. The HC stalks are composed of antiparallel coiled-coils with a globular domain for microtubule binding. Energy from nucleotide hydrolysis at the ATPase domains is converted to mechanical force at the stalk (Burgess *et al*., 2003).

The axonemal dyneins are attached to between the outer microtubule doublets in two distinct complexes; the outer dynein arms (ODAs) and inner dynein arms (IDAs). It is thought that ciliary motility is generated by movement of these dyneins along the microtubules allowing them to slide over each other (Summers & Gibbons, 1971). The doublet sliding is asynchronous with the progression of activity around the axoneme, resulting in a helical beat (Okada *et al*., 2005). The ODAs primarily

control beat frequency regulated by phosphorylation of a regulatory light chain (Christensen *et al*., 2001), while IDAs control the amplitude of the bend in each stroke (Habermacher & Sale, 1997). It is thought that about 60% of patients with PCD have genetic defects that result in loss of the ODAs (Noone *et al*., 2004).

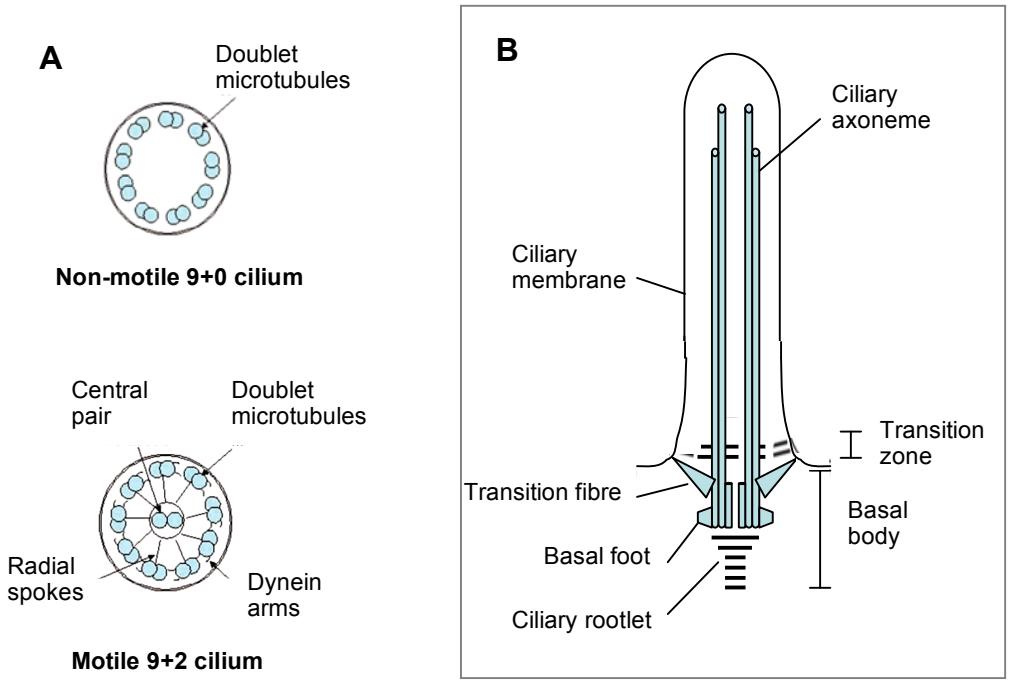

Figure 3.02: General structure of cilia.
A) The axonemal structures of 9+0 and motile 9+2 cilia (adapted from Hildebrandt & Zhou, 2007). B) Structures at the base of the cilium are required to anchor the axonemal microtubules to the membrane and provide a selective barrier separating the cilium from the rest of the cytoplasm.

In 9+2 motile cilia the radial spoke stalks may interact with a subset of IDA proteins (Piperno *et al*., 1992). Phosphoylation and dephosphorylation of radial spoke proteins by signalling kinases and phosphatases may affect this interaction and therefore allow the central apparatus to coordinate dynein activity on certain subsets of microtubules and so regulate the size and shape of the bend during ciliary beating

(reviewed in Omoto *et al*., 1999). It is thought that glutamylation of the microtubule tubulin may also modulate motility by altering dynein arm activity (Kubo *et al*., 2010; Suryavanshi *et al*., 2010).

3.1.2.3 Structures at the base of the cilium anchor the cilium and form a selective barrier

The axonemal microtubules of the cilium are anchored at the cell surface by the basal body. Following cell division each cell contains one newly formed daughter centriole and one older mother centriole that was used as a template for assembly of the daughter centrioles during the division. Basal bodies are derived from these mother centrioles (Piel *et al*., 2000). Centrioles and basal bodies are clusters of nine short triple microtubules arranged in a barrel structure. The outer-most microtubule of each triplet is shorter than the inner two, so the distal end of the centriole is formed by doublet microtubules (Paintrand *et al*., 1992; O'Toole *et al*., 2003). The mother centriole can be distinguished from the daughter at ultrastructural level due to the presence of fibrous distal and subdistal appendages (Paintrand *et al*., 1992). In particular the appendages of mother centrioles contain the protein Odf2, which is not found elsewhere in the cell (Ishikawa *et al*., 2005). Conversion of the mother centriole into a basal body requires formation of tight connections to the plasma membrane. The centriolar appendages are required for this initial attachment (Sorokin, 1968) and in Odf2 deficient mouse cell lines centrioles fail to dock with the plasma membrane and no primary cilia form (Ishikawa *et al*., 2005). Once the basal body has docked with the cell membrane three different structures form that are

thought to assist in anchoring the basal body to the plasma membrane: the ciliary rootlet, basal feet and transition fibres (figure 3.02B).

The proximal end of the basal body is connected to the cell interior by the ciliary rootlet. The main structural component of these rootlets is a coiled-coil protein called rootletin and it is possible that they may have a role in transport of some ciliary components due to the interaction between rooltetin and kinesin-1 (Yang & Li, 2005). However loss of ciliary rootlets does not affect cilium formation or motile ciliary beating and the primary function of the rootlet is therefore considered to be mechanical support of the cilium (Yang *et al*., 2005). This mechanical support is particularly important for very large cilia such as those of mammalian photoreceptor cells and motile cilia since these are subjected to greater mechanical strain; the former due to shear force and the latter due to ciliary beating.

The basal feet are modified centriolar appendages that project outwards from the proximal end of the basal body. These structures may be required to attach the base of the cilium to cytoplasmic microtubules since the ends of these microtubules have been shown to connect with the basal feet (Anderson, 1972). At the distal end of the basal body the transition fibres connect the triplet microtubule barrel to the cell membrane. In trypanosomes and some mammalian cells the base of the cilium forms within a deep cleft in the plasma membrane referred to as the ciliary pocket (Gadelha *et al*., 2009; Molla-Herman *et al*., 2010). In these cells the curved base of the ciliary pocket interacts with the transition fibres. These nine ‘fibres’ or alar sheets are sheet-like structures derived from the distal appendages of the mother centriole (Anderson,

1972). In addition to anchoring the basal body at the membrane, the transition fibres may also be involved in creating a selective barrier restricting movement of vesicles and macromolecules into the cilium. The centrosomal protein CEP164 localises specifically to the transition fibres and its depletion has been shown to disrupt cilium assembly (Graser *et al*., 2007). Transition fibres may therefore be essential for ciliogenesis as well as for basal body anchoring.

Although the ciliary membrane is continuous with the plasma membrane, the ciliary membrane has a distinct protein composition. For example specific ion channels may localise to the cilia of sensory neurons and the membranes of primary cilia contain receptors for extracellular signalling molecules. These proteins must be transported to the ciliary membrane after or during cilium assembly since there is no protein synthesis within the cilium and this requires the presence of a selectively permeable gate at the base of the cilium. In addition to the transition fibres this permeability barrier is also partly formed by another structure at the distal end of the basal body known as the ciliary necklace. This is composed of rows of Y-shaped structures that link the microtubules of the basal body to the ciliary membrane (Gilula & Satir, 1972). It is thought that the ciliary membrane in the necklace region may have a different lipid composition to both the plasma membrane and the rest of the ciliary membrane and can therefore act as a diffusion barrier between these membrane regions (Vieira *et al*., 2006).

The area just distal to the basal body, where the outer microtubule doublets begin to form, is known as the transition zone. The transition zone is thought to act as a

docking site for ciliary proteins and the motors that transport them into the cilium (Cole *et al*., 1998; Deane *et al*., 2001). The ciliary membrane is tightly associated with the axonemal microtubules in this region (Craige *et al*., 2010) and this may also contribute to the selectivity barrier by restricting access of soluble proteins into the cilium. It has been suggested that this selectivity barrier may function in a similar manner to the nuclear pore (Rosenbaum & Witman, 2002). It is possible that some of the transport machinery that moves proteins into the cilium may be able to selectively recognise cargo and then transfer this cargo through the barrier at the transition zone (Ishikawa & Marshall, 2011). However so far no consensus 'ciliary-localisation' sequence equivalent to the nuclear localisation signal has been identified.

3.1.3 Ciliogenesis

3.1.3.1 Intraflagellar transport (IFT)

After docking with the plasma membrane basal bodies nucleate growth of the axonemal microtubules. Since protein synthesis machinery is absent from the cilium, elongation of the axoneme requires import and transport of ciliary proteins from the cytoplasm to the ciliary tip. These proteins are carried towards the tip by a molecular motor driven process called interflagellar transport (IFT). Anterograde protein transport (from the cytoplasm to the ciliary tip) is facilitated by kinesin-2 motors and an associated protein complex, known as the IFT-B complex. The anterograde

machinery is recycled back to the cell body from the tip by retrograde dynein-2 motors in conjuction with another protein complex, the IFT-A complex (figure 3.03).

Like dyneins, proteins of the kinesin superfamily use energy from ATP hydrolysis to drive conformational changes that generate movement along microtubules (Hirokawa & Noda, 2008). It is currently thought that there are 15 kinesin families (termed kinesin-1 to kinesin-14B). These families can be divided into three groups according to the position of the motor domain within the protein described as N (amino-terminal motor domain), M (motor domain located at the middle of the protein) and C (carboxy-terminal motor).

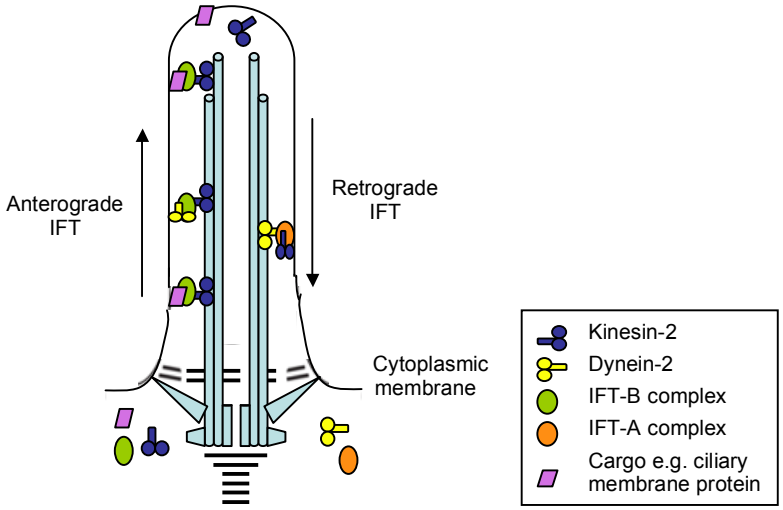

Figure 3.03: Intraflagellar transport. Cargo proteins are carried into the cilium by kinesin-2 and the IFT-B complex and these anterograde transport proteins are recycled back to the cell body by dynein-2 and the IFT-A complex.

In general N kinesins are associated with plus-end directed movement along microtubules and are therefore associated with anterograde transport of cargo away from the cell body. In particular, the N-type kinesin-2 family has been associated with anterograde IFT (Cole *et al*., 1998). In *C. elegans* the kinesin-2 motors KIF-3

and KIF-17 (OSM-3) have both been shown to be required for IFT and although they function partly redundantly only KIF-17 transports cargo to the distal segments of cilia (Ou *et al*., 2005). In mammals KIF17 also has a role in targeting specific nucleotide gated channels to olfactory neuron cilia (Jenkins *et al*., 2006). *Kif3a* and *Kif3b* knockout mice exhibit randomised left-right body determination and die before gestation is complete (Nonaka *et al*., 1998; Marszalek *et al*., 1999). These mice lack the cilia in the ventral node that are required for left-right patterning and these results therefore demonstrate an essential role for KIF3 motors in ciliogenesis.

As described above, dyneins are minus-end directed microtubule associated motor proteins and therefore usually move cargo towards the cell body. Two forms of cytoplasmic dynein have been identified. Cytoplasmic dynein 1 is found in all microtubule containing cells and has a variety of functions in intracellular transport and mitosis while cytoplamic dynein 2 (sometimes called dynein 1b) is exclusive to ciliated cells (Mikami *et al*., 2002). Dynein 2 localises exclusively to the lumen and base of cilia strongly implicating it as the motor for retrograde IFT.

In addition to heavy, intermediate and light chains (HCs ICs and LCs) cytoplasmic dyneins also have light intermediate chain subunits (LICs). LICs are unique to the cytoplasmic form of dynein and the LIC binding site on dynein HCs is well conserved (Habura *et al*., 1999; Mikami *et al*., 2002). The IC, LIC and LC subunits associate with the cargo binding end of the HCs and both LCs and LICs have been implicated in direct cargo binding (Purohit *et al*., 1999; Tai *et al*., 1999) while the ICs may act as scaffolding proteins linking the smaller subunits to the dynein

molecule (Vallee *et al*., 2003). Dynein 2 LIC proteins have been linked to retrograde IFT in both *Chlamydomonas* and *C. elegans*. Mutations in *Chlamydomonas D1bLic* and its *C. elegans* homologue *xbx-1* result in shortened cilia with bulges at the tips that accumulate other IFT proteins (Hou *et al*., 2004; Schafer *et al*., 2003) and such defects are characteristic of a failing of retrograde IFT. In addition to retrograde IFT dynein 2 may also have a role in transport of proteins across the connecting cilia of vertebrate sensory neurons such as those of the retina (Sokolov *et al*., 2002).

The IFT-B and IFT-A complexes bind protein cargo through various protein interaction domains. In vertebrates the IFT-B complex is composed of 14 proteins while the IFT-A complex only contains six known proteins (table 3.1). Most of these proteins are well conserved across all ciliated organisms (Cole 2003; Avidor-Reiss *et al*., 2004). Loss of IFT-B complex proteins results in severely shortened or absent cilia, this is similar to the phenotype of kinesin-2 mutations and suggests that the IFT-B complex is essential for cilium assembly (Pazour *et al*., 2000; Haycraft *et al*., 2003; Follit *et al*., 2006). In contrast, mutations in IFT-A proteins has a much less severe effect on the length of the cilium suggesting IFT-A is not as critical for assembly of the cilium. However IFT-A mutations result in cilia with swollen tips that contain accumulated IFT-B proteins, similar to the effect of dynein 2 mutations, confirming the role of the IFT-A complex in retrograde IFT (Tsao & Gorovsky, 2008; Lee *et al*., 2008; Iomini *et al*., 2009).

	Chlamydomonas reinhardtii	*Caenorhabditis elegans*	*Drosophila melanogaster*	*Homo sapiens*
IFT-A complex	IFT144	DYF-2	Oseg6	WDR19
	IFT140	CHE-11	Oseg3/ RempA	IFT140
	IFT139	ZK328.7	-	THM1/ TTC221B
	IFT122/ FAP80	DAF-10	Oseg1	IFT122/ WDR10
	IFT121	IFTA-1	Oseg4	WDR35
	IFT43	-	CG5780	IFT43/ C14orf179
IFT-B complex	IFT172	OSM-1	Oseg2	IFT172
	IFT88	OSM-5	nompB	IFT88
	IFT81	IFT-81	-	IFT81
	IFT80	CHE-2	Oseg5	IFT80/ WDR56
	IFT74/ IFT72	IFT-74	-	IFT74/ IFT72
	IFT70/ FAP259	DYF-1	CG5142	TTC30A/ TTC30B
	IFT57	CHE-13	IFT57/ CG8853	IFT57
	IFT54/ FAP116	DYF-11	CG3259	IFT54/ TRAF3IP1
	IFT52/ BLD1	OSM-6	IFT52/ CG9595	IFT52/ NGD5
	IFT46	DYF-6	CG15161	IFT46/ C11orf60
	IFT27	-	-	IFT27/ RABL4
	IFT25/ FAP232	-	-	IFT25/ HSPB11
	IFT22/ FAP9	IFTA-2	-	RABL5
	IFT20	Y110A7A.20	IFT20/ CG30441	IFT20
IFT-A accessory complex	TLP1	TUB-1	king tubby	TULP3
IFT-B accessory complex	FAP22	DYF-3	CG17599	CLUAP-1
	DYF13	DYF-13	CG4525	TTC26

Table 3.1: *Chlamydomonas* IFT complex proteins and their orthologues in *C. elegans*, *D. melanogaster* and human. Adapted from Ishikawa & Marshall, 2011 and Avidor-Reiss et al., 2004.

In addition to the IFT-A and B components other proteins are thought to associate with IFT complexes. For example in *C. elegans* DYF-3 and DYF-13 associate with the IFT-B complex and may help it to dock onto kinesin-2 (OSM-3), activating the kinesin-2 motor (Ou *et al*., 2005). Vertebrate tubby-like protein 3 (TULP3) interacts

with IFT-A and may help to localise certain G-protein coupled receptors to the cilium (Mukhopadhyay *et al*., 2010). Some of the protein products of genes implicated in Bardet-Biedl syndrome (referred to as BBS proteins) may also act as IFT accessory proteins. Mutations of *bbs-7* and *bbs-8* in *C. elegans* result in shortened or structurally abnormal cilia with defective chemosensory function (Blacque *et al*., 2004). This suggests BBS proteins may have a role in aiding IFT either by direct interaction with IFT proteins or assisting formation of IFT-motor complexes at the transition zone. *Bbs*-knockout mice are still able to form cilia, however cell type specific membrane proteins fail to localise to the primary cilia (Mykytyn *et al*., 2004; Berbari *et al*., 2008). Similar results have been seen in *C. elegans* (Tan *et al*., 2007). It is therefore possible that BBS proteins also have a role in membrane protein trafficking.

The IFT-B proteins IFT20 and IFT57 have also been implicated in membrane protein trafficking from the Golgi to the cilia. Membrane proteins targeted to the cilia are transported in Golgi derived secretory vesicles and deposited near the base of the cilium. From here they are transferred to the ciliary membrane by IFT (reviewed in Baldari & Rosenbaum, 2010). IFT20 localises to the Golgi as well as the cilia and basal bodies and knockdown of IFT20 has been shown to reduce the amount of the PKD2 calcium ion channel in cilia (Follit *et al*., 2006). IFT57 has recently been shown to interact directly with IFT20 in addition to the endocytosis regulator RAB8 (Omori *et al*., 2008). Since RAB8 has also been implicated in cilium formation and binds directly to basal body components (Yoshimura *et al*., 2007), IFT57 and IFT20 may provide a link between membrane vesicle formation at the Golgi and

incorporation of these vesicles into the ciliary membrane. Several IFT and BBS proteins have structural similarity to scaffold proteins that promote the formation of transport vesicles such as coat protein 1 (COP1) and clathrin. It is therefore possible that these IFT and BBS proteins also carry out similar functions during vesicle trafficking into the cilium (Jin *et al*., 2010).

3.1.3.2 regulation of ciliary length

Cilium assembly at the tip continues even after the cilium has reached its full length (Stephens, 1997) and this is balanced by continuous removal of tubulin subunits from the tip. Ciliary length is highly important for cilium function, particularly for motile cilia since there will be an optimal length that is suitable for producing the appropriate velocity of ciliary beating and fluid flow. The optimal ciliary length will be specific to particular ciliary subtypes. The rates of assembly and disassembly of cilia must therefore be equal to each other in order to maintain ciliary length. It is still not known how this balance is regulated although ciliary length mutations have been identified in *Chlamydomonas* and two of these genes have been found to encode kinases, however their functional targets and possible roles in length control are not clear (reviewed in Wemmer & Marshall, 2007; Ishikawa & Marshall, 2011).

3.1.3.3 Regulation of ciliogenesis

Assembly and disassembly of vertebrate primary cilia are closely linked to the cell cycle. Cilia usually form during G0 or G1 and are removed prior to mitosis. Initiation of ciliogenesis requires conversion of the mother centriole to a basal body. This conversion requires removal of the centrosomal protein CP110 from the mother

centriole. It is not clear how this removal is regulated, however since CP110 is known to be a target of S-phase cyclin dependent kinase it is possible that phosphorylation of CP110 causes it to dissociate from the mother centriole (Chen *et al*., 2002). To re-enter the cell cycle the primary cilium basal body must be converted back to a centriole and relocate to the interior of the cell for formation of the mitotic spindle. This requires disassembly of the cilium. Cilium disassembly may be initiated by a centrosomal kinase, Aurora A. Aurora A is an activator of cyclin-dependent kinase 1- cyclin B and regulates entry into mitosis and deficiency or inhibition of Aurora A has been shown to prevent disassembly of cilia (Pugacheva *et al*., 2007). The mechanism by which Aurora A initiates cilium disassembly is not clear. It has been suggested that Aurora A activates histone deacetylase 6 and this enzyme then deacetylates axonemal microtubules leading to destabilisation of the cilium (Pugacheva *et al*., 2007). However tubulin acetylation is not thought to be a major requirement for microtubule stability (Palazzo *et al*., 2003).

The transcriptional regulation of all the different genes required for ciliogenesis is only beginning to be understood. Expression of the homeobox gene *Noto* is thought to be crucial for formation of vertebrate nodal cilia (Abdelkhalek *et al*., 2004). Noto acts downstream of Foxa2 and T and mice lacking Noto have a reduced number of short, disorganised cilia in the caudal notochord (Beckers *et al*., 2007). The transcription factors Rfx3 and FoxJ1 have both been shown to be essential for ciliogenesis in vertebrates (Bonnafe *et al*., 2004; Brody *et al*., 2000). Daf-19, the *C. elegans* orthologue of Rfx3 has also been shown to regulate expression of many ciliary genes (Efimenko *et al*., 2005) and *Drosophila* Rfx is required for formation of

sensory neuron cilia (Dubruille *et al*., 2002). As discussed in the previous chapter FoxJ1 has been shown to be particularly important for regulating genes required for assembly of motile cilia, although it is not essential for formation of primary cilia (Stubbs *et al*., 2008; Yu *et al*., 2008; Jacquet *et al*., 2009). Recently FoxJ1 and Rfx3 have been shown to share several common regulatory target genes (Thomas *et al*., 2010) and may therefore act cooperatively to regulate assembly of motile cilia. This will be discussed in more detail in the next chapter. Expression of both Rfx3 and FoxJ1 is either strongly reduced or completely abolished in *Noto* mutant mice suggesting that Noto may be an upstream regulator of both transcription factors in vertebrates (Beckers *et al*., 2007).

It is possible that fd3F may be a transcriptional regulator of either Ch cilium assembly or other aspects of Ch neuron morphology. The next section of this chapter therefore describes the generation of an fd3F deletion mutant and the effect of this mutation on adult and larval proprioceptive behaviour and Ch neuron morphology.

3.2 Results

3.2.1 Generation and characterisation of the deficiency mutation *fd3F*^{1}

3.2.1.1 Generation of the *fd3F*^{1} mutation by imprecise P element excision

To determine the function of *fd3F* in Ch neuron differentiation I investigated the effect of fd3F deficiency on this process. Since there is no transposable element insertion available within the *fd3F* coding region I generated an *fd3F* mutant by mobilising a P element in the fly stock P{EP}fd3F^{EP1198} (Berkley *Drosophila* Genome Project, Spradling *et al*., 1999) inserted about 1kb downstream of *fd3F* to create imprecise excisions. The P element can be mobilised by crossing the P element line to flies expressing the Δ2-3 transposase linked to a visible marker (*drop eye* (*Dr*) in this case). This results in excision of the P element. *DrΔ2-3* male offspring from this cross were then crossed to virgin females carrying the X chromosome balancer FM6 which has the dominant marker *Bar* (*FM6ywB*). Flies in which the P element excision has occurred successfully can be identified in the offspring from this cross as females with white eyes, heterozygous for *FM6ywB* and no longer carrying *DrΔ2-3* (to prevent any further hopping of the P element) (figure 3.04).

In most cases this will result in the P element excising correctly leaving the rest of the DNA untouched, however in approximately 10% of cases excision of the P element will also remove some of the flanking DNA sequence. These deletions were detected using single fly PCR. Primer sets that amplify fragments of 700bp, 1.5kb and 2kb from wild type DNA were designed to detect deletions of different sizes.

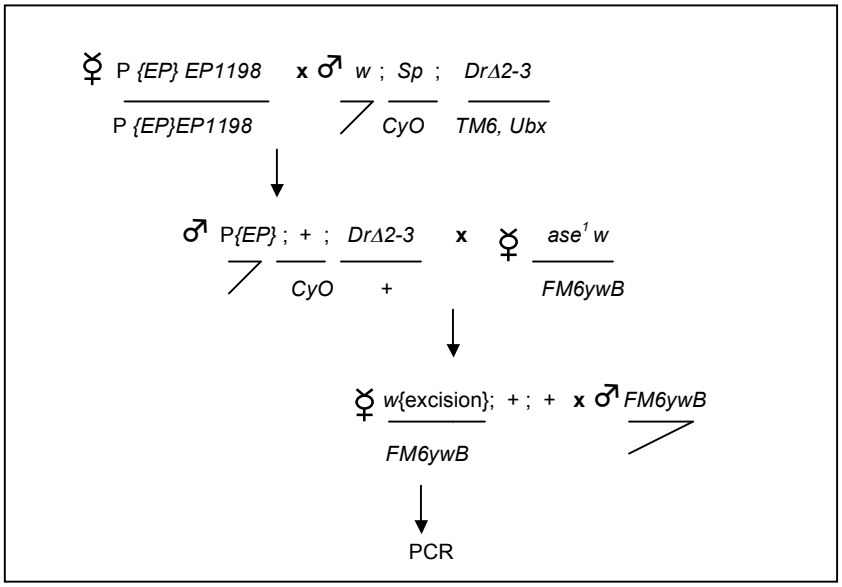

Figure 3.04: Fly crosses set up for P element excision. The *w*[excision]/ *FM6ywB* virgin females collected were crossed individually to *FM6ywB* males and allowed to lay eggs for about 5 days. The females were then collected and screened for deletions using single fly PCR.

Each *w*[excision]/ *FM6ywB* virgin female collected was crossed individually to an *FM6ywB* male (figure 3.04) and allowed to lay eggs for about 5 days at 25^{o}C. The female was then collected and screened for deletions using PCR. Since these flies are heterozygous for the deletion the wild type sized band should be amplified in all cases along with any smaller fragments amplified due to the excision. Due to the difficulty in detecting the 2kb fragment from single fly DNA preparations I extracted genomic DNA from groups of five flies and screened for any deletions in each group by PCR. In groups where a deletion was identified I repeated the PCR using single fly preparations from female progeny of each fly in the group to identify the line containing the deletion.

A total of 231 lines were screened and 12 lines were identified with deletions including one line with a deletion of 1.4 kb. This is sufficient to remove approximately 400bp from the 3' end of the fd3F ORF, which corresponds to most of exon 4 (figure 3.05). This deletion mutation will be named *fd3F*^{1} hereafter.

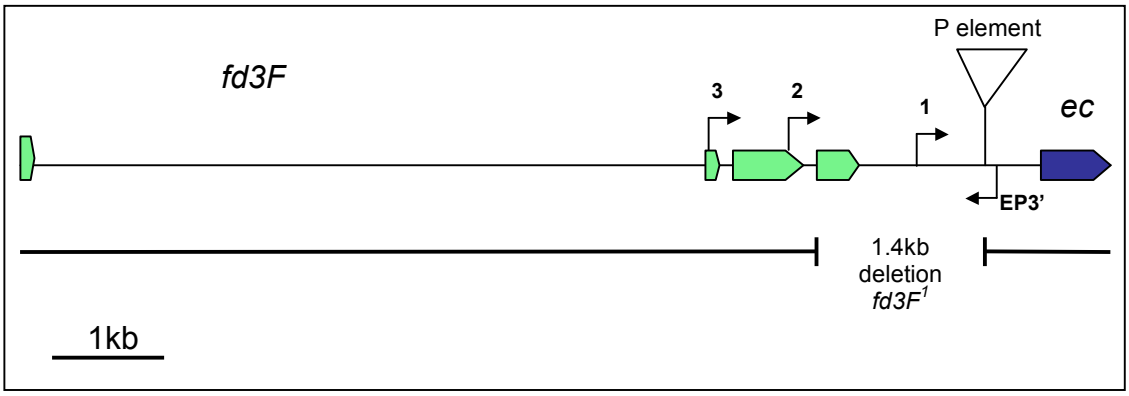

Figure 3.05: Map of *fd3F* showing the position of the P element P{EP}fd3F^{EP1198} in the region between *fd3F* and the adjacent gene *echinus* (*ec*) and the position of the 1.4kb deletion generated in the *fd3F*^{1} line. The approximate positions of the 3' primer (EP3') and the 5' primers used to amplify the 500bp, 1.5kb and 2kb fragments (1, 2 and 3 respectively) are shown.

3.2.1.2 Fertility of *fd3F*^{1} mutant flies

fd3F^{1} homozygotes are viable and fertile. However if *fd3F* is required to regulate the later stages of Ch neuron differentiation it may have a role in regulating ciliogenesis and it is therefore important to consider the possibility that fd3F is also required during spermatogenesis since *Drosophila* sperm are also ciliated. If this is true we would expect some reduction in *fd3F*^{1} male fertility.

To test for any reduction in fertility in *fd3F*^{1} flies young (2-4 day old) *fd3F*^{1} and P{EP}fd3F^{EP1198} males and females were crossed individually to OregonR flies and allowed to lay for 4 days at 25^{o}C, flies were then tipped to new vials and left to lay

for a further 4 days and the progeny in each vial were counted. Flies that are slow to mate between days 1-4 should still produce the same number of progeny as the controls between days 5-8 if there is no reduction in fertility. This should make it possible to distinguish between reduced fertility and any impaired ability to mate due to neurological defects. The results are shown in table 3.2. There was no significant difference in the mean number of progeny produced by either *fd3F* males (Day 1-4 p = 0.07, Day 5-8 p = 0.06) or females (Day 1-4 p = 0.14, Day 5-8 p = 0.41) compared with the number of progeny produced by P{EP}fd3F^{EP1198} males and females crossed to OregonR. This suggests that *fd3F* is not required for male fertility and is therefore unlikely to be involved in spermatogenesis.

	♂		♀	
	P{EP}	*fd3F^{1}*	*P{EP}*	*fd3F^{1}*
Days 1-4	54.8	43.8	36.4	25.6
Days 5-8	68.2	51.3	48.5	54.7

Table 3.2: Mean number of progeny produced by P{EP}fd3F^{EP1198} and *fd3F^{1}* males and females mated with Oregon R flies over 8 days. n= 10 (number of individual crosses) in each case. There is no significant difference between the number of progeny produced by *fd3F^{1}* males or females compared with P{EP} flies (p> 0.05 by *t* test).

3.2.1.3 *fd3F^{1}* mutants show severely reduced *fd3F* mRNA and protein expression

The P element line P{EP}fd3F^{EP1198} was found to have strong fd3F mRNA expression by *in situ* hybridisation (figure 3.06A). In contrast, *fd3F* mRNA expression is very strongly reduced in *fd3F^{1}* mutant embryos and no protein is detected with RbAb-fd3F (fig 3.06B-G). This suggests that the *fd3F* transcripts may be unstable due to loss of the 3' end, however it does not confirm whether *fd3F^{1}*

mutants are protein null or expressing low levels of truncated protein since the antibody used was raised against the C-terminal end of fd3F.

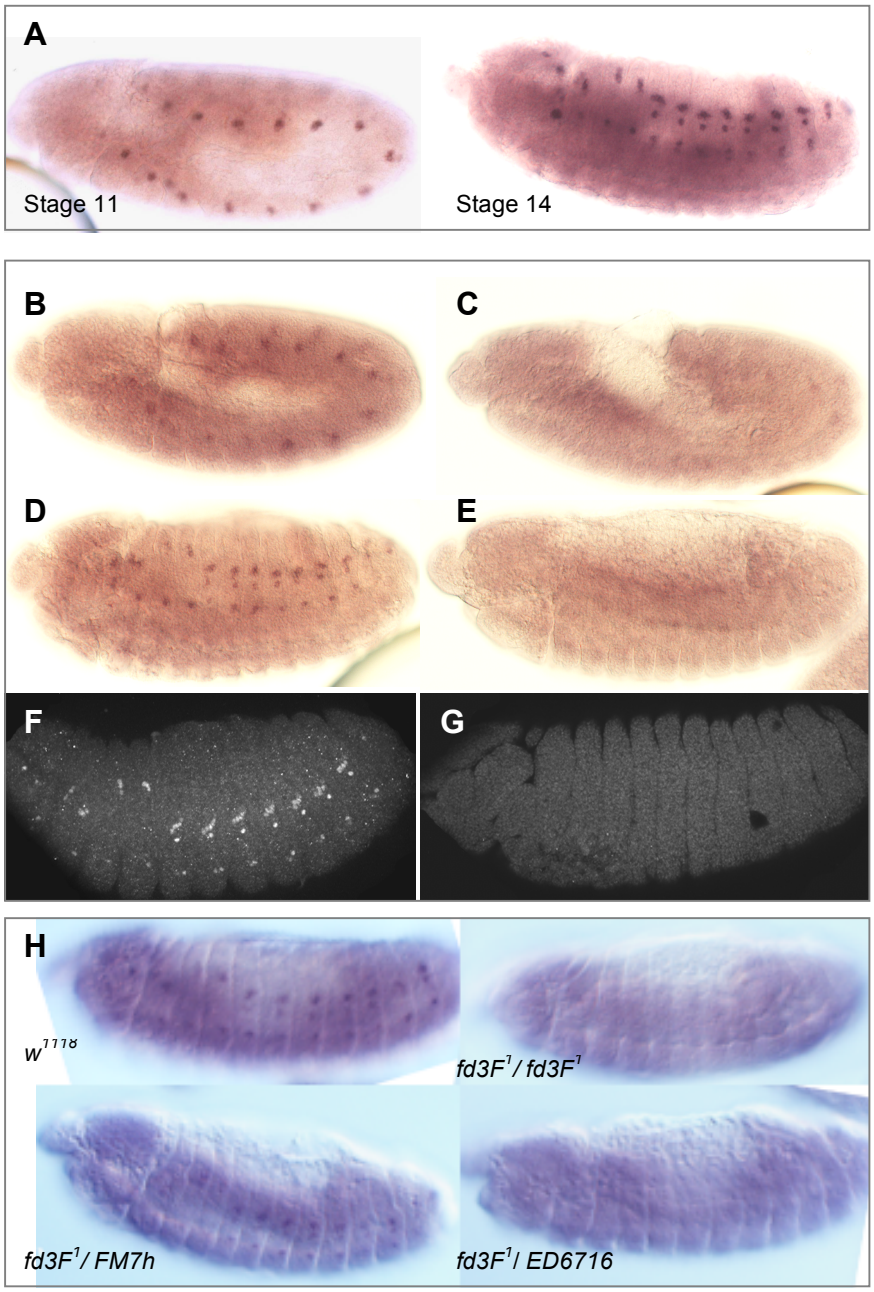

Figure 3.06: *fd3F* expression is lost in *fd3F*^{1} embryos. A) *fd3F* mRNA is expressed at normal levels in the original P element line EP1198. B) - E) *fd3F* mRNA expression in embryos (B & C stage 11, D & E stage 14) *fd3F* expression is strongly reduced in *fd3F*^{1} embryos (C & E) compared with WT (B & D). F & G late stage embryos stained with RbAb-fd3F, F) WT and G) *fd3F*^{1}. H) *fd3F* mRNA is expressed in heterozygotes (*fd3F*^{1}/ *FM7h*) at equal level to WT while expression is almost completely absent in *fd3F*^{1}/ *ED6716* embryos. *w*^{1118} used as WT in all cases.

For this reason I also crossed the *fd3F*^{1} line to the chromosomal deficiency line *Df(1)ED6716* (DrosDel Project, Ryder *et al*., 2004), which deletes a large region of chromosome 1 (from 3F2 to 4B3) including *fd3F*. *fd3F*^{1} males were crossed to *ED6716*/ *FM7h* virgin females in a cage, the embryos were collected and *fd3F* mRNA was detected by *in situ* hybridisation. As expected approximately 50% of the embryos showed almost no staining (predicted to be *fd3F*^{1}/ *ED6716* or hemizygous *ED6716* males), although there was no obvious difference in the expression level in *fd3F*^{1}/ *ED6716* embryos compared with *fd3F*^{1} homozygotes (figure 3.06H). This means that there is still some *fd3F* transcript present in *fd3F*^{1}/ *ED6716* embryos and it is possible that a truncated protein could be expressed. However if there is some active truncated protein produced *fd3F*^{1}/ *ED6716* flies would be expected to exhibit a more severe phenotype than *fd3F*^{1}/ *fd3F*^{1} flies (due to loss of one copy of the truncated fd3F). If on the other hand *fd3F*^{1}/ *ED6716* and *fd3F*^{1}/ *fd3F*^{1} flies exhibit the same phenotype this would mean that the *fd3F*^{1} allele is a genetic null.

3.2.1.4 *fd3F*^{1} adults and larvae exhibit severe proprioception defects

fd3F^{1} adult flies are slow moving and have difficulty walking, climbing and righting themselves after falling. Such poor coordination is characteristic of Ch neuron defects and is similar to the phenotype observed in *ato*^{1} mutants (Jarman *et al*., 1995). Consequently *fd3F*^{1} flies performed very badly in a climbing assay compared with *w*^{1118} controls. In this assay groups of 20-30 flies were placed in a measuring cylinder and banged once on the bench. I compared the percentage of flies climbing more than 10cm within 1min of banging the cylinder: for *w*^{1118} flies this is close to 100%, while in *fd3F*^{1} mutants this drops to about 7% which is similar to the result

obtained with *ato*^{1} flies (figure 3.07A). This experiment was repeated to compare the performance of heterozygous *fd3F*^{1}/ *FM6ywB* flies with w^{1118}, the original P{EP} line and *fd3F*^{1} homozygotes (figure 3.07B). In this experiment the number of flies passing the 10cm threshold within 15s were counted to enable any subtle differences between the heterozygotes and the P{EP} line to be distinguished. There was no significant difference between *fd3F*^{1}/ *FM6ywB* and P{EP}fd3F^{EP1198} flies (p = 0.38) although both are significantly different from *fd3F*^{1} ($p = 1.8 \times 10^{-6}$ and $p = 4.3 \times 10^{-8}$ respectively) suggesting that the *fd3F*^{1} phenotype is recessive and a single wild type copy of *fd3F* is sufficient to rescue the uncoordination.

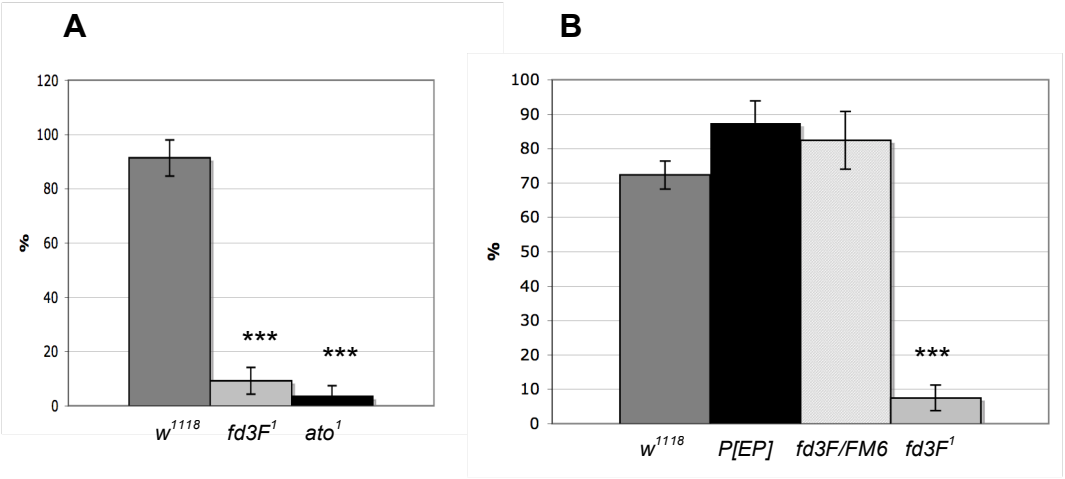

Figure 3.07: Climbing Assays. A) Mean % of flies climbing above 10cm within 1min of banging n=20 in each case (5 groups of flies banged 4 times each). B) Mean % of flies climbing above 10cm within 15s of banging n=6 (6 groups of flies banged once) in each case.
Error bars = standard deviation in all cases. *** Highly significant (p< 0.001 by *t* test).

It is important to confirm that the phenotypic defects caused by this deletion are due to loss of fd3F and not to loss of expression the adjacent gene *echinus* (*ec*). Deletions affecting the *ec* ORF should not have been detected by the PCR screen since the 3'

primer used binds very close to the 3' end of the P element, however the *fd3F*^{1} deletion may remove or disrupt sequences in the regulatory region of *ec*. To ensure that this is not the cause of the *fd3F*^{1} phenotype I have crossed *fd3F*^{1} flies to *ec*^{1} mutant flies. *fd3F*^{1}/ *ec*^{1} adults do not show any of the coordination defects seen in *fd3F*^{1} homozygotes. This was confirmed by repeating the climbing assay. On this occasion however, the flies were banged in a measuring cylinder divided into four 5cm bins and the number of flies in each bin were counted 15s after banging. This should allow more subtle differences in phenotype to be detected. The number of *fd3F*^{1}/ *ec*^{1} flies in each bin was compared to the ratio of flies in each bin observed with either *fd3F*^{1}/ *FM6ywB* or *fd3F*^{1}/ *fd3F*^{1} flies using a Chi-squared test (figure 3.08).

Figure 3.08: Climbing Assay 2.

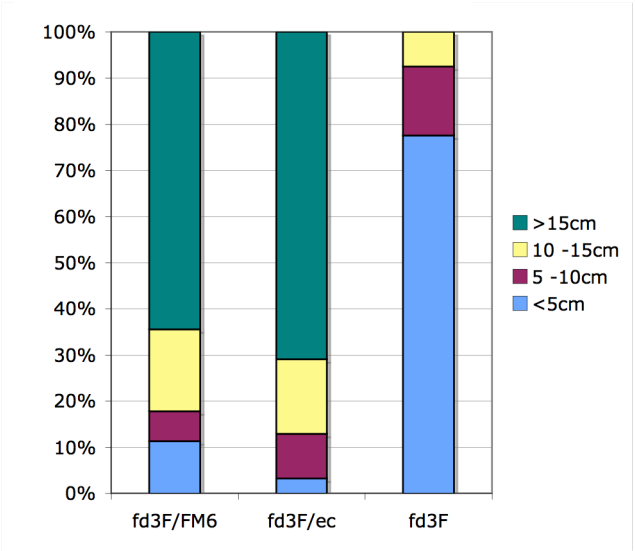

% of flies in each of four 5cm bins 15s after banging. *fd3F*^{1}/ *FM6* and *fd3F*^{1}/ *ec*^{1} n= 62, *fd3F*^{1}/ *fd3F*^{1} n=40 (total number of flies tested).

X^2 test used to compare number of *fd3F*^{1}/ *ec*^{1} flies in each bin to the ratio of distribution of *fd3F*^{1}/ *FM6* and *fd3F*^{1}/ *fd3F*^{1} across the 4 bins.
ΣX^2 *fd3F*^{1}/ *ec*^{1} vs *fd3F*^{1}/ *FM6* = 5.06 (not significant, p> 0.05)
ΣX^2 *fd3F*^{1}/ *ec*^{1}vs *fd3F*^{1}/ *fd3F*^{1} = 569 (highly significant, p< 0.001).

There was a highly significant difference (p< 0.001) between the distributions of *fd3F*^{1}/ *ec*^{1} and *fd3F*^{1}/ *fd3F*^{1} across the four bins, however there was no significant difference between the distributions of *fd3F*^{1}/ *ec*^{1} and *fd3F*^{1}/ *FM6ywB*. Therefore

fd3F^{1} complements *ec*^{1} suggesting that the *fd3F*^{1} phenotype is caused specifically by loss of *fd3F* expression.

To determine whether there was any loss of coordination in *fd3F*^{1} larvae I carried out a crawling assay. Individual larvae were allowed to crawl for 2min on a plain agarose plate and their path lengths were measured using ImageJ software as described for RNAi knockdown larvae in Chapter 2. There is a significant reduction in the path lengths of *fd3F*^{1} and *ato*^{1} larvae compared to w^{1118} controls ($p = 1 \times 10^{-6}$ and $p = 5.7 \times 10^{-6}$ respectively). Although there is quite a lot of individual variation between larvae the *fd3F*^{1} mutants crawl on average half as far as w^{1118} larvae (figure 3.09). This is perhaps unexpected since previous work has shown that perturbing the function of Ch neurons has no effect on the regularity of larval peristaltic contractions or crawling speed (Hughes & Thomas, 2007). There is, however, also a striking difference between the shapes of the tracks of *fd3F*^{1} and w^{1118} larvae. *fd3F*^{1} larvae change direction much more frequently while w^{1118} are able to crawl much further in a straight line (figure 3.09B). There was also a small significant difference observed between *fd3F*^{1} and *ato*^{1} larvae ($p = 0.032$). This may be due to a single neuron of the lch5 cluster still being present in some *ato*^{1} mutant larvae (Jarman *et al.*, 1995) while in *fd3F*^{1} larvae all Ch neurons are impaired resulting in a slightly more severe crawling phenotype in *fd3F*^{1} larvae. However *ato*^{1} larvae crawled in a similarly shaped trail to *fd3F*^{1}.

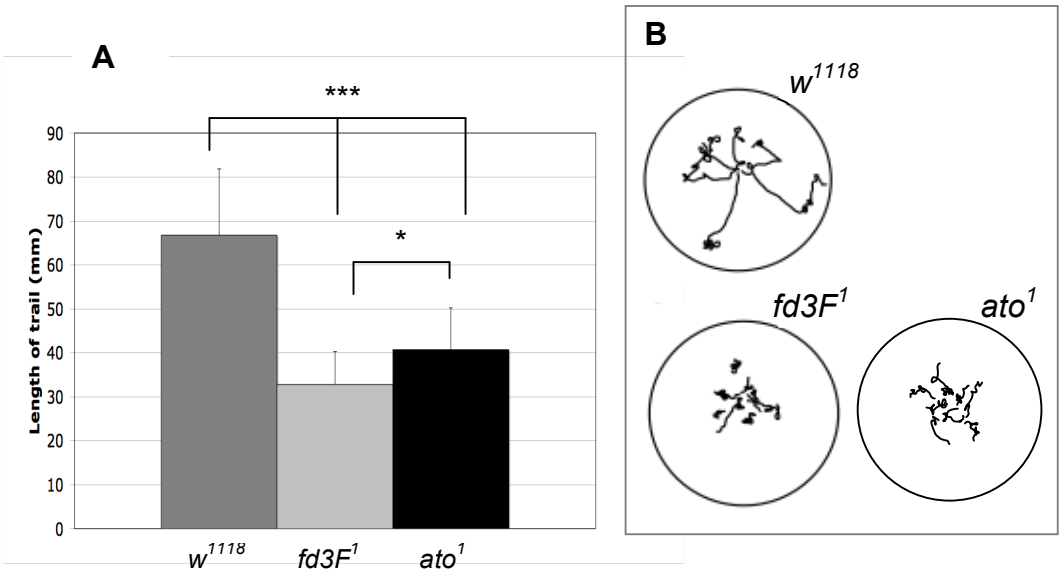

Figure 3.09: Larval crawling analysis. A) Mean length crawled (mm) in 2min by *w*^{1118}, *fd3F*^{1} and *ato*^{1} wandering 3rd instar larvae (n= 23, n= 22 and n= 20 respectively). Error bars = standard deviation. *** highly significant (P< 0.001), * significant (P< 0.05). B) Shape of paths crawled by *w*^{1118}, *fd3F*^{1} (tracks from 6 larvae each) and *ato*^{1} (tracks from 7 larvae).

Taken together these results suggest that *fd3F*^{1} and *ato*^{1} have similar defects in proprioception and the *fd3F*^{1} phenotype is therefore likely to be due to defects in Ch neuron differentiation.

3.2.2 *fd3F*^{1} Ch neuron morphology

3.2.2.1 *fd3F*^{1} Ch neurons do not show gross morphological defects

It is likely that the severe coordination defects observed in *fd3F*^{1} larvae and adults are caused by loss of Ch neuron function. In *ato*^{1} mutants the Ch SOPs fail to form resulting in an absence of Ch neurons (Jarman et al., 1995). Knockdown of *fd3F* by RNAi discussed in the previous chapter also resulted in partial loss of Ch neurons in

embryos. To find out whether there was any loss or morphological defects of Ch neurons in *fd3F*^{1} mutants both embryos and 3rd instar larval pelts were stained with MAb-22C10 and RbAb-HRP. 22C10 is a pan-sensory marker that labels all PNS neurons (but not cilia) in late stage embryos and larvae. RbAb-HRP labels all neurons and cilia in late stage embryos, however in larvae staining in the cilium is no longer seen and instead two strong bands of staining are observed around the basal body and just below the ciliary dilation. In contrast to the RNAi knockdown there were no missing Ch neurons in *fd3F*^{1} embryos suggesting that this aspect of the RNAi phenotype may be due to other off-target effects rather than *fd3F* knockdown.

fd3F^{1} larval Ch neurons also showed no obvious morphological defects (figure 3.10) although there may be some very subtle defects; the inner dendritic segments appear thinner in *fd3F*^{1} Ch neurons and when stained with RbAb-HRP the bands of staining near the basal body and ciliary dilation are more diffuse compared to staining in wild type larvae. This is very similar the RbAb-HRP staining in *fd3F*^{1} embryos, where the ciliary dilation is much less clearly defined than in wild type (figure 3.10A &B). The larval defects were not observed in *fd3F*^{1}/ *FM7-GFP* heterozygotes, which do not show any proprioception defects (figure 3.10E). Ch neurons in *fd3F*^{1} /*ED6716* larvae appear very similar to *fd3F*^{1} Ch neurons (figure 3.10F) suggesting that *fd3F*^{1} is very close to being a genetic null.

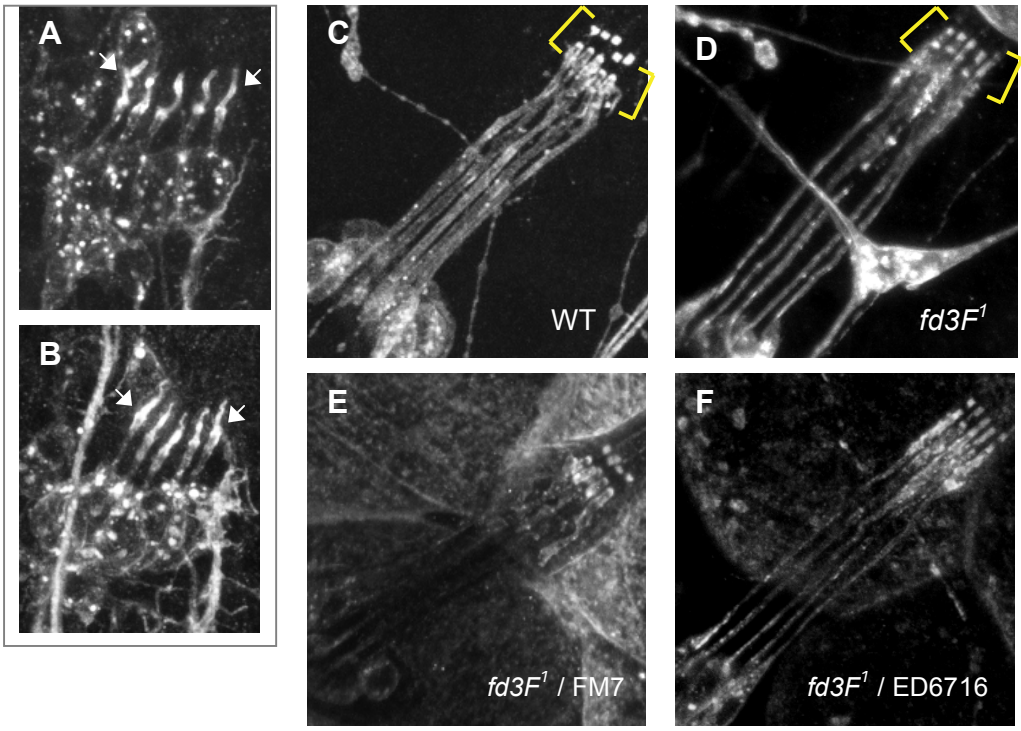

Figure 3.10: Ch neurons in *fd3F*^{1} mutants show only minor morphological defects. A) & B) Lch5 neurons in late stage embryos labelled with RbAb-HRP, staining around the ciliary dilation (arrows) is more diffuse in *fd3F*^{1} embryos (B). C) - F) Lch5 Ch neurons from 3rd instar larval pelts stained with RbAb-HRP. Staining in the lumenal band below the ciliary dilation is more diffuse in *fd3F*^{1} larval Ch neurons (D) (brackets), however staining in *fd3F*^{1}/ *FM7-GFP* heterozygotes (E) appears to be the same as wild type. The Ch neurons of *fd3F*^{1}/ *ED6716* larvae (F) are not substantially more disrupted than *fd3F*^{1} homozygotes.

A *UAS-mCD8-GFP* reporter construct was used to analyse the morphology of adult leg and wing Ch neurons. CD8 is a membrane-associated glycoprotein and, when driven by *elav*-Gal4, mCD8-GFP labels the cell membranes of all PNS neurons including the ciliated dendrites of Ch neurons. As with embryonic and larval Ch neurons there was no obvious difference between Wt and either *fd3F*^{1} or *fd3F*^{1}/ *ED6716* Ch neuron morphology (figure 3.11). Taken together these observations suggest that loss of fd3F expression has no effect on gross morphology of Ch

neurons and this may mean that fd3F only regulates a small subset of Ch-specific differentiation genes. This raises the question as to how *fd3F* deficiency results in the severe defects in adult and larval proprioception. There are two main possibilities: firstly loss fd3F may cause some more subtle changes in morphology that are not detected by immunostaining with these markers, alternatively fd3F may regulate genes required for Ch neuron function but not morphology such as ion channels.

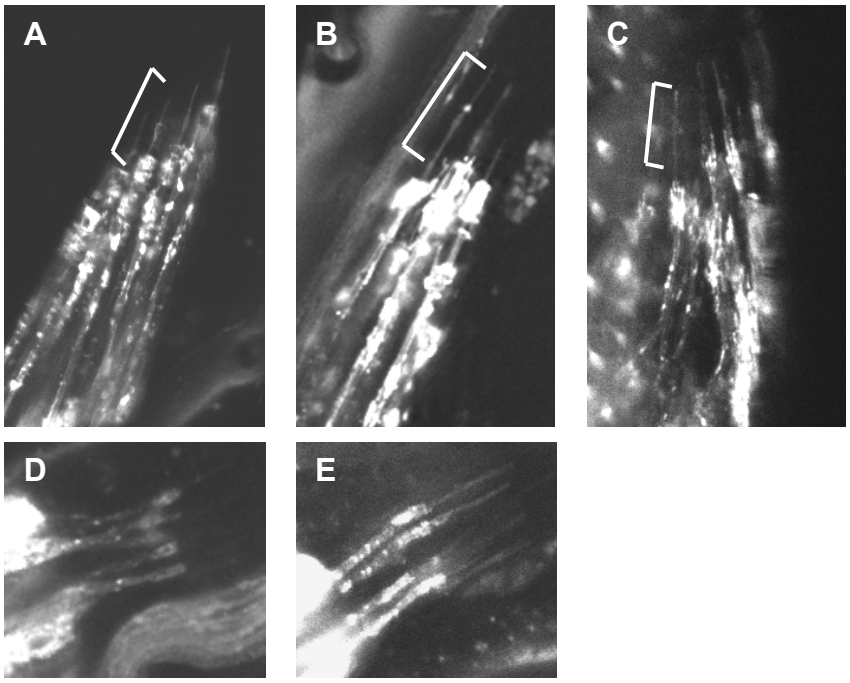

Figure 3.11: Ch neurons from adult legs and wings labelled with mCD8-GFP. Femoral Ch neurons in A) WT, B) *fd3F*^{1}, C) *fd3F*^{1}/ *ED6716* show no obvious morphological differences in the ciliary outer segments (brackets). D & E adult wing Ch neurons, again there is no obvious difference between WT (D) and *fd3F*^{1} (E).

3.2.2.2 Electron microscopy in *fd3F*^{1} adult antennae

To investigate the first possibility adult Ch neuron cilia were analysed in more detail using electron microscopy (Tracy Davey, Newcastle University). Figure 3.12 shows transverse sections through adult antennae showing Johnston's Organ Ch neurons.

Both *fd3F*^{1} and *fd3F*^{1}/ED6716 neurons become swollen close to the tip of the cilium, filling all the space within the dendritic cap and the microtubules appear disorganised (figure 3.12B &C). However further down the cilium the axonemal structure appears no different from wild type (figure 3.12D-F). This might suggest that there is a build up of proteins at the tip of the cilium and this could be caused by defects in retrograde intraflagellar transport (IFT). This seems to contradict the observations in embryos and adult legs (figures 3.10 & 3.11) since there is no visible bulging at the tips of the cilia. This could be because the bulging is too subtle to be seen using immunostaining, or it could be that this phenotype is specific to JO Ch neurons.

Structures at the base of the cilium ciliary including the ciliary rootlet and basal body appear morphologically normal in both *fd3F*^{1} and *fd3F*^{1}/*ED6716* neurons (figure 3.12G &H). The ciliary dilation is present in *fd3F*^{1}/*ED6716* neurons, however it appears to be slightly disrupted and lacks the regular lattice structure seen in wild type cilia (figure 3.12 I &J). If the ciliary dilation is disrupted this would affect the division of the Ch neuron cilium into functionally distinct compartments, leading to defects in Ch neuron physiology. Interestingly in *fd3F*^{1}/*ED6716* cilia one microtubule in each doublet appears to have a higher electron density than the other (figure 3.12L), a feature that is more usually associated with the distal region of the cilium. Observing this in the proximal region could therefore be further indication of disruption of the boundary between these two compartments. The axonemal dynein arms also appear to be missing from mutant cilia (figure 3.12K & L) and this could indicate a loss of motility of Ch neuron cilia in *fd3F*^{1} mutants. Again, this would severely impair Ch neuron function.

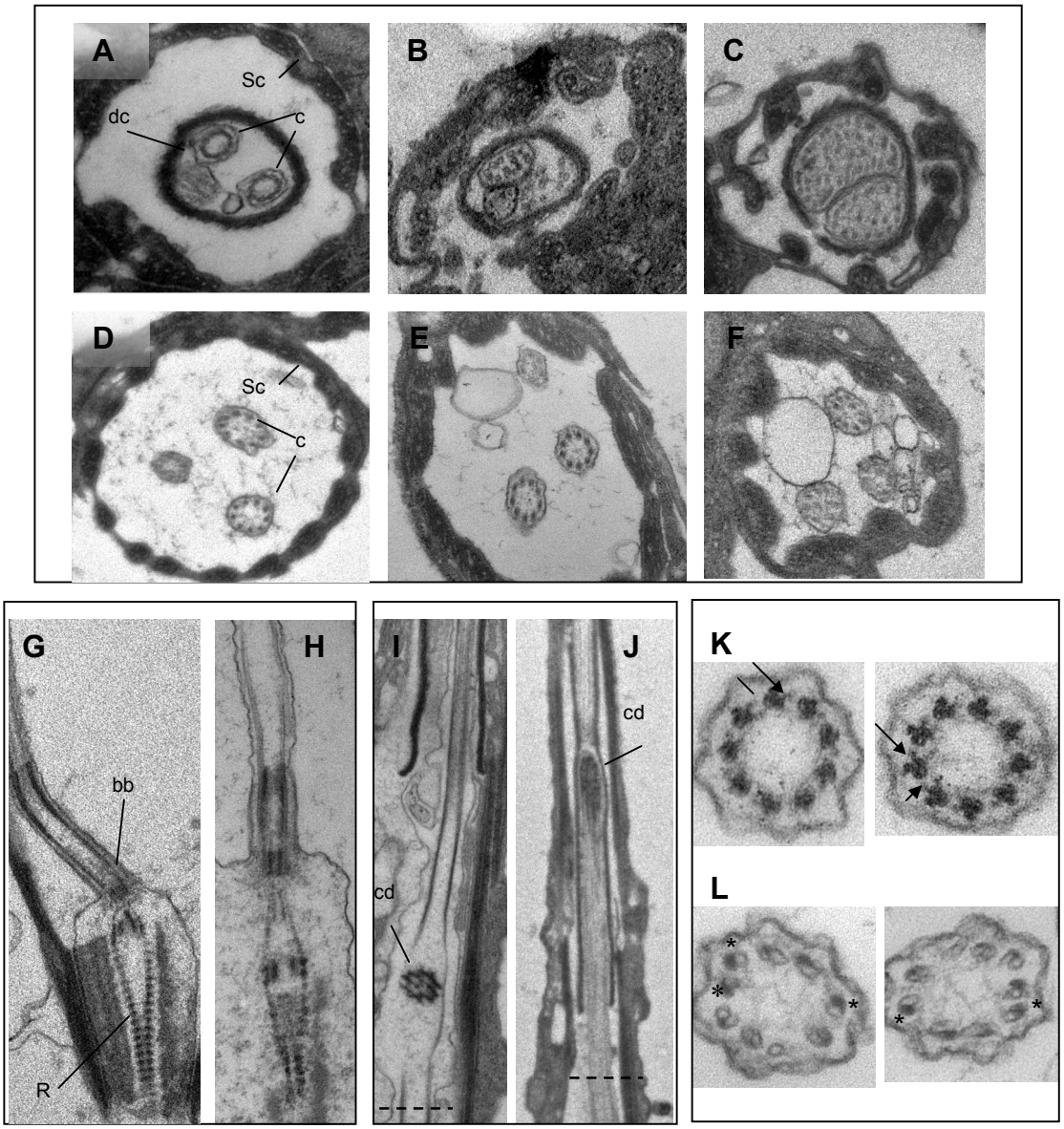

Figure 3.12: Electron microscopy of Johnston's organ (JO) Ch neuron cilia. A-F transverse sections through JO cilia in WT (A & D), *fd3F*^{1} (B & E) and *fd3F*^{1}/ *ED6716* (C & F). Sc = scolopale, dc = dendritic cap, c= cilium. The tips of *fd3F*^{1} and *fd3F*^{1}/ *ED6716* cilia bulge filling the space within the dc (B & C), however sections taken further down the cilia appear no different to WT (D-F). G-J are longitudinal sections, bb= basal body, R = rootlet, cd= ciliary dilation. There is no obvious difference between structures at the base of the cilium in *fd3F*^{1}/ *ED6716* (H) compared with WT (G). The cd is present in *fd3F*^{1}/ *ED6716* (J) but appears disrupted and does not have he regular structure seen in WT (I). K & L close ups of the axonemal structure in the proximal region of cilia. The approximate position of the transverse sections in K & L is indicated by dashed lines in I & J. Dynein arms can be seen in this region in WT (K, indicated by arrows) but they are missing in *fd3F*^{1}/ *ED6716* (L). Also in *fd3F*^{1}/ *ED6716* cilia several of the microtubule doublets appear to have higher electron density in one microtubule of the doublet (asterisks in L), whereas in WT (K) the electron densities associated with the microtubules are more equal.

3.2.2.3 IFT-B complex proteins accumulate at the tips of *fd3F*^{1} cilia

If the swollen ciliary tips of JO neurons observed by electron microscopy are due to a defect in retrograde IFT then proteins of the anterograde IFT-B complex would be expected to accumulate at the ciliary tips since this phenotype is observed in mutants of dynein-2 or IFT-A genes (Schafer *et al*., 2003; Hou *et al*., 2004; Lee *et al*., 2008). To explore this further I used a fly line expressing a nompB-GFP fusion protein (Han *et al*., 2003). NompB is an orthologue of IFT-88 and is known to be a component of the IFT-B complex (Han *et al*., 2003). In 24-48h old pupal antennae nompB-GFP is expressed evenly throughout the JO Ch neuron cilia (figure 3.13A). However when the nompB-GFP line was crossed into the *fd3F*^{1} background nompB-GFP accumulates towards the tips of the cilia (figure 3.13B).

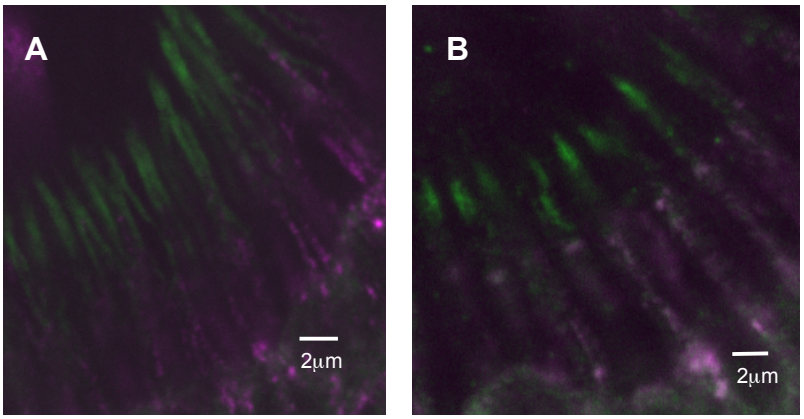

Figure 3.13: The IFT-B component nompB accumulates at the tips of f*d3F*^{1} Ch neuron cilia. JO neuron cilia from 48h old pupal antennae stained with Mab-22C10 (magenta) and RbAb-GFP (green). NompB-GFP is distributed evenly in WT JO neuron ciia (A) however nompB-GFP accumulates at the ciliary tips in JO neurons from f*d3F*^{1}; *nompB-GFP* pupae (B).

This phenotype is characteristic of mutations in the retrograde IFT-A complex proteins (Lee *et al*., 2008) and may therefore imply that fd3F is responsible for regulating expression either IFT-A genes or cytoplasmic dyneins required for

retrograde transport. *fd3F*^{1} JO cilia also appear to be slightly shorter than wild type and again this is characteristic of an IFT-A mutant phenotype, however it seems to contradict the electron microscopy data since the cilia clearly extend up to the dendritic caps.

3.2.2.4 Protein mis-localisation in *fd3F*^{1} Ch neuron cilia

NompC is a transient receptor potential (TRP) channel reported to specifically localise to the distal ciliary segments in Ch neurons (Lee *et al*., 2010; Cheng *et al*., 2010). I therefore initially used MAb -NompC as a marker to label the ciliary outer segments of larval Ch neurons more clearly. However these studies have analysed nompC expression in JO Ch neurons in pupal antennae rather than in larval Ch neurons and I found that, in larvae, MAb-NompC staining is mostly restricted to an area close to the ciliary dilation. While this means that NompC is not a good marker for looking at ciliary tips, I did observe that in both *fd3F*^{1} and *fd3F*^{1}/ *ED6716* larvae the NompC staining has a much less restricted localisation than in wild type and in some cases extends throughout the proximal ciliary segments (figure 3.14A & B). This mis-localisation could indicate some defects in the transport of proteins into Ch neuron cilia in *fd3F*^{1} mutants.

To investigate this further the immunostaining was repeated in 24-48h old pupal antennae. Labelling with MAb-NompC in wild type antennae (figure 3.14C) confirmed the results observed by Lee *et al*., with nompC staining restricted to the distal ciliary tips. In *fd3F*^{1}/ ED6716 antennae, however the nompC staining extends much further along the cilium indicating that nompC is present in the proximal

portion of the cilia as well as the distal tips (figure 3.14D). This suggests that nompC fails to localise correctly in *fd3F*^{1} mutants. This could mean that fd3F regulates genes required for the structural integrity of the ciliary dilation (and therefore division of cilia into functionally distinct compartments) or genes required for specific localisation of proteins within the cilium. If this is the case there may be other functionally or structurally important proteins that are mis-localised in *fd3F*^{1} Ch neuron cilia.

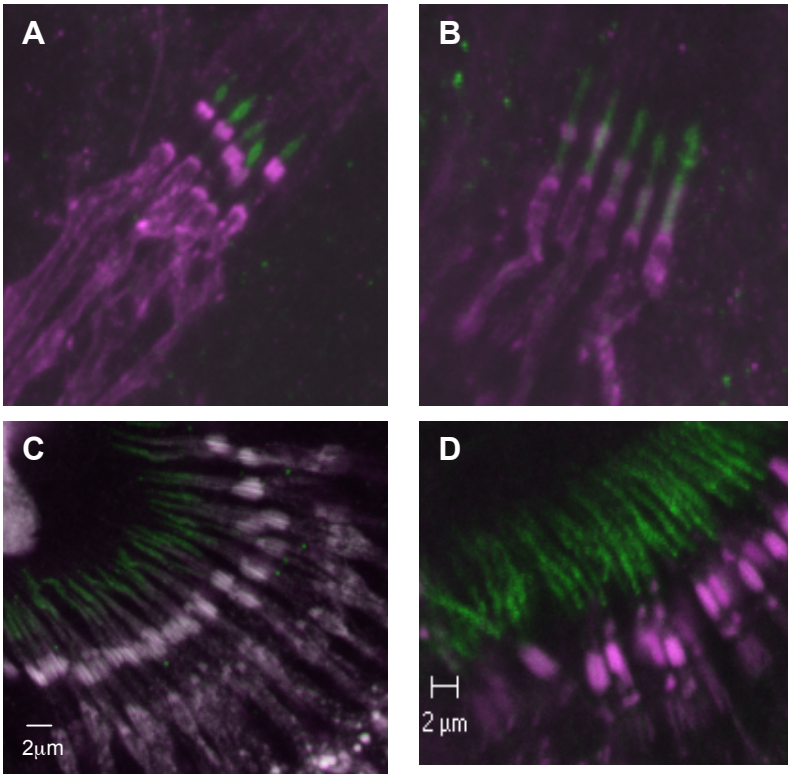

Figure 3.14: Mis-localisation of NompC in *fd3F*^{1}/ *ED6716* Ch neurons. Larval Ch neurons (A & B) and JO neurons in 48h old pupal antennae (C & D) stained with Mab-NompC (green) and RbAb-HRP (magenta). In WT larval Ch neurons (A) NompC is restricted to an area close to the ciliary dilations, whereas in *fd3F*^{1}/ *ED6716* (B) NompC is distributed throughout the cilia. The HRP staining in *fd3F*^{1}/ *ED6716* JO neurons (D) appears different from WT (C) due to the broader lumenal band seen previously in larval Ch neurons (figure 18). However NompC is clearly distributed over a longer section of the cilium in *fd3F*^{1}/ *ED6716* compared to WT.

One protein of particular interest is rempA, an IFT-A component known to localise specifically to the ciliary dilation (Lee *et al*., 2008). Since the electron microscopy data showed disruption of the ciliary dilation in some *fd3F*^{1} JO cilia I decided to investigate whether rempA was also mis-localised in the JO neurons of pupal antennae. To do this I used a line expressing a rempA-YFP fusion protein (Lee *et al*., 2008) and crossed this into the *fd3F*^{1} background. In the wild type background rempA-YFP accumulates at the ciliary dilation of JO Ch neurons as expected. However in *fd3F*^{1}; *rempA-YFP* antennae some YFP expression is seen at the base of the cilium and spreading into the proximal segment, but it fails to accumulate at the ciliary dilation (figure 3.15). This suggests that either disruption to the structure of the ciliary dilation in *fd3F*^{1} Ch neurons prevents rempA from localising there, or that rempA expression in *fd3F*^{1} flies is insufficient to allow accumulation at the dilation and loss of rempA at the ciliary dilation disrupts its structure.

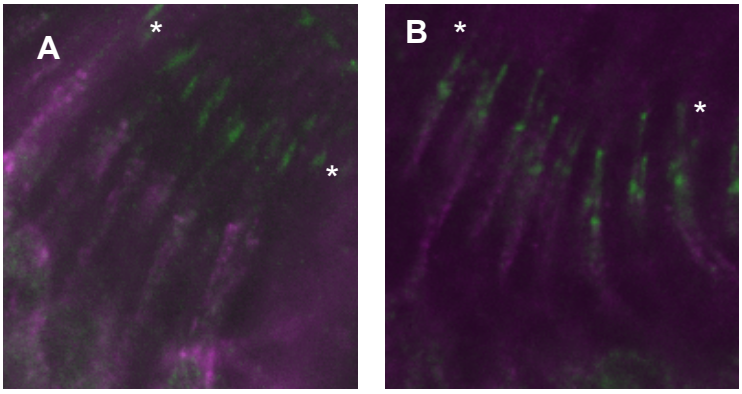

Figure 3.15: Localisation of rempA in *fd3F*^{1} JO neuron cilia. 24-48h old pupal antennae labelled with MAb-22C10 (magenta) and rempA-YFP (green). Asterisks indicate approximate position of the ciliary dilation. A) rempA-YFP localises to the ciliary dilation in the wild type background. B) in the *fd3F*^{1} background rempA-YFP is present at the base of the cilium and in the proximal segment, but fails to accumulate at the ciliary dilation.

3.2.3 Axon guidance in *fd3F*^{1} embryos

The results described so far suggest that loss of fd3F causes subtle defects in the morphology of the Ch neuron cilium. These results may indicate a role for fd3F in regulating retrograde IFT genes, however it is also possible that the severe behavioural phenotype seen in *fd3F*^{1} mutants is caused by the Ch neuron axons failing to terminate in the correct location. One possible way in which fd3F might regulate axon guidance is through transcriptional regulation of *robo3*. Robo3 is the Ch-specific receptor for the midline repellent signal Slit and is essential for termination and arborisation of Ch axons in the correct medio-lateral position in embryos (Zlatic *et al*., 2003). Previous studies have shown that *robo3* expression is *ato*-dependent (Zlatic *et al*., 2003) however *robo3* is expressed only in the late stages of embryogenesis and so cannot be regulated by *ato* directly. *robo3* might therefore be expected to be a candidate regulatory target of *fd3F*.

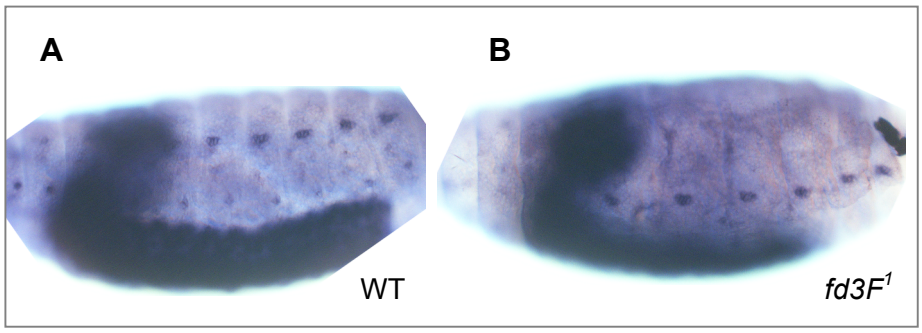

Figure 3.16: *robo3* mRNA *in situ* hybridisation in (A) WT and (B) *fd3F*^{1} embryos. In WT *robo3* is expressed in CNS and Ch neurons. There is no decrease in *robo3* expression level in *fd3F*^{1} embryos. *w*^{1118} used as WT.

robo3 mRNA expression can be detected by *in situ* hybridisation in late stage embryos in Ch neurons and the CNS. However no reduction in *robo3* mRNA was observed in $fd3F^{1}$ embryos (figure 3.16) suggesting that fd3F is not required for *robo3* expression. It is therefore possible that *fd3F* is not required for medio-lateral positioning of terminal Ch axon arbours, although it does not rule out an effect on the dorso-ventral position of the axon terminals.

3.3 Discussion

Loss of fd3F causes a severely uncoordinated phenotype but only subtle defects in Ch neuron morphology

The deletion mutation $fd3F^{1}$ results in strong depletion of *fd3F* mRNA during embryogenesis and $fd3F^{1}$ larvae and adults are severely uncoordinated. The defects observed in adults are characteristic of loss of Ch neuron function since Ch neurons are required to provide the proprioceptive feedback necessary to coordinate walking, climbing and flight and similar defects are seen in ato^{1} mutants that lack Ch neurons (Jarman *et al*., 1995). However previous studies have suggested that inhibition of Ch neuron function by Gal4-driven expression of temperature sensitive *shibire* does not affect the rate of larval peristaltic contractions (Hughes & Thomas, 2007; Song *et al*., 2007). This proprioceptive feedback is instead provided by bipolar dendritic and class I multidendritic neurons. Therefore Ch neuron defects should not affect larval crawling speed.

It is therefore interesting that *fd3F*^{1} larvae crawled a significantly shorter distance in 2min than w^{1118} larvae. The key to this may be the shape of the trails produce by *fd3F*^{1} larvae. Hughes & Thomas measured the rate of peristaltic contractions but discounted any time the larvae spent paused or changing direction. *fd3F*^{1} larvae change direction more frequently than w^{1118} and each turn is accompanied by a brief pause. This could account for the shorter overall path length despite crawling at a similar speed. Indeed other Ch-specific mutations such as *tilB* and *smetana* cause similar crawling defects, shorter path lengths with increased number of turns and decision-making pauses (Caldwell *et al*., 2003). Also Hughes & Thomas observed that when Ch neurons were constitutively inhibited by Gal4-driven expression of tetrodotoxin the larvae had weaker contractions and posture problems. Therefore while the rate of contractions may be unaffected by Ch neuron defects, Ch neurons may be required for the feedback necessary to maintain strong contractions and to crawl in a straight line.

Since the uncoordinated phenotype of *fd3F*^{1} mutants appears to be due to loss of Ch neuron function it is surprising that *fd3F*^{1} Ch neurons exhibit only minor morphological defects. This suggests that fd3F regulates only a small subset of Ch-specific genes, rather than being a general transcriptional regulator of all aspects of Ch neuron differentiation. The subtle defects observed in *fd3F*^{1} Ch neurons do however provide some insight into the types of genes that fd3F might be regulating.

One gene that was considered as potential candidate regulatory target of fd3F was the Ch specific axon guidance receptor *robo3*. This seemed plausible since failure of Ch

axons to project to the correct region of the neuropile would be expected to disrupt Ch neuron function without causing any other morphological defects. However there was no reduction in *robo3* mRNA expression in *fd3F*^{1} embryos suggesting that fd3F does not regulate *robo3*. This means that fd3F deficiency is unlikely to affect the medio-lateral position of Ch axon terminals. Exactly what does regulate *robo3* is therefore still not known since so far there is no evidence that *robo3* is regulated by Rfx. This raises the question of whether there may be other intermediate transcription factors acting downstream of *ato*. Expression of robo3 in *fd3F*^{1} embryos does not preclude fd3F from having a role in regulating axon guidance in the dorso-ventral axis however, although this could be an interesting area to pursue, I decided to focus on understanding how fd3F deficiency causes the subtle morphological defects observed in Ch neuron cilia.

The JO Ch neuron cilia of *fd3F*^{1} adults have swollen tips that accumulate the IFT-B complex protein NompB. This is almost identical to the phenotype caused by mutation of *rempA*, the gene encoding the *Drosophila* orthologue of the IFT-A component IFT140 (Lee *et al*., 2008) and mutations in dynein-2 subunits in *Chlamydomonas* and *C. elegans* (Hou *et al*., 2004; Schafer *et al*., 2003). This suggests that this phenotype may be due to defects in retrograde IFT. It is not clear whether this phenotype is restricted to JO Ch neurons since it is difficult to label the larval ciliary tips clearly and there was no obvious bulging at the tips of embryonic and adult leg Ch neurons. However it may be that the swelling is too subtle to be detected by light microscopy and the cilia of these neurons may still accumulate IFT-B proteins at the tips. It is also unclear whether *fd3F*^{1} Ch neurons have full-length

cilia since the electron microscopy data suggest that the JO cilia extend up to the dendritic cap, however they appear shorter than wild type cilia when labelled with nompB-GFP. The difference in length is, however, not as pronounced as that observed in IFT-A mutants such as *rempA*^{1} where the mutant cilia terminate at the ciliary dilation and therefore do not reach the dendritic cap (Lee *et al*., 2008). It may be that *fd3F*^{1} cilia are long enough to connect to the cap during development and become stretched as development of the adult Ch organs progresses. However these results do imply that, in developing JO Ch neurons at least, fd3F may regulate transcription of IFT-A complex genes or genes encoding dynein-2 subunits.

Interestingly, mutations in the gene *beethoven* (*btv*), which encodes a cytoplasmic dynein-2 heavy chain, cause structural defects in embryonic Ch neurons that appear very similar to the *fd3F*^{1} defects when labelled with anti-HRP (Caldwell *et al*., 2003). In *btv* mutants the main structural defect is thought to be disruption of the ciliary dilation (Eberl *et al*., 2000) suggesting that there is a requirement for retrograde IFT for formation of the ciliary dilation. *Btv* mutants are also deaf and uncoordinated (Eberl *et al*., 2000; Caldwell *et al*., 2003) showing that retrograde transport and integrity of the ciliary dilation are essential for Ch neuron function. In some *fd3F*^{1}/ *ED6716* JO Ch neurons the ciliary dilation appears slightly disrupted (although not as severely as in *btv* mutants) and it is possible that the unusual HRP staining in *fd3F*^{1} embryonic and larval Ch neurons could be due to defects in the ciliary dilation structure.

It is also significant that the TRP ion channel NompC, which normally has a very restricted localisation (Lee *et al*., 2010; Cheng *et al*., 2010), is mis-localised in both *fd3F*^{1} JO and larval Ch neurons. rempA-YFP is also mis-localised in JO Ch neurons. The ciliary dilation separates the cilium into functionally distinct compartments and mis-localisation of NompC and rempA could be due to disruption of the ciliary dilation. It is also possible that rempA expression may be very slightly reduced in *fd3F*^{1} Ch neurons and this could mean there is insufficient rempA present to accumulate at the ciliary dilation. Loss of rempA from the ciliary dilation could be the reason for the disruption in its structure. Alternatively the retrograde transport machinery itself may be particularly important for protein localisation within the cilium. These data support a role for fd3F in regulating retrograde transport genes and/ or genes required for specific localisation of proteins within the Ch neuron cilium. Both *btv* and *rempA* are therefore potential target genes.

Loss of the retrograde IFT machinery and mis-localisation of ion channels within Ch neuron cilia could be sufficient to explain the uncoordinated *fd3F*^{1} phenotype, however this may not be the whole story. The axonemal dynein arms also appear to be missing from *fd3F*^{1} Ch cilia suggesting that fd3F may regulate transcription of some or all of the subunits that make up these dynein arms. The particular axonemal dynein proteins required for Ch cilium motility are not known, however the dynein arm proteins have been identified in other species (for example Andrews *et al*., 1996; Pennarun *et al*., 1999; Bartoloni *et al*., 2002; Supp *et al*., 1997) and many of these have homologues in *Drosophila*. Several axonemal dynein proteins have been identified as RFX targets in mice and the predicted *Drosophila* orthologues of these

proteins are also predicted to be regulatory targets of Rfx (reviewed in Thomas *et al*., 2010). However since dynein arms are a Ch-specific feature it seems reasonable to predict that these genes will also be regulated by a Ch-specific transcription factor such as fd3F.

Studying the morphology of Ch neurons in *fd3F*^{1} mutants has provided some clues as to the Ch differentiation genes that may be regulated by fd3F. However it is also possible that fd3F regulates other genes required for Ch neuron physiology but not morphology such as ion channels. Although I have already established that NompC is expressed at normal levels in *fd3F*^{1} larval and JO Ch neurons (despite being mis-localised) and is therefore not a regulatory target of fd3F, there are other Ch-specific ion channel genes that could potentially be fd3F targets. Two important examples are *nanchung* and *inactive*, the genes encoding two subunits of a Ch-specific TRP channel that is essential for Ch neuron function (Kim *et al*., 2003; Gong *et al*., 2004). The subject of the next chapter is therefore an investigation to identify the regulatory target genes of fd3F.

4

Regulatory Target Genes of fd3F

4.1 Introduction

In chapter 3 I described the effect of the *fd3F*^{1} mutation on Ch neuron morphology. Loss of fd3F appears to cause subtle defects in morphology of the Ch neuron cilium and protein mis-localisation within the cilium. I therefore hypothesised that fd3F may regulate components of the retrograde IFT machinery required for protein localisation and/ or genes required for the structural integrity of the ciliary dilation. However, these genes may not be the only regulatory targets of fd3F. The absence of dynein arms in *fd3F*^{1} Ch neuron cilia suggests fd3F may also regulate genes required for Ch ciliary motility, which is essential for Ch mechanosensory function. It is also possible that fd3F may regulate other genes required for Ch neuron physiology but not morphology such as ion channels. The introduction to this chapter therefore describes the role of Ch organs in mechanosensation and some of the genes known to be required for Ch neuron physiology.

4.1.1 Mechanosensation in *Drosophila*

Mechanosensation involves the transduction of mechanical stimuli such as touch, sound and gravity into electrical signals. In *Drosophila* this is mediated by mechanosensory bristles (touch) and Ch organs (proprioception, gravitaxis and

hearing). Most of the recent work on mechanosensation in *Drosophila* has been to establish the mechanism of auditory transduction by the Johnston's organ (JO) Ch neurons of the antennae. This has led to the identification of several genes required for auditory transduction. Mutants of these genes lack sound evoked potentials and have an uncoordinated phenotype suggesting that similar mechanisms are required for both proprioception and hearing (Eberl *et al.*, 2000). Several of these genes are not required for gross morphology of the Ch neuron and are therefore potential regulatory targets of fd3F.

The JO is a large cluster of several hundred Ch scolopedia, each with two or three neurons, located in the second antennal segment (figure 4.01). The neurons of the JO are considered analogous to the mechanoreceptor hair cells of vertebrate ears such as those of the mammalian cochlea (Boekhoff-Falk, 2005). The *Drosophila* third antennal segment is suspended by the flexible antennal joint and vibrates in response to sound along with a feather-like protrusion called the arista (Göpfert & Robert, 2001a). The third antennal segment and arista therefore act as the sound receiver. The cilia of JO neurons are connected to the third antennal segment via the cap cells and vibration of the receiver is thought to stretch the neurons, directly activating mechanotransduction (Göpfert & Robert, 2002; Caldwell & Eberl, 2002). The JO neuron dendrites are bathed in a K^+ rich, low Ca^{2+} endolymph secreted by the scolopale and movement of the cilium is thought to trigger opening of cation channels resulting in an influx of K^+ and depolarisation of the membrane (Grünert & Gnatzy, 1987). The antennal receiver is also deflected by stimuli such as wind and gravitational force and it has been shown that a separate subset of JO neurons

respond to this stimulation and are required for negative gravitaxic behaviour (Kamikouchi *et al.*, 2009).

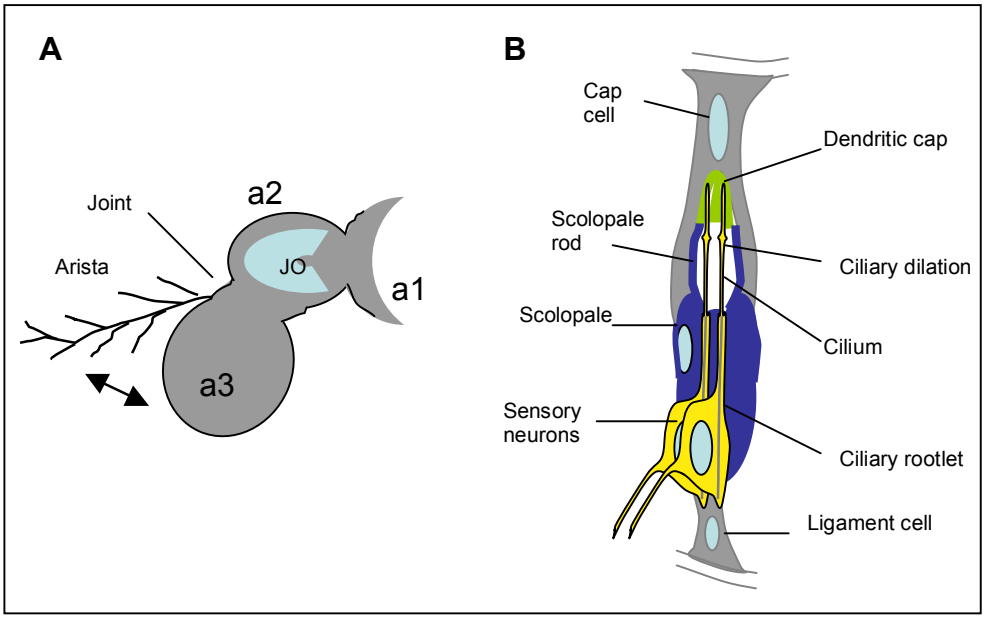

Figure 4.01: The Johnston's Organ. A) Schematic showing the three antennal segments (a1, a2, a3) and the arista. The Johnston's organ (JO) scolopedia are located in the second antennal segment. B) A single JO scolopedium with two Ch neurons. The cap cell is in contact with the a2-a3 joint.

Several studies have measured mechanotransduction activity in JO neurons using laser Doppler vibrometry and measurement of Ca^{2+} signalling (Göpfert & Robert, 2003; Göpfert *et al.*, 2006; Kamikouchi *et al.*, 2009). These studies found that, in addition to the stretching and contraction induced by sound vibrations, Ch neurons also actively vibrate to amplify the mechanotransduction signal at certain frequencies and increase hearing sensitivity. This has also been observed in the auditory systems of mosquitos (Göpfert & Robert, 2001b) and is considered similar to the active contractions of mammalian hair cells (Nobili *et al.*, 1998; Robles & Ruggero, 2001) and active hair bundle twitches in lower vertebrates (Hudspeth *et al.*, 2000).

4.1.2 *Drosophila* mechanosensory genes

Many mechanosensory genes encode the proteins required for cilium assembly such as the IFT-A and IFT-B components and cytoplasmic dyneins and kinesins discussed in the previous chapter. As discussed previously this highlights the importance of Ch neuron cilia for mechanotransduction. Some of the other genes identified encode cytoskeletal-associated proteins such as Crinkled (a homologue of vertebrate myosin VIIA), DmEB1 and NompA (Kiehart *et al*., 2004; Elliott *et al*., 2005; Chung *et al*., 2001). These proteins are required for maintaining the structural integrity of Ch organs, in particular NompA is a zona pellucida (ZP) domain protein that localises to the dendritic cap and is crucial for attachment of the neuron cilium to the cap (Chung *et al*., 2001). However since these cytoskeletal-associated proteins are expressed by either the scolopale or cap cell rather than the neuron their expression cannot be regulated by fd3F since fd3F expression is exclusive to Ch neurons.

Another group of genes shown to be essential for mechanosensation in *Drosophila* are those encoding mechanically gated transient receptor potential (TRP) channels including *nanchung*, *inactive* and *nompC* (Kim *et al*., 2003; Gong *et al*., 2004; Eberl *et al*., 2000). Given the severity of the uncoordinated phenotype of $fd3F^{1}$ mutants and the relatively mild morphological defects of $fd3F^{1}$ Ch cilia it is possible that fd3F regulates Ch-specific TRP channels and these will be discussed in detail in section 4.1.3 below.

Several genes have been shown to be required for active oscillations of the Ch neuron cilium including *btv* and *nompA*, required for structural integrity of the Ch ciliary dilation and connection of the ciliary tip to the dendritic cap respectively (Eberl *et al*., 2000; Chung *et al*., 2001). The ciliary dilation is thought to deform as the cilium stretches and contracts making it a candidate site for transduction (Field & Matheson, 1998). In *nompA* mutants the dendritic caps become detached from cilia and transduction is completely absent (Chung *et al*., 2001) demonstrating that the connection between the ciliary tip and the dendritic cap is essential for transduction.

Another gene found to be essential for active oscillation of Ch neuron cilia is *touch insensitive larva B* (*tilB*) (Eberl *et al*., 2000). TilB is a leucine-rich repeat protein expressed in Ch neurons and sperm. In addition to being deaf *tilB* mutants lack inner and outer dynein arms in both sperm flagella and the proximal region of JO cilia, although TilB itself does not localise to the cilia (Eberl *et al*., 2000; Kavlie *et al*., 2010). It has therefore been proposed that TilB is required for assembly of the axonemal dynein complexes that form the dynein arms prior to their localisation in the cilium (Kavlie *et al*., 2010). Since the dynein arms are known to be required for motility in sperm flagella it has been suggested that the dynein arms of JO cilia generate the motile force that drives active oscillation (Göpfert & Robert, 2003; Nadrowski *et al*., 2010). The axonemal dynein arms appear to be absent from $fd3F^{1}$ JO neuron cilia suggesting that fd3F may regulate expression of either *tilB* or some of the axonemal dynein proteins or both.

4.1.3 Transient receptor potential (TRP) channels and mechanosensation

TRP channels are a superfamily of cation channels with six transmembrane helices, a pore loop between helix 5 and helix 6 and an intracellular domain containing several ankyrin repeats (figure 4.02). TRP genes are expressed across a variety of organisms from archea to mammals (Clapham, 2003) and the amino acid sequences around the pore loop are particularly well conserved in all TRP families highlighting their importance in formation and gating of the channel pore (Nilius *et al*., 2005). TRP channels can be ligand gated (Zhu, 2005; Venkatachalam *et al*., 2003), activated by membrane-bound receptors such as G-protein coupled receptors or receptor tyrosine kinase acting through diacylglycerol (Okada *et al*., 1999; Hisatsune *et al*., 2004) or directly activated by changes in temperature or mechanical stimuli (Clapham, 2003; Maroto *et al*., 2005).

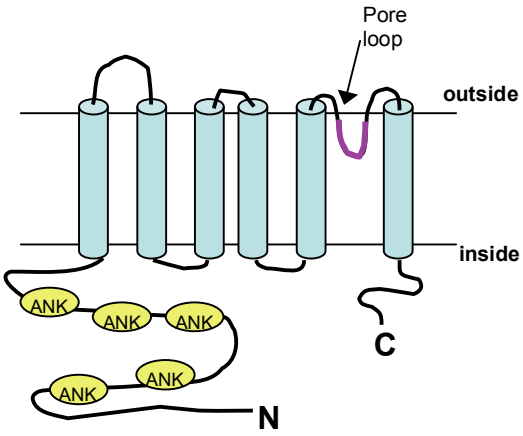

Figure 4.02: TRP channel topology. The N-terminus has a variable number of ankyrin repeats (ANK), from 3 to 29 depending on the TRP channel subfamily and these may be involved in adhesion to the cytoskeleton. The loop between helix 5 and 6 is thought to form the channel pore.

4.1.3.1 Mechanosensory TRP channels in *Drosophila* and other organisms

Several TRP channel subfamilies have been implicated in mechanosensation including TRPA (Corey *et al*., 2004), TRPML (Di Palma *et al*., 2002) and most notably TRPN (Walker *et al*., 2000; Sidi *et al*., 2003) and TRPV (O'neill & Heller, 2005). The TRPV (vanilloid) family channels are Ca^{2+} ion selective channels expressed on both sensory and non-sensory cells. They can be gated by temperature, such as the capsaicin-activated nociceptor TRPV1 (Caterina *et al*., 2000) or by mechanical force. The first members of this family to be characterised were the *C. elegans* proteins Osm-9 and Ocr-1, 2, 3 and 4 (Colbert *et al*., 1997; Tobin *et al*., 2002). Osm-9 can form complexes with any of the Ocrs, in particular Osm-9 and Ocr-2 form a complex that localises to the cilia of ASH sensory neurons that respond to chemical, osmotic and touch stimuli (Tobin *et al*., 2002). Osm-9 mutants lack osmotic avoidance behaviour and are also insensitive to nose touch (Colbert *et al*., 1997) suggesting a role for Osm-9/ Ocr-2 in mechanosensation. The function of Osm-9 can be rescued by expression of its mammalian homologue TRPV4 (Leidtke *et al*., 2003), which is known to act as a sensor for osmotic pressure.

Two TRPV family members *nanchung* (*nan*) and *inactive* (*iav*) have been identified in *Drosophila* (Kim *et al*., 2003; Gong *et al*., 2004). The Iav protein is closely related to the Osm-9 while Nan is related to the Ocr proteins (O'Neil & Heller, 2005). Both *nan* and *iav* are exclusively expressed in Ch neurons and an Iav-GFP fusion protein was found to localise to the proximal region of the Ch cilium (Kim *et al*., 2003; Gong *et al*., 2004). Deletion mutations of *nan* result in flies that are mildly uncoordinated with almost a complete lack of antennal sound evoked potentials (Kim

et al., 2003). Similar defects have been observed in *iav* mutants (Gong *et al*., 2004), suggesting that both Nan and Iav are essential for Ch neuron function. Nan and Iav are also reciprocally dependent on each other for stability and correct localisation within the membrane of the Ch neuron cilium (Gong *et al*., 2004). This is similar to the interdependence of Osm-9 and Ocr-2 in *C. elegans* ASH neurons, both proteins must be co-expressed to allow their localisation in the neuron cilium (Tobin *et al*., 2002).

Expression of Nan or Iav in mammalian cell lines induces sensitivity to changes in osmotic pressure of the surrounding fluid (Kim *et al*., 2003; Gong *et al*., 2004) and this is similar to the osmosensitivity of cells expressing TRPV4 (Liedtke *et al*., 2000; Strotmann *et al*., 2000). Since TRPV4 is thought to be closely related to Nan and Iav and can be activated by mechanical stress as well as osmotic pressure (Gao *et al*., 2003) several studies have tried to establish a role for TRPV4 in mammalian hearing. TRPV4 is expressed in vertebrate cochlear hair cells (Liedtke *et al*., 2000) however TRPV4 knockout mice do not exhibit any loss of response to auditory stimuli suggesting that TRPV4 is either not required for transduction in cochlear hair cells or functions redundantly with other TRP channels (Liedtke & Friedman, 2003). In contrast TRPML3 mutations have been found to cause deafness and balance defects in mice making this channel the most likely candidate for mammalian hearing transduction (Di Palma *et al*., 2002). However in *Drosophila* no TRPML homologues have been associated with mechanosensation.

TRPA1 knockdown in zebrafish hair cells in culture has been shown to reduce sound evoked potentials (Corey *et al*., 2004). Two TRPA channels genes, *painless* and *pyrexia*, have been identified in *Drosophila*. These channels are expressed in a subset of JO neurons and cap cells respectively, however mutation of *painless* or *pyrexia* has no effect on auditory transduction and these channels are instead thought to be required for gravitaxis (Sun *et al*., 2009). These TRPA channels are also required for nociception in larvae (Lee *et al*., 2005). This suggests there may be some divergence in the mechanosensory roles of different TRP families between vertebrates and invertebrates.

The *Drosophila* TRPN family channel NompC is expressed in both ES and Ch neurons and mutation of *nompC* has been shown to severely reduce transduction in the neurons of mechanosensory bristles (Kernan *et al*., 1994; Walker *et al*., 2000; Gillespie & Walker, 2001). Interestingly TRPN1 has also been found to be important for auditory sensation in zebrafish larvae (Sidi *et al*., 2003) and the *C. elegans* TRPN channel TRP-4 is essential for transduction in mechanosensory neurons (Kang *et al*., 2010). In JO neurons NompC localises to the distal regions of the cilia, which may allow it to be gated directly by movement of the dendritic cap (Lee *et al*., 2010; Cheng *et al*., 2010; Laing *et al*., 2011). However detection of gravity and wind appears to be independent of NompC suggesting its role in antennae may be restricted to auditory transduction (Effertz *et al*., 2011).

4.1.3.2 NompC and Nan/Iav have distinct roles in *Drosophila* mechanosensation

In contrast to *nan* and *iav* mutants, sound evoked potentials in *nompC* mutant JO neurons were found to be only around 50% reduced (Eberl *et al*., 2000) suggesting that NompC is only partially responsible for transduction in Ch neurons. The active antennal vibrations required to amplify the mechanosensory potentials are, however, severely reduced in *nompC* mutants (Göpfert *et al*., 2006) and *nompC* mutants have impaired hearing sensitivity (Effertz *et al*., 2011). In *nan* and *iav* mutants these active vibrations have actually been shown to increase (Göpfert *et al*., 2006). These results suggest that while active amplification is dependent on NompC, Nan/Iav may be required to adjust the amplification gain. This means that NompC may act as the mechanotransducer in the non-motile distal portion of the cilium while Nan/Iav may act as a secondary channel that is required not only to depolarise the membrane and trigger action potentials but also to modulate active oscillations of the proximal region (Göpfert *et al*., 2006). The excessive mechanical oscillations in *nan* and *iav* mutant antennae may be analogous to the over-activation of mechanical feedback that produces the ringing sound in tinnitus patients (Fettiplace & Hackney, 2006; Robles & Ruggero, 2001). As with *nan* and *iav* mutants chronic forms of tinnitus are also associated with hearing loss (Baguley, 2002).

The mechanism by which the *Drosophila* NompC and Nan/Iav channels are gated is still unclear. Gating mechanisms such as phosphorylation or signalling pathways used by other TRPV channels such as TRPV4 (Xu *et al*., 2003; Nilius *et al*., 2004) are not fast enough to explain the rapid auditory transduction observed in JO neurons (Eberl *et al*., 2000; Gong *et al*., 2004). The Nan/Iav channel is therefore likely to be

directly gated by mechanical stress in a similar manner to *C. elegans* Osm-9/Ocr-2. The Osm-9/Ocr-2 channel is attached to both the cytoskeleton and extracellular matrix and movement of the neuron cilium relative to extracellular structures could pull the channel open (Tobin *et al*., 2002). However since Nan/Iav localisation is restricted to the proximal region of Ch cilia it is not clear how extracellular mechanical force is transmitted from the ciliary tip to the Nan/Iav channel.

NompC may be gated directly by movement of the dendritic cap. However, in contrast to the *nompA* mutant phenotype, *nompC* mutant ciliary tips do not detach from the dendritic caps and NompC is therefore not necessary to maintain the connection between these structures (Walker *et al*., 2000). To date there is no evidence of a direct interaction between NompC and NompA or any other extracellular matrix protein. One striking feature of the TRPN family proteins however is the large number of ankyrin repeats in the amino-terminal domain (NompC has 29 ankyrin repeats compared with only 5 in Nan and Iav) (Walker *et al*., 2000). It has been proposed that these ankyrin repeats may form one helical turn and could function as a gating spring during mechanosensation (Howard & Bechstedt, 2004). NompC has also been found to co-localise with cytoskeletal microtubules in cell culture and the ankyrin repeats are required for this co-localisation (Cheng *et al*., 2010). This suggests that the ankyrin repeats may be involved in attaching NompC to the axomemal microtubules of neuron cilia. Deletion of some or all of the ankyrin repeats from the amino-terminus of NompC has been shown to prevent proper localisation of NompC and results in similar defects to NompC deficiency (Cheng *et al*., 2010). Cheng et al. have therefore suggested a model in which NompC may be

connected to both the extracellular matrix via connections with the dendritic cap and axonemal microtubules via the ankyrin repeats and movement of NompC could therefore be transmitted down the axoneme to Nan/ Iav.

Alternatively NompC and Nan/Iav function may be physically linked by protein components of the ciliary dilation. DCX-EMAP is a microtubule associated protein that localises to the tubular body of campaniform sensilla and the ciliary dilation of Ch neurons (Bechstedt *et al*., 2010). Mutations in DCX-EMAP result in loss of the regularly structured, electron dense material from the ciliary dilation and causes deafness and uncoordination. This was found to be due to loss of both initial mechanosensory response and active amplification (Bechstedt *et al*., 2010). Bechstedt et al. therefore proposed that DCX-EMAP is required to organise protein material within the ciliary dilation and that these protein components may be involved in gating Nan/Iav and NompC as the ciliary dilation is stretched and compressed.

4.2 Results

4.2.1 RNA *in situ* hybridisation screen to identify regulatory targets of fd3F

In the previous chapter I have described the apparent discrepancy between the severe proprioceptive defects in *fd3F*^{1} mutants and the relatively minor defects in the morphology of their Ch neurons. From this I concluded that *fd3F* must regulate a small subset of Ch-specific genes that are crucial for Ch neuron function but not gross structural morphology. To fully understand the role of *fd3F* in Ch neuron differentiation it is therefore important to identify which genes *fd3F* regulates. To investigate this I began by screening 19 genes by *in situ* hybridisation in *fd3F*^{1} embryos to search for genes with reduced levels of mRNA expression compared to wild type. The genes selected for this screen were chosen from genes identified in the *ato* microarray data that were shown to have Ch-specific or Ch-enriched expression patterns (Cachero *et al*., 2011) as well as some late expressing genes known to be essential for Ch neuron function. All genes included in this screen are summarised in table 4.1. After discovering more about the detailed morphology of *fd3F*^{1} Ch neuron cilia (described in Chapter 3) the screen was expanded to include other genes featured in the ato microarray data that may be required for those morphological features. These genes are listed in table 4.2. In the descriptions below the results of the two screens are combined for clarity.

Gene	Enrichment at atot3 (catot4)	Expression Pattern	Expression in *fd3F*^{1} embryos	Other information/ function
CG6129	5.5	Ch-enriched (stage 11-17)	Not affected	Formation of ciliary rootlet
CG6980	25.7	Ch-specific (stage 11-17)	Reduced expression	TPR domain
CG17564	16.4	Ch-specific (stage 11-16)	Not affected	
CG11253	18.4 (20.8)	Ch-specific (stage 11-16)	Moderately reduced expression	Homologue of ZMYND10/ BLU
CG3085	9.3	Ch-specific (stage 11-16)	Not affected	
CG10339	7.6	Ch-specific (stage 13-17)	Reduced expression	Carboxylesterase activity
CG31291	8.8	Ch-enriched (stage 11-16)	Not affected	
CG3769	9.8 (16.1)	Ch-enriched (stage 11-15)	Reduced expression	Dynein-2 LIC Retrograde transport
CG13125	9.4	Ch-specific (stage 11-16)	Not affected	
CG31320		Ch-specific (stage 11-16)	Reduced expression	Homologue of HEATR2
nan	(2.1)	Ch-specific (stages 15-17)	Reduced expression	TRPV
iav	absent	Ch-specific (stages 15-17)	Reduced expression	TRPV
CG5359	2.2 (5.0 at atot1)	Ch-specific (stage 11-14)	Not affected	Dynein-2 LC, retrograde transport?
king tubby	1.1 (4.2 at atot1)	Pan-neural (stage 11-17)	Not affected	IFT-A accessory, retrograde transport
dila/ CG1625	9.3	Ch-enriched (stage 11-16)	Not affected	Transition zone protein
robo3	absent	Ch neurons & CNS (late stages)	Not affected	Axon guidance
CG15161	6.9	Ch-enriched (stage 11-16)	Not affected	IFT-B
btv	8.7 (16.3)	Ch-enriched (stage 11-15)	Moderately reduced expression	Dynein-2 HC, retrograde transport
Dhc93AB	3.8	Ch-specific (stage 11-16)	Reduced expression	Axonemal Dynein

Table 4.1: Genes selected for the initial *in situ* hybridisation screen. Most were selected for their high enrichment (fold change) in Ch cells at the atot3 or catot4 time points in the microarray data (Cachero et al., 2011). Others such as *nan*, *iav* & *robo3* were selected due to their reported Ch-specific expression and importance in Ch neuron function. *CG31320* was selected due to predicted protein-protein interactions with other Ch genes. Expression patterns are described as Ch-specific, Ch-enriched (high expression in Ch cells, low in ES cells) or pan-neural (all PNS and CNS) along with approximate embryonic stages when expression can be seen. This screen identified 9 genes with reduced expression in *fd3F*^{1} embryos.

Gene	Enrichment at catot4	Expression Pattern	Expression in *fd3F*^{1} embryos	Function
rempA	4.4	Ch-enriched (stages 11-16)	Moderately reduced expression	IFT-A
Oseg6	7.4	Ch-enriched (stages 11-16)	Moderately reduced expression	IFT-A
nompB		Ch-enriched (stages 11-16)	Not affected	IFT-B
Dhc62B	6.1	Ch-specific (stages 12-15)	No expression	Axonemal Dynein
Dhc16F	2.9	Ch-specific (stages 12-15)	Reduced expression	Axonemal Dynein
CG13930	5.7	Ch-specific (stages 12-15)	No expression	Axonemal Dynein
smet/ CG31623	8.6	Ch-specific (stages 11-16)	Reduced expression	Dynein arm assembly
tilB	3.9	Ch-specific (stages 11-17)	Reduced expression	Dynein arm assembly
CG14905	27.3	Ch-specifc (Stages 11-16)	Reduced expression	Dynein arm assembly
tektin-A	8.0	Ch-specific	Reduced expression	IDA assembly/ attachment
tektin-C	2.1	Ch-specific	Not affected	IDA assembly/ attachment
CG8800	2.5	Ch-specific	No expression	Axonemal dynein
CG6971	6.0	Ch-specific	Reduced expression	Axonemal dynein
CG16789/ Iqca	6.6	Ch-specific	Not affected	AAA-type ATPase, dynein HC?

Table 4.2: Genes added to the in situ hybridisation screen based on the morphology of *fd3F*^{1} Ch neurons and targets identified by the initial screen. These include IFT-A genes, the IFT-B gene *nompB* as a negative control and genes predicted to have a role in motility of the Ch cilium.

4.2.1.1 Many Ch-specific or enriched genes are not down-regulated in *fd3F*^{1} embryos

About half of the genes analysed in the initial screen showed no loss of expression in *fd3F*^{1} mutants. This is not surprising given the lack of severe morphological defects observed in *fd3F*^{1} Ch neurons. While the function of many of these genes is not

known, those with known function are all directly involved in formation of structural features of Ch neurons (figure 4.03). These are discussed in detail below.

(i) IFT-B complex genes

IFT-B complex proteins are required for anterograde IFT during ciliogenesis. The IFT-B proteins connect cargo proteins to the kinesins that transport cargo from the base of the cilium towards the tip. Mutation of IFT-B genes severely impairs ciliogenesis resulting in either very truncated or missing cilia (Iomini *et al*., 2001; Wang *et al*., 2009; Fan *et al*., 2010). fd3F would therefore not be expected to regulate IFT-B genes since *fd3F*^{1} mutants are able to form full-length cilia. My screens included two genes known to encode IFT-B proteins: *CG15161*, a homologue of *Chlamydomonas* and vertebrate IFT-46 and *dyf-6* in *C. elegans* expressed exclusively in ciliated cells (Hou *et al*., 2007; Bell *et al*., 2006; Avidor-Reiss *et al*., 2004) and *no mechanoreceptor potential B* (*nompB*), a homologue of *Chlamydomonas* IFT-88 and mammalian Polaris (Eberl *et al*., 2000; Han *et al*., 2003). NOMPB localises to sensory cilia and *nompB* mutants have truncated cilia characteristic of IFT-B mutants (Han *et al*., 2003). *CG15161* and *nompB* are expressed in both Ch and ES neurons in *Drosophila* embryos and, as expected, neither showed any reduced expression in *fd3F*^{1} mutants (figure 4.03A &B).

(ii) Dilatory (*dila*, *CG1625*)

dila encodes a coiled-coil domain protein expressed in ES and Ch neurons (Cachero *et al*., 2011). In Ch neurons DILA localises to the basal body and transition zone at the base of the cilium and is essential for assembly of cilia (Ma & Jarman, 2011).

Despite its Ch-enriched expression pattern there was no loss of *dila* expression in *fd3F*^{1} embryos and again this was to be expected since *fd3F*^{1} Ch cilia do not show the severe truncation observed in *dila* mutants (figure 4.03C).

(iii) CG6129

CG6129 encodes the only Drosophila homologue of the mammalian Rootletin family proteins (Laurençon *et al*., 2007). Rootletin is an essential structural component of the ciliary rootlets of motile cilia and is required to anchor the cilium (Yang *et al*., 2005). It associates with the proximal ends of basal bodies and is required for basal body and centrosome cohesion in mammalian cells (Yang *et al*., 2002; Bahe *et al*., 2005; Yang *et al*., 2006). Knockdown of *CG6129* by RNAi results in disruption of ciliary rootlets and dissociation of basal bodies in adult JO Ch neurons (Katarzyna Styczynska, unpublished) suggesting that *Drosophila* CG6129 is also functionally similar to mammalian rootletin. However this phenotype was not observed in *fd3F* mutants and it is therefore not surprising that there was no decrease in *CG6129* expression in *fd3F*^{1} embryos (figure 4.03D).

(iv) robo3

As discussed in the previous chapter *robo3* encodes a Ch specific receptor for the midline repellent slit (Zlatic *et al*., 2003). *robo3* was considered to be a good candidate for an fd3F target since it is expressed too late during development to be regulated by ato directly and mis-localisation of Ch axon terminals would be expected to cause proprioceptive defects without affecting morphology of Ch cilia.

However no reduction in *robo3* mRNA was observed in *fd3F*^{1} embryos suggesting that this is not the case.

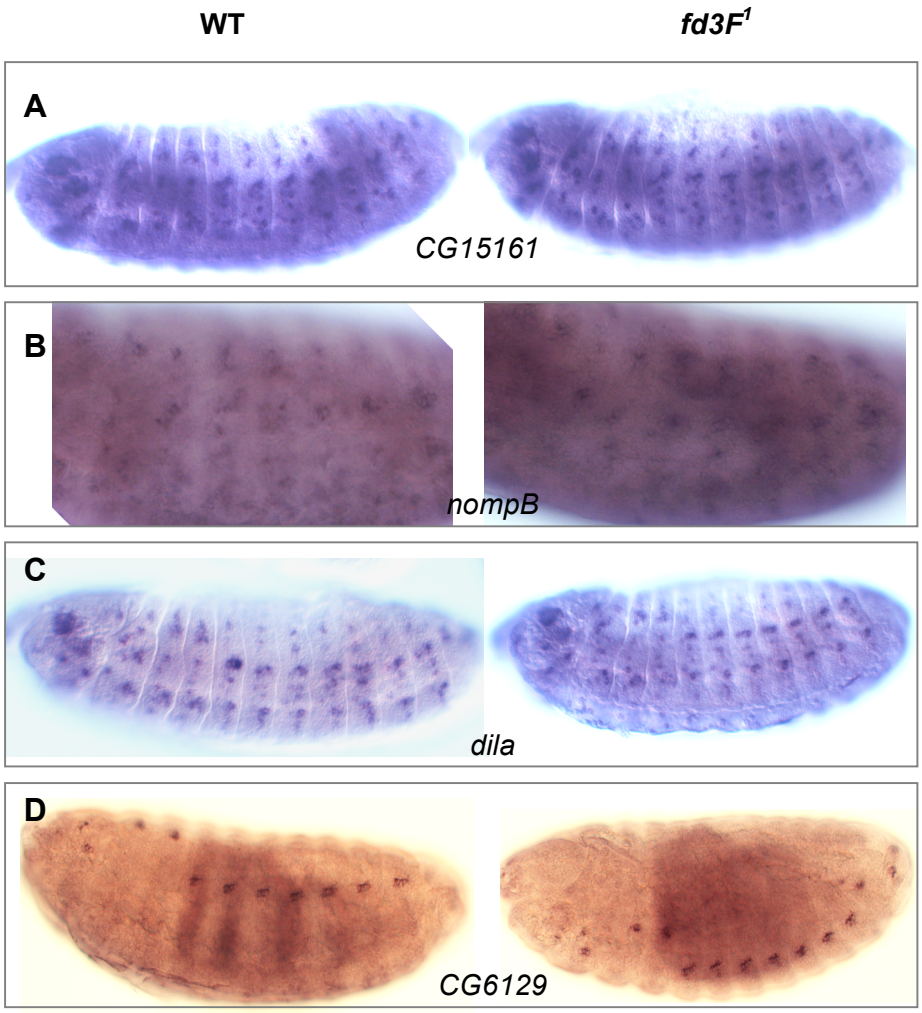

Figure 4.03: Genes with unaltered expression in *fd3F*^{1} embryos. A & B genes of the anterograde ITF-B complex *CG15161* (IFT46) and *nompB* (IFT88). C & D other genes required for formation of Ch cilia, *CG6129* (*rootletin*) and *dila* (*CG1625*).

4.2.1.2 Genes down-regulated in *fd3F*^{1} embryos

The two screens did however identify 20 genes with reduced mRNA expression in *fd3F*^{1} embryos. Although the degree of loss of expression varied between genes

(summarised in table 4.1 & 4.2) suggesting that many of these genes may be only partially regulated by fd3F. These target genes are described in detail below. Crucially all of the target genes identified are known or predicted to have either a very subtle or no effect on Ch neuron morphology.

(i) TRPV ion Channel genes

nanchung (*nan*) and *inactive* (*iav*) encode two subunits of a vanilloid transient receptor potential (TRPV) cation channel. This channel is exclusively expressed in Ch neurons where it localises to the proximal segment of the cilium (Kim *et al*., 2003; Gong *et al*., 2004). The Nan/Iav channel has also been shown to be essential for Ch neuron function (Kim *et al*., 2003; Gong *et al*., 2004). The proprioceptive defects observed in *nan* and *iav* mutants are very similar to those observed in $fd3F^{1}$ flies. *nan* and *iav* were therefore considered to be good candidates to be regulatory targets of fd3F and were included in the initial screen despite being expressed too late during embryogenesis to feature in the *ato* microarray data. *nan* and *iav* expression is clearly reduced in $fd3F^{1}$ embryos although it is not completely absent suggesting these genes may be at least partially regulated by other transcription factors (figure 4.04). Loss of the Nan/Iav channel in $fd3F^{1}$ mutants would certainly impair Ch neuron function and would also not be expected to affect structural morphology so this can at least partially explain the $fd3F^{1}$ phenotype.

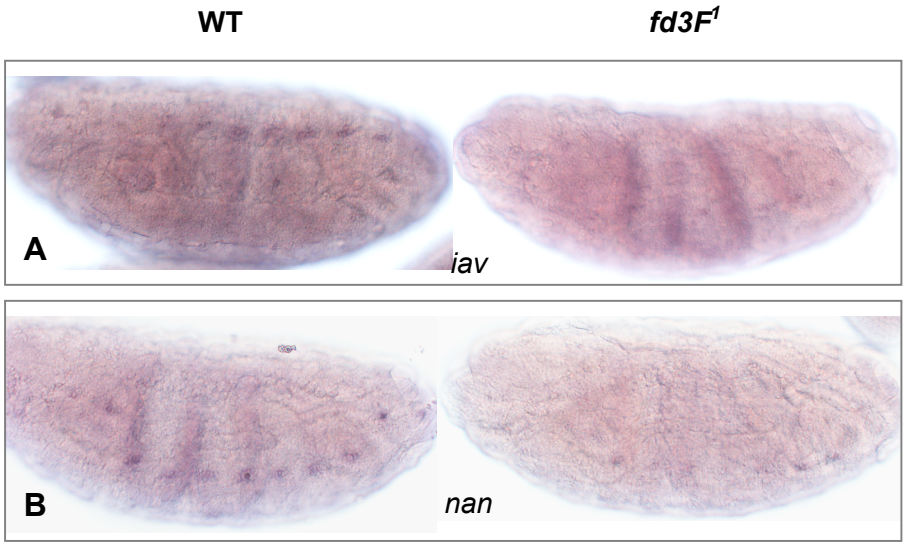

Figure 4.04: Expression of the TRPV channels is reduced in *fd3F*^{1} embryos. RNA in situ hybridisation for A) *iav* and B) *nan* show reduced expression in *fd3F*^{1} embryos compared with WT.

(ii) Retrograde transport genes

Retrograde IFT is required to move cargo form the ciliary tip back towards the cell body and this is particularly important for recycling the anterograde transport machinery. Dyneins act as the retrograde transport motors and cargo is attached to these dyneins via interaction with IFT-A complex proteins. In *Drosophila* the IFT-A complex is thought to be composed of five proteins: *oseg1*, *reduced mechanoreceptor potential A* (*rempA*/ *oseg3*), *oseg4*, *oseg6* and *CG5780*. I found down-regulation of two of these genes (*rempA* and *oseg6*) in *fd3F*^{1} embryos.

rempA encodes the *Drosophila* homologue of mammalian IFT140. *rempA* mutants have shortened cilia and accumulate the IFT-B complex protein NompB towards the tips of the cilia (Lee *et al*., 2008), however although NompB does appear to

accumulate in *fd3F*^{1} JO cilia *fd3F*^{1} Ch cilia appear to be of normal length. This slightly less severe morphological effect could be because *rempA* is only partially knocked down in *fd3F*^{1} mutants (figure 4.05C). RempA-YFP has been shown to localise to the ciliary dilation in Ch neurons and the ciliary dilation is absent in *rempA* mutants (Lee *et al*., 2008). The Nan/ Iav channel is also mislocalised in *rempA* mutants, spreading into the distal segment of the cilium rather than being restricted to the proximal segment (Lee *et al*., 2008) suggesting that in addition to recycling the anterograde transport machinery IFT-A proteins may have a role in segregating proteins between the two compartments of the cilium. Since *oseg6* is also down-regulated in *fd3F*^{1} embryos it is possible that fd3F is at least partly responsible for regulation of IFT-A genes in Ch neurons (figure 4.05D).

I also observed moderate down-regulation of *beethoven* (*btv*), which encodes a cytoplasmic dynein heavy chain (motor) protein predicted to have a role in retrograde IFT (figure 4.05B). *btv* mutants have strongly reduced sound-evoked potentials (Eberl et al., 2000; Tauber et al., 2001) and *btv* mutant larvae show an impaired ability to crawl in a straight line similar to the crawling defects of both *ato*^{1} and *fd3F*^{1} larvae (Caldwell *et al*., 2003). Taken together these defects suggest that *btv* is essential for Ch neuron function, however Ch neurons in *btv*^{1} mutants show only minor morphological defects; embryonic Ch neurons have normal length cilia but lack a clearly defined ciliary dilation while adult JO neuron ciliary dilations lack the regular substructure seen in wild type (Caldwell *et al*., 2003; Eberl *et al*., 2000). Notably the embryonic Ch neuron morphology at least seems very similar to that seen in *fd3F*^{1} embryos (see previous chapter).

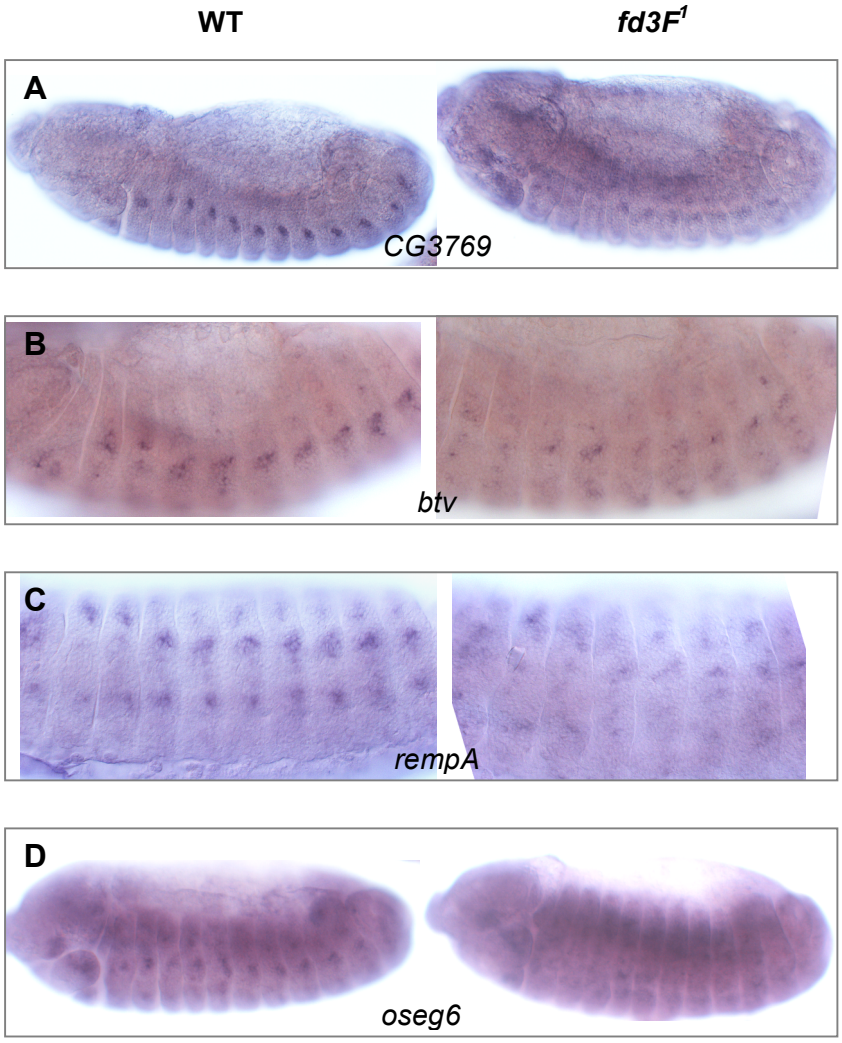

Figure 4.05: Retrograde transport genes down-regulated in *fd3F*^{1} embryos. A & B cytoplasmic dynein-2 genes, *btv* (heavy chain) and *CG3769* (D2LIC). C & D IFT-A complex genes, *rempA* (IFT140) and *oseg6* (IFT144).

Interestingly I also saw down-regulation of *CG3769* (figure 4.05A), a predicted orthologue of *Chlamydomonas* dynein-2 light intermediate chain (LIC) (Mische *et al*., 2008). Dynein LICs are thought to bind directly to dynein heavy chains and mediate the attachment of cargo (Purohit *et al*., 1999). LICs are also unique to the cytoplasmic form of dynein, which is required for IFT and trafficking rather than

ciliary motility (Vallee *et al*., 2004; Hook & Vallee 2006) and the dynein-2 form is required for IFT during cilium assembly. It is therefore likely that *CG3769* is involved in retrograde IFT. *CG3769* also has a Ch-enriched expression pattern similar to that of other genes required for IFT. Although the *CG3769* mutant phenotype is not known, the effect on Ch neuron morphology would not be expected to be any more severe than that of *btv* or the IFT-A complex genes making it a plausible regulatory target of fd3F. The enhancer for *CG3769* has been identified (Katarzyna Styczynska, unpublished) and contains at least one well-conserved forkhead factor binding site. *CG3769* could therefore be regulated by fd3F directly.

(iii) Axonemal Dyneins

The initial screen also identified *Dhc93AB* as a regulatory target of *fd3F* (figure 4.06A). *Dhc93AB* encodes another dynein heavy chain protein and is a predicted orthologue of mouse axonemal dynein *Dnahc11* and *Dnahc9*. Unlike other dynein motors such as *btv*, *Dhc93AB* expression is Ch-specific and since Ch cilia (but not ES cilia) are thought to be motile (Göpfert & Robert, 2003), Dhc93AB may be a component of the axonemal dynein arms required for motility of the Ch cilium. Loss of *Dhc93AB* expression in $fd3F^{1}$ mutants could explain the missing dynein arms observed in $fd3F^{1}$ Ch cilia by electron microscopy and defects in ciliary motility could also explain the uncoordinated phenotype of $fd3F^{1}$ flies.

It is possible therefore, that one key role of *fd3F* is in regulating genes required for motility of the Ch cilium. To investigate this the second screen included three other predicted axonemal dynein genes that could have a role in motility. *Dhc16F* (a

predicted orthologue of human *DNAH6*), *Dhc62B* (possible orthologue of *DNAH7* and *DNAH3*) and *CG13930* (*IC138*, *wdr78*) all featured in the *ato* microarray data although they were not among the most highly enriched genes and so had not been included in the original screen. *Dhc62B* and *CG13930* are strongly down-regulated in $fd3F^{1}$ embryos and there was also some loss of *Dhc16F* expression (figure 4.06). Subsequently two other genes predicted to encode axonemal dynein light chains, *CG8800* and *CG6971*, were also found to have reduced expression in $fd3F^{1}$ embryos (Petra zur Lage, unpublished).

I also observed reduced expression of *smetana* (*smet*) in $fd3F^{1}$ embryos (figure 4.06E). Smet is encoded by *CG31623*, the gene previously called *dtr* (Daniel Eberl, personal communication to Andrew Jarman), and is known to be required for Ch neuron motility. The precise role of Smet is not known, however like TilB it contains leucine-rich repeats and so may be involved in dynein arm assembly along with TilB. Three other non-dynein genes required for motility of Ch cilia (*tilB*, *tektin-A* and *CG14905*) also showed reduced or no expression in $fd3F^{1}$ embryos (Petra zur Lage, unpublished). Tektins are required for ciliary stability and have been suggested to have a role in inner dynein arm assembly or attachment (Tanaka *et al*., 2004; Amos *et al*., 2008). CG14905 is a predicted orthologue of Chlamydomonas ODA-1, which is also required for dynein arm assembly (Fowkes & Mitchell, 1998). fd3F could therefore be the main regulator ciliary motility genes in *Drosophila* Ch neurons.

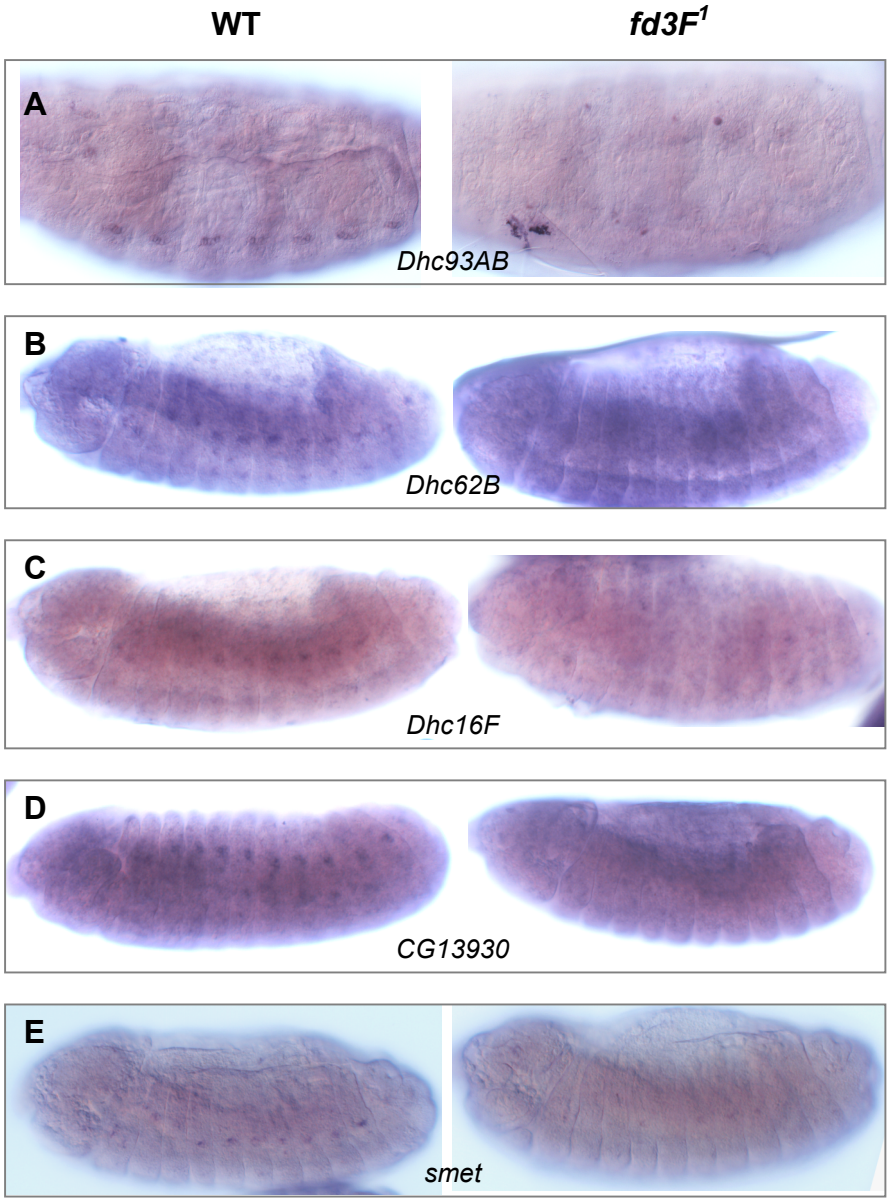

Figure 4.06: fd3F regulates genes required for motility of the Ch neuron cilium. A-D axonemal dynein genes, Dhc93AB (Dnahc11), Dhc62B, Dhc16F and CG13930 (Dnai/ Wdr78). E) smetana is thought to be required for dynein arm assembly. All are absent or severely reduced in fd3F^{1} embryos.

(iv) Other fd3F target genes

The four other Ch-specific genes (figure 4.07) found to have reduced expression in *fd3F*^{1} embryos are described below. Much less is known about the function of these genes compared to the other identified fd3F targets, however the specificity of their expression patterns would suggest they have an important role in Ch neuron specialisation. Two of these genes (*CG31320* and *CG11253*) have human homologues.

CG31320 encodes a predicted orthologue of HEATR2. HEAT repeat containing proteins have been associated with a variety of functions including intracellular vesicle trafficking and chromatin remodelling (Neuwald & Hirano, 2000) although the exact role of CG31320 in Ch neurons is not known. Knockdown of *CG31320* by RNAi results in an uncoordinated phenotype in adult flies but causes only minor defects in Ch neuron morphology (Girish Mali, unpublished) making it a plausible fd3F target. *CG11253* encodes a zinc finger protein and is predicted to be an orthologue of *BLU* (*ZMYND10*), which is thought to act as a tumour suppressor (Liu *et al*., 2003; Qiu *et al*., 2004). *Zmynd10*, the mouse orthologue of *BLU* has also been identified as a ciliary gene (McClintock *et al*., 2008). In addition CG11253 has been shown to interact with TilB (CG14620) in a yeast-two-hybrid screen (Giot *et al*., 2003) so it is possible that CG11253 may also be required for ciliary motility.

CG6980 is a Ch-specific tetratricopeptide repeat (TPR) family gene. TPR folds mediate reversible protein-protein interactions and are found in proteins with a variety of functions. In particular, TPR repeats have been identified in proteins

encoded by the Oseg genes, which are known to be involved in intraflagellar transport (Avidor-Reiss *et al*., 2004) and also in kinesin light chain proteins (EMBL InterPro). It is therefore possible that CG6980 may have a role in IFT or transport of proteins within Ch neuron cilia.

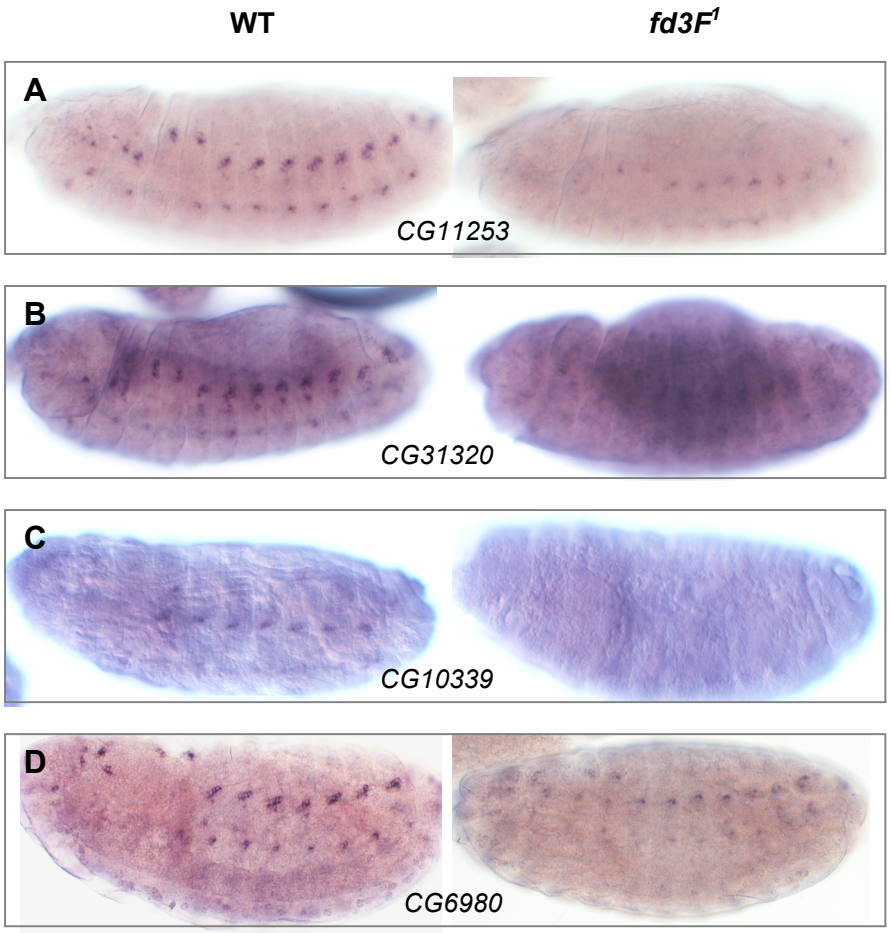

Figure 4.07: Uncharacterised Ch-specifc genes with reduced expression in *fd3F*^{1} embryos.

CG10339 encodes a predicted carboxylesterase expressed exclusively in Ch neurons. The role of *CG10339* in Ch neuron differentiation is not clear, however the specificity of its expression and the fact that it is knocked down in *fd3F*^{1} embryos

supports a role in either assembly of axonemal dyneins or compartmentalisation of the Ch cilium.

4.2.1.3 Verification of fd3F target genes using RT-PCR

RNA was extracted from w^{1118} and $fd3F^{1}$ embryos as described in materials and methods. Since the majority of the identified target genes exhibited strongest expression during the later stages of embryogenesis (stages13 to 17) embryo collection was timed to ensure that most embryos would be between these stages. Flies were allowed to lay eggs for 14 hours at 25°C and the plates were then changed and the resulting embryos were aged at 25°C for a further 5 hours. Approximately 30mg of embryos were collected for each genotype for RNA extraction. The concentration of RNA obtained was calculated from measuring the OD at 260nm and equal concentrations of RNA from each genotype were reverse transcribed to produce complete cDNA.

Small fragments of several of the target genes were amplified from w^{1118} and $fd3F^{1}$ cDNA by PCR. The relative concentration of amplified product was then estimated by comparing the intensity of bands on an electrophoresis gel. Two genes not thought to be targets (*CG15161* and *CG3085*) were used as controls and, as expected, in both cases there was no difference in the intensity of the bands amplified from w^{1118} and $fd3F^{1}$ cDNA (figure 4.08). Expression of two other IFT-A complex genes *oseg1* and *oseg4* in $fd3F^{1}$ embryos was also tested by this method since it was not possible to make successful *in situ* probes for these genes.

CG6980, *CG3769*, *iav*, *Dhc93AB*, *rempA* and *oseg6* all showed some reduction in product amplified from *fd3F*^{1} cDNA compared with *w*^{1118} cDNA (figure 4.08). *CG6980*, *CG3769*, *iav* and *rempA* all appear to be about 50% reduced while *Dhc93AB* is about 30% reduced. While this is consistent with the *in situ* data as there is still some residual mRNA expression observed for all of these genes, the reduction in expression does not seem as dramatic as that observed by *in situ* hybridisation. This could be because, since the PCR is not quantitative, the amplification reaction reaches an end point faster when *w*^{1118} cDNA is used as a template and the *fd3F*^{1} amplification catches up. The relative amount of product from each reaction is therefore not a true reflection of the difference in cDNA level for each gene.

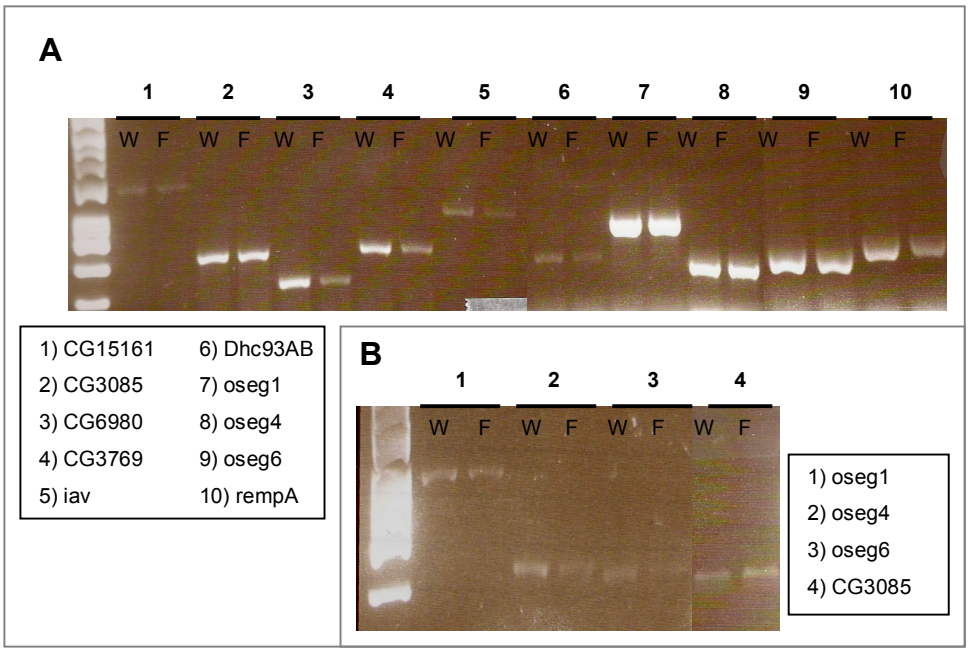

Figure 4.08: RT-PCR to confirm reduced expression of target genes in *fd3F*^{1} embryos. Fragments amplified from complete cDNA from *w*^{1118} (W) and *fd3F*^{1}(F) embryos. A) 25 cycles, *CG15161* and *CG3085* amplified as controls (no reduced expression in *fd3F*^{1}) 5μl loaded. *CG6980*, *CG3769*, *iav*, *Dhc93AB* and *rempA* expression is reduced in *fd3F*^{1} embryos. B) 20 cycles, 2μl loaded. *CG3085* used as a control. *Oseg4* and *oseg6* expression is reduced in *fd3F*^{1} embryos, *oseg1* expression may be slightly reduced.

This may also explain the very slight reduction in the amount of *oseg6* amplified from *fd3F*^{1} cDNA compared with *w*^{1118} despite the observed down-regulation shown by RNA *in situ* and also why *oseg1* and *oseg4* initially showed no reduced expression in *fd3F*^{1} embryos by this method. When the number of cycles used in the PCR reaction was reduced (figure 4.08B) there was a clear reduction in the level of *oseg4* and *oseg6* cDNA amplified (almost 50% reduced) however there was still only minimal reduction in the level of *oseg1*. This could be because *fd3F* has less influence over the regulation of *oseg1* or it may be that *oseg1* has stronger expression in ES cells than some of the other Ch-enriched genes during the developmental stages of the embryos used for the RNA preparation. Gene expression in ES cells would not be expected to be affected by *fd3F* deficiency but would contribute to the total mRNA expression of whole embryos. Quantitative RT-PCR (qRT-PCR) could be used to resolve whether the differences in band intensity (particularly those observed for *oseg1*, *4* and *6*) represent real changes in mRNA expression.

4.2.1.4 Expression of target genes in *fd3F*^{1}/ *ED6716* embryos

All of the target genes identified also showed reduced expression in *fd3F*^{1}/ *ED6716* embryos. Virgin female *ED6716*/ *FM7h* flies were crossed to *fd3F*^{1} males and the *in situs* for several of the target genes were repeated on the resulting embryos. In each case approximately 50% of the embryos showed reduced mRNA expression compared to wild type (table 4.3). These embryos are predicted to be *fd3F*^{1}/ *ED6716* females and hemizygous *ED6716* males, although it was not possible to detect a difference in expression level between these two groups. To confirm this result *in situ* hybridisations were also repeated using *dila* and *CG15161* probes as controls. In

both cases fewer than 10% of the embryos showed any reduction in staining compared to wild type.

	fd3F^{1} x ED6716/ FM7h		Wild type	
Gene	**% embryos with reduced expression**	**Total number of embryos counted**	**% embryos with reduced expression**	**Total number of embryos counted**
Btv	46.0	76	7.8	64
CG10339	47.7	65	8.5	47
CG11253	56.0	75	8.1	74
RempA	42.0	69	6.2	65
CG15161	6.7	60	5.0	60
dila	9.3	54	7.7	52

Table 4.3: Percentage of embryos collected from *fd3F^{1}* x *ED6716/ FM7h* and wild type (*w^{1118}*) cages with reduced staining in RNA in situs. Only embryos from stages expected to have the strongest expression were counted (stages 13-15 in most cases, stage 16-17 for *CG10339*).

There appeared to be little difference in the level of down-regulation in *fd3F^{1}/ED6716* compared with *fd3F^{1}* homozygotes for most of the target genes suggesting that *fd3F^{1}* may be close to a genetic null. Since expression of target genes is not completely lost even in *fd3F^{1}/ ED6716* embryos, it is likely that these genes are co-regulated by other transcription factors and loss of fd3F is therefore not sufficient to completely abolish expression of its target genes. Many fd3F targets are also predicted to be regulated by Rfx and this will be discussed further later in this chapter.

4.2.2 *nan* and *iav* are directly regulated by fd3F

4.2.2.1 The enhancers of *nan* and *iav* contain two conserved forkhead factor binding sites

The enhancers for *nan* and *iav* have been identified in earlier work and enhancer-GFP reporter lines are available for both genes (Kim *et al*., 2003; Lynn Powell, unpublished). The GFP reporter constructs include 560bp of sequence upstream of *nan* and 600bp of sequence upstream of *iav* cloned into the PH-Stinger vector. These constructs were injected into *w*; *Δ2-3* flies and the resulting transformant lines express GFP specifically in Ch neurons in late stage embryos and larvae. When *nan*-GFP and *iav*-GFP lines were crossed into the $fd3F^{1}$ background GFP expression (both mRNA and protein) was completely abolished (figure 4.09). This indicates that fd3F is required to allow expression from these enhancers. However the fact that *iav* mRNA expression does not completely disappear in $fd3F^{1}$ embryos (as shown by both *in situ* hybridisation and RT-PCR) suggests that there may also be a secondary enhancer that is not dependent on fd3F.

Both the *nan* and *iav* enhancers were found to have two sites closely matching the consensus sequence for a forkhead factor binding site (fkh) (A/G)(T/C)(A/C)AA(T/C)A (Lee & Frasch 2004) and these are highly conserved across *Drosophila* species (figure 4.09B &C). These sites will be referred to as iav-fkh1, iav-fkh2, nan-fkh1 and nan-fkh2 hereafter and the sequences of these sites are listed in table 4.4 below.

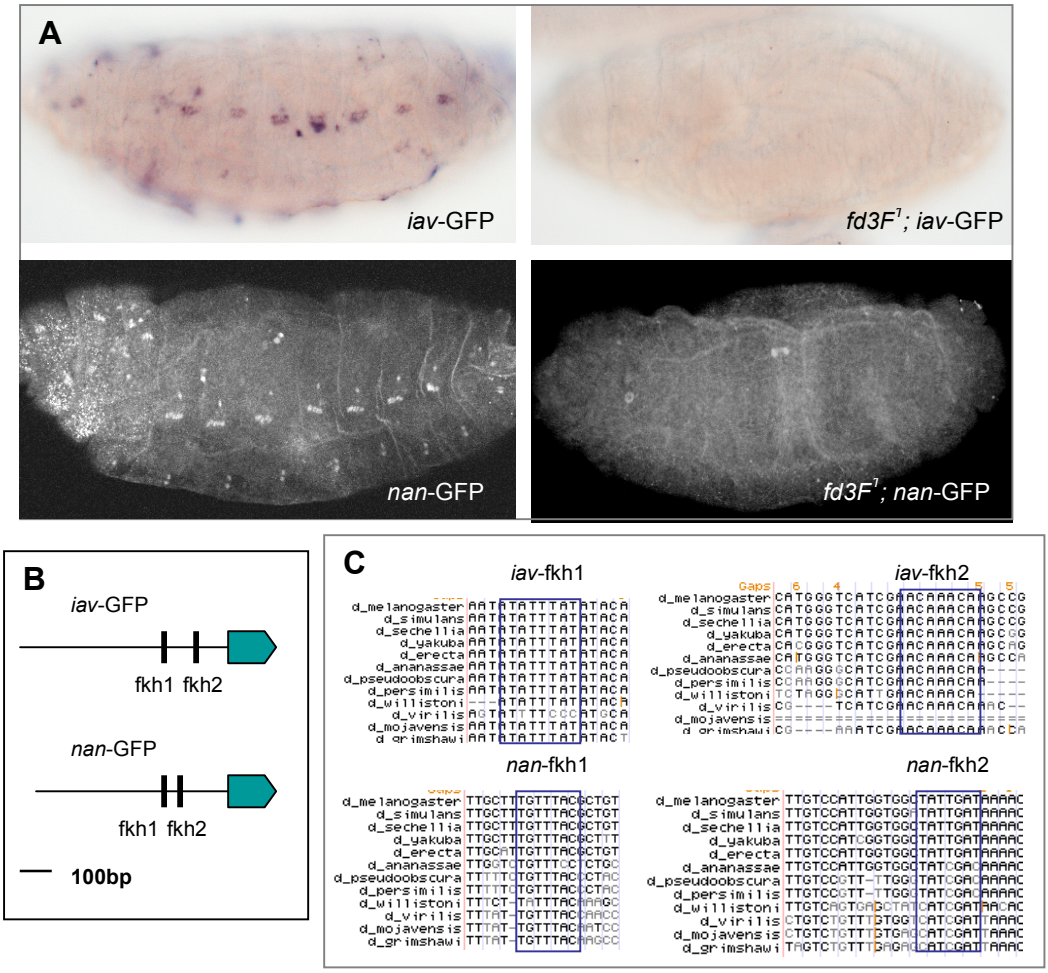

Figure 4.09: Expression from *iav* and *nan* enhancers is *fd3F*-dependent. A) GFP expression driven by *iav*-GFP and *nan*-GFP enhancer constructs detected by mRNA in situ and anti-GFP respectively. GFP expression is abolished in *fd3F*^{1} background. B) Maps of *iav*-GFP and *nan*-GFP enhancer constructs, both include two forkhead factor binding sites (fkh1 & 2). C) Alignments showing conservation of fkh sites from *iav* and *nan* enhancers across several *Drosophila* species (from UCSC Genome Browser).

iav-fkh1	ATAAATA (reverse strand)
iav-fkh2	ACAAACA (forward strand)
nan-fkh1	GTAAACA (reverse strand)
nan-fkh2	ATCAATA (reverse strand)

Table 4.4: Sequences of conserved fkh sites in *iav* and *nan* enhancers

In both cases the fkh sites are located either side of a conserved Rfx binding site (X-box) (GTNRCC(N1-3)RGYAAC) suggesting that a combination of fd3F and RFX may be required to regulate *nan* and *iav* expression. This will be discussed later in the chapter.

4.2.2.2 Mutation of fkh sites in *iav* and *nan* enhancers

To investigate whether these sites are required for expression of *nan* and *iav* I used site directed mutagenesis to disrupt all four sites in the original enhancer constructs. Mutations in the 5th and 6th positions within the fkh site consensus (A and C/T) have previously been shown to prevent forkhead factor binding in vitro (Kaufmann *et al*., 1995). These bases were therefore changed to CG in each case. Three different mutant constructs were made for each enhancer; one with both fkh sites mutated (*iav*-F1F2-GFP and *nan*-F1F2-GFP) and one with each fkh site mutated individually (*iav*-F1-GFP, *iav*-F2-GFP, *nan*-F1-GFP and *nan*-F2-GFP). The constructs were sequenced to ensure they contained the correct mutation and that no other bases in the sequence had been altered during mutagenesis and then injected into *w*; *Δ2-3* flies.

Several transformant lines were obtained for each mutant construct. Mutation of both fkh sites simultaneously (*iav*-F1F2-GFP and *nan*-F1F2-GFP) resulted in complete loss of GFP expression in embryos (figure 4.10). This was confirmed by anti-GFP immunostaining in embryos from three different transformant lines for each construct. In both cases knocking out the fkh1 site had no effect on GFP expression (*iav*-F1-GFP and *nan*-F1-GFP, figure 4.10). However mutation of the fkh2 site in

each construct (*iav*-F2-GFP and *nan*-F2-GFP, figure 4.10) completely abolished GFP expression. Again each of these results was confirmed in embryos from two or three independent transformant lines. This implies that the *iav*-fkh2 and *nan*-fkh2 sites are essential to allow transcription from these enhancers.

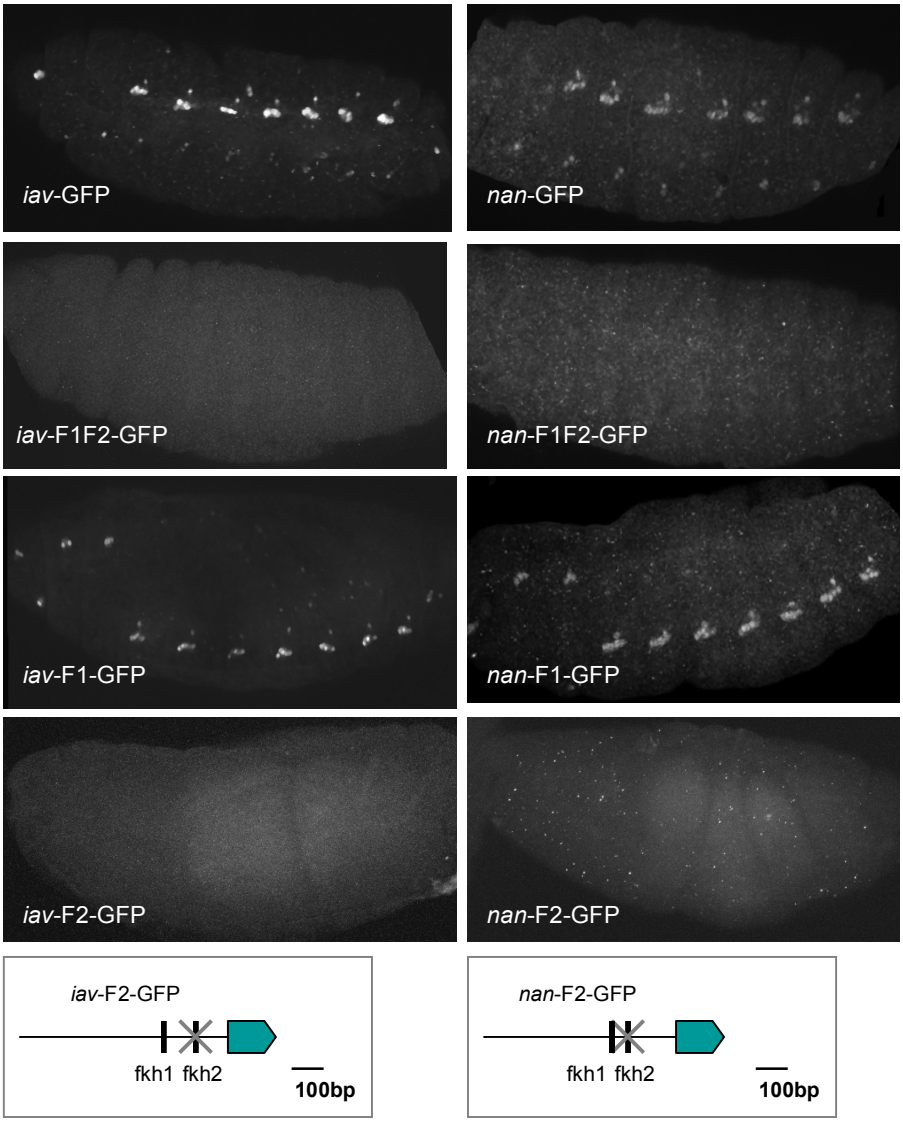

Figure 4.10: Mutation of fkh sites in *iav*-GFP and *nan*-GFP enhancer constructs. Embryos stained with MAb-GFP. In both constructs mutation of both fkh sites (F1F2) abolishes GFP expression while mutation of fkh1 alone (F1) has no effect on GFP expression. However in both cases mutation of fkh2 alone (F2) is sufficient to prevent GFP expression.

4.2.2.3 The fd3F forkhead domain binds specifically to *iav*-fkh2 and *nan*-fkh2 *in vitro*

In order to determine whether fd3F is able to bind to these predicted fkh sites in the *nan* and *iav* enhancers I carried out an electrophoresis mobility shift assay (EMSA) as described below. Purified fd3F forkhead domain was able to bind to radioactively labelled DNA fragments containing *iav*-fkh2 and *nan*-fkh2 but was unable to bind when these sites were mutated.

(i) Expression and purification of the fd3F forkhead domain

The predicted fd3F forkhead domain ($fd3F^{fd}$) is composed of 94 amino acids located near the N-terminus of the protein. I therefore decided to express a 120 amino acid peptide that includes this region. Expression of the forkhead domain only rather than the whole protein should make it more likely to fold correctly when over-expressed in *E. coli* and reduce the chance of forming insoluble aggregates. Several previous studies of other forkhead factor proteins have shown that the forkhead domain alone is sufficient for sequence-specific DNA binding (Kaufmann *et al*., 1995; Perez-Sanchez *et al*., 2000; Pierrou *et al*., 1994). The full-length fd3F ORF had already been amplified from cDNA and cloned into pSC-A vector (see Chapter 5) and a 360bp region from the 5' end of *fd3F* including the complete forkhead domain but not the ATG start codon was amplified from this clone. This 360bp fragment was then cloned into pGEX-2T to allow expression of $fd3F^{fd}$ as a GST fusion protein. The cloned $fd3F^{fd}$ was then sequenced to ensure no base changes had occurred that could alter the amino acid sequence.

The pGEX- fd3F^{fd} construct was used to transform competent BL21 *E. coli* that allow IPTG inducible expression of GST- fd3F^{fd}. Transformed cells from a single colony were grown to OD_{550} of 0.36 and then induced using either 0.5mM or 0.1mM IPTG for between 1 and 4 hours at both 37^{o}C and 20^{o}C to determine the optimal conditions for a high yield of soluble protein expression. Small samples were taken every hour from cultures under each of these conditions, resuspended in PBS and then sonicated and centrifuged to separate soluble and insoluble fractions (as described in materials & methods). The soluble and insoluble fractions were then run on an SDS-PAGE gel next to an uninduced control sample. When cultures were induced at 37^{o}C most of the GST-fd3F^{fd} produced was in the insoluble phase even after only 2h induction. The results for induction at 20^{o}C are shown in figure 4.11A. Induction at 20^{o}C with 0.5mM IPTG produced a good yield of soluble fusion protein after 2h induction however GST- fd3F^{fd} became increasingly insoluble with longer induction times. Large-scale induction of GST- fd3F^{fd} expression was therefore carried out at 20^{o}C for 2h using 0.5mM IPTG.

Fd3F^{fd} was purified from the soluble fraction by overnight incubation with glutathione-sepharose beads (see materials & methods for detailed protocol). After incubation a small sample of the supernatant was kept for comparison on SDS-PAGE (unbound supernatant, figure 4.11). Initially 12.5mM reduced glutathione in 50mM Tris pH8 was used to elute fd3F^{fd} from the beads, however this produced a very low yield of purified fd3F^{fd}. I therefore repeated the purification and tried three alternative elution buffers. The first (12.5mM reduced glutathione in 50mM Tris + 0.1% triton-X-100) had no effect on the yield of eluted protein however both buffer 2

(50mM reduced glutathione in 250mM Tris pH8) and buffer 3 (buffer 2 + 0.4% deoxycholate) gave a good yield of purified fd3F^{fd} (elution 1 & 2, figure 4.11B). The approximate protein concentration of the fractions eluted with buffer 2 and 3 was calculated from the OD measured at 280nm. The fraction eluted using buffer 3 was used for the DNA binding assays since the strong detergent should help to prevent the protein from denaturing or aggregating.

(ii) fd3F^{fd} binds specifically to DNA containing iav-fkh2 and nan-fkh2

Double-stranded DNA probes were designed containing the *iav*-fkh2 and *nan*-fkh2 sequences. In each case the top strand was labelled with γ^{33}P-ATP. The labelled probes were incubated with purified fd3F^{fd} at the following concentrations: 0.5uM, 5uM, 12.5uM and 25uM and then run on an acrylamide gel. fd3F^{fd} was able to bind to both these DNA probes at protein concentrations above 12.5mM. I therefore used fd3F^{fd} at 12.5uM final concentration in all subsequent competitive mobility shift assays since the effect of adding competitor DNA should be more noticeable if the amount of protein used is close to the minimum required for binding.

Two other double-stranded probes containing mutated *iav*-fkh2 and *nan*-fkh2 sites. In each case the mutation was identical to that used in the *iav*-F2-GFP and *nan*-F2-GFP reporter constructs described above. These probes were left unlabelled and used as competitors in EMSA experiments (figure 4.11C). Addition of mutant probes even at 100-fold excess had no effect on fd3F^{fd} binding to the ^{33}P labelled probes. This suggests that fd3F^{fd} is unable to bind to these mutated forkhead factor binding sites. In addition when cold non-mutated probes were added as specific competitors at

100-fold excess binding of fd3F^{fd} to labelled DNA was strongly reduced (although addition at 50-fold excess had no effect). I therefore concluded that fd3F^{fd} is able to bind specifically to *iav*-fkh2 and *nan*-fkh2.

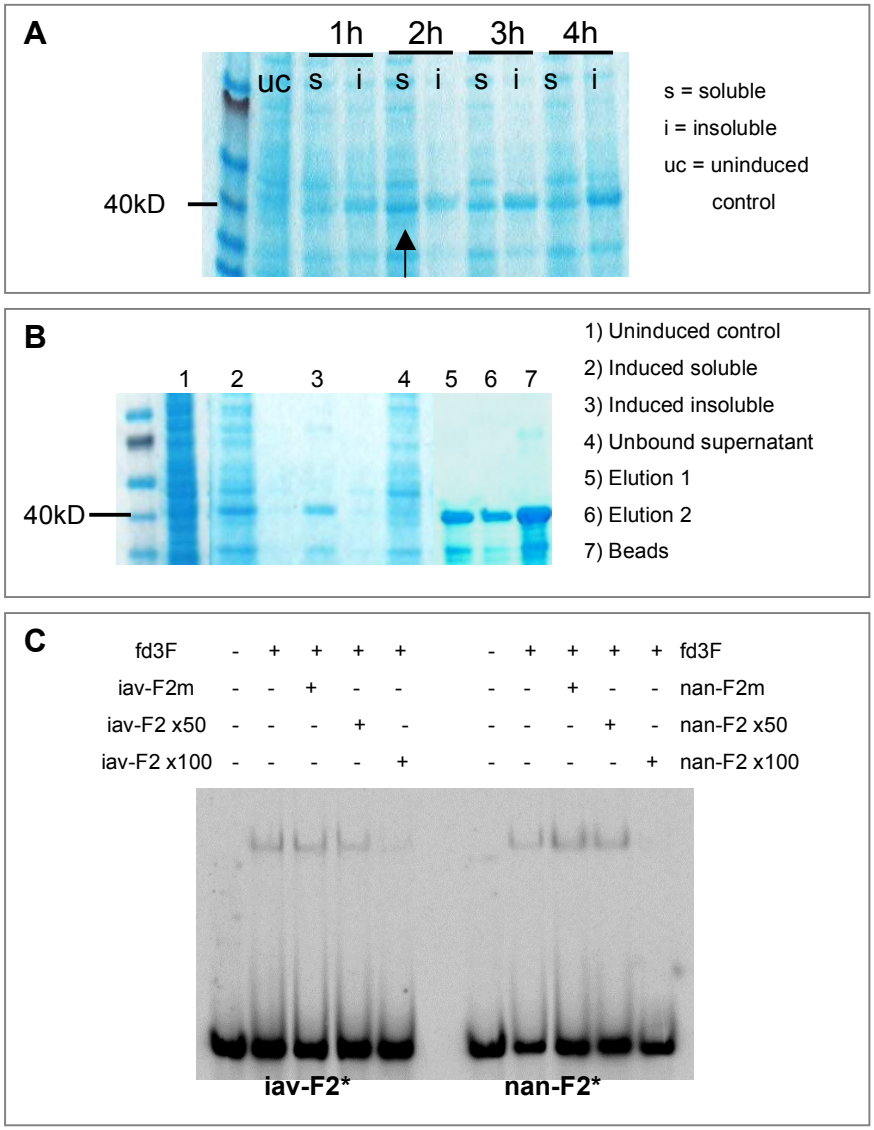

Figure 4.11: The fd3F forkhead domain binds specifically to *iav*-F2 and *nan*-F2 sites. A) Timecourse for IPTG induced expression of GST-fd3F^{fd} (0.5mM IPTG at 20^{o}C). Soluble and insoluble fractions from samples taken every hour for 4h. GST-fd3F^{fd} (40kD approx) is mostly in the soluble phase after 2h induction. B) SDS-PAGE showing GST-fd3F^{fd} at various stages of expression and purification. C) Competition EMSA using radioactively labelled iav-F2* and nan-F2* probes (see materials & methods for sequences). fd3F^{fd} and unlabelled competitors added as shown above.

This result, taken together with those described above, suggests that fd3F regulates *iav* and *nan* expression directly.

4.2.3 fd3F and Rfx may act co-operatively to regulate expression of Ch genes

4.2.3.1 *iav* and *nan* enhancers contain conserved X-boxes

As described above, alignment of the *nan* and *iav* enhancer sequences from different *Drosophila* species identified highly conserved X-boxes in both enhancers (figure 4.12). In both cases the X-box is located within 40bp of the fkh2 site. It is therefore possible that fd3F and Rfx may act co-operatively to regulate *nan* and *iav* expression. To test whether the X-boxes in these enhancers (referred to as *iav*-X and *nan*-X hereafter) are required to allow transcription of *nan* and *iav* the *iav*-X and *nan*-X sites were mutated in the enhancer-GFP constructs. In both X-boxes the middle pair of cytosines (CC) was changed to a pair of adenines (AA). This mutation was chosen since previous studies have shown that mutations in this position prevented Rfx binding to DNA in *in vitro* binding assays (Iwama et al., 1999; Sun et al., 1996). The mutations were confirmed by sequencing and the *iav*-X-GFP and *nan*-X-GFP constructs were injected into *w*; *Δ2-3* embryos.

iav-X	GTTA**CC**AGGACAAC
nan-X	GTTG**CC**AATGCAAC

Table 4.5: Sequences of conserved X-boxes in *iav* and *nan* enhancers. The pair of C residues (bold) were mutated to AA in *iav*-X-GFP and *nan*-X-GFP constructs.

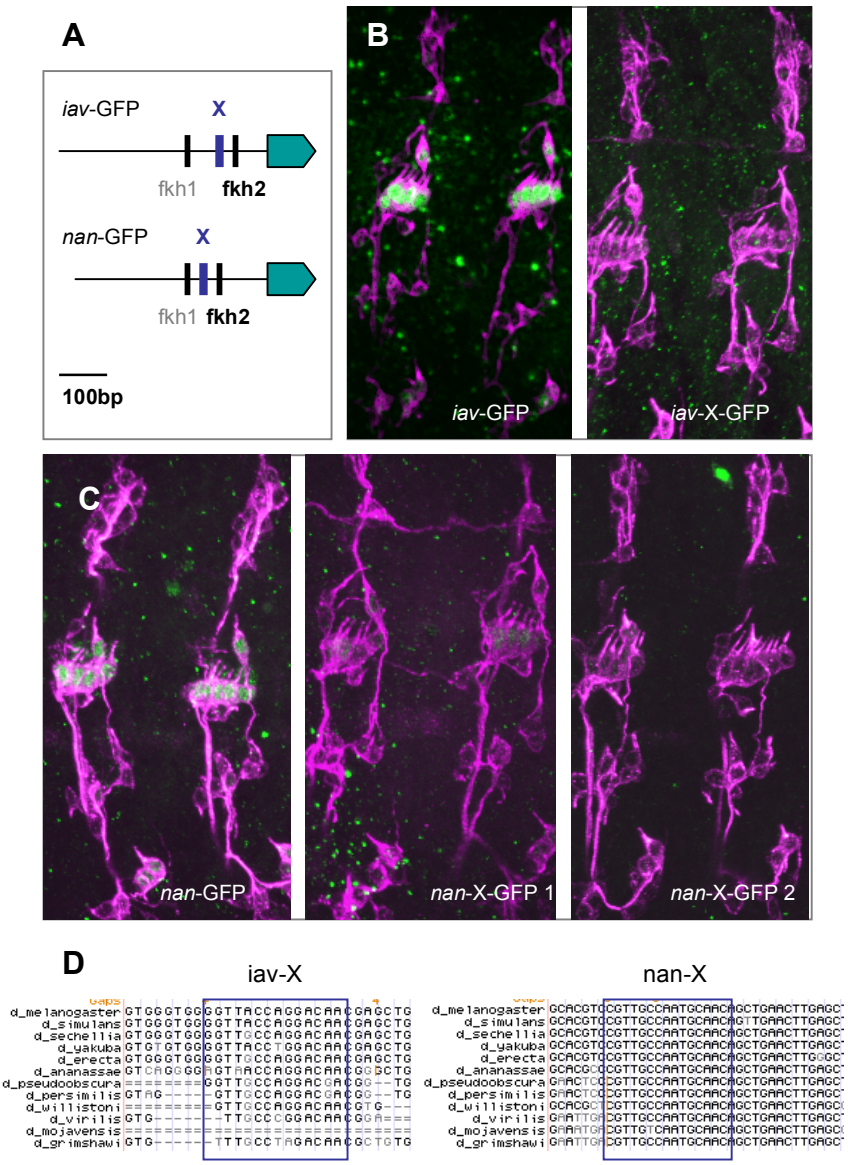

Figure 4.12: Expression from *iav*-GFP and *nan*-GFP enhancer constructs is also dependent on X-boxes. A) In both iav and nan enhancer there is an X-box close to the critical fkh2 site. B & C late stage embryos stained with RbAb-GFP (green) and MAb-22C10 (magenta). B) Mutation of the X-box in *iav*-GFP construct (*iav*-X) severely reduces GFP expression. C) Mutation of the X-box in nan-GFP construct causes either strong down regulation of GFP expression in some transformants (*nan*-X-GFP 1) or complete loss of GFP expression (*nan*-X-GFP 2) in other independent transformant lines. D) Alignments showing conservation of X-box sequences in *iav* and *nan* enhancers (from UCSC Genome Browser).

Embryos from the resulting *iav*-X-GFP and *nan*-X-GFP transformant lines were then examined for GFP expression. In three independent *iav*-X-GFP lines GFP expression was completely lost and there was a partial reduction in GFP expression in the fourth line (figure 4.12). GFP expression was also abolished in one *nan*-X-GFP line while in two other lines expression was strongly reduced (figure 4.12). Therefore in order to be expressed *iav* and *nan* require a functional X-box as well as the fd3F binding sites in their enhancers. The reason why GFP expression is not completely lost in all the lines could be a positional effect, for example if the transgene was inserted close to a particularly strong enhancer or a site which could act as an alternative X-box. This suggests that *nan* and *iav* are regulated by both fd3F and Rfx and neither of these transcription factors is sufficient on its own to activate expression of these genes.

4.2.3.2 Other predicted fd3F target genes may be co-regulated by Rfx

Nan and *iav* may not be the only genes to be co-regulated by fd3F and Rfx. Several other fd3F target genes have already been identified as potential Rfx targets including *btv*, *CG3769* and *Dhc93AB* (Thomas *et al*., 2010). *CG3769* has two conserved X-boxes in its enhancer as well as several fkh sites. Mutation of one of these X-boxes in a GFP enhancer line results in a strong reduction in GFP expression and mutation of a nearby fkh site also reduces GFP expression in Ch neurons (Katarzyna Styczynska, unpublished). Therefore, as with *nan* and *iav*, *CG3769* expression in Ch neurons may require both fd3F and Rfx. In addition *rempA*, *oseg6* and *CG11253* have all been found to have no detectable mRNA expression in *rfx*

mutant embryos in *in situ* hybridisations (Daniel Moore, unpublished). It is therefore likely that these genes are also co-regulated by fd3F and Rfx.

Since the enhancers of *iav*, *nan* and *CG3769* all share a similar motif of a highly conserved fkh site close to a conserved X-box and that in each case both sites appear to be required for expression, the upstream regions of other fd3F target genes were analysed to see if they also contain this motif. Alignments were generated using UCSC Genome Browser and for each of the target genes sequences closely matching the consensus for an fkh site and an X-box were identified at peaks of high conservation in either the upstream region or 5'UTR (figure 4.13). Some sites matched the consensus sequences more closely than others, however the pair of conserved fkh and X-box sites appears to be a common regulatory motif in the enhancers of all predicted fd3F target genes. It is therefore possible that fd3F may always act in conjunction with Rfx to regulate Ch-specific gene expression.

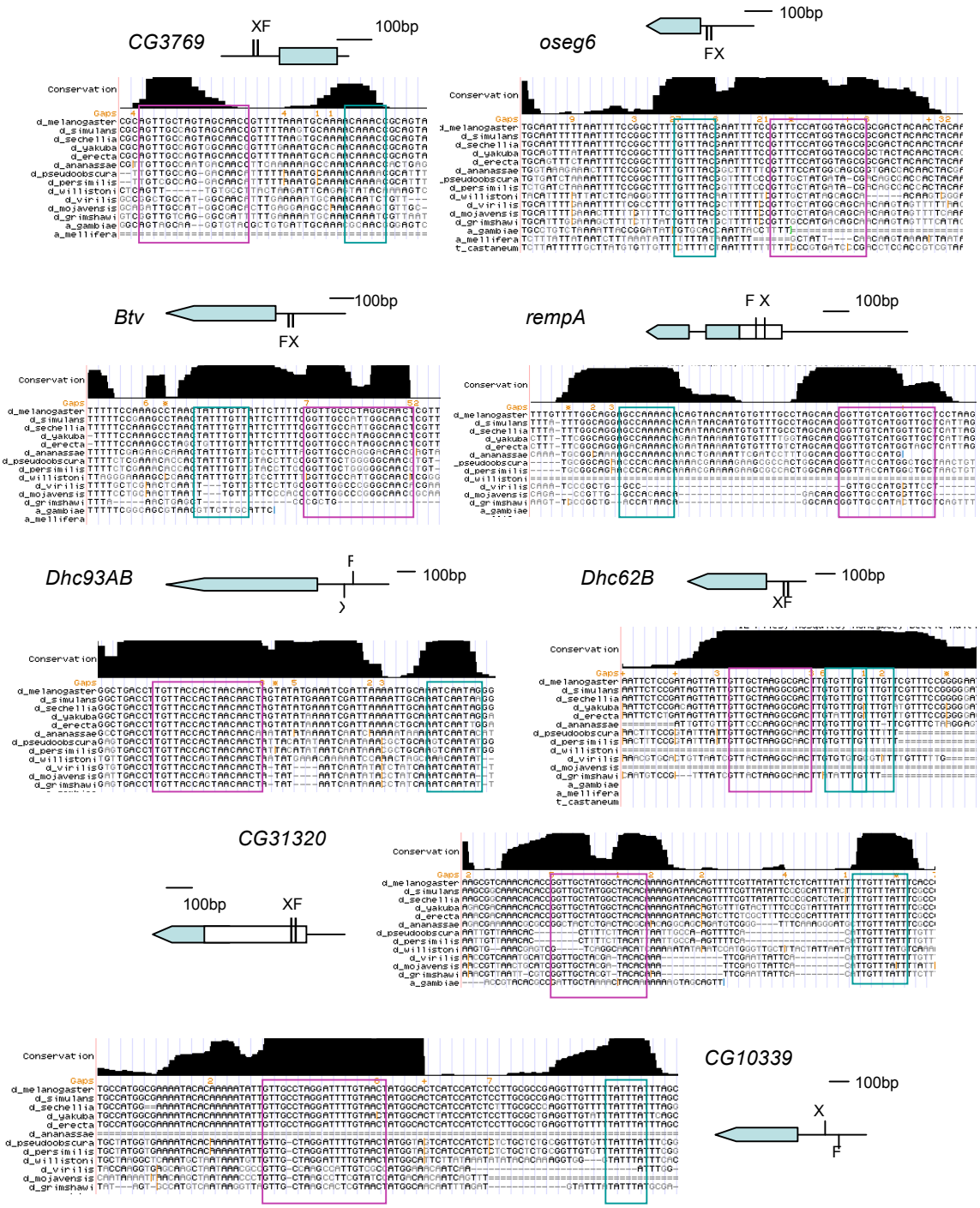

Figure 4.13: Conserved pairs of fkh sites and X-boxes in the upstream regions of predicted fd3F target genes. Alignments from UCSC Genome Browser, Fkh sites RYMAAYA (green boxes) X-boxes RYYRCC{N_{1-3}}RGYAAC (pink). All are within 100bp of the start of the gene or in some cases in the 5'UTR. *CG3769*, *btv* and *Dhc93AB* are predicted to be Rfx target genes, while *oseg6* and *rempA* may not have been picked up by these screens since due to the X-boxes being a less close match to the consensus.

4.3 Discussion

4.3.1 fd3F regulates genes required for specialisation of the proximal Ch cilium

I have shown that fd3F is required for expression of a subset of Ch-specific and Ch-enriched genes, confirming its regulatory role in Ch neuron differentiation. However not all Ch-specific genes are regulated by fd3F suggesting that, rather than being a master regulator, fd3F is concerned with regulating specific aspects of Ch dendrite specialisation. This finding is not surprising given the relatively mild morphological defects observed in *fd3F*^{1} mutant Ch neurons. Several of the target genes identified by the *in situ* hybridisation screen also showed reduced expression in *fd3F*^{1} embryos in RT-PCR experiments. However these results are not quantitative and qRT-PCR would need to be used to confirm that the band intensities in figure 4.08 represent real differences in mRNA expression, particularly in the case of *oseg1* and *oseg4* for which there is no supporting *in situ* data.

The regulatory target genes identified so far fall into two categories: Ch-specific genes required for mechanosensory function of the proximal region of the cilium (*nan*, *iav*, axonemal dyneins) and Ch-enriched genes with a role in retrograde transport. It is possible that, in addition to their role in core ciliogenesis, components of the retrograde transport machinery also play a secondary role in generating and maintaining separation of the two ciliary compartments. This is supported by previous studies that showed both *btv* and *rempA* are required to form the ciliary dilation that separates these compartments (Eberl *et al*., 2000; Lee *et al*., 2008). This

would also explain the mis-localisation of NompC in *fd3F*^{1} JO neurons described in the previous chapter. This may be the reason why retrograde transport genes are expressed at much higher levels in Ch neurons than ES neurons (which do not have compartmentalised cilia) compared with IFT-B complex genes where the difference in expression level between the two neuron types is less marked. The IFT-B components are essential for core ciliogenesis in both Ch and ES cells, whereas the IFT-A components and cytoplasmic dyneins are required at higher levels in Ch neurons due to their additional function in maintaining compartmentalisation. It therefore seems likely that all genes regulated by fd3F are involved in construction and specialisation of the proximal region of the Ch cilium.

The identification of genes required for mechanosensory function of Ch neurons as fd3F targets is supported by electrophysiology experiments carried out by Martin Göpfert (unpublished data, figure 4.14). To determine the level of Ch neuron function in *fd3F* mutants, compound action potentials (CAP) were recorded from the antennal nerve of adult flies. Unlike wild type flies, *fd3F*^{1} flies showed no antennal nerve CAP in response to JO stimulation. This is indicative of loss of function of the Nan/ Iav channel, however the effect in *fd3F*^{1} flies is more severe than expected from the loss of *nan* or *iav* genes alone. This suggests that *fd3F* regulates additional physiological or structural aspects of Ch ciliary dendrite or neuronal differentiation. Significantly, Martin Göpfert also found that active amplification was completely absent in JO neurons of *fd3F*^{1} mutants (figure 4.14).

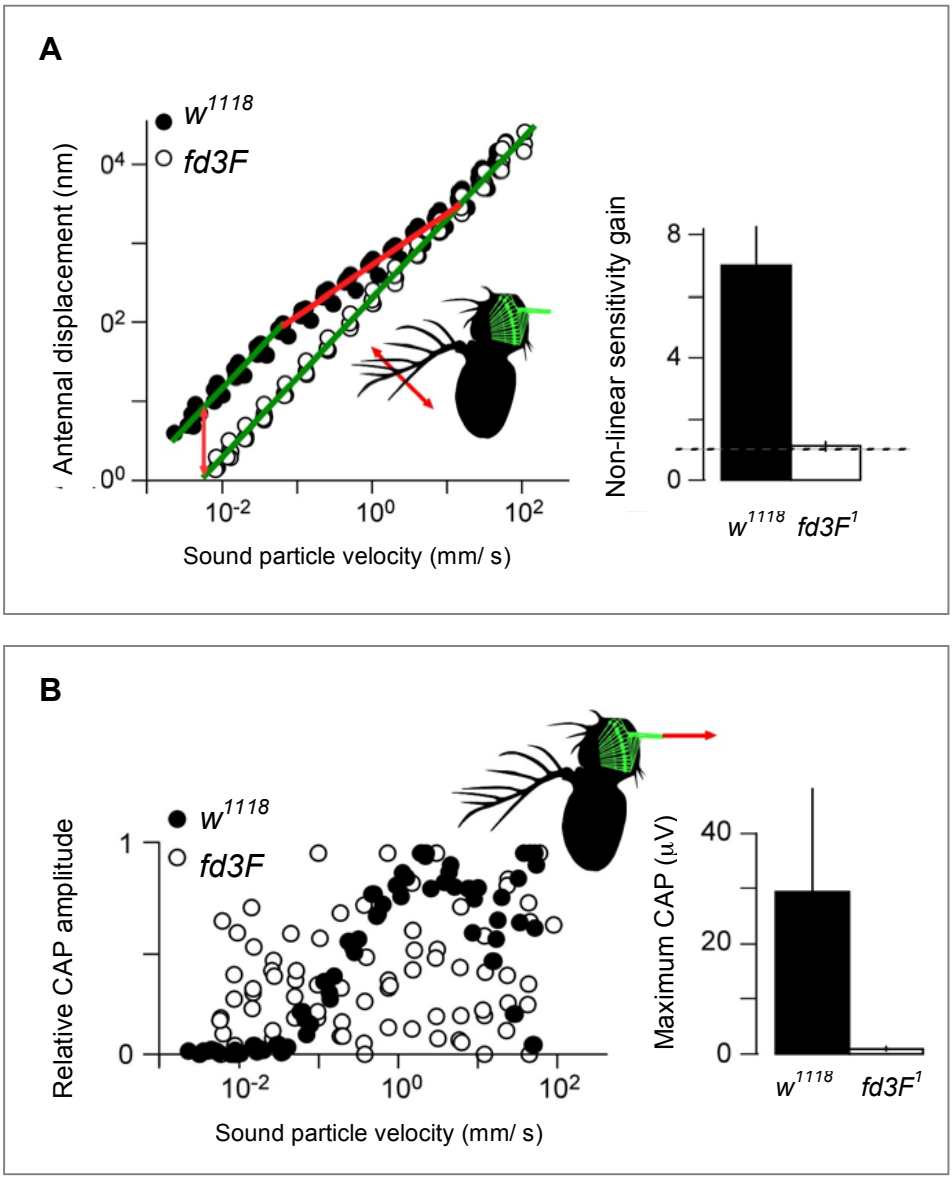

Figure 4.14: Results of electrophysiology experiments by Martin Göpfert showing that *fd3F*^{1} mutants are deaf. A (Left): antennal displacement amplitude as a function of the sound particle velocity, as measured at the arista tip (inset, red arrow). Green lines indicate linearity, red lines non-linearity. The orange arrow indicates the non-linear sensitivity gain due to mechanical amplification by JO neurons. (Right): Non-linear sensitivity gain. A gain of one (dotted horizontal line) signals the absence of amplification. B (Left): Relative compound action potential (CAP) amplitudes in the antennal nerve (inset) as a function of the sound particle velocity. Corresponding absolute values of the maximum amplitudes in A. N = 5 flies per strain. Figure by Martin Göpfert.

Mis-localisation of the mechanotransduction channel NompC may contribute to this, however loss of *nan* or *iav* alone would be expected to increase active amplification, since the Nan/ Iav channel regulates amplification gain (Göpfert *et al.*, 2006). This therefore suggests that fd3F also regulates genes required to generate active amplification and is supported by down-regulation of expression of *tilB* and *smet* in $fd3F^{1}$ embryos. The fact that several axonemal dynein genes are not expressed in $fd3F^{1}$ embryos strongly supports a role for these dyneins in generating the motile force required for amplification.

Several of the genes identified as possible regulatory targets of fd3F have no known function. However it is likely that they are involved in similar processes to other fd3F targets and are therefore required for formation or function of the proximal ciliary zone. For example *CG6980* is a Ch-specific gene encoding a protein with TPR domains, a structural feature that is shared with the *oseg* genes that encode IFT components (Avidor-Reiss *et al*., 2004). It is therefore possible that CG6980 is a component of a transport complex involved in targeting ciliary proteins to the appropriate ciliary compartment, maybe by helping to select proximal region-specific targets. CG11253 is predicted to interact with TilB (Giot *et al.*, 2003) and so may be required for axonemal dynein assembly or transport of dynein arms into the cilium.

4.3.2 fd3F could modulate Rfx activity to promote specialisation of Ch cilia

The majority of fd3F targets are still expressed at a low level in *fd3F*^{1} embryos implying that they are partially regulated by other transcription factors. I have shown that both *nan* and *iav* require the general ciliogenesis factor, Rfx as well as fd3F for their expression. The upstream sequences of other fd3F targets were examined to determine whether any might share this mode of regulation. In all cases examined the upstream sequences contained a closely spaced combination of conserved X box-like and Fkh motifs. This pair of motifs was usually very close to the transcriptional or translational start site. Therefore it appears that most, if not all, *fd3F* targets may also be regulated by *Rfx*. Some such as *btv*, *Dhc93AB* and *CG3769* were already predicted to be Rfx targets (Thomas *et al.*, 2010). However it had been assumed that Rfx does not regulate IFT-A genes. It has been shown by *in situ* hybridisation that at least some IFT-A genes (*rempA*, *Oseg6* and *Oseg1*) are indeed *Rfx* targets (Daniel Moore, unpublished), and these genes show the X-box/ Fkh site combination of motifs.

Interestingly, this site combination is shared by both Ch-specific and Ch-enriched genes. The reason for this shared regulation of Ch-specific targets could be that while *Rfx* is required for all ciliated neurons in *Drosophila*, fd3F is expression is restricted to Ch neurons. Fd3F may therefore modulate expression of some Rfx target genes in Ch neurons. For instance, in the case of Ch-specific genes such as *nan*, *iav* and axonemal dynein genes *Rfx* is not sufficient to regulate them in the absence of *fd3F*. However, in the case of Ch-enriched fd3F target genes such as *btv*, *rempA* and

CG3769, Rfx regulates expression at low level in both ES and Ch cell and this may be sufficient for their core ciliogenesis role in both neuron subtypes. Fd3F enhances expression of these genes in Ch neurons. Therefore these genes are still expressed at a reduced level in *fd3F*^{1} embryos while their expression is completely absent from Rfx mutant embryos.

This supports the notion that Rfx cooperates with cell-type specific transcription factors to regulate the genes required for cilia specialisation (Efimenko *et al*., 2005; Silverman & Leroux, 2009; Thomas *et al*., 2010). For example Daf-19, the *C. elegans* orthologue of Rfx, is entirely responsible for regulation of some core ciliogenesis genes but only partially regulates genes required for ciliary specialisation (Efimenko *et al*., 2005). These specialisation genes would therefore also require cell-type specific factors for their expression. As with the *Drosophila* IFT-A genes the enhancers of some ciliary specialisation genes in *C. elegans* contain X-box variants that deviate from the usual consensus, although they are within 100bp of the translation start sites (Efimenko *et al*., 2005). This is probably the reason that the IFT-A X-boxes have not been detected in previous bioinformatic analyses.

However there are other Ch-specific and Ch-enriched genes that do not appear to be fd3F targets. For example *CG3085* and *CG17564* are not down-regulated in *fd3F*^{1} embryos despite Ch-specific expression and *CG6129* is Ch-enriched gene that is unaffected by loss of fd3F. This result is particularly surprising since *CG6129* is required to form the ciliary rootlet, an important distinguishing feature of Ch as opposed to ES neurons. It is possible that the difference in level of Rfx expression in

Ch and ES cells may be sufficient to control appropriate expression of these genes. However, if these expression patterns cannot be achieved by regulation by Rfx alone it implies that there must be other as yet unidentified Ch-specific transcription factors that regulate expression of these genes. In the case of *CG6129* mutation of either a conserved X-box or a nearby fkh site in its upstream region results in loss of expression in GFP-enhancer lines (Katarzyna Styczynska, unpublished). This suggests that *CG6129* is regulated by Rfx, possibly in conjunction with another forkhead transcription factor in Ch neurons. One possible candidate is CG32006, another uncharacterised forkhead factor expressed in Ch neurons (ranked 27th at *ato*t3 with a fold change of 7.15; Cachero *et al*., 2011).

4.3.3 Is fd3F functionally analogous to FoxJ1?

FoxJ1 is thought to be responsible for regulating genes associated with specialisation of motile cilia in vertebrates (Stubbs *et al*., 2008; Yu *et al*., 2008; Jacquet *et al*., 2009). Some FoxJ1 target genes, such as the axonemal dynein genes *dnahc9* and *dnahc11* (orthologues of *Dhc93AB*), are also regulated by Rfx3 (El Zein *et al*., 2009; Chen *et al*., 1998; Thomas *et al*., 2010). This suggests that FoxJ1 and Rfx3 may work in combination in a similar way to fd3F/ Rfx. The results described so far therefore suggest a striking resemblance between the roles of fd3F and FoxJ1, however it is not clear whether *fd3F* is truly related to *Foxj1*or if this is an example of convergence of gene function.

fd3F appears to be present in all insects and crustacea, however it does not appear to be closely related to any of the fox gene subfamilies. The *foxj1* subfamily can be traced back to before the divergence of fungi and metazoans, however bioinformatics analyses have failed to identify any members in insects (Larroux *et al*., 2008; Mazet *et al*., 2003). Phylogenetic analysis of forkhead genes in mosquito has however identified a new subfamily FoxJx that includes *fd3F* and a forkhead gene from *Aedes aegypti* (Hansen *et al*., 2007). This subfamily is related to FoxN and FoxJ1 as well as FoxO and FoxP. *fd3F* could therefore be distantly related to the FoxJ subfamily.

A number of *Foxj1* target genes have been identified from studies of ependymal cells in *Foxj1* knockout mice (Jacquet *et al*., 2009) as well as other studies in *Xenopus* and zebrafish (Stubbs *et al*., 2008; Yu *et al*., 2008). Almost all of these genes are associated with ciliary motility, such as axonemal dynein subunits and tektins. Interestingly, the *Drosophila* homologues of some of these genes are *fd3F* targets, such as *Dhc93AB* (*Dnahc9*), *CG6971* (*Dnali1*), *tektin-A* (*tekt4*) and *CG13930* (zebrafish *wdr78*). In fact, FoxJ1a has been shown to associate with the promoters of zebrafish *dnah9* and *wdr78 in vivo* indicating that both genes are directly regulated by FoxJ1a (Yu *et al*., 2008). This suggests that there may be an ancestral relationship between fd3F and FoxJ1 despite the lack of any obvious sequence homology.

However, unlike *fd3F*, *foxj1* targets are primarily concerned with motility and there are no IFT genes are among the targets. Therefore if fd3F is derived from *Foxj1* it must have acquired an additional function in the regulation of retrograde transport genes and the TRPV channel genes *nan* and *iav*. Also there are a number of FoxJ1

targets that are not fd3F targets. Many of these are likely to be required for sperm motility but are not expressed in Ch neurons and, since *fd3F*^{1} flies show no reduction in fertility, fd3F does not appear to be required for motile sperm. This means that fd3F is more a regulator of Ch-specific specialisation rather than a regulator of motility genes. It is also possible however that fd3F has acquired its function as a regulator of retrograde transport genes because only a portion of the Ch cilium is motile. Targeting dynein arms to the proximal region and maintaining this localisation may be essential for motility and this may require the retrograde transport machinery.

It is also not clear why some motility genes such as *tektin-C* and *CG16789* (*Iqca*) are not regulated by fd3F. Both are predicted orthologues of FoxJ1 target genes and both are expressed in Ch neurons, however neither showed any reduced expression in *fd3F*^{1} embryos (Petra zur Lage, unpublished). It is possible that in *Drosophila* Ch neurons these genes have functions other than ciliary motility. For example tektins are also required for axonemal stability (Amos, 2008) and the AAA-type ATPase encoded by *CG16789* could have a more general function as a chaperone or secretory protein. Again, The Ch-specific expression pattern of these genes indicates the presence of alternative intermediate regulators of Ch-specific differentiation.

There are also a few examples of *Foxj1* expression in non-motile cilia. For example *Foxj1* is required for basal body anchoring in pulmonary cells (Gomperts *et al*., 2004) and *Foxj1* has been shown to be sufficient to promote longer cilia on neural tube floorplate cells, modulating their receptivity to Shh (Cruz *et al*., 2010). However

loss of fd3F does not appear to affect basal body anchoring or ciliary length, suggesting that these functions are not conserved. Ch cilia may be more similar to the motile 9+0 cilia of the embryonic node and zebrafish floor plate since they share the same axonemal structure. FoxJ1 and fd3F may therefore share more common targets in these ciliated cell types. The node cilia also express and *rfx3* as well as *Foxj1* and the long 9+0 cilia of the chick floor plate also express both these transcription factors (Cruz *et al*., 2010) suggesting a similar mode of co-regulation of targets to that identified in other motile cilia. However in these cases *Foxj1* knockdown did not affect formation of full-length cilia or expression of motility genes such as *Dnahc11* in chick floor plate. This suggests redundancy with Rfx3 or, in the case of the chick floor plate, another transcription factor such as FoxA2.

Therefore, while fd3F may share some functional similarity with FoxJ1, some of its functions are not replicated and fd3F appears to have evolved some functions that are unique to Ch neurons. However, given that FoxJ1 is expressed in a much broader variety of ciliated cell types in vertebrates it is perhaps not surprising that the regulatory targets of fd3F and FoxJ1 have diverged.

5

Mis-expression of *fd3F* and Analysis of the 5' end of the *fd3F* ORF

5.1 Introduction

So far I have shown that fd3F deficiency results in coordination defects in both adult flies and larvae and that these defects are caused by loss of genes required for the structure and function of the proximal segments of Ch neuron cilia. However in order to fully investigate the role of fd3F as a regulator of Ch-specific specialisation I decided to analyse the effect of ectopically expressing fd3F, particularly the effect of expressing fd3F in ES neurons. While mis-expression of fd3F is unlikely to have any impact on the gross morphology of ES neurons (since fd3F deficiency in Ch neurons causes only subtle defects) it may alter the expression profile of these neurons. For example mis-expression of fd3F may be sufficient to drive expression of target genes such as *nan* and *iav* in ES cells.

To do this I have made a construct that allows expression of the fd3F ORF under control of the yeast upstream activation sequence (UAS) that is specifically recognised by Gal4 transcriptional activator. This can be used to express fd3F in both Ch and non-Ch neurons in fly lines expressing Gal4 under control of pan-sensory or pan-neural enhancers (*Sca-Gal4* and *elav-Gal4*). The UAS/ Gal4 system was

developed in1993 (Brand & Perrimon, 1993) and is an effective system for targeted expression of genes in specific subsets of cells. The *UAS-fd3F* construct can also be used to ectopically express fd3F in the $fd3F^{1}$ background in order to rescue the mutant phenotype.

5.2 Results

5.2.1 Generation of a UAS-*fd3F* construct

I have used the UAS/ Gal4 system for both mis-expression of fd3F in ES cells and also to ectopically express fd3F in the $fd3F^{1}$ background to try to rescue the mutant phenotype. Due to the presence of the 5kb intron in the *fd3F* gene I decided to clone the *fd3F* open reading frame only. The *fd3F* ORF as annotated in FlyBase plus 9bp of upstream sequence (including the ribosome binding site) and 20bp of downstream sequence was amplified from complete embryonic cDNA. This 1.2kb fragment was first cloned into pSC-A vector and sequenced. The sequencing results showed two base changes in the sequence that would be expected to affect the fd3F amino acid sequence and these were therefore corrected by site directed mutagenesis. After ensuring that the sequence contained no other mutations the *fd3F* fragment was cut out using EcoRI and XhoI and subcloned into pUAST (figure 5.01A). The resulting clone was then re-sequenced prior to injecting into *w*; *Δ2-3* embryos.

From these injections I obtained five independent transformant lines. Flies from each of these lines were crossed to *elav-Gal4* flies and the resulting embryos were stained

with RbAb-fd3F. Embryos from all five UAS-fd3F lines were found to express fd3F in the ES cells and CNS as well as Ch cells (figure 5.01B) showing that this construct is able to express fd3F protein under control of the UAS enhancer.

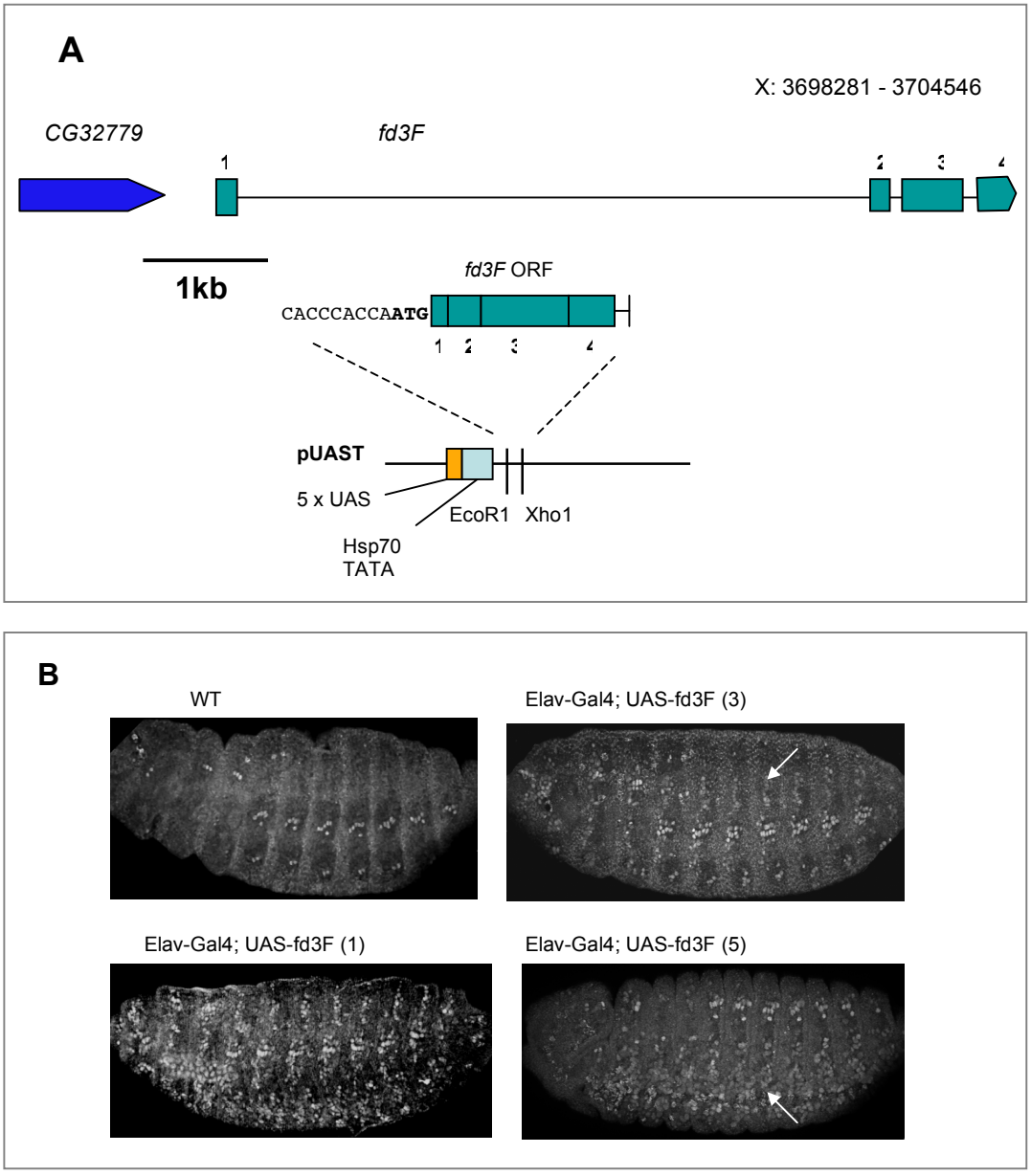

Figure 5.01: UAS-*fd3F* construct. A) The *fd3F* ORF was amplified from complete cDNA and cloned into pUAST vector between EcoR1 and Xho1. B) Late stage embryos stained with RbAb-fd3F, embryos are from w^{1118} (wild type) and three independent transformant lines (1, 3 and 5). Driving expression of this construct with *Elav-Gal4* results in fd3F expression in ES cells and CNS (arrows) in addition to Ch neurons.

As expected these lines have a range of levels of ectopic expression depending on the position of the insertion of the *UAS-fd3F* transgene. Insertions close to strong enhancers will have stronger UAS/ Gal4 controlled expression. Lines 2 and 4 showed much weaker ectopic expression than the other lines and were therefore not used for subsequent mis-expression and rescue experiments.

5.2.2 Mis-expression of fd3F in ES cells

Elav-Gal4; UAS-*fd3F* adult flies showed no obvious behavioural phenotype, however all failed to unfold their wings after eclosion. The reason for this effect is not clear although it may be caused by some adverse effect of expressing fd3F in the CNS or the wing disc. Unlike mis-expression of ato (Jarman & Ahmed, 1998), mis-expression of fd3F did not cause loss of adult mechanosensory bristles, nor was there any effect on the gross morphology of ES neuron dendrites (figure 5.02A). This is not surprising given that *fd3F* mutation results in only subtle morphological defects and loss of fd3F only affects a subset of Ch-specific genes. Interestingly ectopic expression of *fd3F* using both *sca-Gal4* and *elav-Gal4* did not cause mis-expression of *iav*, *nan*, or *CG6980* (figure 5.02B). However, since all of these genes are expected to require high levels of Rfx in addition to fd3F to allow expression, expressing fd3F alone may not be sufficient to drive expression of these target genes in ES cells. Although Rfx is expressed in ES cells during embryogenesis by the late stages when these genes are normally strongly expressed Rfx is almost completely

absent in ES cells while remaining strong in Ch neurons. It may therefore be necessary to mis-express both fd3F and Rfx at the same time to induce mis-expression of fd3F target genes.

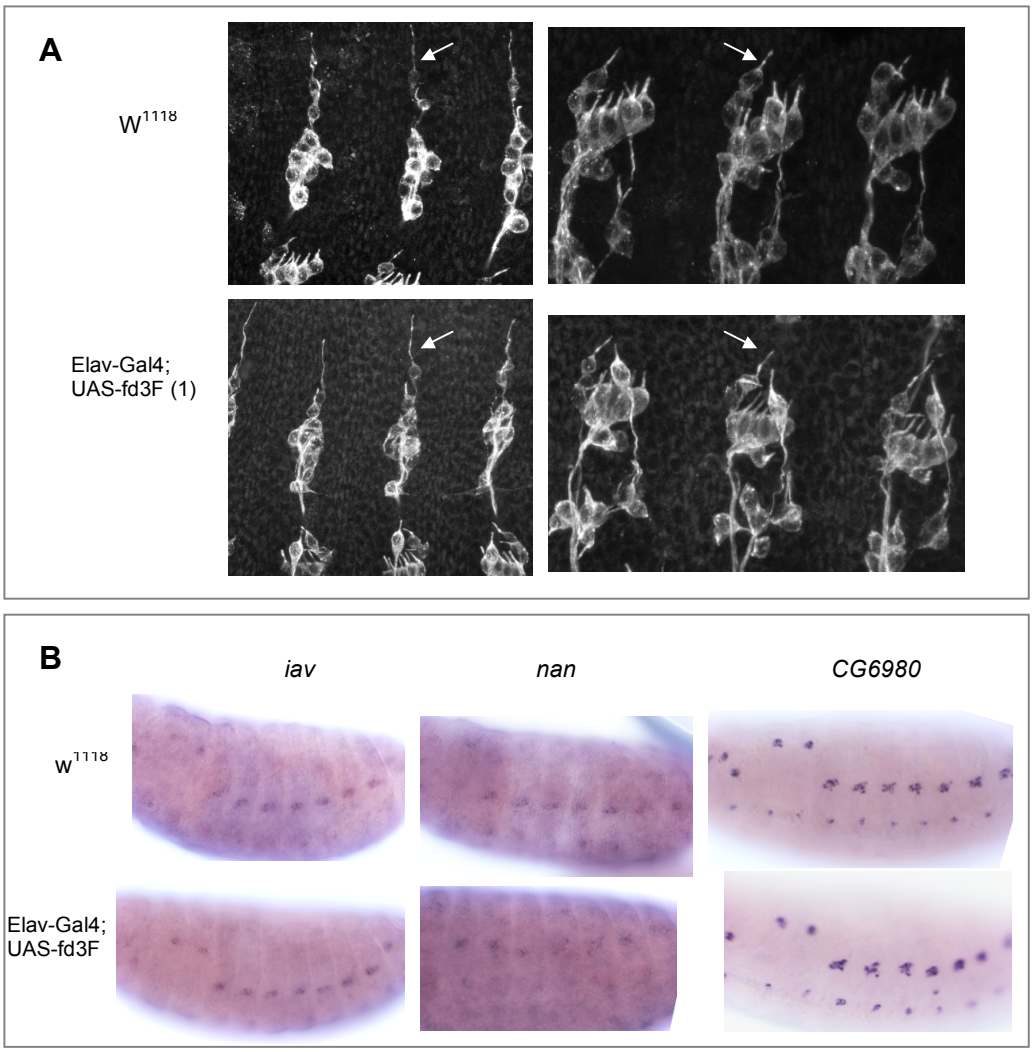

Figure 5.02: Mis-expression of fd3F has no effect on ES dendrite morphology or gene expression. A) Late stage embryos stained with MAb-22C10, expression of fd3F in non-Ch cells has no effect on dendrite thickness or length (arrows). B) RNA in situs show expression of *iav*, *nan* and *CG6980* in late stage embryos. Expression of fd3F throughout the PNS is not sufficient to cause expression of any of these genes in non-Ch cells.

5.2.3 Using UAS-*fd3F* to rescue the *fd3F*^{1} phenotype

To test whether ectopic expression of *fd3F* could rescue the *fd3F*^{1} phenotype *UAS-fd3F* lines and *sca-Gal4* lines were crossed into the *fd3F*^{1} background. I also generated an *fd3F*^{1}, *elav-Gal4* line by recombination. *fd3F*^{1}; *UAS-fd3F* lines were then crossed to *fd3F*^{1}; *sca-Gal4* or *fd3F*^{1}, *elav-Gal4* to allow ectopic expression of fd3F in the mutant background. However *fd3F*^{1},*elav-Gal4*/ *fd3F*^{1}; *UAS-fd3F*/+ adults showed no improvement in their coordination compared with *fd3F*^{1} adults. It is possible that this is because *elav-Gal4* does not drive fd3F expression at the correct time in the adult SOPs to allow normal differentiation of Ch neurons.

Despite the high levels of *fd3F* transcript produced in *fd3F*^{1}; *sca-Gal4*/ *UAS-fd3F* embryos (figure 5.03A), ectopic expression of fd3F failed to restore wild type levels of fd3F target genes (figure 5.03B). This was true for three different *UAS-fd3F* lines (lines 1, 3 and 5), which were found to have the strongest ectopic expression of fd3F. Similar results were seen when *elav-Gal4* was used to drive fd3F expression. As with the adult phenotype, this could be due to inappropriate timing of fd3F expression, however this seems unlikely since high levels of *fd3F* transcript can be detected from stage 11 onwards when expression is driven by *sca-Gal4* in embryos. This coincides with the onset of expression of most of its target genes.

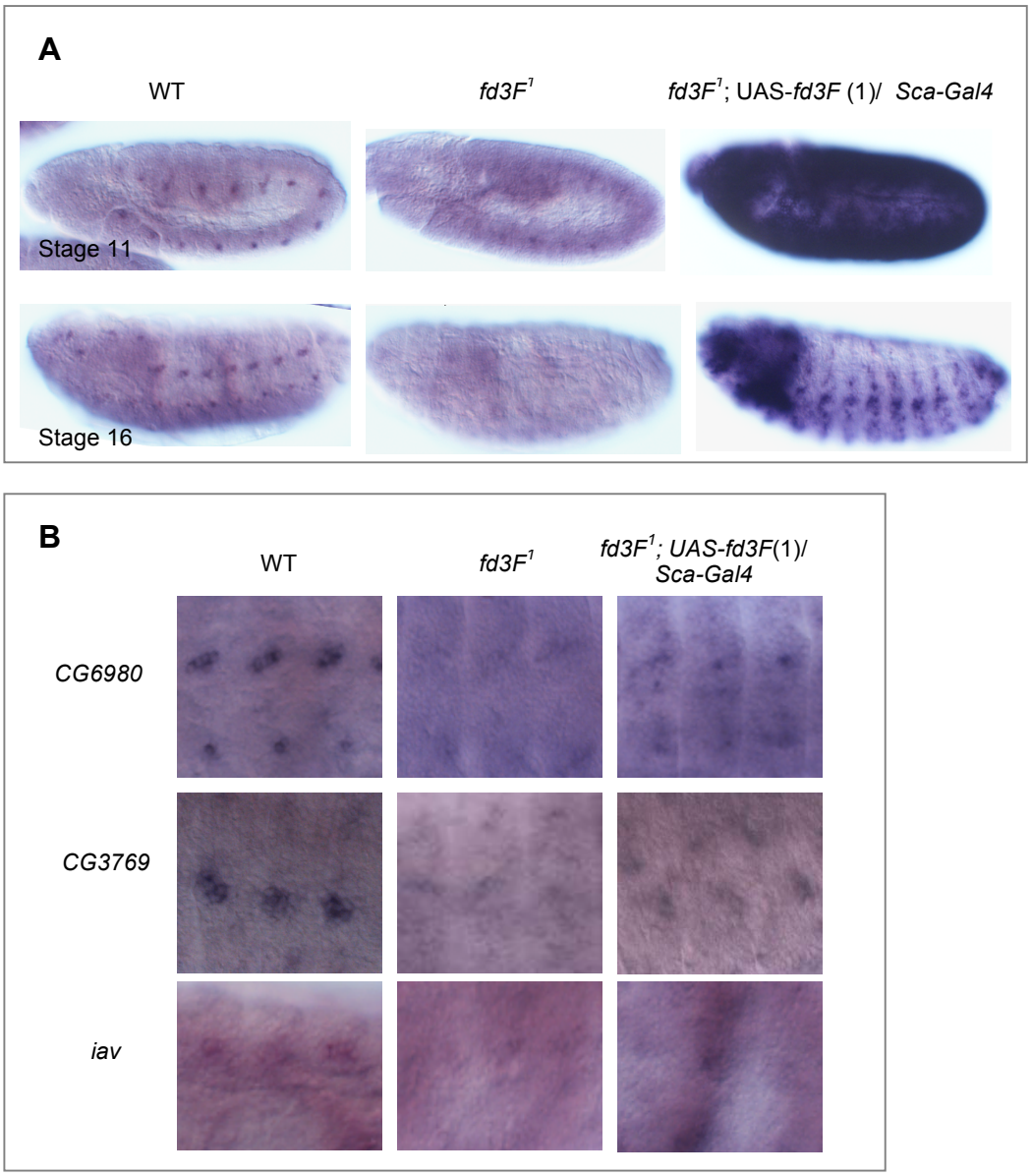

Figure 5.03: The UAS-*fd3F* construct failed to restore wild type levels of fd3F target gene expression. A) Ectopic expression of *fd3F* is sufficient to restore high levels of *fd3F* mRNA expression in *fd3F*^{1} background at appropriate embryonic stages when driven by *sca-Gal4*. B) Each panel shows three abdominal segments. UAS-*fd3F* fails to rescue expression of *CG6980*, *CG3769* and *iav* in the *fd3F*^{1} background. There may be some subtle increase in expression of these genes in Ch neurons compared with *fd3F*^{1} but this is nowhere near the wild type expression level.

All the evidence so far suggests that the phenotype observed in *fd3F*^{1} mutants is due to loss of fd3F. Both *fd3F* mRNA and protein are not detected in *fd3F*^{1} embryos and a mutation of the adjacent gene *ec*^{1} complements *fd3F*^{1} suggesting that *ec* is not affected by the imprecise P element excision. Also several of the genes that are down-regulated in *fd3F*^{1} embryos are also down-regulated in *fd3F* RNAi lines (Petra zur Lage, unpublished). It is therefore surprising that ectopic expression of fd3F does not rescue the *fd3F*^{1} phenotype. In addition to inappropriate timing of fd3F expression, another reason for this could be that the fd3F protein produced by the *UAS-fd3F* construct is not functional. I therefore decided to investigate what could be causing this lack of function.

5.2.3.1 The protein produced by the *UAS-fd3F* construct may be non-functional

Although there were no point mutations found in the *UAS-fd3F* sequence and the forkhead domain is capable of binding to fkh sites in DNA (as this construct was also used to make the fd3F^{fd} expression construct used for EMSA described in chapter 4) it is possible that the annotated start site of *fd3F* is not correct and that part of the 5'UTR may be included in the open reading frame. The absence of this region could affect the overall folding of the fd3F protein or it could mean that the protein lacks critical peptide motifs or domains. An earlier FlyBase annotation of *fd3F* (prior to the May 2011 update) included both a non-coding region at the 5' end of exon 1 and an additional 5' non-coding exon upstream of *CG32779* (figure 5.04A). To investigate this I amplified the 5' end of *fd3F* from complete cDNA by PCR. This showed that both the non-coding portion of exon 1 and a non-coding upstream exon

are present in *fd3F* cDNA and therefore mature mRNA transcripts (figure 5.04). The size of this fragment implies that *CG32779* is spliced out.

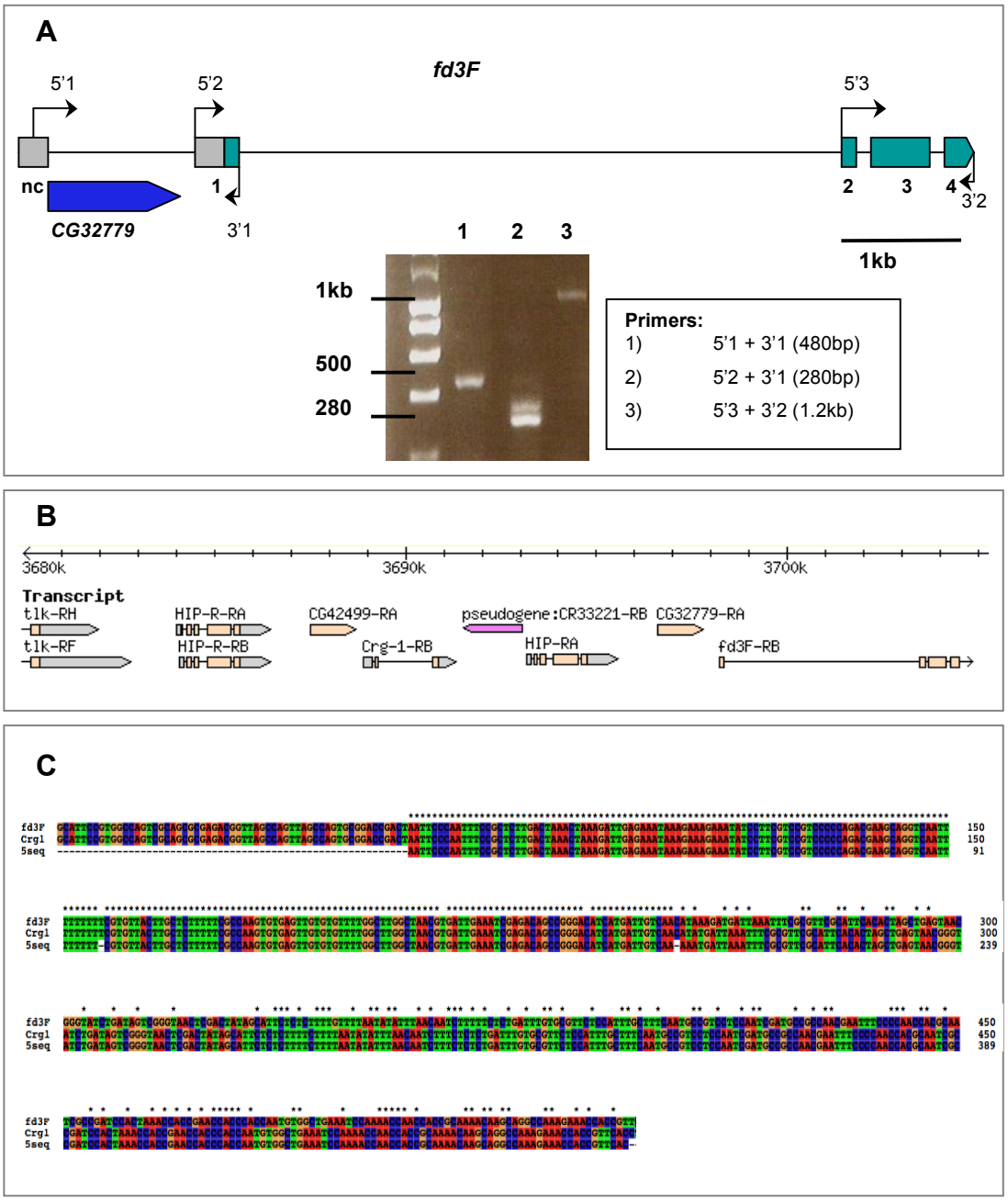

Figure 5.04: Amplifying the 5' end of *fd3F*. A) The 5' end of *fd3F* was amplified from complete cDNA using primers at the approximate positions shown. The 3' end was also amplified as a control. The non-coding region of exon1 and the 5' non-coding exon (nc) can both be amplified from cDNA. B) The locus upstream of fd3F (from GBrowse) showing duplication of the *HIP* gene (*HIP-R*). *Crg-1* is a duplication of the 5'end of *fd3F*, *CG42499* is a duplication of *CG32779*. C) Alignment of amplified fragment 1 (5 seq) with *fd3F* 5'end and *Crg-1* (ClustalX). The amplified fragment is a closer match to *Crg-1*.

However there is an added complication in that the locus upstream of *fd3F* is the site of a large gene duplication event (figure 5.04B). The gene *Crg-1* (located 9kb upstream of *fd3F*) is thought to have arisen from duplication of the 5' end of *fd3F* (Hogan & Bettencourt, 2009). Although the 5' end of fd3F is almost identical to *Crg-1* their sequences differ by 4 extra nucleotides present in *fd3F*. When the amplified 5' fragment was cloned into pSC-A and sequenced I found that the sequence of the amplified fragment aligned more closely to *Crg-1* than *fd3F* (figure 5.04C). The *Crg-1* sequence was obtained from 7 different clones. It is therefore not clear whether this 5' non-coding region really exists in *fd3F* mRNA. Sequence analysis of the *fd3F* 5' non-coding region revealed two alternative in frame ATG codons, however there is also an in frame stop codon just downstream of both of these. Therefore even if this 5' region does exist in *fd3F* mRNA it is unlikely that anything upstream of the predicted start of the ORF is translated.

5.2.3.2 Could *CG32779* be part of the *fd3F* ORF?

There is, however a third possibility. The gene immediately upstream of *fd3F* (*CG32779*) may form part of the *fd3F* ORF. As I described briefly in chapter 2 the annotated ATG start codon of fd3F is actually poorly conserved in other *Drosophila* species and in at least three other *Drosophila* species the region homologous to *CG32779* forms part of the *fd3F* ORF. This could add another 1.2kb to the *fd3F* ORF, doubling the size of the protein. I used western blotting to try to detect whether the fd3F protein was a larger size than expected, however all of the bands detected using RbAb-fd3F in protein extract from w^{1118} embryos were also present in extract from $fd3F^{1}$ embryos (figure 5.05). Since RbAb-fd3F recognises the 3' end of fd3F,

which is missing in *fd3F*^{1}, this suggests that all the bands detected are non-specific. It is perhaps not surprising that fd3F cannot be detected however, since it is expressed in such a small proportion of cells in the whole embryo.

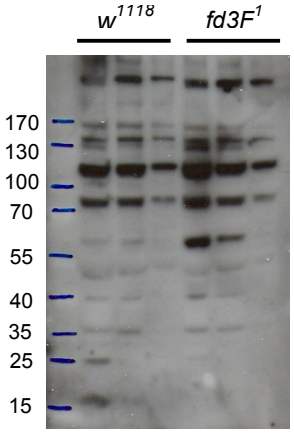

Figure 5.05: Western blot showing proteins detected using RbAb-fd3F. Protein extract from whole *w*^{1118} and *fd3F*^{1} embryos (three different dilutions of each extract) run on an SDS-PAGE gel and blotted onto membrane. fd3F should be at least 40kD. None of the bands present in the *w*^{1118} extract appear to be missing in *fd3F*^{1}.

I therefore tried to amplify larger fragments from complete cDNA. On this occasion I used 3' primers that complement sequences closer to the 3' end of fd3F (the region not duplicated in *Crg-1*) to avoid amplifying *Crg-1* (figure 5.06). All three sets of primers amplified only a single fragment from cDNA and in each case the fragment was approximately 1kb larger than expected (figure 5.06). Sequence analysis of these fragments confirmed the inclusion of all of *CG32779* apart from the stop codon and allowed the splice site to be identified (3bp from the 3' end of *CG32779* to 3bp upstream of the *fd3F* forkhead domain, figure 5.06B). This suggests that *CG32779* may in fact form part of the *fd3F* ORF and, since this implies that half the fd3F protein is missing in the original UAS construct, this could be the reason why the original construct failed to rescue the *fd3F*^{1} phenotype. I therefore cloned this new full length ORF into pUAST to create an alternative rescue construct. This new construct has now been shown to be sufficient to induce ectopic expression of some

predicted fd3F target genes (*iav*, *CG31320* and *CG11253*) in ES cells in embryos when its expression is driven by *sca-Gal4* in the wild type background (Petra zur Lage, unpublished). Although the rescue experiments have not yet been carried out these results do at least show that CG32779-fd3F is functional and capable of switching on expression of fd3F target genes.

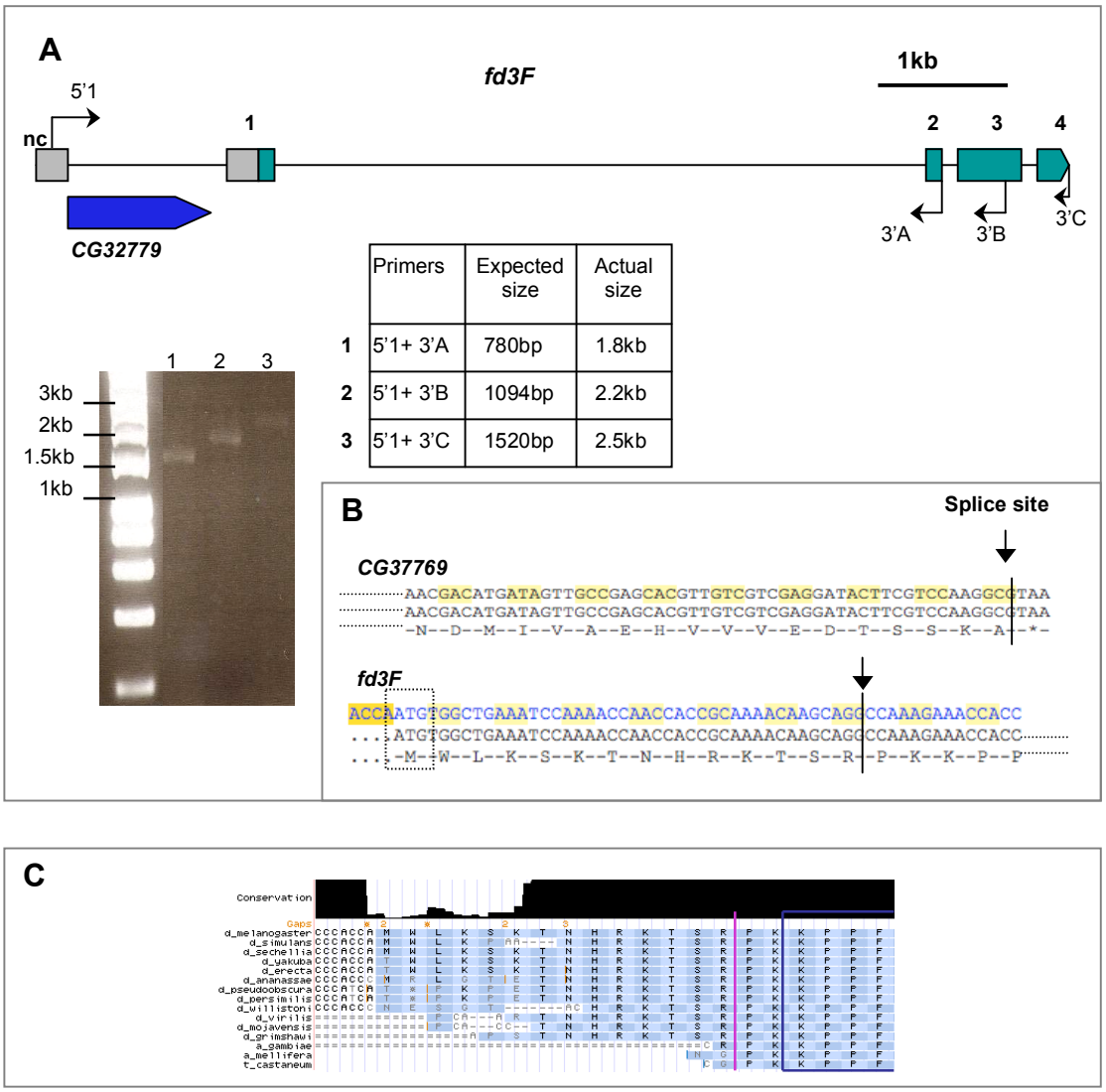

	Primers	Expected size	Actual size
1	5'1+ 3'A	780bp	1.8kb
2	5'1+ 3'B	1094bp	2.2kb
3	5'1+ 3'C	1520bp	2.5kb

Figure 5.06: *CG32779* may form part of the *fd3F* ORF. A) Map of *fd3F* showing the approximate positions of primers used for RT-PCR. All three amplified fragments are about 1kb larger than expected. The sequence of these fragments confirmed the inclusion of *CG32779*. B) Splice sites identified from analysis of the fragment sequences (Ensembl), dotted box shows the annotated start codon. C) Alignment of *fd3F* with other *Drosophila* species, mosquito, honeybee and beetle (UCSC Genome Browser), pink line shows the splice site, blue box shows the start of the forkhead domain.

5.3 Discussion

5.3.1 CG32779-fd3F could be an alternative splice variant of fd3F

There are two main reasons to consider that CG32779 forms part of the fd3F protein. Firstly, the splice site within *fd3F* exon 1 occurs at the point at which the sequence becomes much more highly conserved (figure 5.06C) and secondly, in other *Drosophila* species the region homologous to *CG32779* forms part of the *fd3F* ORF. However it was also possible to amplify the region used to make the original UAS construct, a region that includes the annotated ATG start codon which would be spliced out if *CG32779* is included in the extended form of the transcript. This suggests that there may be two alternative splice forms of *fd3F*, one corresponding to the FlyBase annotation (*fd3F-RB*) and the other extended form including *CG32779*. Due to the failure of the shorter fd3F-RB protein to rescue the $fd3F^{1}$ phenotype when ectopically expressed it is possible that this version of the protein is not functional. *CG32779-fd3F* may therefore be the major splice form. Indeed ectopic expression of CG32779-fd3F (but not fd3F-RB) appears to be sufficient to induce ectopic expression of at least some fd3F target genes (Petra zur Lage, unpublished).

However there are still some questions remaining. For example, *CG42499* (the duplicate of *CG32779*) appears not to be included in the *Crg-1* ORF as shown by amplification of the 5' end of *Crg-1* (figure 5.04). It seems odd that *CG42499*/ *Crg-1* would be spliced differently since this region is almost identical to the 5'end of fd3F. Also *CG32779* is not enriched at any of the time points in the *ato* microarray data

(Cachero *et al*., 2011). Compound expression measurements from 13 of the oligonucleotide probes used in the microarray experiments that are specific to *CG32779* and *CG42499* indicate a very low level of expression of these genes (Ian Simpson, personal communication). The expression level would be expected to be close to that of the 3' end of *fd3F* if *fd3F* and *CG32779* are truly part of the same transcript. So far no *CG32779* expression has been detected in embryonic Ch neurons by *in situ* hybridisation (Petra zur Lage, personal communication). While this could be a problem with the *in situ* probe it seems strange that the 5' end of the *CG32779-fd3F* transcript would be so much more difficult to detect than the 3'end of *fd3F*. It may be that the *fd3F* transcript is spliced differently in the embryonic and larval/ pupal stages. The *fd3F-RB* form may be the more common form in the embryo (accounting for the absence of detectable *CG32779* transcript in *in situs* and in the microarray data) whereas *CG32779-fd3F* may be the form required during differentiation of adult Ch organs and may therefore be more easily detected in leg or eye-antennal discs.

These results therefore suggest that the *CG32779-fd3F* form is only a minor splice variant. If this is true, however it is not clear why the fd3F-RB form of the protein is not able to rescue the $fd3F^{1}$ phenotype. It is possible that the precise timing and level of fd3F expression is important for its function. It may not be possible to reproduce this accurately using the UAS/ Gal4 system, which seems to produce much more than the wild type level of transcript when driven by *sca-Gal4* in the $fd3F^{1}$ background. Therefore in order to fully rescue the $fd3F^{1}$ phenotype it may be necessary to express an *fd3F* transgene under control of its endogenous enhancer. For

this reason I have decided to use two fosmid constructs (FlyFos Project, Max Plank Institute; Ejsmont *et al*., 2009) that contain both the full genomic sequence of *fd3F* and the surrounding sequence (FlyFos024749, X: 3686452-3719552 and FlyFos021777, X: 3691489-3721908) to rescue the $fd3F^{1}$ phenotype. These constructs are designed to allow ϕ31 mediated transgenesis into flies carrying *attP* landing sites. The resulting transgenic flies can be crossed to the $fd3F^{1}$ line to allow expression of the fd3F transgene under control of its endogenous enhancer in the $fd3F^{1}$ background.

5.3.2 Evolutionary evidence for CG32779-fd3F

There is, however, some evolutionary evidence to suggest that CG32779 may encode part of the functional fd3F protein. The homologues of *fd3F* and *CG32779* in several other *Drosophila* species (including *D. yakuba*, *D. persimilis*, and *D. mojavensis*) form part of the same ORF. There is also evidence of conservation of CG32779-fd3F- like proteins in mosquito (*Culex*, *Aedes* and *Anopheles*). *D. melanogaster* fd3F also appears to be related to ant proteins annotated as PCM1-like. The forkhead domains of the ant PCM1 proteins are very similar to the forkhead domains of fd3F and its homologues in other *Drosophila* species as well as forkhead proteins from other hymenoptera species (figure 5.07).

The hymenopteran genes also have an extensive region upstream of the forkhead domain, although this region does not have any obvious homology to *CG32779*.

However this region does include a short peptide motif (EADFEDKNLSWLLNFKFDEF) that appears to be shared by CG32779 and is also present in the N-terminal region of other *Drosophila* fd3F homologues (figure 5.08).

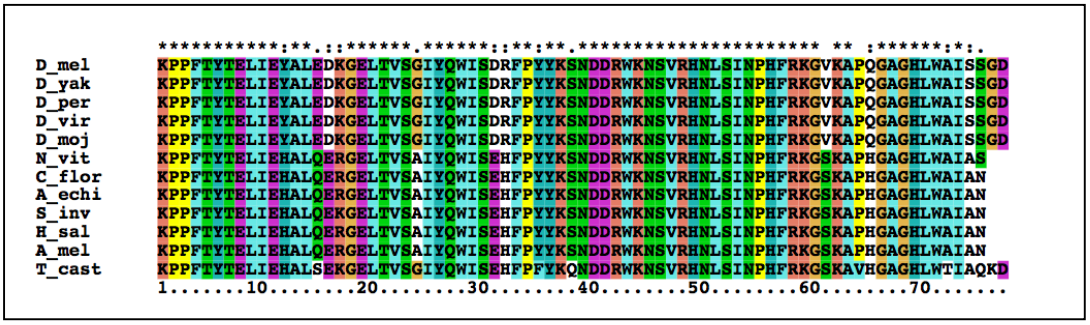

Figure 5.07 Alignment of forkhead domains from fd3F and related insect forkhead proteins. Sequences from *D. melanogaster* fd3F and homologues in *D. yakuba*, *D. persimilis*, *D. virilis*, *D. mojavensis*, aligned to related sequences from *Nasonia*, *Camponotus*, *Acromyrmex*, *Solenopsis*, *Harpegnathos*, *Apis* and *Tribolium* species using ClustalX.

A related peptide can also be identified in the upstream region of a forkhead protein from the flour beetle *T. castaneum* (IESDCTDGNLSWLLNYRIHEL). The conservation of this peptide in the N-terminal portion of these forkhead proteins suggests it may be important for their function, for example as a co-factor binding site. Therefore the presence of this peptide in CG32779 strongly supports it forming part of the functional fd3F ORF. Interestingly, a similar situation is found in another uncharacterised *D. melanogaster* forkhead gene expressed in Ch neurons: *CG32006*. The region upstream of the CG32006 forkhead domain contains a short peptide motif (ELTNLNWLLRNQNLT) that is conserved in related genes in other insect species and shares some similarity with the CG32779 motif. The CG32006 peptide motif is also conserved in several lower vertebrate foxJ1 proteins (figure 5.08B) suggesting

there may be some (albeit very tenuous) evolutionary link between CG32006, CG32779-fd3F and foxJ1.

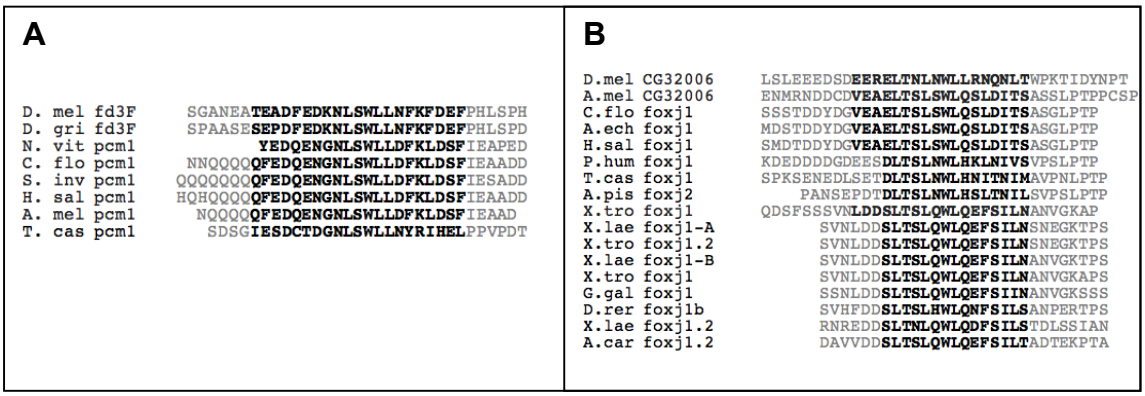

Figure 5.08 Conserved peptide in the N-terminal region of fd3F-related genes.
A) Hymenopteran PCM1 genes share a short peptide upstream of the forkhead domain a similar peptide can be identified in CG32779 (*D. mel* fd3F) and the *D. grimshawi* fd3F homologue by BLAST search. B) A similar peptide is also present upstream of the CG32006 forkhead domain. This peptide appears to be conserved in foxJ1 homologues from other insects and lower invertebrates (*C. floridanus*, *A. echinatior*, *H. saltator*, *T. castaneum*, *A. pisum*, *X. laevis*, *X. tropicalis*, *G. gallus*, *D. rerio*, *A. carolinensis*).

If *CG32779* does encode part of the functional fd3F protein it will be interesting to discover its role in fd3F function. We have already established that the forkhead domain is encoded by the 'fd3F' half of the transcript. This domain must be able to fold independently since it can bind specifically to fkh sites in DNA *in vitro* in the absence of the rest of the protein (Chapter 4). Therefore the portion of the protein encoded by *CG32779* is not required for primary DNA binding. It is possible that part of CG32779 may be close to the C-terminal end of fd3F when folded and the presence or absence of CG32779 could therefore affect the fold of the C-terminus. Alternatively CG32779 may be required for binding transcriptional co-activators

such as chromatin remodelling enzymes or histone acetylases or for interaction with the core transcription machinery. The conserved peptide in CG32779 may have a role in binding one of these cofactors. CG32779 could even contain the domain required for direct interaction with Rfx. The presence of CG32779 would therefore be essential for fd3F to function as a transcriptional regulator. If this is true it would certainly explain why the original rescue construct did not work and may serve as a warning to confirm that the annotation of a gene is correct before embarking on similar projects in the future.

6

General Discussion

In this study I have shown that fd3F is an important intermediate regulator of Ch neuron differentiation. Fd3F regulates expression of Ch-specific differentiation genes and its expression pattern makes it a likely candidate to be a direct target of Ato. Fd3F therefore provides a link between Ch SOP specification by transient expression of *ato* and Ch-specific differentiation. The evidence described in Chapter 4 suggests that fd3F may act in conjunction with the well-known intermediate regulator of ciliated sensory neuron differentiation, Rfx, to control expression of a subset of Ch-specific genes. The predicted role of fd3F within the regulatory network governing differentiation of Ch neurons is shown in figure 6.01.

It is interesting that, rather than being a master regulator of all Ch genes, fd3F appears to be responsible for regulating genes relating to one particular feature of the Ch neuron: the proximal segment of the cilium. The specialised features of this segment of the cilium, such as axonemal dynein arms and the Nan/ Iav channel, are particularly important for Ch neuron physiology. Ch neuron differentiation is therefore not just a model for studying neurogenesis but perhaps also for studying ciliary specialisation in general.

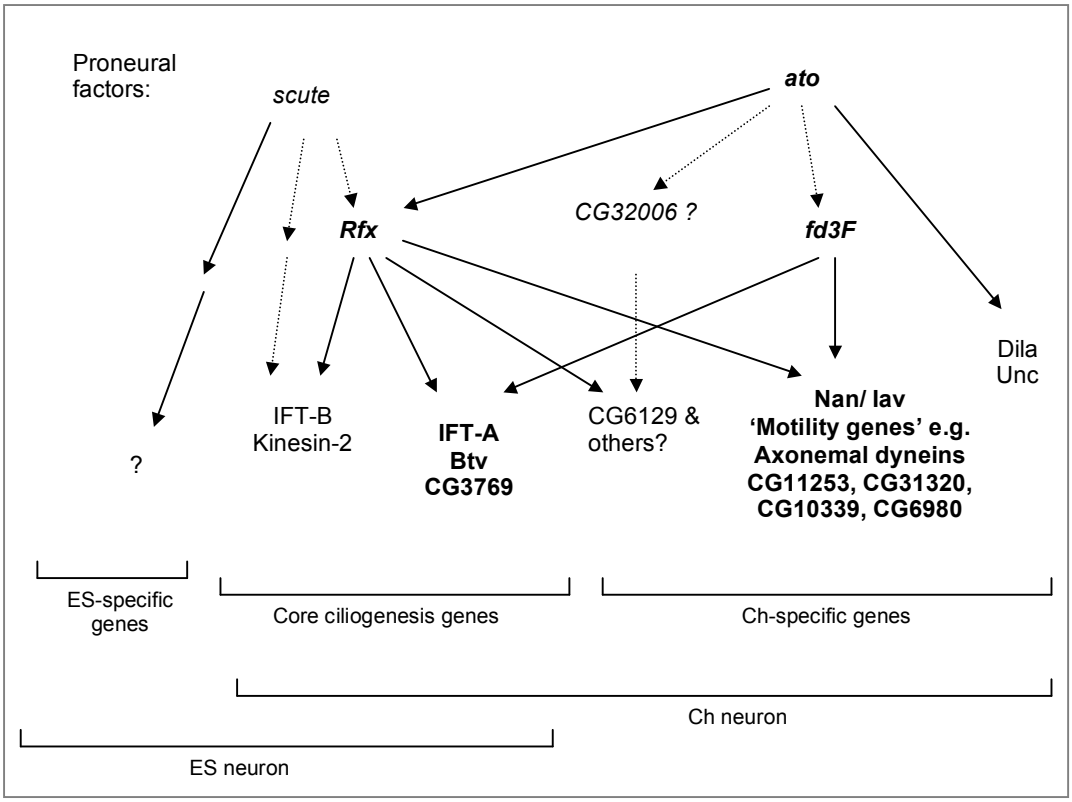

Figure 6.01: Summary diagram showing how fd3F might fit into the regulatory network that controls Ch-specific differentiation. Genes discussed in detail in this thesis are shown in bold, solid and dashed arrows represent putative direct and indirect regulation respectively. Some Ch-specific genes such as *dila* and *unc* are regulated by ato directly, while the TRPV channel genes *nan* and *iav* and axonemal dynein genes are regulated by fd3F, possibly in conjunction with Rfx. Rfx regulates core ciliogenesis genes in both Ch and ES cells, however fd3F enhances expression of IFT-A genes and some dynein-2 subunits such as *btv* and *CG3769* in Ch neurons. These retrograde transport genes may have a secondary role in ensuring proper protein localisation within the compartmentalised Ch-cilium. Other Ch-specific genes such as *CG6129* do not appear to require fd3F for their expression and may therefore be regulated by another Ch-specific transcription factor e.g. CG32006. Adapted from Cachero *et al*., 2011.

6.1 *Drosophila* Ch neuron differentiation as a model for studying differentiation of specialised cilia

Cilia can have diverse and highly specialised structures. For instance, vertebrate olfactory neurons can have up to eight elongated cilia extending from a single dendrite and the outer segments of rod and cone cilia have unique, highly specialised structures for phototransduction. While the same basic mechanisms are involved in the construction of all cilia and have been well characterised, the mechanisms regulating ciliary diversity are poorly understood. It is not clear, for example, how the general process of IFT is modified for formation of specialised ciliary structures. Ciliary specialisation also requires specific sensory receptors to be localised to the cilium and many of the proteins involved in targeting these receptors to the ciliary membrane in particular cell types are not known.

As discussed in Chapter 3 ciliogenesis has become an important area of research in recent years due to the link established between cilia and a number of human diseases. Many of these so-called ciliopathies are thought to be related to the role of the IFT machinery of primary cilia in developmental signalling pathways such as Sonic Hedgehog (Shh) and Wnt signalling. Loss of primary cilia therefore results in severe developmental defects. However since the *Drosophila* Hh and Wnt pathways are independent of ciliogenesis, Ch cilia are likely to be more useful as a model for formation of specialised motile cilia. Structurally Ch cilia may be considered to be most similar to the motile cilia of the embryonic node and zebrafish ependymal cells since they share the same 9+0 axonemal structure. In terms of function, however Ch

cilia are probably most closely related to the mechanosensory hair cells of the vertebrate cochlea.

6.1.1 Similarities between Ch neurons and vertebrate cochlear hair cells

Hearing impairment affects over 249 million people worldwide. In the majority of cases this is due to degeneration of the hair cells of the inner ear. It is hoped that understanding how hair cell differentiation is regulated during development will lead to regenerative treatments for hearing loss. In mammals hair cell fate is determined by expression of the Ato homologue Atoh1 (Bermingham *et al*., 1999). However, the gene regulatory pathways that govern subsequent differentiation into hair cells or supporting cells are still to be determined. The mechanosensory function of hair cells is dependent on rows of stereocilia arranged in ascending height order. Unlike the mechanosensory cilia of Ch neurons these are not true cilia, however they rely on the presence of a true cilium, the kincilium, during their development.

In *Drosophila* the Ch neurons of the Johnston's organ are required to generate sound evoked potentials and are functionally very similar to vertebrate cochlear hair cells. The third antennal segment vibrates in response to sound and this physically distorts the JO Ch cilia, resulting in opening of mechanosensory ion channels and depolarisation of the neuron. Similarly, in vertebrates sound vibrations are converted to oscillations in fluid pressure that travel down the cochlear duct and induce oscillations in the basilar membrane. These vibrations cause deflection of hair cell bundles and opening of mechanically gated ion channels. This leads to depolarisation of the hair cell and activation of afferent neurons. Similar to the Ch dendritic cap the

extracellular tip links between hair cell stereocilia are also essential for mechanosensory function. Vibrations of the vertebrate basilar membrane are amplified by active oscillation of the outer hair cells, increasing hearing sensitivity. This is analogous to the active oscillations observed in the proximal segments of Ch neuron cilia (Göpfert & Robert, 2003). Fd3F regulates the genes required for the ciliary motility that is necessary to produce these oscillations as well as the Nan/ Iav channel, which is required for auditory mechanosensation.

While the structures of Ch neurons and hair cells are quite different, these cell types do appear to be functionally and possibly developmentally related. Both cell types are specified by Ato-family transcription factors and just as fd3F regulates genes required for Ch ciliary motility, the forkhead factor FoxJ1b is required for kinocilium formation in zebrafish hair cells (Yu *et al*., 2008). Understanding the regulation of Ch ciliary differentiation could therefore contribute some insight into the regulation of hair cell specialisation.

6.1.2 Ch cilia differentiation as a model for other ciliary specialisations

Specialisation of Ch cilia requires development of specific ciliary structures such as the ciliary dilation and the axonemal dynein arms of the proximal segment. The nompC and Nan/ Iav ion channels must also localise to the distal and proximal segments respectively. I have shown that all of these specialisations are dependent on fd3F. Similar specialisation processes also occur in during ciliary differentiation in other organisms. Ciliary specialisation has been most extensively studied in *C. elegans* sensory neurons and has been shown to involve both localisation of different

sets of signalling molecules to the ciliary membrane and modulation of IFT (Bae *et al*., 2006; Evans *et al*., 2006; Mukhopadhyay *et al*., 2007).

Cell-type specific regulation of IFT may contribute to generating ciliary structural diversity. For example, in *C. elegans* the OSM-3 kinesin is required for assembly of the outer segments of ASH and ASI neuron cilia but not AWB neuron cilia (Mukhopadhyay *et al*., 2007). The distal ends of ASH/ ASI neuron cilia have a singlet microtubule axonemal structure that is dependent on OSM-3 for assembly, whereas the distal segments of AWB neuron cilia display unusual irregular morphology (Snow *et al*., 2004; Ward *et al*., 1975). OSM-3 acts as a kinesin-2 dependent accessory motor in ASH cilia, while in AWB cilia OSM-3 is restricted to the middle segments and acts in a kinesin-2 independent manner. Significantly, this modulation of IFT may be dependent on the forkhead transcription factor, FKH-2. FKH-2 is exclusively expressed in AWB neurons and is required for AWB cell fate. It has been proposed that FKH-2 regulates AWB-specific genes some of which modulate IFT processes such as localisation of OSM-3 (Mukhopadhyay *et al*., 2007). Since fd3F appears to be required to increase the level of expression of some retrograde IFT genes (Chapter 4), Ch ciliary specialisation may also involve modulation of IFT.

Targeting the correct ion channels and receptors to the ciliary membrane in specific cell types is obviously extremely important for ciliary function. For example, in vertebrates the polycystin complex mediates the mechanosensory function of both node cilia and renal epithelial primary cilia. PC1 (PKD1) acts as a G-protein coupled

receptor, whereas PC2 (PKD2) is a TRPP family ion channel. PKD1 and PKD2 are evolutionarily conserved (Yoder *et al*., 2002; Nauli *et al*., 2003) and are associated with autosomal polycystic kidney disease in humans. Like the Nan/ Iav and NompC TRP channels in Ch neuron cilia PC1 and PC2 are essential for the Ca^{2+} influx required for the mechanosensory response, in this case to fluid-flow stimulation (Nauli *et al*., 2003). Mice with the *Pkd1* mutation lack both PC1 and PC2 and also develop *situs inversus* and kidney cysts (Pennekamp *et al*., 2002; Nauli *et al*., 2003).

However the exact proteins and mechanisms involved in trafficking cell-type specific cargos into cilia and protein distribution within the ciliary membrane is still poorly understood. It is likely that the IFT machinery is involved in this and GFP-tagged membrane proteins such as the TRPV channels Osm9 and Ocr2 in *C. elegans* and PKD2 in *Chlamydomonas* have also been shown to display IFT-like movement (Qin *et al*., 2005; Huang *et al*., 2007). However movement of PKD-2 in *C. elegans* cilia is not thought to be dependent on IFT, although IFT may be required to control abundance of PKD-2 in the cilium (Bae *et al*., 2006). Fd3F regulates expression of ion channels in the Ch cilium in two ways; firstly by direct regulation of expression of *nan* and *iav* and secondly through an indirect effect on NompC localisation within the cilium (described in Chapter 3). While the exact cause of NompC mis-localisation is not clear, it is possible that this is related to the effect of fd3F on the expression of retrograde transport components.

6.2 The role of retrograde IFT in protein localisation

One role of fd3F appears to be to enhance expression of genes such as *btv*, *CG3769* and IFT-A complex genes in Ch neurons. These genes are likely to be required for retrograde IFT however, as discussed in Chapter 4, it is also possible that they have a role in protein localisation within the cilium. For example *btv* and *rempA* are known to be required for maintaining the structure of the ciliary dilation that separates the two compartments of Ch cilia (Eberl *et al*., 2000; Lee *et al*., 2008). Btv is also required to restrict Iav to the proximal portion of the cilium (Lee *et al*., 2008). The proximal and distal segments of the Ch cilium contain distinct sets of proteins and correct protein localisation is therefore extremely important to Ch neuron function. A role for the retrograde IFT machinery in protein localisation would explain the need for much higher levels of expression of retrograde IFT genes in Ch neurons than in ES neurons. This secondary function of retrograde IFT proteins has only recently begun to be explored.

Recent research has revealed a function for IFT-A proteins in trafficking membrane proteins into cilia allowing them to be transported towards the ciliary tip. This function appears to be independent of cytoplasmic dyneins (Mukhopadhyay *et al*., 2010; Qin *et al*., 2011). This secondary function of IFT-A proteins may be particularly important to the mechanism of signalling pathways mediated by primary cilia. For example the Shh pathway is activated by Shh binding to a negative regulator, Patched1 (Ptch1), thereby releasing Smoothened (Smo) from inhibition. Smo controls gene expression by activating the Gli family of transcription factors

(Gli1, 2 and 3) (Varjosalo M & Taipale J, 2008). In the absence of Shh Ptch1 localises to the ciliary membrane and Smo localises to the cytoplasm. This localisation is reversed upon exposure to Shh (Corbit *et al*., 2005; Rohatgi *et al*., 2007). Proper ciliary protein localisation is therefore essential to this pathway. Mutations in the IFT-A protein Thm1 (IFT139) causes overactivation of the Hh pathway in mice (Tran *et al*., 2008) while the Hh pathway is disrupted by mutations in IFT-B components, kinesins or cytoplasmic dyneins. This suggests a role for IFT-A proteins in this pathway that is separate from retrograde IFT.

The IFT-A protein IFT122 (a homologue of oseg1) has been shown to control ciliary localisation of a subset of Shh pathway components (Qin *et al*., 2011). In mice *Ift122* mutant cilia accumulate Gli2 and Gli3 at the tips, while the TULP3 protein fails to localise to the tips (Qin *et al*., 2011). Loss of TULP3 from ciliary tips suggests that IFT122 may be involved in loading cargo onto IFT particles prior to anterograde transport. IFT122 has also been shown to bind directly TULP3 allowing it to enter the cilium and IFT122 and TULP3 together mediate ciliary localisation of a subset of G-protein coupled receptors (GPCRs) (Mukhopadhyay *et al*., 2010). In contrast to Gli proteins and GPCRs, localisation of Smo to the ciliary membrane is not affected by loss of TULP3 or IFT122 suggesting that different IFT-A proteins and/ or accessory proteins may be required for trafficking vesicles containing different membrane proteins (Mukhopadhyay *et al*., 2010; Qin *et al*., 2011).

Similarly, in *Drosophila* Ch neurons localisation of Iav to the ciliary membrane requires rempA but not cytoplasmic dynein (Lee *et al*., 2008). This could imply a

role for rempA in trafficking membrane proteins into the cilium in addition to maintaining the structure of the ciliary dilation. Interestingly, I found that although the NompC ion channel appears to be successfully trafficked into Ch cilia in *fd3F*^{1} mutants it is no longer restricted to distal region of the cilium. In addition to this rempA itself fails to specifically localise to the ciliary dilation. This may indicate that the ciliary dilation structure is disrupted in *fd3F*^{1} mutants, preventing segregation of the two ciliary compartments. However it could also suggest a more direct role for retrograde transport components in protein localisation that goes beyond allowing cargo proteins to access the cilium.

The ciliary membrane forms a specialised domain of the plasma membrane with a distinct protein and lipid composition (Bloodgood *et al*., 1995). Recently studies have suggested that IFT particles associate with lipid rafts, discrete membrane patches that sequester specialised protein complexes, in the flagellar membrane of African trypanosomes (Tyler *et al*., 2009). It is not known, however whether this involves IFT-B or IFT-A complexes or both. This suggests an alternative means by which IFT proteins may be involved in localisation of ciliary membrane proteins in addition to vesicle trafficking. It also provides insight into how specialised cellular functions may be segregated to discrete regions of the membrane. The compartmentalisation of Ch cilia may make them a particularly interesting model in which to study this since not only is the protein composition of the cilium different from the rest of the cytoplasmic membrane, but different ion channels localise to the proximal and distal regions of the ciliary membrane.

6.3 Transcriptional regulation of ciliogenesis

My work has established the function of fd3F as a transcriptional regulator of Ch ciliary specialisation. As discussed in Chapter 4, fd3F appears to modulate the function of the general ciliogenesis regulator Rfx to allow differentiation of Ch-specific features. Fd3F could therefore be considered analogous to vertebrate FoxJ1, which may act in conjunction with Rfx to regulate differentiation of motile cilia (Thomas *et al*., 2010). However, as described in chapters 4 and 5, the evolutionary relationship between *fd3F* and *foxj1* appears to be quite weak. Also fd3F is not strictly a regulator of motility genes so much as a regulator of Ch specialisation. In this respect it is perhaps more similar to *C. elegans* FKH-2, which regulates differentiation of specific morphological features of AWB neurons (Mukhopadhyay *et al*., 2007). However some FoxJ1 family transcription factors may have a role in subtype-specific specialisation. For example, FoxJ1b is required for ciliogenesis in the zebrafish ear and pronephric ducts (Yu *et al*., 2008). In pronephric ducts FoxJ1b regulates formation of motile cilia, whereas in inner ear hair cells *foxj1b* function is modulated by Atoh1b and in this particular context FoxJ1b regulates differentiation of hair cells with immotile kinocilia (Yu *et al*., 2011).

It is still not clear exactly how differentiation of morphologically and functionally diverse cilia is regulated at the transcriptional level. However, the emerging theme appears to be that Rfx is required to regulate basic assembly of all cilia and that subtype-specific transcription factors interact with Rfx to produce particular ciliary specialisations. The role of fd3F in Ch neuron differentiation appears to conform to

this. It is unclear, however whether the variety of specialised cilia types in vertebrates can be explained by Rfx and FoxJ1 regulation alone. The genes regulated by these transcription factors may be context dependent as in the case of FoxJ1b in zebrafish, alternatively other transcription factors may cooperate with Rfx and/ or FoxJ1 to produce certain ciliary adaptations. Even in the case of Ch cilia there are some subtype-specific features such as the ciliary rootlet that do not require fd3F, implying that other Ch-specific transcription factors are involved.

6.4 Conclusions

fd3F regulates genes required for differentiation of unique features of Ch neuron cilia. However there are other aspects of Ch-specific differentiation, such as expression of axon guidance receptors, which do not require fd3F suggesting that there must be other intermediate transcription factors that regulate Ch neuron differentiation. In order to build up an accurate picture of the regulatory networks involved in neural differentiation it will be necessary to identify these transcription factors and their regulatory targets. One possible candidate is CG32006, another uncharacterised forkhead transcription factor expressed in Ch neurons. It will be interesting to discover whether CG32006 regulates some of the other Ch-specific genes not found to be fd3F targets. Also, since fd3F is not required for spermatogenesis it will be interesting to learn what regulates genes required for specialised features of sperm flagella.

The function of fd3F provides some insight into the general regulatory mechanisms involved in ciliary diversification. It now seems likely that the complex structure of the Ch neuron cilium requires at least one other intermediate transcription factor in addition to fd3F and Rfx. Just how closely this reflects the regulation of ciliary specialisation in other organisms is still to be determined.

7

Materials and Methods

7.1 Fly stocks

Fly stocks were raised on standard cornmeal-yeast-agar medium (1 litre: 25g cornflour, 50g sugar, 17.5g yeast, 10g agar, boiled, cooled to 40^{o}C and poured into vials or bottles to set) prepared by the media kitchen of the Wellcome Trust Centre for Cell Biology. The rearing temperatures used were 18^{o}C or 21^{o}C for stocks, 25^{o}C for most experiments and 29^{o}C for some UAS-Gal4 crosses. OrR and w^{1118} flies were used as wild type strains throughout. The deletion allele $fd3F^{1}$ was isolated by imprecise excision of a P element in the line P{EP}EP1198 (as described in chapter 3). Other fly stocks are listed in appendix A.

7.2 Molecular Biology

7.2.1 Preparation of genomic DNA from adult flies

50 adult flies were anaesthetised and frozen in lysis buffer (100mM Tris-HCl pH9, 100mM EDTA, 1% SDS) in a 1.5ml eppendorf tube. After thawing the flies were homogenised with a rotating pestle for 1min and the sample was then incubated at 70^{o}C for 30min. 150µl of 8M cold potassium acetate was then added to denature the proteins. After incubating on ice for 20min the mixture was centrifuged at 14000 rpm

for 20min at 4°C. The superantant was retained and genomic DNA was precipitated using 0.9 volumes of cold isopropanol. After mixing carefully the samples were centrifuged at 14000rpm for 5min. The DNA pellet was washed in 70% ethanol and resuspended in TE. Dnase-free Rnase was used to remove RNA from the sample. 1µl of 10mg/ml Rnase was added and the sample was incubated at 37°C for 30min. Phenol-chloroform extraction was then performed until no protein precipitation was detected in the interphase. Genomic DNA was precipitated by addition of 0.1 volume of 3M sodium actetate (pH5.5) and 2.5 volumes of 100% ethanol. This solution was incubated at -20°C overnight. The DNA was spun down at 14000rpm for 15min and the pellet was washed with 70% ethanol and resuspended in 300µl of TE.

This method was also used for DNA extraction from groups of five flies in the initial PCR screen for imprecise excisions.

7.2.2 Preparation of genomic DNA from single flies

The single fly DNA preparations used in the screen for imprecise excisions were carried out as follows. Individual female flies were squashed using a yellow pipette tip in 'squishing buffer' (10mM Tris-HCl pH8.2, 1mM EDTA, 25mM NaCl and 200µg/ml Proteinase K (Roche, cat. 01135836001)) (Gloor et al., 1993). The samples were then incubated at 37°C for 30min and then heated to 95°C for 2min to inactivate the Proteinase K. The sample was then stored at -20°C until needed. This sample was used directly as a template for PCR reactions without need for further purification.

7.2.3 Preparation of plasmid DNA

During cloning experiments, plasmid DNA was prepared using Fastplasmid Miniprep kit (Eppendorf, discontinued) or GeneJET Miniprep kit (Fermentas, cat. K0503) according to the manufacturers' instructions.

7.2.4 Preparation of plasmid DNA for microinjection

Bacterial cultures were grown overnight at 37^{o}C. 50ml of this culture was transferred to a falcon tube and centrifuged at 4500rpm at 4^{o}C for 15min. The pellet was drained thoroughly and resuspended carefully in 2ml of Solution I (50mM glucose, 25mM Tris-HCl pH8.0, 10mM EDTA pH8.0, 5mg/ml lysozyme added just before use). After 10min incubation at room temperature 4ml of Solution II (0.2M NaOH, 1% SDS) were added and mixed thoroughly but not vigorously. Following 10min incubation at 4^{o}C with occasional mixing 3ml of Solution III (3M KAcO, 1.3M HCOOH) were added. The solution was mixed quickly and thoroughly and placed on ice for 15min. The mixture was then centrifuged at 4500rpm for 15min at 4^{o}C. The superantant was transferred to a clean falcon tube avoiding transfer of any precipitate. Nucleic acids were precipitated by addition of 0.6 volumes of isopropanol. After incubating the sample for 5min at room temperature it was centrifuged at 4000rpm for 10min. The supernatant was discarded and the pellet washed twice with 70% ethanol.

The pellet was resuspended in 1ml of TE, split equally between two 1.5ml eppendorf tubes and chilled on ice for 5min. One volume of cold 5M LiCl was added and the solution was mixed thoroughly and left on ice for 5min. The tubes were then

centrifuged at 14000rpm at 4°C for 5min and the supernatant was transferred to clean eppendorf tubes. An equal volume of isopropanol was added and the tubes were left on ice for 10min. The precipitated DNA was collected by centrifugation at 4°C for 5min. The supernatant was discarded and the pellets air dried, resuspended in 300µl TE and pooled together. 1µl of DNase-free RNase (10mg/ml) was added and the mixture was incubated at 37°C for 1h. After cooling on ice one volume of PEG/ NaCl (15% PEG, 1.6M NaCl) was added and the sample was left on ice for 5min and then centrifuged at 14000rpm for 5min. The supernatant was discarded and the pellet was resuspended in 300µl TE. Phenol-chloroform extraction was then performed until no protein precipitation was detected in the interphase. The DNA was precipitated by the addition of 1/20 volume of 3M NaAcO (pH5.6) and 2 volumes of 100% ethanol. The tube was incubated at -20°C overnight. The DNA was spun down at 14000rpm for 15min and the pellet was washed with 70% ethanol, air dried and resuspended in 100µl of water.

DNA concentration was calculated by measuring absorbance at 260nm. The absorbance of the sample at 280nm was used as an indicator of the protein content and the ratio 260/280 used as a purity index.

7.2.5 RNA Preparations

Embryos laid overnight (15h approximately) on red wine agar plates were aged for a further 5h at 25°C before being collected into a sieve and washed for 4min in 50% bleach to remove the chorion. The embryos were then rinsed with distilled water and dried on tissue. 20-30mg of embryos were then collected into a pre-weighed

eppendorf and homogenised with a rotating pestle in 600ul of lysis buffer RLT (RNeasy mini kit, Qiagen) + 10μl/ml β-mercaptoethanol until no whole embryos remained. RNA was then extracted using the RNeasy mini kit (Qiagen, cat. 74106) following the manufacturer's protocol 'Total RNA from animal tissues'. Genomic DNA was removed from the samples using the DNase1 kit (Qiagen, cat. 79254) according to the manufacturer's instructions. RNA was eluted in RNase-free water and kept at -20^{o}C.

RNA quality was assessed by electrophoresis on a 1% agarose gel. The concentration of RNA was calculated from the absorbance measured at 260nm.

7.2.6 Reverse Transcription

Complete embryonic cDNA was synthesised using embryonic RNA as a template and primed with an oligodT primer. 1μg RNA was used in each 20μl reverse transcription reaction (ImProm-II reverse transcriptase kit, Promega cat. A3802). Reactions were carried out according to the manufacturer's protocol.

7.2.7 Polymerase chain reaction (PCR)

All PCR reactions carried out using Roche Taq polymerase (cat. 11146173001), buffer and dNTP mix according to the manufacturer's instructions. All primers used were synthesised by Sigma Aldrich. Briefly, for 25μl reactions the conditions used were: 1μl gDNA or 2μl cDNA, 2.5μl of each primer (10mM), 1μl dNTP mix (10mM each dNTP), 2.5μl 10X buffer (100mM Tris-HCl, 15mM $MgCl_2$, 500mM KCl,

pH8.3), 0.25µl Taq, water up to 25µl. The cycling reactions were carried out using either Biometra or Techne thermal cyclers.

The cycling conditions were:

2min	94°C	
30s	94°C	
30s	58°C	30 cycles
1min/ kbp	72°C	
10min	72°C	
pause	4°C	

unless otherwise described in the results chapters. All primers used are listed in appendix B.

7.2.8 Separation of DNA fragments by gel electrophoresis

DNA mixtures were analysed using standard agarose electrophoresis. For most experiments 1% agarose gels were prepared in 1X TAE containing 0.7µl/ml GelRed (Biotium, cat. 41003). In all cases molecular weight markers were used to estimate the size and quantity of the analysed fragments. Gels were run at 80V-150V depending on the gel and tank sizes.

7.2.9 Purification of DNA from PCR reactions and agarose gels

DNA fragments from PCR mixtures or bands sliced from agarose gels were purified using the Illustra GFX PCR DNA and gel band purification kit (GE Healthcare, cat. 28-9034-70) according to the manufacturer's instructions.

7.2.10 DNA restriction

DNA restriction enzymes were acquired from Roche, Promega and NEB. Restriction digests were carried out according to each manufacturer's instructions. All reactions were performed for 2-12h at 37^{o}C.

7.2.11 DNA dephosphorylation

To prevent re-circularisation of plasmid DNA during cloning, linearised vectors were dephosphorylated before ligation reactions. The phosphate removal was done using Antarctic Phosphatase (NEB, cat. M0289S) following the munfacturer's instructions. No clean-up was performed after dephosphorylation.

7.2.12 DNA ligation

Ligation reactions were performed using the LigaFast kit (Promega, cat. M8221). Ligation mixtures were used to transform *E. coli* without any further purification.

7.2.13 DNA sequencing

DNA sequencing reactions were using the BigDye Terminator v3.1 Cycle sequencing kit (Applied Biosystems, cat. 4337454). Reaction mixtures consisted of 3.0μl of reaction mix, 100-200ng of template, 0.32μl of sequencing primer (10μM) and water to a final volume of 10μl.

The cycling conditions used were:

1min	96^{o}C	
10s	96^{o}C	25 cycles
5s	50^{o}C	
1min 15s	60^{o}C	

After the reaction was completed the reaction was sent to the GenePool sequencing facility, Edinburgh University, Kings Buildings.

7.2.14 *E. coli* transformation

E. coli XL1-Blue competent cells were prepared by the $CaCl_2$ procedure (Sambrook & Russell, 2001). At the end of the protocol cells were aliquoted, snap frozen in liquid nitrogen and kept at -80^{o}C until use.

When needed an aliquot of competent cells was thawed and kept on ice for 10min. 10-100ng of DNA were added to 30µl of compentent cells, mixed gently and kept on ice for 30min. The mixture was then heat shocked in a water bath at 42^{o}C for 45s and then allowed to recover on ice for 2min. 50µl of Luria-Bertani (LB) medium (for 1L: 10g Tryptone, 5g yeast extract, 5g NaCl, pH7.0) was added to the tubes and incubated at 37^{o}C for 1h. The total volume of the transformation mixture was spread onto an LB plate with the appropriate antibiotic. The plates were incubated at 37^{o}C overnight. For blue/ white screening 40µl of X-gal and 100µl of 100mM IPTG were spread onto the plates prior to spreading the cells.

In the case of cloning into pSC-A the Strataclone kit (Stratagene, cat. 240205) was used for ligation and transformation according to the manufacturer's instructions.

7.2.15 Site directed mutagenesis

The Site-Directed Mutagenesis QuickChange II XL kit (Stratagene, cat. 200522-5) was used according to the manufacturer's instructions. Mutagenesis primer sequences are given in appendix B (all synthesised by Eurofins MWG).

7.2.16 Bacterial growth culture

Bacterial cultures were grown overnight in LB medium by incubation at 37^{o}C in an orbital shaker with moderate agitation (250rpm). Ampicillin was added to cultures at a final concentration of 100μg/ml. Plates were 1.5% agar in LB medium supplemented with the appropriate antibiotic.

7.3 Immunohistochemistry

7.3.1 Fixation of samples for RNA and protein detection

i) Embryos

Embryos were collected on red wine agar plates and transferred to a sieve. The embryos were then dechorionated in 50% household bleach for 4min and then thoroughly washed to remove the bleach. The embryos were then transferred to a scintillation vial containing 3.75ml of PBS, 1.25ml of 37% formaldehyde and 5ml of heptane. The embryos were then fixed by shaking for 20min on an orbital shaker at room temperature. After shaking the lower phase was removed with a fine pastette. 10ml of methanol was then added and the vial shaken vigorously for 30s to break the vitelline membrane of the embryos. The embryos were then allowed to sink to the

bottom of the vial and transferred to a clean eppendorf tube with a cut pipette tip. The embryos were then rinsed twice with methanol to remove residual heptane. In the case of *in situ* hybridisation, embryos were kept frozen at -20^{o}C until required. Embryos required for immunostaining were washed 4 times with PBT (0.3% Triton-X-100 in PBS) and used immediately.

ii) Imaginal discs

Larval and early pupal imaginal discs were dissected in PBS and then fixed for 1h in 3.7% formaldehyde in PBS. The discs were then rinsed 3 times with PBTween (0.1% Tween20 in PBS). For immunostaining the discs were then washed twice for 10min in PBT and used immediately. For in situ hybridisation the discs were dehydrated in an ethanol series: 30%, 50% and 70% in PBTween, 5min each wash and then stored in 100% ethanol at -20^{o}C until needed.

iii) Larval pelts

Third instar larvae were chilled on ice for 20min in PBS and then dissected at room temperature in a drop of PBS in a Stylgard dish. The larval body was fully opened and pinned onto the plate and the internal tissues were removed. The sample was then fixed in 3.7% formaldehyde in PBS for 1h. After fixation the sample was rinsed twice with PBT and the pins were then removed and the pelts transferred to 900µl of PBT in a clean eppendorf and used immediately for immunostaining.

iv) Pupal antennae

24-48h old pupae were transferred to a drop of PBS on a Stylgard dish. The tops of the pupal casings were removed and the pupae were transferred to a clean eppendorf and fixed in 3.7% formaldehyde in PBS for 1h. The pupae were then washed twice with PBT (10min each wash) and then pinned to a Stylgard dish. The antennae (and the covering membrane) were then dissected in a drop of PBT and transferred to 700µl of PBT in a clean eppendorf. The antennae were then used immediately for immunostaining. All subsequent washed were performed on the bench allowing the antennae at least 10min to sink to the bottom of the tube before the wash solution was removed.

v) Adult legs and wings

Legs and wings were dissected under a drop of PBT and transferred quickly to 3.7% formaldehyde in PBT for fixation. Samples were fixed for 1-2h and then washed several times in PBT before mounting onto a microscope slide in Vectashield medium (Vector Labs, cat. H-1000).

7.3.2 Immunostaining

Fixed tissues were blocked for 2-4h in 2% bovine serum albumin (BSA, Roche) in PBT at room temperature on a rotating wheel. Primary antibody was then prepared in 2% BSA, 5% normal goat serum (NGS, Jackson labs) in PBT (see appendix C for antibody dilutions). The sample was then incubated at 4^{o}C overnight. Unbound antibody was then removed by 4 quick rinses and three 15min washes with PBT. Seconsary antibodies (Alexa fluorochrome conjugated, Molecular Probes) were

added to a concentration of 1:500 in 0.5% BSA, 5% NGS in PBT. Samples were incubated for 2h at room temperature on a rotating wheel. The samples were then rinsed and washed three times for 15min in PBT. The samples were then mounted on microscope slides in Vectashield medium (Vector labs, cat. H-1000), covered with coverslips and sealed with nail varnish. Slides were kept at 4^{o}C in the dark.

7.3.3 Fd3F antibody preparation

To make the fd3F antibody a synthetic peptide matching the C-terminal region of fd3F (sequence NH_2- NLNYFGYNPGSDIVAC -COOH) was synthesised by CovalAb and purified by HPLC. This peptide was injected into two rabbits to produce anti-fd3F antisera (CovalAb/ Eurogentec). The serum was purified using Melon Gel IgG Spin Purification Kit (Thermo Scientific, cat. 42506) and was used 1:100 for immunostainings.

7.3.4 RNA in situ probe preparation

DIG-labelled antisense RNA probes were prepared from either PCR products bearing the promoter sequence for the T7 RNA polymerase (See appendix for primers). or from pSC-A vector with the sequence of interest inserted into the cloning site. Clones were chosen with the sequence oriented so that the T7 promoter present in the plasmid drove synthesis of antisense RNA. The synthesis reactions were carried out using a DIG RNA labelling kit (Roche, cat. 11274015001) following the manufacturer's instructions. Probes were purified using the RNeasy Mini Kit (Qiagen, cat. 74106) according to the manufacturer's protocol (RNA Clean up). Probes were stored at -20^{o}C until used.

7.3.5 RNA *in situ* hybridisation

Embryos were re-hydrated in 70%, 50% and 30% methanol in PBTween (5min each wash) and imaginal discs were re-hydrated in 70%, 50% and 30% ethanol (5min each wash). They were then washed for 5min in PBTween and then post-fixed in 3.7% formaldehyde in PBTween on a rotating wheel at room temperature. The fixing solution was removed by washing 5 times for 5min with PBTween. Samples were then incubated in a solution of 50% PBTween, 50% Hybridisation buffer (50% deionised formamide, 5X SSC, 100µg/ml E. coli tRNA, 50µg/ml heparin, 0.1% Tween20, pH6.5) for 10min on the rotating wheel. This solution was then discarded and 500µl of fresh hybridisation buffer was added to the sample. The tube was then transferred to a heat block at 70^{o}C and left to pre-hybridise for 2-4h. The probe was then diluted in hybridisation buffer, heat shocked at 94^{o}C for 2min and chilled immediately on ice to remove secondary structure in the RNA. The sample was then incubated with the probe overnight at 70^{o}C.

The following day the probe was removed and the sample was washed at 70^{o}C in preheated solutions as follows: 1 x hybridisation buffer, 1 x 50% hybridisation buffer in PBTween, 4 x PBTween for 30min each. The sample was then washed for 5min with PBTween at room temperature and then incubated with anti-DIG alkaline phosphate conjugate (Roche, cat. 11093274910) 1:2000 in PBTween for 2h at room temperature on the rotating wheel. The excess antibody was then removed by washing with PBTween 3 times for 20min each. The samples were then transferred to a microtitre plate and rinsed with reaction solution (100mM Tris-HCl pH9.5,

100mM NaCl) three times to remove residual PBTween. The sample was then stained using an NBT/ BCIP solution (20µl/ml NBT/BCIP, Roche, cat. 11681451001 in reaction solution). The samples were kept in the dark during colour development and the intensity of the staining was checked occasionally using a stereomicroscope. When the staining was satisfactory the reaction was stopped by washing several times with PBTween. The embryos or discs were mounted on microscope slides with 70% glycerol in PBTween, covered with coverslips and sealed with nail varnish. Slides were kept at 4^{o}C.

7.3.6 Simultaneous RNA/ protein detection

RNA was detected first following the RNA in situ protocol described above. After the stopping NBT/ BCIP colour reaction with PBTween, the embryos were rinsed several times with PBT and transferred to a clean eppendorf tube. The embryos were then blocked for 2h or overnight in 2% BSA in PBT at room temperature on the rotating wheel. Primary antibody was then added at the appropriate concentration and incubated overnight at 4^{o}C as in the immunostaining protocol described above. The embryos were then washed as described earlier and HRP-conjugated secondary antibody (Molecular Probes) was added at 1:500 dilution in 5% NGS in PBT. Embryos were incubated for 2h at room temperature on the rotating wheel. Excess antibody was then removed by three quick rinses and three 15min washes with PBT. The embryos were then transferred to a microtitre plate and washed several times with PBS to remove any residual Triton-X. The DAB staining solution (1 drop buffer, 2 drops DAB, 1 drop H_2O_2 in 2.5ml water; Peroxidase Substrate kit, Vector, cat. SK-4100) was then added to the embryos. After a 5-15min incubation to allow

the colour to develop the embryos were rinsed with PBT and then mounted onto slides in 70% glycerol. Slides were stored at 4^{o}C.

7.3.7 Microscopy

Chromogenic stainings were imaged using an Olympus Provis system consisting of an Olympus AX70 microscope and a DP50 Olympus digital camera.

Fluorescent stainings were imaged using a Zeiss LSM Pascal system with the LSM Zeiss capture software. The same confocal gain settings were applied to both control and tested samples. In most cases a complete Z-stack was acquired and rendered on a 3D projection.

7.3.8 Transmission Electron Microscopy

Whole adult flies were rinsed in 0.5% Triton-X-100 in water to permeablise the cuticle. Dissections were carried out in 0.1M phosphate buffer PB (1:1 Na2HPO4 and NaH_2PO4 in water, pH7.4). After removing the head, the proboscis was removed to facilitate infiltration of the fix. The heads were then fixed in 2.5% glutaraldehyde and 2% paraformaldehyde in 0.1M PB pH7.4 overnight at 4^{o}C. Heads were then washed in PB, postfixed with OsO_4, dehydrated in an ethanol series and embedded in Polybed812. Ultrathin (75nm) sections of the antennae were then stained with aqueous uranyl-acetate and lead citrate and examined with a Philips CM100 Compustage (FEI) microscope with images collected using an AMT CCD camera (Electron Microscopy Research Services, Newcastle University Medical School).

7.4 Injection of DNA to make transgenic fly lines

Constructs of interest were cloned into either pUAST or pHStinger vectors as described above. These vectors contain P element repeats flanking the sequence of interest allowing it to be integrated into the genome in lines expressing the Δ2-3 transposase. The plasmid DNA was injected into syncytical blastoderm *w; Δ2-3* embryos at a concentration of approximately 500ng/ul.

Cages of flies were set up a couple of days in advance and red wine agar plates with added yeast paste were changed regularly to encourage egg laying. On the day of injection the plates were changed at least twice to ensure removal of older embryos. Embryos were then collected once an hour for injection. The embryos were dechorionated for 3min in 50% bleach and then rinsed with water. The embryos were then lined up on a block of agar under a dissection microscope with the micropyle side (anterior) pointing towards the edge of the agar. They were then transferred to a coverslip coated with double-sided sticky tape with the posterior of the embryos pointing towards the edge of the coverslip. The coverslip was attached to a slide using a drop of hydrocarbon oil and put into a desiccating chamber for 9 or 10min. The embryos were then covered with series 700 halocarbon oil to prevent further dehydration and injected at 18^{o}C using a standard microscope and microinjecting device. Injected embryos were covered with series 95 halocarbon oil and left at 18^{o}C overnight. The embryos were then transferred to 21^{o}C and left to develop for a further 24h. The hatched larvae were then collected and transferred to standard food vials, about 20 larvae per vial, and left at 25^{o}C until eclosure. The individual flies

were crossed to w^{1118} flies and their progeny were screened for transformants on the basis of eye colour, ranging form pale yellow to red. The transformants were crossed to w^{1118} until the transgene segregated from the transposase (identified as loss of mosaic eye colour). The insertion was then mapped genetically.

7.5 Behaviour Analyses

7.5.1 Climbing Assay

All climbing assays were carried out at 21°C between 12.00 and 2.00pm. Virgin females were collected and left to mate with males for 48h. The females were then separated and left for a further 2 days to recover from being anaesthetised. For threshold tests 20 mated female flies were transferred to a measuring cylinder marked at 10cm. After a 1min recovery period the cylinder was banged firmly once on the bench and the percentage of flies passing the 10cm threshold within 1min or 15s of banging (as described in chapter 3) was recorded. This was repeated 5 times each for 4 groups of flies from each line. This mean percentage of flies crossing the 10cm threshold was then calculated and the significance of the result was tested using the Student *t*-test. The lines tested by this method were $fd3F^{1}$, $fd3F^{1}$/ *FM6ywB*, *P{EP}EP1198*, ato^{1} and w^{1118} (wild type).

For distribution tests 10-12 mated female flies were placed in a measuring cylinder marked at 5cm, 10cm, 15cm and 20cm. After a 1min recovery period the cylinder was banged firmly on the bench and the flies were filmed for 30s with a standard

digital camera. This was repeated with six sets of flies for each line tested. Afterwards each 30s film was paused after 15s and the number of flies in each of the four sections of the cylinder was counted. The results for each line were pooled and the ratio of flies in each section of the cylinder was calculated. The significance of the results was tested using the Chi-squared test. The lines tested by this method were *fd3F*^{1}, *fd3F*^{1}/ *FM6ywB* and *fd3F*^{1}/ *ec*^{1}.

7.5.2 Larval crawling assay

All tests were carried out at 21^{o}C at approximately the same time each day. Individual third instar larvae were rinsed briefly in water to remove any residual food and placed in the centre of a 1% agarose plate. The larvae were then left for 1min to recover from handling and then to crawl for 2min. During the 2min crawl the path taken by the larva was traced onto the lid of the plate. The lids were then imaged using a scanner and the paths were measured using ImageJ software. The diameter of the plate was used as a standard to convert the measurements into milimeters. Mean path lengths were then calculated and the significance tested using the Student *t*-test.

7.6 *in vitro* DNA binding assays

7.6.1 Expression and purification of fd3F forkhead domain

fd3F^{fd} was amplified from the complete cDNA (from 5-21h old embryos) and cloned in pGEX-2T. The pGEX- *fd3F*^{fd} plasmid was used to transform BL21-pLysS *E. coli* as described above. For large-scale expression of fd3F^{fd} for purification 400ml of

bacterial culture was grown up to OD_{550} of 0.35 and expression of $fd3F^{fd}$ was then induced with 0.5M IPTG for 2h at 20°C. Following induction the culture was spun down at 4500rpm, resuspended in 5ml ice cold PBS with 1mg/ml lysozyme and sonicated at 6μ (3x 10s). Triton-X-100 was then added to 0.1% final concentration and the cell lysate was centrifuged at 15000rpm for 15min to separate soluble and insoluble fractions. GST- $fd3F^{fd}$ was purified from the soluble cell lysate by overnight incubation at 4°C with glutathione sepharose beads (GE Healthcare) on a rotating wheel. The beads were then washed five times with PBS and GST- $fd3F^{fd}$ was eluted with buffer 2 (50mM reduced glutathione in 250mM Tris pH8) for 2h at room temperature, followed by elution with buffer 3 (buffer 2 + 0.4% deoxycholate) overnight at 4°C.

Samples taken at various stages were boiled for 3min in gel loading buffer (50mM Tris-HCl pH6.8, 2% SDS, 0.1% bromophenol blue, 10% glycerol, 0.1M DTT) and then run on an SDS-PAGE gel (RunBlue 4-12% gradient, Expedeon, cat. NXG41212). Gels were stained with InstantBlue stain (Expedeon, cat. ISB1L).

7.6.2 Gel Mobility Shift Assay

The following synthetic complementary 36-bp oligonucleotides containing a central fkh site were used in gel retardation experiments. Fkh sites are shown in bold.

IavF2 5' ATCATGGGTCATCGA**ACAAACA**AGCCGAGAAGGTTGT

NanF2 5' GCACGGAAATGTTTT**ATCAATA**GCCACCAATGGACAA

IavF2mut 5' ATCATGGGTCATCGA**ACAACGA**AGCCGAGAAGGTTGT

NanF2mut 5' GCACGGAAATGTTTT**ATCACGA**GCCACCAATGGACAA

The top strand of each oligo was labelled with [γ^{33}P]ATP (10μCi/ μl) (Amersham) using T4 polynucleotide kinase (New England Biolabs, cat. M0201). The oligos were added at 1μM concentration. Unincorporated [γ^{33}P]ATP was removed using ProbeQuant G-50 microcolumns (GE Healthcare, cat. 28-9034-08) according to the manufacturer's instructions. The labelled sample recovered from the column was then hybridised to the unlabelled complimentary strand.

The hybridisation conditions were as follows:

5min 95^{o}C
10min 68^{o}C
10min 42^{o}C
10min 37^{o}C

γ^{33}P labelled duplexes were used at 0.1nM in 20μl reaction mixtures in binding buffer (10mM Tris HCl, 1mM DTT, 1mM EDTA and 100mM NaCl). The duplexes were incubated with purified fd3F^{fd} (12.5μM in binding buffer) for 20min on ice. The reaction mixture was then electrophoresed on a 6% polyacrylamide gel in 0.5x TBE at 40mA for 1h. The gels were dried and exposed to a phosphoimager screen. For competition assays 10nM unlabelled DNA was mixed with 0.1nM labelled DNA prior to adding fd3F^{fd}.

7.7 Western Blotting

Embryos were collected overnight on red wine agar plates and transferred to a sieve. The embryos were then dechorionated with 50% bleach for 4min, rinsed and

transferred to an eppendorf tube. 500µl of lysis buffer (50mM Tris pH7.5, 125mM NaCl, 1.5mM $MgCl_2$, 1mM EDTA, 5% glycerol, 0.4% NP-40, 0.1% Tween, 1mM DTT, 1 CompleteMini protease inhibitor tablet per 10ml) was added and the embryos were then homogenised with a rotating pestle. The sample was centrifuged for 5min at 14000rpm and the supernatant was transferred to a clean tube. Three different dilutions (1:10, 1:100 and 1:1000) were made for both the w^{1118} and $fd3F^{1}$ samples and 20µl of each was boiled for 3min with 5µl gel loading buffer (as above). The samples were then run on an SDS-PAGE gel (4-12%, as above) at 175V for 1hr.

Once the gel had run to the bottom it was soaked for 15min in transfer buffer (25mM Tris, 192mM Glycine, 20% methanol). During this time a PVDF membrane was rinsed in methanol and then soaked on transfer buffer for 10min. The membrane was then placed on top of the gel with two sheets of 3MM blotting paper (wet with transfer buffer) on either side. The gel was then blotted onto the membrane at 90V for 1h with stirring to prevent over-heating. The PVDF membrane was blocked with 5% dried milk in PBT for 1h at room temperature with gentle shaking and then incubated with RbAb-fd3F (diluted 1:5000 in block) overnight. The following day the membrane was washed 4 times for 10min with PBT and then HRP conjugated secondary antibody was added (diluted 1:5000 in block). After incubating for 1h at room temperature the membrane was washed 4times for 10min with PBT. The membrane was then developed using the ECL plus kit (GE Healthcare, cat. RPN2132) according to the manufacturer's instructions. After the reaction the membrane was wrapped in Saran wrap and exposed to photographic film (1min exposure).

APPENDIX A

Fly Stocks

General fly stocks

Genotype	Nature of allele	Source/ Reference
w^{1118}	Used as wild type	Bloomington
Δ2-3	Source of transposase	Bloomington
ato^{1}	*ato* null mutant	Jarman et al., 1994
sca-Gal4	GAL4 driver	Egger et al., 2002
elav-Gal4	GAL4 driver	Bloomington
yw; 109-68Gal4	GAL4 driver	Jarman & Ahmed, 1998
yw; Pin/ Cyo	Visible dominant balancer	Bloomington
yw;; Ly/ TM3, Sb	Visible dominant balancer	Bloomington
FM6, ywB	Visible dominant balancer	Bloomington
FM7Bar, GFP	Visible dominant balancer	Donated by Dr Pennetta
FM6 ywB; Cyo	Visible dominant balancers	Bloomington

Chapter 2

Genotype	Annotation
UAS-dsfd3F^{37745}	RNAi line (Chr2), Vienna Drosophila RNAi Center
UAS-dsfd3F^{37746}	RNAi line (Chr3), Vienna Drosophila RNAi Center

Chapter 3

Genotype	Annotation
P{EP}fd3F^{EP1198}	P element insertion line
fd3F^{1}/ FM6ywB	fd3F deletion allele (heterozygous)
fd3F^{1}	fd3F deletion allele
Df(1)ED6716/ FM7h	Chromosomal deficiency in the region of fd3F (3F3-4B4) Bloomington
Df(1)ED6716/ FM7, GFP	Chromosomal deficiency in the region of fd3F (3F3-4B4)
yw; mCD8-GFP	Labels neuron membranes with GFP
fd3F^{1}, elav-Gal4	GAL4 driver in fd3F^{1} background (recombined)
fd3F^{1},elav-Gal4/ FM6ywB; mCD8-GFP	Labels neuron membranes with GFP in *fd3F^{1}* background
fd3F^{1}; Pin/ Cyo	fd3F deletion with visible dominant balancer
nompB-GFP	GFP protein fusion donated by Maurice Kernan
fd3F^{1}; nompB-GFP/ Cyo; nompB-GFP	nompB-GFP in fd3F^{1} background
RempA-YFP; TM6B	YFP protein fusion (Lee et al., 2008)
fd3F^{1}; RempA-YFP	RempA-YFP in fd3F^{1} background

Chapter 4

Genotype	Annotation
iav-GFP	Promoter fusion (550bp upstream sequence in PHStinger vector) by Lynn Powell
nan-GFP	Promoter fusion (600bp upstream sequence in PHStinger vector) by Lynn Powell
fd3F^{1}; iav-GFP	Promoter fusion in *fd3F^{1}* background
fd3F^{1}; nan-GFP	Promoter fusion in *fd3F^{1}* background
iav-F1-GFP	Site directed mutagenesis of fkh site furthest from start of gene
iav-F2-GFP	Site directed mutagenesis of fkh site nearest start of gene
iav-F1F2-GFP	Site directed mutagenesis of both fkh sites
nan-F1-GFP	Site directed mutagenesis of fkh site furthest from start of gene
nan-F2-GFP	Site directed mutagenesis of fkh site nearest start of gene
nan-F1F2-GFP	Site directed mutagenesis of both fkh sites
iav-X-GFP	Site directed mutagenesis of X-box site
nan-X-GFP	Site directed mutagenesis of X-box site

Chapter 5

Genotype	Annotation
UAS-fd3F(1)/ Cyo	fd3F ORF (as annotated in FlyBase) in PUAST. Chr2
UAS-fd3F(2)	fd3F ORF (as annotated in FlyBase) in PUAST. Chr2
UAS-fd3F(3)	fd3F ORF (as annotated in FlyBase) in PUAST. Chr3
UAS-fd3F(4)	fd3F ORF (as annotated in FlyBase) in PUAST. Chr2
UAS-fd3F(5)	fd3F ORF (as annotated in FlyBase) in PUAST. Chr2
$fd3F^{1}$*; sca-Gal4*	GAL4 driver in $fd3F^{1}$ background
$fd3F^{1}$*; UAS-fd3F(1)/ Cyo*	UAS-fd3F in $fd3F^{1}$ background, used for rescue
$fd3F^{1}$*;; UAS-fd3F(3)*	UAS-fd3F in $fd3F^{1}$ background, used for rescue
$fd3F^{1}$*; UAS-fd3F(5)*	UAS-fd3F in $fd3F^{1}$ background, used for rescue

APPENDIX B

Primers

Chapter 3

Name	Sequence (5'-3')	Application
EP 3'B	CGGTTTCGAGAGCAAAGAAC	3' primer for P element hop
5'fd3F 1	TGAATATTCGTGAATACTACCAGGC	5' primer for P element hop (500bp approx)
5'fd3F 5	TACCACGATGTCCTGTTGGA	5' primer for P element hop (1.5kb approx)
5'fd3F 6b	CCATTTCCAGCGGAGATTCC	5' primer for P element hop (2kb approx)

Chapter 4: Site directed mutagenesis

Name	Sequence (5'-3')
iav-F1 fwd	CTAGCACTAAGTTATAATTACAATAATAATAATGAAGGCAAAAATATCGTTAT ATACATAATTCAATAAAAAAAAACAAAAAGAAATTATATATT
iav-F1 rev	AATTATATAATTTCTTTTTGTTTTTTTTTATTGAATTATGATATATAACGATA TTTTTGCCTTCATTATTATTATTGTAATTATAACTTAGTGCTA
iav-F2 fwd	TCTTGATATCATGGGTCATCGAACAACGAAGCCGAGAAGGTT
iav-F2 rev	AACCTTCTCGGCTTCGTTGTTCGATGACCCATGATATCAAGA
nan-F1 fwd	AGCTGAACTTGAGCTCCTTTGCTTTCGTTACGCTGTGTTGC
nan-F1 rev	GCAACACAGCGTAACGAAAGCAAAGGAGCTCAAGTTCAGCT
nan-F2 fwd	GAGGTCCTTGTCCCATTGGTGGCTCGTGATAAAACATTTCCG
nan-F2 rev	CGGAAATGTTTTATCACGAGCCACAATGGACAAGGACCTC
iav-X fwd	GGCTGGGTGGGTGGGGTTAAAAGGACAACGAGCTGGCTTC
iav-X rev	GAAGCCAGCTCGTTGTCCTTTTAACCCCACCCACCCAGCC
nan-X fwd	CATTTCCGTGCACGTCCGTTGAAAATGCAACAGCTGAACTTGAG
nan-X rev	CTCAAGTTCAGCTGTTGCATTTTCAACGGACGTGCACGGAAATG

Chapter 4: Primers for *in situ* probes

Name	Sequence (5'-3')
fd3F 5'B	TAACCCACATTTTCGGAAGG
fd3F 3' T7	GTAATACGACTCACTATAGGGCGGTTGAACTCGTCGCTGAAG
iav 5'4	GTCGGAGAAGGAATGGATGGATGA
iav rv3	GTAATACGACTCACTATAGGGCCAGGACATGGGCTGAAACTGT
nan fw2	TCAATAGCCACCAATTGGACA
nan rv2	GTAATACGACTCACTATAGGGCCCAAAACTAAGCGGAAGCAC
robo3 5'	CCACCATCTTCTGGACCATC
robo3 3' T7	GTAATACGACTCACTATAGGGCTGGGTATCCAAGTCCTGCTC
rempA 5'	CTGCTCTTTCCCAGCAAATC
rempA 3' T7	GTAATACGACTCACTATAGGGCTTCAGGACTTGCTTCCTCGT
btv 5'	AGAATCATGCGGTGATCCTC
btv 3' T7	GTAATACGACTCACTATAGGGCCAAGGATTCGGATTGCAGTT
Dhc93AB 5'	GGTGGCTGCTCTTCAGAATC
Dhc93AB 3' T7	GTAATACGACTCACTATAGGGCCGCTTCTCATTGGGCTTTAG
nompB 5'	GCGTTTCGAGTTGCTAAAGG
nompB 3' T7	GTAATACGACTCACTATAGGGCGCTTTGCAGACGGGTGTATT
Dhc16F 5'	AACGTTCTCCTCCGCAGTAA
Dhc16F 3' T7	GTAATACGACTCACTATAGGGCAGGGATTGTTTTCCCATTCC
Dhc62B 5'	CAGCAGTGACAAGGAAACGA
Dhc62B 3' T7	GTAATACGACTCACTATAGGGCGGTAGCATCGATCCGTCAGT
CG13930 5'	ACGGAGGTACAGGAACATGG
CG13930 3' T7	GTAATACGACTCACTATAGGGCATCAGCCGGTACTTGGTCAC
Primers for *king tubby*, *CG5359*, *CG6129* and *CG15161* probes from Sebastian Cachero. *GFP* and *dila* probes from Lina Ma. Primers for all other probes from Petra zur Lage. These primers were also used for RT-PCR experiments.	

Chapter 4: fd3F forkhead domain for cloning into PGEX-2T

Name	Sequence (5'-3')	Restriction site
f domain 5'	CGGGATCCTGGCTGAAATCCAAAACC	BamH1
f domain 3'	GCGAATTCTCACTCACGGTTAATCGACTC	EcoR1

Chapter 5

Name	Sequence (5'-3')	Description
F1 forward	GCGCGAATTCCACCCACCAATGTGGCTGAAATC	UAS-fd3F construct, EcoR1 site
F2 reverse	GGGCTCGAGCGCTGAAACTGGAGTCTGTTG	UAS-fd3F construct, Xho1 site
5'1 (5'nc1)	AATTCCCAATTTCCGCTCTT	5' non-coding exon
5'2 (5'ex1)	TAAATTTCGCGTTCGCATTC	Start of fd3F ORF (as annotated on FlyBase)
5'3 (F2 fwd)	GCGCGAATTCCGATCGTTTCCCCTACTACA	Start of fd3F exon 2
3'1 (exon1 3')	GTGAACGGTGGTTTCTTTGG	3' end of fd3F exon 1
3'2 (F2 reverse)	GGGCTCGAGCGCTGAAACTGGAGTCTGTTG	3' end of fd3F ORF
3'A (f dom 3')	GCGAATTCTCACTCACGGTTAATCGACTC	3' of fd3F forkhead domain, rev strand
3'B (3'fd3F 4)	CGTCGCTCAACAGATCGTT	Mid-exon 3, rev strand
3'C (F2 rev)	GGGCTCGAGCGCTGAAACTGGAGTCTGTTG	3' end of fd3F ORF

APPENDIX C

Primary Antibodies

Antibody	Dilution	Reference/ source
Mouse α 22C10	1:200	Developmental Biology Hybridoma Bank, Iowa
Rabbit α HRP	1:500	Jackson Immuno Research laboratories
Rabbit α GFP	1:500	Molecular probes, Invitrogen
Rabbit α Atonal	1:2000	Jarman et al., 1995
Rabbit α couch potato	1:1000	Bellen et al., 1992
Sheep α DIG-AP	1:2000	Roche
Mouse α NompC	1:100	Donated by Jonathan Howard
Rabbit α fd3F	1:100	CovalAb/ Eurogentec (see materials & Methods)

References

Abdelkhalek HB, Beckers A, Schuster-Gossler K, Pavlova MN, Burkhardt H, Lickert H, Rossant J, Reinhardt R, Schalkwyk LC, Müller I, Herrmann BG, Ceolin M, Rivera-Pomar R, Gossler A. The mouse homeobox gene Not is required for caudal notochord development and affected by the truncate mutation. 2004 Genes Dev. Jul 15;18(14):1725-36.

Accili D, Arden KC. FoxOs at the crossroads of cellular metabolism, differentiation, and transformation. Cell. 2004 May 14;117(4):421-6

Aerts S, Quan XJ, Claeys A, Naval Sanchez M, Tate P, Yan J, Hassan BA. Robust target gene discovery through transcriptome perturbations and genome-wide enhancer predictions in Drosophila uncovers a regulatory basis for sensory specification. PLoS Biol. 2010 Jul 27;8(7):e1000435.

Alonso M. C & Cabrera C. V. (1988) The achaete-scute gene complex of Drosophila melanogaster comprises four homologous genes. *EMBO J.* 7: 2585-91

Amos LA. The tektin family of microtubule-stabilizing proteins. Genome Biol. 2008;9(7):229.

Anderson RG. The three-dimensional structure of the basal body from the rhesus monkey oviduct. J Cell Biol. 1972 Aug;54(2):246-65.

Andrade YN, Fernandes J, Vázquez E, Fernández-Fernández JM, Arniges M, Sánchez TM, Villalón M, Valverde MA. TRPV4 channel is involved in the coupling of fluid viscosity changes to epithelial ciliary activity. J Cell Biol. 2005 Mar 14;168(6):869-74.

Andrews KL, Nettesheim P, Asai DJ, Ostrowski LE Identification of seven rat axonemal dynein heavy chain genes: expression during ciliated cell differentiation. Mol Biol Cell. 1996 Jan;7(1):71-9.

Ansley SJ, Badano JL, Blacque OE, Hill J, Hoskins BE, Leitch CC, Kim JC, Ross AJ, Eichers ER, Teslovich TM, Mah AK, Johnsen RC, Cavender JC, Lewis RA, Leroux MR, Beales PL, Katsanis N. Basal body dysfunction is a likely cause of pleiotropic Bardet-Biedl syndrome. Nature. 2003 Oct 9;425(6958):628-33

Artavanis-Tsakonas, S; Rand, M. D; Lake, R. J. (1999) Notch signalling: cell fate control and signal integration in development. *Science* 284: 770-6.

Avidor-Reiss T, Maer AM, Koundakjian E, Polyanovsky A, Keil T, Subramaniam S, Zuker CS. Decoding cilia function: defining specialized genes required for compartmentalized cilia biogenesis. Cell. 2004 May 14;117(4):527-39.

Bae YK, Qin H, Knobel KM, Hu J, Rosenbaum JL, Barr MM. General and cell-type specific mechanisms target TRPP2/PKD-2 to cilia. Development. 2006 Oct;133(19):3859-70.

Baguley DM. Mechanisms of tinnitus. Br Med Bull. 2002;63:195-212.

Bahe S, Stierhof YD, Wilkinson CJ, Leiss F, Nigg EA. Rootletin forms centriole-associated filaments and functions in centrosome cohesion. J Cell Biol. 2005 Oct 10;171(1):27-33.

Baldari CT, Rosenbaum J. Intraflagellar transport: it's not just for cilia anymore. Curr Opin Cell Biol. 2010 Feb;22(1):75-80.

Bartoloni L, Blouin JL, Pan Y, Gehrig C, Maiti AK, Scamuffa N, Rossier C, Jorissen M, Armengot M, Meeks M, Mitchison HM, Chung EM, Delozier-Blanchet CD, Craigen WJ, Antonarakis SE. Mutations in the DNAH11 (axonemal heavy chain dynein type 11) gene cause one form of situs inversus totalis and most likely primary ciliary dyskinesia. Proc Natl Acad Sci U S A. 2002 Aug 6;99(16):10282-6.

Bechstedt S, Albert JT, Kreil DP, Müller-Reichert T, Göpfert MC, Howard J. A doublecortin containing microtubule-associated protein is implicated in mechanotransduction in Drosophila sensory cilia. Nat Commun. 2010 Apr 12;1:11.

Beckers A, Alten L, Viebahn C, Andre P, Gossler A. The mouse homeobox gene Noto regulates node morphogenesis, notochordal ciliogenesis, and left right patterning. Proc Natl Acad Sci U S A. 2007 Oct 2;104(40):15765-70.

Bell LR, Stone S, Yochem J, Shaw JE, Herman RK. The molecular identities of the Caenorhabditis elegans intraflagellar transport genes dyf-6, daf-10 and osm-1. Genetics. 2006 Jul;173(3):1275-86.

Bellen HJ, Kooyer S, D'Evelyn D, Pearlman J. The Drosophila couch potato protein is expressed in nuclei of peripheral neuronal precursors and shows homology to RNA-binding proteins. Genes Dev. 1992 Nov;6(11):2125-36.

Berbari NF, Lewis JS, Bishop GA, Askwith CC, Mykytyn K. Bardet-Biedl syndrome proteins are required for the localization of G protein-coupled receptors to primary cilia. Proc Natl Acad Sci U S A. 2008 Mar 18;105(11):4242-6

Bermingham NA, Hassan BA, Price SD, Vollrath MA, Ben-Arie N, Eatock RA, Bellen HJ, Lysakowski A, Zoghbi HY. Math1: an essential gene for the generation of inner ear hair cells. Science. 1999 Jun 11;284(5421):1837-41.

Bertrand, N; Castro, S. C; Guillemot, F. (2002) Proneural genes and the specification of neural cell types. *Nature Rev. Neuroscience* 3: 517-528

Bhalerao S, Berdnik D, Török T, Knoblich JA. Localization-dependent and -independent roles of numb contribute to cell-fate specification in Drosophila. Curr Biol. 2005 Sep 6;15(17):1583-90.

Biggs WH 3rd, Cavenee WK, Arden KC Identification and characterization of members of the FKHR (FOX O) subclass of winged-helix transcription factors in the mouse.
Mamm Genome. 2001 Jun;12(6):416-25.

Biggs WH 3rd, Meisenhelder J, Hunter T, Cavenee WK, Arden KC. Protein kinase B/Akt-mediated phosphorylation promotes nuclear exclusion of the winged helix transcription factor FKHR1. Proc Natl Acad Sci U S A. 1999 Jun 22;96(13):7421-6.

Blacque OE, Reardon MJ, Li C, McCarthy J, Mahjoub MR, Ansley SJ, Badano JL, Mah AK, Beales PL, Davidson WS, Johnsen RC, Audeh M, Plasterk RH, Baillie DL, Katsanis N, Quarmby LM, Wicks SR, Leroux MR. Loss of C. elegans BBS-7 and BBS-8 protein function results in cilia defects and compromised intraflagellar transport. Genes Dev. 2004 Jul 1;18(13):1630-42.

Blochlinger K, Jan LY, Jan YN. Transformation of sensory organ identity by ectopic expression of Cut in Drosophila. Genes Dev. 1991 Jul;5(7):1124-35.

Bloodgood, R. A., Woodward, M. P. and Young, W. W. (1995). Unusual distribution of a glycolipid antigen in the flagella of Chamydomonas. Protoplasma 185, 123-130.

Bodmer R, Barbel S, Sheperd S, Jack JW, Jan LY, Jan YN. Transformation of sensory organs by mutations of the cut locus of D. melanogaster. Cell. 1987 Oct 23;51(2):293-307.

Boekhoff-Falk G. Hearing in Drosophila: development of Johnston's organ and emerging parallels to vertebrate ear development. Dev Dyn. 2005 Mar;232(3):550-8.

Bonnafe E, Touka M, AitLounis A, Baas D, Barras E, Ucla C, Moreau A, Flamant F, Dubruille R, Couble P, Collignon J, Durand B, Reith W. The transcription factor RFX3 directs nodal cilium development and left-right asymmetry specification. Mol Cell Biol. 2004 May;24(10):4417-27.

Brand AH, Perrimon N. Targeted gene expression as a means of altering cell fates and generating dominant phenotypes. Development. 1993 Jun;118(2):401-15.

Bressac C, Joly D, Devaux J, Serres C, Feneux D, Lachaise D. Comparative kinetics of short and long sperm in sperm dimorphic Drosophila species. Cell Motil Cytoskeleton. 1991;19(4):269-74.

Brewster R & Bodmer R (1995) Origin and specification of type II sensory neurons in Drosophila *Development* 121: 2923-2936

Brody SL, Yan XH, Wuerffel MK, Song SK, Shapiro SD. Ciliogenesis and left-right axis defects in forkhead factor HFH-4-null mice. Am J Respir Cell Mol Biol. 2000 Jul;23(1):45-51.

Brown, N. L; Paddock S. W; Sattler C. A; Cronmiller C; Thomas B. J; Carroll S. B. (1996) Daughterless is required for Drosophila photoreceptor cell determination, eye morphogenesis, and cell cycle progression. *Dev Biol.* 179: 65-78.

Burgess SA, Walker ML, Sakakibara H, Knight PJ, Oiwa K. Dynein structure and power stroke. Nature. 2003 Feb 13;421(6924):715-8.

Cabrera C. V, Martinez-Arias A, Bate M. (1987)The expression of three members of the achaete-scute gene complex correlates with neuroblast segregation in Drosophila. *Cell.* 50: 425-33

Cabrera CV, Alonso MC, Huikeshoven H. Regulation of scute function by extramacrochaete in vitro and in vivo. Development. 1994 Dec;120(12):3595-603.

Cachero S, Simpson TI, Zur Lage PI, Ma L, Newton FG, Holohan EE, Armstrong JD, Jarman AP. The gene regulatory cascade linking proneural specification with differentiation in Drosophila sensory neurons. PLoS Biol. 2011 Jan 4;9(1):e1000568.

Caldwell JC, Eberl DF. Towards a molecular understanding of Drosophila hearing. J Neurobiol. 2002 Nov 5;53(2):172-89.

Caldwell JC, Miller MM, Wing S, Soll DR, Eberl DF. Dynamic analysis of larval locomotion in Drosophila chordotonal organ mutants. Proc Natl Acad Sci U S A. 2003 Dec 23;100(26):16053-8.

Caldwell SA, Jackson SR, Shahriari KS, Lynch TP, Sethi G, Walker S, Vosseller K, Reginato MJ. Nutrient sensor O-GlcNAc transferase regulates breast cancer tumorigenesis through targeting of the oncogenic transcription factor FoxM. Oncogene. 2010 May 13;29(19):2831-42.

Campos-Ortega JA, Hartenstein V
The Embryonic Development of Drosophila melanogaster.
1997 Second Edition, Springer ISBN 3-54057079-9

Carlsson P, Mahlapuu M. Forkhead transcription factors: key players in development and metabolism. Dev Biol. 2002 Oct 1;250(1):1-23.

Caterina MJ, Leffler A, Malmberg AB, Martin WJ, Trafton J, Petersen-Zeitz KR, Koltzenburg M, Basbaum AI, Julius D. Impaired nociception and pain sensation in mice lacking the capsaicin receptor. Science. 2000 Apr 14;288(5464):306-13.

Cederberg A, Grønning LM, Ahrén B, Taskén K, Carlsson P, Enerbäck S. FOXC2 is a winged helix gene that counteracts obesity, hypertriglyceridemia, and diet-induced insulin resistance. Cell. 2001 Sep 7;106(5):563-73.

Chanet S, Vodovar N, Mayau V, Schweisguth F. Genome engineering-based analysis of Bearded family genes reveals both functional redundancy and a nonessential function in lateral inhibition in Drosophila. Genetics. 2009 Aug;182(4):1101-8.

Chapin HC, Caplan MJ. The cell biology of polycystic kidney disease. J Cell Biol. 2010 Nov 15;191(4):701-10.

Chen J, Knowles HJ, Hebert JL, Hackett BP. Mutation of the mouse hepatocyte nuclear factor/forkhead homologue 4 gene results in an absence of cilia and random left-right asymmetry. J Clin Invest. 1998 Sep 15;102(6):1077-82.

Chen Z, Indjeian VB, McManus M, Wang L, Dynlacht BD. CP110, a cell cycle-dependent CDK substrate, regulates centrosome duplication in human cells. Dev Cell. 2002 Sep;3(3):339-50.

Cheng LE, Song W, Looger LL, Jan LY, Jan YN. The role of the TRP channel NompC in Drosophila larval and adult locomotion. Neuron. 2010 Aug 12;67(3):373-80.

Chien C. T; Hsiao C. D; Jan L.Y; Jan Y. N. (1996) Neuronal type information encoded in the basic-helix-loop-helix domain of proneural genes. *Proc Natl Acad Sci U S A*. 93: 13239-44

Christensen ST, Guerra C, Wada Y, Valentin T, Angeletti RH, Satir P, Hamasaki T. A regulatory light chain of ciliary outer arm dynein in Tetrahymena thermophila. J Biol Chem. 2001 Jun 8;276(23):20048-54.

Chung YD, Zhu J, Han Y, Kernan MJ. nompA encodes a PNS-specific, ZP domain protein required to connect mechanosensory dendrites to sensory structures. Neuron. 2001 Feb;29(2):415-28.

Cirillo LA, McPherson CE, Bossard P, Stevens K, Cherian S, Shim EY, Clark KL, Burley SK, Zaret KS. Binding of the winged-helix transcription factor HNF3 to a linker histone site on the nucleosome. EMBO J. 1998 Jan 2;17(1):244-54.

Cirillo LA, Zaret KS. Specific interactions of the wing domains of FOXA1 transcription factor with DNA. J Mol Biol. 2007 Feb 23;366(3):720-4.

Clapham DE. TRP channels as cellular sensors. Nature. 2003 Dec 4;426(6966):517-24.

Clark KL, Halay ED, Lai E, Burley SK.Co-crystal structure of the HNF-3/fork head DNA-recognition motif resembles histone H5.Nature. 1993 Jul 29;364(6436):412-20.

Colbert HA, Smith TL, Bargmann CI. OSM-9, a novel protein with structural similarity to channels, is required for olfaction, mechanosensation, and olfactory adaptation in Caenorhabditis elegans. J Neurosci. 1997 Nov 1;17(21):8259-69.

Cole DG, Diener DR, Himelblau AL, Beech PL, Fuster JC, Rosenbaum JL. Chlamydomonas kinesin-II-dependent intraflagellar transport (IFT): IFT particles contain proteins required for ciliary assembly in Caenorhabditis elegans sensory neurons. J Cell Biol. 1998 May 18;141(4):993-1008.

Cole DG. The intraflagellar transport machinery of Chlamydomonas reinhardtii. Traffic. 2003 Jul;4(7):435-42.

Corbit KC, Aanstad P, Singla V, Norman AR, Stainier DY, Reiter JF. Vertebrate Smoothened functions at the primary cilium. Nature. 2005 Oct 13;437(7061):1018-21.

Corbit KC, Shyer AE, Dowdle WE, Gaulden J, Singla V, Chen MH, Chuang PT, Reiter JF. Kif3a constrains beta-catenin-dependent Wnt signalling through dual ciliary and non-ciliary mechanisms. Nat Cell Biol. 2008 Jan;10(1):70-6.

Corey DP, García-Añoveros J, Holt JR, Kwan KY, Lin SY, Vollrath MA, Amalfitano A, Cheung EL, Derfler BH, Duggan A, Géléoc GS, Gray PA, Hoffman MP, Rehm HL, Tamasauskas D, Zhang DS. TRPA1 is a candidate for the mechanosensitive transduction channel of vertebrate hair cells. Nature. 2004 Dec 9;432(7018):723-30.

Cortellino S, Wang C, Wang B, Bassi MR, Caretti E, Champeval D, Calmont A, Jarnik M, Burch J, Zaret KS, Larue L, Bellacosa A. Defective ciliogenesis, embryonic lethality and severe impairment of the Sonic Hedgehog pathway caused by inactivation of the mouse complex A intraflagellar transport gene Ift122/Wdr10, partially overlapping with the DNA repair gene Med1/Mbd4. Dev Biol. 2009 Jan 1;325(1):225-37.

Craige B, Tsao CC, Diener DR, Hou Y, Lechtreck KF, Rosenbaum JL, Witman GB. CEP290 tethers flagellar transition zone microtubules to the membrane and regulates flagellar protein content. J Cell Biol. 2010 Sep 6;190(5):927-40.

Crozatier M, Vincent A. Control of multidendritic neuron differentiation in Drosophila: the role of Collier.Dev Biol. 2008 Mar 1;315(1):232-42.

Cruz C, Ribes V, Kutejova E, Cayuso J, Lawson V, Norris D, Stevens J, Davey M, Blight K, Bangs F, Mynett A, Hirst E, Chung R, Balaskas N, Brody SL, Marti E, Briscoe J. Foxj1 regulates floor plate cilia architecture and modifies the response of cells to sonic hedgehog signalling. Development. 2010 Dec;137(24):4271-82.

Cuesta I, Zaret KS, Santisteban P. The forkhead factor FoxE1 binds to the thyroperoxidase promoter during thyroid cell differentiation and modifies compacted chromatin structure. Mol Cell Biol. 2007 Oct;27(20):7302-14.

Culí J, Martín-Blanco E, Modolell J. (2001) The EGF receptor and N signalling pathways act antagonistically in Drosophila mesothorax bristle patterning. *Development.* 128(2): 299-308.

Deane JA, Cole DG, Seeley ES, Diener DR, Rosenbaum JL. Localization of intraflagellar transport protein IFT52 identifies basal body transitional fibers as the docking site for IFT particles. Curr Biol. 2001 Oct 16;11(20):1586-90.
Decoding cilia function: defining specialized genes required for compartmentalized cilia biogenesis. Cell. 2004 May 14;117(4):527-39.

Di Palma F, Belyantseva IA, Kim HJ, Vogt TF, Kachar B, Noben-Trauth K. Mutations in Mcoln3 associated with deafness and pigmentation defects in varitint-waddler (Va) mice. Proc Natl Acad Sci U S A. 2002 Nov 12;99(23):14994-9.

Dickinson M (1990) Linear and nonlinear encoding properties of an identified mechanoreceptor on the fly wing measured with mechanical noise stimuli. J Exp Biol 151:219-244

Dietzl G, Chen D, Schnorrer F, Su KC, Barinova Y, Fellner M, Gasser B, Kinsey K, Oppel S, Scheiblauer S, Couto A, Marra V, Keleman K, Dickson BJ. A genome-wide transgenic RNAi library for conditional gene inactivation in Drosophila. Nature. 2007 Jul 12;448(7150):151-6.

Doroquez D. B, Orr-Weaver T. L, Rebay I. (2007) Split ends antagonizes the Notch and potentiates the EGFR signaling pathways during Drosophila eye development. *Mech Dev.* 124: 792-806.

Dubruille R, Laurençon A, Vandaele C, Shishido E, Coulon-Bublex M, Swoboda P, Couble P, Kernan M, Durand B. Drosophila regulatory factor X is necessary for ciliated sensory neuron differentiation. Development. 2002 Dec;129(23):5487-98.

Eberl DF, Hardy RW, Kernan MJ. Genetically similar transduction mechanisms for touch and hearing in Drosophila. J Neurosci. 2000 Aug 15;20(16):5981-8.

Effertz T, Wiek R, Göpfert MC. NompC TRP channel is essential for Drosophila sound receptor function. Curr Biol. 2011 Apr 12;21(7):592-7.

Efimenko E, Bubb K, Mak HY, Holzman T, Leroux MR, Ruvkun G, Thomas JH, Swoboda P. Analysis of xbx genes in C. elegans. Development. 2005 Apr;132(8):1923-34.

Ejsmont RK, Sarov M, Winkler S, Lipinski KA, Tomancak P. A toolkit for high-throughput, cross-species gene engineering in Drosophila. Nat Methods. 2009 Jun;6(6):435-7.

El Zein L, Ait-Lounis A, Morlé L, Thomas J, Chhin B, Spassky N, Reith W, Durand B. RFX3 governs growth and beating efficiency of motile cilia in mouse and controls the expression of genes involved in human ciliopathies. J Cell Sci. 2009 Sep 1;122(Pt 17):3180-9.

Elliott SL, Cullen CF, Wrobel N, Kernan MJ, Ohkura H. EB1 is essential during Drosophila development and plays a crucial role in the integrity of chordotonal mechanosensory organs. Mol Biol Cell. 2005 Feb;16(2):891-901.

Elstob PR, Brodu V, Gould AP (2001) spalt-dependent switching between two cell fates that are induced by the Drosophila EGF receptor. Development 128, 723–732.

Evans JE, Snow JJ, Gunnarson AL, Ou G, Stahlberg H, McDonald KL, Scholey JM. Functional modulation of IFT kinesins extends the sensory repertoire of ciliated neurons in Caenorhabditis elegans. J Cell Biol. 2006 Feb 27;172(5):663-9.

Fan ZC, Behal RH, Geimer S, Wang Z, Williamson SM, Zhang H, Cole DG, Qin H Chlamydomonas IFT70/CrDYF-1 is a core component of IFT particle complex B and is required for flagellar assembly. Mol Biol Cell. 2010 Aug 1;21(15):2696-706.

Ferri AL, Lin W, Mavromatakis YE, Wang JC, Sasaki H, Whitsett JA, Ang SL. Fxa1 and Foxa2 regulate multiple phases of midbrain dopaminergic neuron development in a dosage-dependent manner. Development. 2007 Aug;134(15):2761-9.

Fettiplace R, Hackney CM. The sensory and motor roles of auditory hair cells. Nat Rev Neurosci. 2006 Jan;7(1):19-29.

Field LH & Matheson T (1998) Chordotonal organs of insects. Advances in Insect Physiology 27: 1-228.

Fisher A and Caudy M. The function of hairy-related bHLH repressor proteins in cell fate decisions Bioessays, 1998. 20, 298-306.

Follit JA, Tuft RA, Fogarty KE, Pazour GJ. The intraflagellar transport protein IFT20 is associated with the Golgi complex and is required for cilia assembly. Mol Biol Cell. 2006 Sep;17(9):3781-92.

Fowkes ME, Mitchell DR. The role of preassembled cytoplasmic complexes in assembly of flagellar dynein subunits. Mol Biol Cell. 1998 Sep;9(9):2337-47.

Gadelha C, Rothery S, Morphew M, McIntosh JR, Severs NJ, Gull K. Membrane domains and flagellar pocket boundaries are influenced by the cytoskeleton in African trypanosomes. Proc Natl Acad Sci U S A. 2009 Oct 13;106(41):17425-30

Gajiwala KS, Burley SK. Winged helix proteins. Curr Opin Struct Biol. 2000 Feb;10(1):110-6.
Gallardo TD, John GB, Bradshaw K, Welt C, Reijo-Pera R, Vogt PH, Touraine P, Bione S, Toniolo D, Nelson LM, Zinn AR, Castrillon DH. Sequence variation at the human FOXO3 locus: a study of premature ovarian failure and primary amenorrhea. Hum Reprod. 2008 Jan;23(1):216-21.

Gao X, Wu L, O'Neil RG. Temperature-modulated diversity of TRPV4 channel gating: activation by physical stresses and phorbol ester derivatives through protein kinase C-dependent and -independent pathways. J Biol Chem. 2003 Jul 18;278(29):27129-37.
Genes Dev. 2003 Jan 1;17(1):1-6.

Gerdes JM, Liu Y, Zaghloul NA, Leitch CC, Lawson SS, Kato M, Beachy PA, Beales PL, DeMartino GN, Fisher S, Badano JL, Katsanis N. Disruption of the basal body compromises proteasomal function and perturbs intracellular Wnt response. Nat Genet. 2007 Nov;39(11):1350-60.

Gho M, Bellaïche Y, Schweisguth F. Revisiting the Drosophila microchaete lineage: a novel intrinsically asymmetric cell division generates a glial cell. Development. 1999 Aug;126(16):3573-84.

Ghysen, A., and O'Kane, C. Detection of neural enhancer-like elements in the genome of Drosophila. Development 1989. 705, 35-52.

Gibert J. M & Simpson P. (2003) Evolution of cis-regulation of the proneural genes. *Int J Dev Biol* 47: 643-651.

Gillespie PG, Walker RG. Molecular basis of mechanosensory transduction. Nature. 2001 Sep 13;413(6852):194-202.

Gilley J, Coffer PJ, Ham J. FOXO transcription factors directly activate bim gene expression and promote apoptosis in sympathetic neurons. J Cell Biol. 2003 Aug 18;162(4):613-22.

Gilula NB, Satir P. The ciliary necklace. A ciliary membrane specialization. J Cell Biol. 1972 May;53(2):494-509.

Giot L, Bader JS, Brouwer C, Chaudhuri A, Kuang B, Li Y, Hao YL, Ooi CE, Godwin B, Vitols E, Vijayadamodar G, Pochart P, Machineni H, Welsh M, Kong Y, Zerhusen B, Malcolm R, Varrone Z, Collis A, Minto M, Burgess S, McDaniel L, Stimpson E, Spriggs F, Williams J, Neurath K, Ioime N, Agee M, Voss E, Furtak K, Renzulli R, Aanensen N, Carrolla S, Bickelhaupt E, Lazovatsky Y, DaSilva A, Zhong J, Stanyon CA, Finley RL Jr, White KP, Braverman M, Jarvie T, Gold S, Leach M, Knight J, Shimkets RA, McKenna MP, Chant J, Rothberg JM. A protein interaction map of Drosophila melanogaster. Science. 2003 Dec 5;302(5651):1727-36.

Gloor GB, Preston CR, Johnson-Schlitz DM, Nassif NA, Phillis RW, Benz WK, Robertson HM, Engels WR. Type I repressors of P element mobility. Genetics. 1993 Sep;135(1):81-95.

Gohlke JM, Armant O, Parham FM, Smith MV, Zimmer C, Castro DS, Nguyen L, Parker JS, Gradwohl G, Portier CJ, Guillemot F. Characterization of the proneural gene regulatory network during mouse telencephalon development. BMC Biol. 2008 Mar 31;6:15.

Gomperts BN, Gong-Cooper X, Hackett BP. Foxj1 regulates basal body anchoring to the cytoskeleton of ciliated pulmonary epithelial cells. J Cell Sci. 2004 Mar 15;117(Pt 8):1329-37.

Gong Z, Son W, Chung YD, Kim J, Shin DW, McClung CA, Lee Y, Lee HW, Chang DJ, Kaang BK, Cho H, Oh U, Hirsh J, Kernan MJ, Kim C. Two interdependent TRPV channel subunits, inactive and Nanchung, mediate hearing in Drosophila. J Neurosci. 2004 Oct 13;24(41):9059-66.

Göpfert MC, Albert JT, Nadrowski B, Kamikouchi A. Specification of auditory sensitivity by Drosophila TRP channels. Nat Neurosci. 2006 Aug;9(8):999-1000.

Göpfert MC, Robert D. Active auditory mechanics in mosquitoes. Proc Biol Sci. 2001 Feb 22;268

Göpfert MC, Robert D. Biomechanics. Turning the key on Drosophila audition. Nature. 2001 Jun 21;411(6840):908.

Göpfert MC, Robert D. Motion generation by Drosophila mechanosensory neurons. Proc Natl Acad Sci U S A. 2003 Apr 29;100(9):5514-9.

Göpfert MC, Robert D. The mechanical basis of Drosophila audition. J Exp Biol. 2002 May;205(Pt 9):1199-208.

Gould AP, Elstob PR, Brodu V. Insect oenocytes: a model system for studying cell-fate specification by Hox genes. J Anat. 2001 Jul-Aug;199(Pt 1-2):25-33.

Goulding SE, zur Lage P, Jarman AP. amos, a proneural gene for Drosophila olfactory sense organs that is regulated by lozenge. Neuron. 2000 Jan;25(1):69-78.

Graser S, Stierhof YD, Lavoie SB, Gassner OS, Lamla S, Le Clech M, Nigg EA. Cep164, a novel centriole appendage protein required for primary cilium formation. J Cell Biol. 2007 Oct 22;179(2):321-30.

Grossniklaus U, Cadigan KM, Gehring WJ. Three maternal coordinate systems cooperate in the patterning of the Drosophila head. Development. 1994 Nov;120(11):3155-71.

Grueber WB, Jan LY, Jan YN. Different levels of the homeodomain protein cut regulate distinct dendrite branching patterns of Drosophila multidendritic neurons.Cell. 2003 Mar 21;112(6):805-18.

Grueber WB, Ye B, Moore AW, Jan LY, Jan YN. Dendrites of distinct classes of Drosophila sensory neurons show different capacities for homotypic repulsion. Curr Biol. 2003 Apr 15;13(8):618-26.

Grünert, U., Gnatzy, W. K+ and Ca++ in the receptor lymph of arthropod cuticular mechanoreceptors. J. Comp. Physiol.,1987. 161, 329-333.

Gupta BP, Rodrigues V. Atonal is a proneural gene for a subset of olfactory sense organs in Drosophila.Genes Cells. 1997 Mar;2(3):225-33.

Habermacher G, Sale WS. Regulation of flagellar dynein by phosphorylation of a 138-kD inner arm dynein intermediate chain. J Cell Biol. 1997 Jan 13;136(1):167-76.

Habura A, Tikhonenko I, Chisholm RL, Koonce MP. Interaction mapping of a dynein heavy chain. Identification of dimerization and intermediate-chain binding domains. J Biol Chem. 1999 May 28;274(22):15447-53.

Häcker U, Grossniklaus U, Gehring WJ, Jäckle H. Developmentally regulated Drosophila gene family encoding the fork head domain. Proc Natl Acad Sci U S A. 1992 Sep 15;89(18):8754-8.

Hacker, U., Kaufmann, E., Hartmann, C., Jurgens, G., Knochel, W., Jaeckle, H. The Drosophila fork head domain protein crocodile is required for the establishment of head structures. EMBO J. 1995 14(21): 5306--5317.

Hackett BP, Brody SL, Liang M, Zeitz ID, Bruns LA, Gitlin JD. Primary structure of hepatocyte nuclear factor/forkhead homologue 4 and characterization of gene expression in the developing respiratory and reproductive epithelium. Proc Natl Acad Sci U S A. 1995 May 9;92(10):4249-53.

Han YG, Kwok BH, Kernan MJ. Intraflagellar transport is required in Drosophila to differentiate sensory cilia but not sperm. Curr Biol. 2003 Sep 30;13(19):1679-86.

Hansen IA, Sieglaff DH, Munro JB, Shiao SH, Cruz J, Lee IW, Heraty JM, Raikhel AS. Forkhead transcription factors regulate mosquito reproduction. Insect Biochem Mol Biol. 2007 Sep;37(9):985-97.

Hartenstein AY, Rugendorff A, Tepass U, Hartenstein V The function of the neurogenic genes during epithelial development in the Drosophila embryo. Development 1992 116, 1203–1220

Hatta M, Liu F, Cirillo LA Acetylation curtails nucleosome binding, not stable nucleosome remodeling, by FoxO1. Biochem Biophys Res Commun. 2009 Feb 20;379(4):1005-8.

Haycraft CJ, Banizs B, Aydin-Son Y, Zhang Q, Michaud EJ, Yoder BK. Gli2 and Gli3 localize to cilia and require the intraflagellar transport protein polaris for processing and function. PLoS Genet. 2005 Oct;1(4):e53.

Haycraft CJ, Schafer JC, Zhang Q, Taulman PD, Yoder BK. Identification of CHE-13, a novel intraflagellar transport protein required for cilia formation. Exp Cell Res. 2003 Apr 1;284(2):251-63.

Hellman NE, Liu Y, Merkel E, Austin C, Le Corre S, Beier DR, Sun Z, Sharma N, Yoder BK, Drummond IA. The zebrafish foxj1a transcription factor regulates cilia function in response to injury and epithelial stretch. Proc Natl Acad Sci U S A. 2010 Oct 26;107(43):18499-504.

Hirokawa N, Noda Y. Intracellular transport and kinesin superfamily proteins, KIFs: structure, function, and dynamics. Physiol Rev. 2008 Jul;88(3):1089-118

Hisatsune C, Kuroda Y, Nakamura K, Inoue T, Nakamura T, Michikawa T, Mizutani A, Mikoshiba K. Regulation of TRPC6 channel activity by tyrosine phosphorylation. J Biol Chem. 2004 Apr 30;279(18):18887-94.

Ho SR, Wang K, Whisenhunt TR, Huang P, Zhu X, Kudlow JE, Paterson AJ. O-GlcNAcylation enhances FOXO4 transcriptional regulation in response to stress. FEBS Lett. 2010 Jan 4;584(1):49-54.

Hogan CC, Bettencourt BR. Duplicate gene evolution toward multiple fates at the Drosophila melanogaster HIP/HIP-Replacement locus. J Mol Evol. 2009 Apr;68(4):337-50.

Holohan E. E, zur Lage P. I, Jarman A. P. (2006) Multiple enhancers contribute to spatial but not temporal complexity in the expression of the proneural gene, amos. *BMC Dev Biol.* 6: 53.

Höök P, Vallee RB. The dynein family at a glance. J Cell Sci. 2006 Nov 1;119(Pt 21):4369-71.

Hori S, Nomura T, Sakaguchi S. Control of regulatory T cell development by the transcription factor Foxp3. Science. 2003 Feb 14;299(5609):1057-61.

Hou Y, Pazour GJ, Witman GB. A dynein light intermediate chain, D1bLIC, is required for retrograde intraflagellar transport. Mol Biol Cell. 2004 Oct;15(10):4382-94.

Hou Y, Qin H, Follit JA, Pazour GJ, Rosenbaum JL, Witman GB. Functional analysis of an individual IFT protein: IFT46 is required for transport of outer dynein arms into flagella. J Cell Biol. 2007 Feb 26;176(5):653-65.

Howard J, Bechstedt S. Hypothesis: a helix of ankyrin repeats of the NOMPC-TRP ion channel is the gating spring of mechanoreceptors. Curr Biol. 2004 Mar 23;14(6):R224-6.

Hu B, Lefort K, Qiu W, Nguyen BC, Rajaram RD, Castillo E, He F, Chen Y, Angel P, Brisken C, Dotto GP. Control of hair follicle cell fate by underlying mesenchyme through a CSL-Wnt5a-FoxN1 regulatory axis. Genes Dev. 2010 Jul 15;24(14):1519-32.

Huang K, Diener DR, Mitchell A, Pazour GJ, Witman GB, Rosenbaum JL. Function and dynamics of PKD2 in Chlamydomonas reinhardtii flagella. J Cell Biol. 2007 Nov 5;179(3):501-14.

Huang ML, Hsu CH, Chien CT. The proneural gene amos promotes multiple dendritic neuron formation in the Drosophila peripheral nervous system. Neuron. 2000 Jan;25(1):57-67.

Huangfu D, Liu A, Rakeman AS, Murcia NS, Niswander L, Anderson KV. Hedgehog signalling in the mouse requires intraflagellar transport proteins. Nature. 2003 Nov 6;426(6962):83-7.

Hudspeth AJ, Choe Y, Mehta AD, Martin P. Putting ion channels to work: mechanoelectrical transduction, adaptation, and amplification by hair cells. Proc Natl Acad Sci U S A. 2000 Oct 24;97(22):11765-72.

Hudspeth AJ, Corey DP. Sensitivity, polarity, and conductance change in the response of vertebrate hair cells to controlled mechanical stimuli. Proc Natl Acad Sci U S A. 1977 Jun;74(6):2407-11.

Hughes CL, Thomas JB. A sensory feedback circuit coordinates muscle activity in Drosophila. Mol Cell Neurosci. 2007 Jun;35(2):383-96.

Hummel T, Krukkert K, Roos J, Davis G, Klämbt C. Drosophila Futsch/22C10 is a MAP1B-like protein required for dendritic and axonal development. Neuron. 2000 May;26(2):357-70.

Hutterer A, Knoblich JA.
Numb and alpha-Adaptin regulate Sanpodo endocytosis to specify cell fate in Drosophila external sensory organs. EMBO Rep. 2005 Sep;6(9):836-42.

Hwang RY, Zhong L, Xu Y, Johnson T, Zhang F, Deisseroth K, Tracey WD. Nociceptive neurons protect Drosophila larvae from parasitoid wasps. Curr Biol. 2007 Dec 18;17(24):2105-16.

Inbal A, Levanon D, Salzberg A. (2003). Multiple roles for u-turn/ventral veinless in the development of Drosophila PNS. *Development.* 130: 2467-78.

Iomini C, Babaev-Khaimov V, Sassaroli M, Piperno G. Protein particles in Chlamydomonas flagella undergo a transport cycle consisting of four phases. J Cell Biol. 2001 Apr 2;153(1):13-24.

Iomini C, Li L, Esparza JM, Dutcher SK. Retrograde intraflagellar transport mutants identify complex A proteins with multiple genetic interactions in Chlamydomonas reinhardtii. Genetics. 2009 Nov;183(3):885-96.

Ishikawa H, Kubo A, Tsukita S, Tsukita S. Odf2-deficient mother centrioles lack distal/subdistal appendages and the ability to generate primary cilia. Nat Cell Biol. 2005 May;7(5):517-24.

Ishikawa H, Marshall WF. Ciliogenesis: building the cell's antenna. Nat Rev Mol Cell Biol. 2011 Apr;12(4):222-34.

Iwama A, Pan J, Zhang P, Reith W, Mach B, Tenen DG, Sun Z. Dimeric RFX proteins contribute to the activity and lineage specificity of the interleukin-5 receptor alpha promoter through activation and repression domains. Mol Cell Biol. 1999 Jun;19(6):3940-50.

Jacquet BV, Salinas-Mondragon R, Liang H, Therit B, Buie JD, Dykstra M, Campbell K, Ostrowski LE, Brody SL, Ghashghaei HT. FoxJ1-dependent gene expression is required for differentiation of radial glia into ependymal cells and a subset of astrocytes in the postnatal brain. Development. 2009 Dec;136(23):4021-31.

Jan YN, Jan LY.HLH proteins, fly neurogenesis, and vertebrate myogenesis. Cell. 1993 Dec 3;75(5):827-30.

Jarman AP, Ahmed I. The specificity of proneural genes in determining Drosophila sense organ identity. Mech Dev. 1998 Aug;76(1-2):117-25

Jarman AP, Grau Y, Jan LY, Jan YN. atonal is a proneural gene that directs chordotonal organ formation in the Drosophila peripheral nervous system. Cell. 1993 Jul 2;73(7):1307-21.

Jarman AP, Grell EH, Ackerman L, Jan LY, Jan YN. Atonal is the proneural gene for Drosophila photoreceptors.Nature. 1994 Jun 2;369(6479):398-400.

Jarman AP, Sun Y, Jan LY, Jan YN. Role of the proneural gene, atonal, in formation of Drosophila chordotonal organs and photoreceptors. Development. 1995 Jul;121(7):2019-30.

Jarman, A. P. (2002) Studies of machanosensation using the fly. *Human Molecular Genetics* 11: 1215-1218

Jenkins PM, Hurd TW, Zhang L, McEwen DP, Brown RL, Margolis B, Verhey KJ, Martens JR. Ciliary targeting of olfactory CNG channels requires the CNGB1b subunit and the kinesin-2 motor protein, KIF17. Curr Biol. 2006 Jun 20;16(12):1211-6.

Jafar-Nejad H, Andrews HK, Acar M, Bayat V, Wirtz-Peitz F, Mehta SQ, Knoblich JA, Bellen HJ. Sec15, a component of the exocyst, promotes notch signaling during the asymmetric division of Drosophila sensory organ precursors. Dev Cell. 2005 Sep;9(3):351-63.

Jiménez F & Campos-Ortega J. A. (1990) Defective neuroblast commitment in mutants of the achaete-scute complex and adjacent genes of D. melanogaster. *Neuron.* 5: 81-9

Jin H, White SR, Shida T, Schulz S, Aguiar M, Gygi SP, Bazan JF, Nachury MV. The conserved Bardet-Biedl syndrome proteins assemble a coat that traffics membrane proteins to cilia. Cell. 2010 Jun 25;141(7):1208-19.

Johnson UG, Porter KR. Fine structure of cell division in Chlamydomonas reinhardi. Basal bodies and microtubules. J Cell Biol. 1968 Aug;38(2):403-25.

Jonassen JA, San Agustin J, Follit JA, Pazour GJ Deletion of IFT20 in the mouse kidney causes misorientation of the mitotic spindle and cystic kidney disease. J Cell Biol. 2008 Nov 3;183(3):377-84.

Kageyama R, Ohtsuka T and Tomita K. The bHLH gene Hes1 regulates differentiation of multiple cell types Mol. Cells 2000 10, 1-7.

Kamikouchi A, Inagaki HK, Effertz T, Hendrich O, Fiala A, Göpfert MC, Ito K. The neural basis of Drosophila gravity-sensing and hearing. Nature. 2009 Mar 12;458(7235):165-71.

Kamikouchi A, Shimada T, Ito K. (2006). Comprehensive classification of the auditory sensory projections in the brain of the fruit fly Drosophila melanogaster. *J Comp Neurol.* 499: 317-56.

Kang L, Gao J, Schafer WR, Xie Z, Xu XZ. C. elegans TRP family protein TRP-4 is a pore-forming subunit of a native mechanotransduction channel. Neuron. 2010 Aug 12;67(3):381-91.

Katsanis N. The oligogenic properties of Bardet-Biedl syndrome. Hum Mol Genet. 2004 Apr 1;13 Spec No 1:R65-71.

Katz F, Moats W, Jan YN. A carbohydrate epitope expressed uniquely on the cell surface of Drosophila neurons is altered in the mutant nac (neurally altered carbohydrate). EMBO J. 1988 Nov;7(11):3471-7.

Kaufmann E, Müller D, Knöchel W. DNA recognition site analysis of Xenopus winged helix proteins. J Mol Biol. 1995 Apr 28;28(2):239-54.

Kavlie RG, Kernan MJ, Eberl DF. Hearing in Drosophila requires TilB, a conserved protein associated with ciliary motility. Genetics. 2010 May;185(1):177-88.

Kernan M, Cowan D, Zuker C. Genetic dissection of mechanosensory transduction: mechanoreception-defective mutations of Drosophila. Neuron. 1994 Jun;12(6):1195-206.

Kernan MJ. Mechanotransduction and auditory transduction in Drosophila. Pflugers Arch. 2007 Aug;454(5):703-20.

Kidd T, Brose K, Mitchell KJ, Fetter RD, Tessier-Lavigne M, Goodman CS, Tear G. Roundabout controls axon crossing of the CNS midline and defines a novel subfamily of evolutionarily conserved guidance receptors. Cell. 1998 Jan 23;92(2):205-15.

Kiehart DP, Franke JD, Chee MK, Montague RA, Chen TL, Roote J, Ashburner M. Drosophila crinkled, mutations of which disrupt morphogenesis and cause lethality, encodes fly myosin VIIA. Genetics. 2004 Nov;168(3):1337-52.

Kim J, Chung YD, Park DY, Choi S, Shin DW, Soh H, Lee HW, Son W, Yim J, Park CS, Kernan MJ, Kim C. A TRPV family ion channel required for hearing in Drosophila. Nature. 2003 Jul 3;424(6944):81-4.

Kim MD, Jan LY, Jan YN. The bHLH-PAS protein Spineless is necessary for the diversification of dendrite morphology of Drosophila dendritic arborization neurons.Genes Dev. 2006 Oct 15;20(20):2806-19.

Kops GJ, Dansen TB, Polderman PE, Saarloos I, Wirtz KW, Coffer PJ, Huang TT, Bos JL, Medema RH, Burgering BM. Forkhead transcription factor FOXO3a protects quiescent cells from oxidative stress. Nature. 2002 Sep 19;419(6904):316-21.

Kozminski KG, Johnson KA, Forscher P, Rosenbaum JL. A motility in the eukaryotic flagellum unrelated to flagellar beating. Proc Natl Acad Sci U S A. 1993 Jun 15;90(12):5519-23.

Kramer-Zucker AG, Olale F, Haycraft CJ, Yoder BK, Schier AF, Drummond IA. Cilia-driven fluid flow in the zebrafish pronephros, brain and Kupffer's vesicle is required for normal organogenesis. Development. 2005 Apr;132(8):1907-21.

Kubo T, Yanagisawa HA, Yagi T, Hirono M, Kamiya R. Tubulin polyglutamylation regulates axonemal motility by modulating activities of inner-arm dyneins. Curr Biol. 2010 Mar 9;20(5):441-5.

Lai CS, Fisher SE, Hurst JA, Vargha-Khadem F, Monaco AP. A forkhead-domain gene is mutated in a severe speech and language disorder. Nature. 2001 Oct 4;413(6855):519-23.

Laoukili J, Stahl M, Medema RH. FoxM1: at the crossroads of ageing and cancer. Biochim Biophys Acta. 2007 Jan;1775(1):92-102.

Larroux C, Luke GN, Koopman P, Rokhsar DS, Shimeld SM, Degnan BM. Genesis and expansion of metazoan transcription factor gene classes. Mol Biol Evol. 2008 May;25(5):980-96.

Laurençon A, Dubruille R, Efimenko E, Grenier G, Bissett R, Cortier E, Rolland V, Swoboda P, Durand B. Identification of novel regulatory factor X (RFX) target genes by comparative genomics in Drosophila species. Genome Biol. 2007;8(9):R195.

Lee E, Sivan-Loukianova E, Eberl DF, Kernan MJ. An IFT-A protein is required to delimit functionally distinct zones in mechanosensory cilia. Curr Biol. 2008 Dec 23;18(24):1899-906.

Lee HH, Frasch M. Survey of forkhead domain encoding genes in the Drosophila genome: Classification and embryonic expression patterns.Dev Dyn. 2004 Feb;229(2):357-66.

Lee J, Moon S, Cha Y, Chung YD. Drosophila TRPN(=NOMPC) channel localizes to the distal end of mechanosensory cilia. PLoS One. 2010 Jun 8;5(6):e11012.

Lee Y, et al. (2005) Pyrexia is a new thermal transient receptor potential channel endowing tolerance to high temperatures in Drosophila melanogaster. Nat Genet 37:305-310.

Lehmann OJ, Sowden JC, Carlsson P, Jordan T, Bhattacharya SS.
Fox's in development and disease. Trends Genet. 2003 Jun;19(6):339-44.

Li JB, Gerdes JM, Haycraft CJ, Fan Y, Teslovich TM, May-Simera H, Li H, Blacque OE, Li L, Leitch CC, Lewis RA, Green JS, Parfrey PS, Leroux MR, Davidson WS, Beales PL, Guay-Woodford LM, Yoder BK, Stormo GD, Katsanis N, Dutcher SK. Comparative genomics identifies a flagellar and basal body proteome that includes the BBS5 human disease gene. Cell. 2004 May 14;117(4):541-52.

Li S, Weidenfeld J, Morrisey EE Transcriptional and DNA binding activity of the Foxp1/2/4 family is modulated by heterotypic and homotypic protein interactions.
Mol Cell Biol. 2004 Jan;24(2):809-22.

Li W, Wang F, Menut L, Gao FB.BTB/POZ-zinc finger protein abrupt suppresses dendritic branching in a neuronal subtype-specific and dosage-dependent manner. Neuron. 2004 Sep 16;43(6):823-34.

Liang X, Madrid J, Saleh HS, Howard J. NOMPC, a member of the TRP channel family, localizes to the tubular body and distal cilium of Drosophila campaniform and chordotonal receptor cells. Cytoskeleton (Hoboken). 2011 Jan;68(1):1-7.

Liedtke W, Choe Y, Martí-Renom MA, Bell AM, Denis CS, Sali A, Hudspeth AJ, Friedman JM, Heller S. Vanilloid receptor-related osmotically activated channel (VR-OAC), a candidate vertebrate osmoreceptor. Cell. 2000 Oct 27;103(3):525-35.

Liedtke W, Friedman JM. Abnormal osmotic regulation in trpv4-/- mice. Proc Natl Acad Sci U S A. 2003 Nov 11;100(23):13698-703.

Liedtke W, Tobin DM, Bargmann CI, Friedman JM. Mammalian TRPV4 (VR-OAC) directs behavioral responses to osmotic and mechanical stimuli in Caenorhabditis elegans. Proc Natl Acad Sci U S A. 2003 Nov 25;100

Lim L, Zhou H, Costa RH. The winged helix transcription factor HFH-4 is expressed during choroid plexus epithelial development in the mouse embryo. Proc Natl Acad Sci U S A. 1997 Apr 1;94(7):3094-9.

Liu XQ, Chen HK, Zhang XS, Pan ZG, Li A, Feng QS, Long QX, Wang XZ, Zeng YX.
Alterations of BLU, a candidate tumor suppressor gene on chromosome 3p21.3, in human nasopharyngeal carcinoma. Int J Cancer. 2003 Aug 10;106(1):60-5.

Logan CV, Abdel-Hamed Z, Johnson CA. Molecular genetics and pathogenic mechanisms for the severe ciliopathies: insights into neurodevelopment and pathogenesis of neural tube defects. Mol Neurobiol. 2011 Feb;43(1):12-26.

Lorenzo IM, Liedtke W, Sanderson MJ, Valverde MA. TRPV4 channel participates in receptor-operated calcium entry and ciliary beat frequency regulation in mouse airway epithelial cells.

Luck DJ. Genetic and biochemical dissection of the eucaryotic flagellum. J Cell Biol. 1984 Mar;98(3):789-94.

Ma L, Jarman AP. Dilatory is a Drosophila protein related to AZI1 (CEP131) that is located at the ciliary base and is required for cilium formation J Cell Sci. **2011** Aug 1;124(Pt 15):2622-30.

MacDermot KD, Bonora E, Sykes N, Coupe AM, Lai CS, Vernes SC, Vargha-Khadem F, McKenzie F, Smith RL, Monaco AP, Fisher SE. Identification of FOXP2 truncation as a novel cause of developmental speech and language deficits. Am J Hum Genet. 2005 Jun;76(6):1074-80.

Marinez C, Modolell J, Garrell J. (1993) Regulation of the proneural gene achaete by helix-loop-helix proteins. *Mol Cell Biol.* 13: 3514-21

Maroto R, Raso A, Wood TG, Kurosky A, Martinac B, Hamill OP. TRPC1 forms the stretch-activated cation channel in vertebrate cells. Nat Cell Biol. 2005 Feb;7(2):179-85.

Marszalek JR, Ruiz-Lozano P, Roberts E, Chien KR, Goldstein LS. Situs inversus and embryonic ciliary morphogenesis defects in mouse mutants lacking the KIF3A subunit of kinesin-II.

Martynoga B, Morrison H, Price DJ, Mason JO. Foxg1 is required for specification of ventral telencephalon and region-specific regulation of dorsal telencephalic precursor proliferation and apoptosis. Dev Biol. 2005 Jul 1;283(1):113-27.

Matsuzaki H, Daitoku H, Hatta M, Aoyama H, Yoshimochi K, Fukamizu A. Acetylation of Foxo1 alters its DNA-binding ability and sensitivity to phosphorylation. Proc Natl Acad Sci U S A. 2005 Aug 9;102(32):11278-83.

Matsuzaki H, Daitoku H, Hatta M, Tanaka K, Fukamizu A. Insulin-induced phosphorylation of FKHR (Foxo1) targets to proteasomal degradation. Proc Natl Acad Sci U S A. 2003 Sep 30;100(20):11285-90.

Maung SM, Jarman AP. Functional distinctness of closely related transcription factors: a comparison of the Atonal and Amos proneural factors. Mech Dev. 2007 Sep-Oct;124(9-10):647-56.

Mazet F, Yu JK, Liberles DA, Holland LZ, Shimeld SM. Phylogenetic relationships of the Fox (Forkhead) gene family in the Bilateria. Gene. 2003 Oct 16;316:79-89.

McClintock TS, Glasser CE, Bose SC, Bergman DA. Tissue expression patterns identify mouse cilia genes. Physiol Genomics. 2008 Jan 17;32(2):198-206.

McGrath J, Somlo S, Makova S, Tian X, Brueckner M. Two populations of node monocilia initiate left-right asymmetry in the mouse. Cell. 2003 Jul 11;114(1):61-73.

McVittie A. Flagellum mutants of Chlamydomonas reinhardii. J Gen Microbiol. 1972 Aug;71(3):525-40.

Merritt DJ, Whitington PM. Central projections of sensory neurons in the Drosophila embryo correlate with sensory modality, soma position, and proneural gene function. J Neurosci. 1995 Mar;15(3 Pt 1):1755-67.

Mikami A, Tynan SH, Hama T, Luby-Phelps K, Saito T, Crandall JE, Besharse JC, Vallee RB. Molecular structure of cytoplasmic dynein 2 and its distribution in neuronal and ciliated cells. J Cell Sci. 2002 Dec 15;115(Pt 24):4801-8.

Mische S, He Y, Ma L, Li M, Serr M, Hays TS. Dynein light intermediate chain: an essential subunit that contributes to spindle checkpoint inactivation. Mol Biol Cell. 2008 Nov;19(11):4918-29.

Molla-Herman A, Ghossoub R, Blisnick T, Meunier A, Serres C, Silbermann F, Emmerson C, Romeo K, Bourdoncle P, Schmitt A, Saunier S, Spassky N, Bastin P, Benmerah A. The ciliary pocket: an endocytic membrane domain at the base of primary and motile cilia. J Cell Sci. 2010 May 15;123(Pt 10):1785-95.

Moscoso del Prado J & Garcia Bellido A. (1984). Genetic regulation of the AS-C of D. melanogaster. *Dev Genes & Evol* 193: 242-5

Mukhopadhyay S, Lu Y, Qin H, Lanjuin A, Shaham S, Sengupta P. Distinct IFT mechanisms contribute to the generation of ciliary structural diversity in C. elegans. EMBO J. 2007 Jun 20;26(12):2966-80.

Mukhopadhyay S, Wen X, Chih B, Nelson CD, Lane WS, Scales SJ, Jackson PK. TULP3 bridges the IFT-A complex and membrane phosphoinositides to promote trafficking of G protein-coupled receptors into primary cilia. Genes Dev. 2010 Oct 1;24(19):2180-93.

Myat, M.M., Andrew, D.J. Fork head prevents apoptosis and promotes cell shape change during formation of the Drosophila salivary glands. Development 2000 127(19): 4217--4226.

Myatt SS, Lam EW. The emerging roles of forkhead box (Fox) proteins in cancer. Nat Rev Cancer. 2007 Nov;7(11):847-59.

Mykytyn K, Mullins RF, Andrews M, Chiang AP, Swiderski RE, Yang B, Braun T, Casavant T, Stone EM, Sheffield VC. Bardet-Biedl syndrome type 4 (BBS4)-null mice implicate Bbs4 in flagella formation but not global cilia assembly. Proc Natl Acad Sci U S A. 2004 Jun 8;101(23):8664-9.

Mykytyn K, Nishimura DY, Searby CC, Shastri M, Yen HJ, Beck JS, Braun T, Streb LM, Cornier AS, Cox GF, Fulton AB, Carmi R, Lüleci G, Chandrasekharappa SC, Collins FS, Jacobson SG, Heckenlively JR, Weleber RG, Stone EM, Sheffield VC. Identification of the gene (BBS1) most commonly involved in Bardet-Biedl syndrome, a complex human obesity syndrome. Nat Genet. 2002 Aug;31(4):435-8

Nadrowski B, Effertz T, Senthilan PR, Göpfert MC. Antennal hearing in insects--new findings, new questions. Hear Res. 2011 Mar;273(1-2):7-13.

Nakamura N, Ramaswamy S, Vazquez F, Signoretti S, Loda M, Sellers WR. Forkhead transcription factors are critical effectors of cell death and cell cycle arrest downstream of PTEN. Mol Cell Biol. 2000 Dec;20(23):8969-82.

Nauli SM, Alenghat FJ, Luo Y, Williams E, Vassilev P, Li X, Elia AE, Lu W, Brown EM, Quinn SJ, Ingber DE, Zhou J. Polycystins 1 and 2 mediate mechanosensation in the primary cilium of kidney cells. Nat Genet. 2003 Feb;33(2):129-37.

Neuwald AF, Aravind L, Spouge JL, Koonin EV. AAA+: A class of chaperone-like ATPases associated with the assembly, operation, and disassembly of protein complexes. Genome Res. 1999 Jan;9(1):27-43.

Neuwald AF, Hirano T. HEAT repeats associated with condensins, cohesins, and other complexes involved in chromosome-related functions. Genome Res. 2000 Oct;10(10):1445-52.

Nilius B, Talavera K, Owsianik G, Prenen J, Droogmans G, Voets T. Gating of TRP channels: a voltage connection? J Physiol. 2005 Aug 15;567(Pt 1):35-44.

Nilius B, Vriens J, Prenen J, Droogmans G, Voets T. TRPV4 calcium entry channel: a paradigm for gating diversity. Am J Physiol Cell Physiol. 2004 Feb;286(2):C195-205.

Nobili R, Mammano F, Ashmore J. How well do we understand the cochlea? Trends Neurosci. 1998 Apr;21(4):159-67.

Nonaka S, Tanaka Y, Okada Y, Takeda S, Harada A, Kanai Y, Kido M, Hirokawa N. Randomization of left-right asymmetry due to loss of nodal cilia generating leftward flow of extraembryonic fluid in mice lacking KIF3B motor protein. Cell. 1998 Dec 11;95(6):829-37.

Noone PG, Leigh MW, Sannuti A, Minnix SL, Carson JL, Hazucha M, Zariwala MA, Knowles MR. Primary ciliary dyskinesia: diagnostic and phenotypic features. Am J Respir Crit Care Med. 2004 Feb 15;169(4):459-67.

O'Callaghan CL, Sikand K, Rutman A, Hirst RA. The effect of viscous loading on brain ependymal cilia. Neurosci Lett. 2008 Jul 4;439(1):56-60.

O'Connor-Giles KM, Skeath JB Numb inhibits membrane localization of sanpodo, a four-pass transmembrane protein, to promote asymmetric divisions in Drosophila. Dev Cell 2003 5: 231–243

Okabe M, Okano H. Two-step induction of chordotonal organ precursors in Drosophila embryogenesis. Development. 1997 124: 1045-53.

Okada T, Inoue R, Yamazaki K, Maeda A, Kurosaki T, Yamakuni T, Tanaka I, Shimizu S, Ikenaka K, Imoto K, Mori Y. Molecular and functional characterization of a novel mouse transient receptor potential protein homologue TRP7. Ca(2+)-permeable cation channel that is constitutively activated and enhanced by stimulation of G protein-coupled receptor. J Biol Chem. 1999 Sep 24;274(39):27359-70.

Okada Y, Takeda S, Tanaka Y, Belmonte JC, Hirokawa N. Mechanism of nodal flow: a conserved symmetry breaking event in left-right axis determination. Cell. 2005 May 20;121(4):633-44.

Omori Y, Zhao C, Saras A, Mukhopadhyay S, Kim W, Furukawa T, Sengupta P, Veraksa A, Malicki J. Elipsa is an early determinant of ciliogenesis that links the IFT particle to membrane-associated small GTPase Rab8. Nat Cell Biol. 2008 Apr;10(4):437-44.

Omoto CK, Gibbons IR, Kamiya R, Shingyoji C, Takahashi K, Witman GB. Rotation of the central pair microtubules in eukaryotic flagella. Mol Biol Cell. 1999 Jan;10(1):1-4.

O'Neil RG, Heller S. The mechanosensitive nature of TRPV channels. Pflugers Arch. 2005 Oct;451(1):193-203.

Orenic T. V, Held L. I Jr, Paddock S.W, Carroll S. B. (1993)The spatial organization of epidermal structures: hairy establishes the geometrical pattern of Drosophila leg bristles by delimiting the domains of achaete expression. *Development*. 118: 9-20.

Orgogozo V, Schweisguth F, Bellaïche Y. (2001) Lineage, cell polarity and inscuteable function in the peripheral nervous system of the Drosophila embryo. *Development* 128: 631-643

O'Toole ET, Giddings TH, McIntosh JR, Dutcher SK. Three-dimensional organization of basal bodies from wild-type and delta-tubulin deletion strains of Chlamydomonas reinhardtii. Mol Biol Cell. 2003 Jul;14(7):2999-3012.

Ou G, Blacque OE, Snow JJ, Leroux MR, Scholey JM. Functional coordination of intraflagellar transport motors. Nature. 2005 Jul 28;436(7050):583-7.

Paik JH, Ding Z, Narurkar R, Ramkissoon S, Muller F, Kamoun WS, Chae SS, Zheng H, Ying H, Mahoney J, Hiller D, Jiang S, Protopopov A, Wong WH, Chin L, Ligon KL, DePinho RA. FoxOs cooperatively regulate diverse pathways governing neural stem cell homeostasis. Cell Stem Cell. 2009 Nov 6;5(5):540-53.

Paintrand M, Moudjou M, Delacroix H, Bornens M. Centrosome organization and centriole architecture: their sensitivity to divalent cations. J Struct Biol. 1992 Mar-Apr;108(2):107-28.

Palazzo A, Ackerman B, Gundersen GG. Cell biology: Tubulin acetylation and cell motility. Nature. 2003 Jan 16;421(6920):230.

Park M, Wu X, Golden K, Axelrod JD, Bodmer R. The wingless signaling pathway is directly involved in Drosophila heart development. Dev Biol. 1996 Jul 10;177(1):104-16.

Parrish JZ, Kim MD, Jan LY, Jan YN. Genome-wide analyses identify transcription factors required for proper morphogenesis of Drosophila sensory neuron dendrites.Genes Dev. 2006 Apr 1;20(7):820-35.

Pazour GJ, Dickert BL, Vucica Y, Seeley ES, Rosenbaum JL, Witman GB, Cole DG. Chlamydomonas IFT88 and its mouse homologue, polycystic kidney disease gene tg737, are required for assembly of cilia and flagella. J Cell Biol. 2000 Oct 30;151(3):709-18.

Pennarun G, Escudier E, Chapelin C, Bridoux AM, Cacheux V, Roger G, Clément A, Goossens M, Amselem S, Duriez B. Loss-of-function mutations in a human gene related to Chlamydomonas reinhardtii dynein IC78 result in primary ciliary dyskinesia. Am J Hum Genet. 1999 Dec;65(6):1508-19.

Pennekamp P, Karcher C, Fischer A, Schweickert A, Skryabin B, Horst J, Blum M, Dworniczak B. The ion channel polycystin-2 is required for left-right axis determination in mice. Curr Biol. 2002 Jun 4;12(11):938-43.

Pérez-Sánchez C, Gómez-Ferrería MA, de La Fuente CA, Granadino B, Velasco G, Esteban-Gamboa A, Rey-Campos J FHX, a novel fork head factor with a dual DNA binding specificity. J Biol Chem. 2000 Apr 28;275(17):12909-16.

Piel M, Meyer P, Khodjakov A, Rieder CL, Bornens M. The respective contributions of the mother and daughter centrioles to centrosome activity and behavior in vertebrate cells. J Cell Biol. 2000 Apr 17;149(2):317-30.

Pierrou S, Hellqvist M, Samuelsson L, Enerbäck S, Carlsson P. Cloning and characterization of seven human forkhead proteins: binding site specificity and DNA bending EMBO J. 1994 Oct 17;13(20):5002-12.

Piperno G, Mead K, Shestak W. The inner dynein arms I2 interact with a "dynein regulatory complex" in Chlamydomonas flagella. J Cell Biol. 1992 Sep;118(6):1455-63.

Powell LM, Deaton AM, Wear MA, Jarman AP. Specificity of Atonal and Scute bHLH factors: analysis of cognate E box binding sites and the influence of Senseless. Genes Cells. 2008 Sep;13(9):915-29.

Powell LM, Zur Lage PI, Prentice DR, Senthinathan B, Jarman AP. The proneural proteins Atonal and Scute regulate neural target genes through different E-box binding sites. Mol Cell Biol. 2004 Nov;24(21):9517-26.

Pugacheva EN, Jablonski SA, Hartman TR, Henske EP, Golemis EA. HEF1-dependent Aurora A activation induces disassembly of the primary cilium. Cell. 2007 Jun 29;129(7):1351-63.

Purohit A, Tynan SH, Vallee R, Doxsey SJ. Direct interaction of pericentrin with cytoplasmic dynein light intermediate chain contributes to mitotic spindle organization. J Cell Biol. 1999 Nov 1;147(3):481-92.

Qin H, Burnette DT, Bae YK, Forscher P, Barr MM, Rosenbaum JL. Intraflagellar transport is required for the vectorial movement of TRPV channels in the ciliary membrane. Curr Biol. 2005 Sep 20;15(18):1695-9.

Qin J, Lin Y, Norman RX, Ko HW, Eggenschwiler JT. Intraflagellar transport protein 122 antagonizes Sonic Hedgehog signaling and controls ciliary localization of pathway components. Proc Natl Acad Sci U S A. 2011 Jan 25;108(4):1456-61.

Qiu GH, Tan LK, Loh KS, Lim CY, Srivastava G, Tsai ST, Tsao SW, Tao Q. The candidate tumor suppressor gene BLU, located at the commonly deleted region 3p21.3, is an E2F-regulated, stress-responsive gene and inactivated by both epigenetic and genetic mechanisms in nasopharyngeal carcinoma. Oncogene. 2004 Jun 10;23(27):4793-806.

Rawlins E. L, Lovegrove B, Jarman A. P. (2003) Echinoid facilitates Notch pathway signalling during Drosophila neurogenesis through functional interaction with Delta. *Development.* 130: 6475-84.

Reeves N, Posakony JW. Genetic programs activated by proneural proteins in the developing Drosophila PNS. Dev Cell. 2005 Mar;8(3):413-25.

Ringo DL. Flagellar motion and fine structure of the flagellar apparatus in Chlamydomonas. J Cell Biol. 1967 Jun;33(3):543-71.

Robles L, Ruggero MA. Mechanics of the mammalian cochlea. Physiol Rev. 2001 Jul;81(3):1305-52.

Rodríguez I, Hernández R, Modolell J, Ruiz-Gómez M. (1990) Competence to develop sensory organs is temporally and spatially regulated in Drosophila epidermal primordia. *EMBO J.* 9: 3583-92

Rohatgi R, Milenkovic L, Scott MP. Patched1 regulates hedgehog signaling at the primary cilium. Science. 2007 Jul 20;317(5836):372-6.

Roos J, Hummel T, Ng N, Klämbt C, Davis GW. Drosophila Futsch regulates synaptic microtubule organization and is necessary for synaptic growth. Neuron. 2000 May;26(2):371-82.

Rosenbaum JL, Witman GB. Intraflagellar transport. Nat Rev Mol Cell Biol. 2002 Nov;3(11):813-25.

Ruiz-Gómez M & Ghysen A. (1993) The expression and role of a proneural gene, achaete, in the development of the larval nervous system of Drosophila. *EMBO J.* 12: 1121-30

Rusten TE, Cantera R, Urban J, Technau G, Kafatos FC, Barrio R Spalt restricts EGFR mediated induction of chordotonal precursors in the embryonic PNS of Drosophila. Development 2001 128, 711–722.

Ryder E, Blows F, Ashburner M, Bautista-Llacer R, Coulson D, Drummond J, Webster J, Gubb D, Gunton N, Johnson G, O'Kane CJ, Huen D, Sharma P, Asztalos Z, Baisch H, Schulze J, Kube M, Kittlaus K, Reuter G, Maroy P, Szidonya J, Rasmuson-Lestander A, Ekström K, Dickson B, Hugentobler C, Stocker H, Hafen E, Lepesant JA, Pflugfelder G, Heisenberg M, Mechler B, Serras F, Corominas M, Schneuwly S, Preat T, Roote J, Russell S. The DrosDel collection: a set of P-element insertions for generating custom chromosomal aberrations in Drosophila melanogaster. Genetics. 2004 Jun;167(2):797-813.

Salzberg A, D'Evelyn D, Schulze K. L, Lee J. K, Strumpf D, Tsai L, Bellen H. J. (1994) Mutations affecting the pattern of the PNS in Drosophila reveal novel aspects of neuronal development. *Neuron.* 13: 269-87

Sambrook J. & Russell DW. Molecular Cloning: A Laboratory Manual vol. 3. 3rd Edition, 2001. Cold Spring Harbor Laboratory Press.

Satir P, Sleigh MA. The physiology of cilia and mucociliary interactions. Annu Rev Physiol. 1990;52:137-55.

Schafer JC, Haycraft CJ, Thomas JH, Yoder BK, Swoboda P. XBX-1 encodes a dynein light intermediate chain required for retrograde intraflagellar transport and cilia assembly in Caenorhabditis elegans. Mol Biol Cell. 2003 May;14(5):2057-70.

Seo S, Lim JW, Yellajoshyula D, Chang LW, Kroll KL. Neurogenin and NeuroD direct transcriptional targets and their regulatory enhancers.EMBO J. 2007 Dec 12;26(24):5093-108.
Seoane J, Le HV, Shen L, Anderson SA, Massagué J. Integration of Smad and forkhead pathways in the control of neuroepithelial and glioblastoma cell proliferation. Cell. 2004 Apr 16;117(2):211-23.

Shen W, Scearce LM, Brestelli JE, Sund NJ, Kaestner KH. Foxa3 (hepatocyte nuclear factor 3gamma) is required for the regulation of hepatic GLUT2 expression and the maintenance of glucose homeostasis during a prolonged fast. J Biol Chem. 2001 Nov 16;276(46):42812-7.

Shim EY, Woodcock C, Zaret KS. Nucleosome positioning by the winged helix transcription factor HNF3. Genes Dev. 1998 Jan 1;12(1):5-10.

Sidi S, Friedrich RW, Nicolson T. NompC TRP channel required for vertebrate sensory hair cell mechanotransduction. Science. 2003 Jul 4;301(5629):96-9.

Siegrist SE, Haque NS, Chen CH, Hay BA, Hariharan IK. Inactivation of both Foxo and reaper promotes long-term adult neurogenesis in Drosophila. Curr Biol. 2010 Apr 13;20(7):643-8.

Silverman MA, Leroux MR. Intraflagellar transport and the generation of dynamic, structurally and functionally diverse cilia. Trends Cell Biol. 2009 Jul;19(7):306-16.

Simpson JH, Bland KS, Fetter RD, Goodman CS. Short-range and long-range guidance by Slit and its Robo receptors: a combinatorial code of Robo receptors controls lateral position. Cell. 2000 Dec 22;103(7):1019-32.

Singson A, Leviten MW, Bang AG, Hua XH, Posakony JW. Direct downstream targets of proneural activators in the imaginal disc include genes involved in lateral inhibitory signaling. Genes Dev. 1994 Sep 1;8(17):2058-71.

Skeath J. B & Carroll S. B. (1991) Regulation of achaete-scute gene expression and sensory organ pattern formation in the Drosophila wing. *Genes Dev.* 5: 984-95

Snow JJ, Ou G, Gunnarson AL, Walker MR, Zhou HM, Brust-Mascher I, Scholey JM. Two anterograde intraflagellar transport motors cooperate to build sensory cilia on C. elegans neurons. Nat Cell Biol. 2004 Nov;6(11):1109-13.

Sokolov M, Lyubarsky AL, Strissel KJ, Savchenko AB, Govardovskii VI, Pugh EN Jr, Arshavsky VY. Massive light-driven translocation of transducin between the two major compartments of rod cells: a novel mechanism of light adaptation. Neuron. 2002 Mar 28;34(1):95-106.

Song W, Onishi M, Jan LY, Jan YN. Peripheral multidendritic sensory neurons are necessary for rhythmic locomotion behavior in Drosophila larvae. Proc Natl Acad Sci U S A. 2007 Mar 20;104(12):5199-204.

Sorokin SP. Reconstructions of centriole formation and ciliogenesis in mammalian lungs. J Cell Sci. 1968 Jun;3(2):207-30.

Spradling, A.C., Stern, D., Beaton, A., Rhem, E.J., Laverty, T., Mozden, N., Misra, S., Rubin, G.M. (1999). The Berkeley Drosophila genome project gene disruption project. Single P-element insertions mutating 25% of vital Drosophila genes. Genetics 153(1): 135--177.

Srivatsan S, Peng SL. Foxj1 protects against autoimmunity and inhibits thymocyte egress. J Immunol. 2005 Dec 15;175(12):7805-9.

Steffen W, Linck RW. Evidence for tektins in centrioles and axonemal microtubules. Proc Natl Acad Sci U S A. 1988 Apr;85(8):2643-7.

Stephens RE. Synthesis and turnover of embryonic sea urchin ciliary proteins during selective inhibition of tubulin synthesis and assembly. Mol Biol Cell. 1997 Nov;8(11):2187-98.

Strotmann R, Harteneck C, Nunnenmacher K, Schultz G, Plant TD. OTRPC4, a nonselective cation channel that confers sensitivity to extracellular osmolarity. Nat Cell Biol. 2000 Oct;2(10):695-702.

Stroud JC, Wu Y, Bates DL, Han A, Nowick K, Paabo S, Tong H, Chen L Structure of the forkhead domain of FOXP2 bound to DNA. Structure. 2006 Jan;14(1):159-66.

Stubbs JL, Oishi I, Izpisúa Belmonte JC, Kintner C. The forkhead protein Foxj1 specifies node-like cilia in Xenopus and zebrafish embryos. Nat Genet. 2008 Dec;40(12):1454-60.

Sugimura K, Yamamoto M, Niwa R, Satoh D, Goto S, Taniguchi M, Hayashi S, Uemura T. Distinct developmental modes and lesion-induced reactions of dendrites of two classes of Drosophila sensory neurons.J Neurosci. 2003 May 1;23(9):3752-60.

Sukhanova M. J, Deb D. K, Gordon G. M, Matakatsu M. T, Du W. (2007) Proneural basic helix-loop-helix proteins and epidermal growth factor receptor signalling coordinately regulate cell type specification and cdk inhibitor expression during development. *Mol Cell Biol.* 27: 2987-96.

Summers KE, Gibbons IR. Adenosine triphosphate-induced sliding of tubules in trypsin-treated flagella of sea-urchin sperm. Proc Natl Acad Sci U S A. 1971 Dec;68(12):3092-6.

Sun Y, Jan L. Y, Jan Y. N. (1998)Transcriptional regulation of atonal during development of the Drosophila peripheral nervous system. *Development.* 125: 3731-40

Sun Y, Liu L, Ben-Shahar Y, Jacobs JS, Eberl DF, Welsh MJ. TRPA channels distinguish gravity sensing from hearing in Johnston's organ. Proc Natl Acad Sci U S A. 2009 Aug 11;106(32):13606-11.

Sun Z, Yergeau DA, Wong IC, Tuypens T, Tavernier J, Paul CC, Baumann MA, Auron PE, Tenen DG, Ackerman SJ. Interleukin-5 receptor alpha subunit gene regulation in human eosinophil development: identification of a unique cis-element that acts like an enhancer in regulating activity of the IL-5R alpha promoter. Curr Top Microbiol Immunol. 1996; 211:173-87.

Supp DM, Witte DP, Potter SS, Brueckner M. Mutation of an axonemal dynein affects left-right asymmetry in inversus viscerum mice. Nature. 1997 Oct 30;389(6654):963-6.

Suryavanshi S, Eddé B, Fox LA, Guerrero S, Hard R, Hennessey T, Kabi A, Malison D, Pennock D, Sale WS, Wloga D, Gaertig J. Tubulin glutamylation regulates ciliary motility by altering inner dynein arm activity. Curr Biol. 2010 Mar 9;20(5):435-40.

Tabin CJ, Vogan KJ. A two-cilia model for vertebrate left-right axis specification. Genes Dev. 2003 Jan 1;17(1):1-6.

Tai AW, Chuang JZ, Bode C, Wolfrum U, Sung CH. Rhodopsin's carboxy-terminal cytoplasmic tail acts as a membrane receptor for cytoplasmic dynein by binding to the dynein light chain Tctex-1. Cell. 1999 Jun 25;97(7):877-87.

Tan PL, Barr T, Inglis PN, Mitsuma N, Huang SM, Garcia-Gonzalez MA, Bradley BA, Coforio S, Albrecht PJ, Watnick T, Germino GG, Beales PL, Caterina MJ, Leroux MR, Rice FL, Katsanis N. Loss of Bardet Biedl syndrome proteins causes defects in peripheral sensory innervation and function. Proc Natl Acad Sci U S A. 2007 Oct 30;104(44):17524-9.

Tanaka H, Iguchi N, Toyama Y, Kitamura K, Takahashi T, Kaseda K, Maekawa M, Nishimune Y. Mice deficient in the axonemal protein Tektin-t exhibit male infertility and immotile-cilium syndrome due to impaired inner arm dynein function. Mol Cell Biol. 2004 Sep;24(18):7958-64.

Tauber E, Eberl DF. Song production in auditory mutants of Drosophila: the role of sensory feedback. J Comp Physiol A. 2001 Jun;187(5):341-8.

Teilmann SC, Byskov AG, Pedersen PA, Wheatley DN, Pazour GJ, Christensen ST. Localization of transient receptor potential ion channels in primary and motile cilia of the female murine reproductive organs. Mol Reprod Dev. 2005 Aug;71(4):444-52.

Thomas J, Morlé L, Soulavie F, Laurençon A, Sagnol S, Durand B. Transcriptional control of genes involved in ciliogenesis: a first step in making cilia. Biol Cell. 2010 Jul 9;102(9):499-513.

Tobin D, Madsen D, Kahn-Kirby A, Peckol E, Moulder G, Barstead R, Maricq A, Bargmann C. Combinatorial expression of TRPV channel proteins defines their sensory functions and subcellular localization in C. elegans neurons. Neuron. 2002 Jul 18;35(2):307-18.

Todi S. V, Sharma Y, Eberl D. F. (2004) Anatomical and molecular design of the Drosophila antenna as a flagellar auditory organ. *Microsc Res Tech*. 63: 388-99

Tran H, Brunet A, Grenier JM, Datta SR, Fornace AJ Jr, DiStefano PS, Chiang LW, Greenberg ME. DNA repair pathway stimulated by the forkhead transcription factor FOXO3a through the Gadd45 protein. Science. 2002 Apr 19;296(5567):530-4.

Tran PV, Haycraft CJ, Besschetnova TY, Turbe-Doan A, Stottmann RW, Herron BJ, Chesebro AL, Qiu H, Scherz PJ, Shah JV, Yoder BK, Beier DR. THM1 negatively modulates mouse sonic hedgehog signal transduction and affects retrograde intraflagellar transport in cilia. Nat Genet. 2008 Apr;40(4):403-10

Tran PV, Haycraft CJ, Besschetnova TY, Turbe-Doan A, Stottmann RW, Herron BJ, Chesebro AL, Qiu H, Scherz PJ, Shah JV, Yoder BK, Beier DR. THM1 negatively modulates mouse sonic hedgehog signal transduction and affects retrograde intraflagellar transport in cilia. Nat Genet. 2008 Apr;40(4):403-10.

Tsai KL, Huang CY, Chang CH, Sun YJ, Chuang WJ, Hsiao CD. Crystal structure of the human FOXK1a-DNA complex and its implications on the diverse binding specificity of winged helix/forkhead proteins. J Biol Chem. 2006 Jun 23;281(25):17400-9

Tsao CC, Gorovsky MA. Tetrahymena IFT122A is not essential for cilia assembly but plays a role in returning IFT proteins from the ciliary tip to the cell body. J Cell Sci. 2008 Feb 15;121(Pt 4):428-36.

Tyler KM, Fridberg A, Toriello KM, Olson CL, Cieslak JA, Hazlett TL, Engman DM. Flagellar membrane localization via association with lipid rafts. J Cell Sci. 2009 Mar 15;122(Pt 6):859-66.

Uemura T, Shepherd S, Ackerman L, Jan LY, Jan YN. numb, a gene required in determination of cell fate during sensory organ formation in Drosophila embryos. Cell. 1989 Jul 28;58(2):349-60.

Umesono Y, Hiromi Y, Hotta Y.
Context-dependent utilization of Notch activity in Drosophila glial determination.
Development. 2002 May;129(10):2391-9.

Vallee R.B., Williams J.C., Varma D, Barnhart LE. Dynein: An Ancient Motor Protein Involved in Multiple Modes of Transport. J Neurobiol. 2004 Feb 5;58(2):189-200.

Van De Bor, V. and Giangrande, A. Notch signaling represses the glial fate in fly PNS. Development 2001 128, 1381-1390.

van der Horst A, de Vries-Smits AM, Brenkman AB, van Triest MH, van den Broek N, Colland F, Maurice MM, Burgering BM. FOXO4 transcriptional activity is regulated by monoubiquitination and USP7/HAUSP. Nat Cell Biol. 2006 Oct;8(10):1064-73.

Van Doren M, Ellis HM, Posakony JW. The Drosophila extramacrochaetae protein antagonizes sequence-specific DNA binding by daughterless/achaete-scute protein complexes. Development. 1991 Sep;113(1):245-55.

Van Doren M, Powell P. A, Pasternak D, Singson A, Posakony J. W. (1992) Spatial regulation of proneural gene activity: auto- and cross-activation of achaete is antagonized by extramacrochaetae. *Genes Dev.* 6: 2592-605.

Varjosalo M, Taipale J. Hedgehog: functions and mechanisms. Genes Dev. 2008 Sep 15;22(18):2454-72.

Venkatachalam K, Zheng F, Gill DL. Regulation of canonical transient receptor potential (TRPC) channel function by diacylglycerol and protein kinase C. J Biol Chem. 2003 Aug 1;278(31):29031-40.

Vieira OV, Gaus K, Verkade P, Fullekrug J, Vaz WL, Simons K. FAPP2, cilium formation, and compartmentalization of the apical membrane in polarized Madin-Darby canine kidney (MDCK) cells. Proc Natl Acad Sci U S A. 2006 Dec 5;103(49):18556-61.

Vining MS, Bradley PL, Comeaux CA, Andrew DJ. Organ positioning in Drosophila requires complex tissue-tissue interactions. Dev Biol. 2005 Nov 1;287(1):19-34.

Walker RG, Willingham AT, Zuker CS. A Drosophila mechanosensory transduction channel. Science. 2000 Mar 24;287(5461):2229-34.

Wallace K, Liu TH, Vaessin H. The pan-neural bHLH proteins DEADPAN and ASENSE regulate mitotic activity and cdk inhibitor dacapo expression in the Drosophila larval optic lobes. Genesis. 2000 Jan;26(1):77-85.

Wang VY, Hassan BA, Bellen HJ, Zoghbi HY. Drosophila atonal fully rescues the phenotype of Math1 null mice: new functions evolve in new cellular contexts. Curr Biol. 2002 Sep 17;12(18):1611-6.

Wang Z, Fan ZC, Williamson SM, Qin H. Intraflagellar transport (IFT) protein IFT25 is a phosphoprotein component of IFT complex B and physically interacts with IFT27 in Chlamydomonas. PLoS One. 2009;4(5):e5384.

Ward S, Thomson N, White JG, Brenner S. Electron microscopical reconstruction of the anterior sensory anatomy of the nematode Caenorhabditis elegans. J Comp Neurol. 1975 Apr 1;160(3):313-37.

Warner FD, Satir P. The structural basis of ciliary bend formation. Radial spoke positional changes accompanying microtubule sliding. J Cell Biol. 1974 Oct;63(1):35-63.

Weigel D, Jürgens G, Küttner F, Seifert E, Jäckle H. The homeotic gene fork head encodes a nuclear protein and is expressed in the terminal regions of the Drosophila embryo. Cell. 1989 May 19;57(4):645-58.

Wemmer KA, Marshall WF. Flagellar length control in chlamydomonas--paradigm for organelle size regulation. Int Rev Cytol. 2007;260:175-212.

Wijchers PJ, Burbach JP, Smidt MP. In control of biology: of mice, men and Foxes. Biochem J. 2006 Jul 15;397(2):233-46.

Witman GB, Plummer J, Sander G. Chlamydomonas flagellar mutants lacking radial spokes and central tubules. Structure, composition, and function of specific axonemal components. J Cell Biol. 1978 Mar;76(3):729-47.

Xu H, Zhao H, Tian W, Yoshida K, Roullet JB, Cohen DM. Regulation of a transient receptor potential (TRP) channel by tyrosine phosphorylation. SRC family kinase-dependent tyrosine phosphorylation of TRPV4 on TYR-253 mediates its response to hypotonic stress. J Biol Chem. 2003 Mar 28;278(13):11520-7.

Yamagata K, Daitoku H, Takahashi Y, Namiki K, Hisatake K, Kako K, Mukai H, Kasuya Y, Fukamizu A. Arginine methylation of FOXO transcription factors inhibits their phosphorylation by Akt. Mol Cell. 2008 Oct 24;32(2):221-31.

Yamasaki Y, Lim YM, Niwa N, Hayashi S, Tsuda L. Robust specification of sensory neurons by dual functions of charlatan, a Drosophila NRSF/REST-like repressor of extramacrochaetae and hairy. Genes Cells. 2011 Aug;16(8):896-909.

Yan J, Xu L, Crawford G, Wang Z, Burgess SM. The forkhead transcription factor FoxI1 remains bound to condensed mitotic chromosomes and stably remodels chromatin structure.
Mol Cell Biol. 2006 Jan;26(1):155-68.

Yang J, Adamian M, Li T. Rootletin interacts with C-Nap1 and may function as a physical linker between the pair of centrioles/basal bodies in cells. Mol Biol Cell. 2006 Feb;17(2):1033-40.

Yang J, Gao J, Adamian M, Wen XH, Pawlyk B, Zhang L, Sanderson MJ, Zuo J, Makino CL, Li T. The ciliary rootlet maintains long-term stability of sensory cilia. Mol Cell Biol. 2005 May;25(10):4129-37.

Yang J, Gao J, Adamian M, Wen XH, Pawlyk B, Zhang L, Sanderson MJ, Zuo J, Makino CL, Li T. The ciliary rootlet maintains long-term stability of sensory cilia. Mol Cell Biol. 2005 May;25(10):4129-37.

Yang J, Li T. The ciliary rootlet interacts with kinesin light chains and may provide a scaffold for kinesin-1 vesicular cargos. Exp Cell Res. 2005 Oct 1;309(2):379-89.

Yang J, Liu X, Yue G, Adamian M, Bulgakov O, Li T. Rootletin, a novel coiled-coil protein, is a structural component of the ciliary rootlet. J Cell Biol. 2002 Nov 11;159(3):431-40.

Yang Q, Kong Y, Rothermel B, Garry DJ, Bassel-Duby R, Williams RS. The winged-helix/forkhead protein myocyte nuclear factor beta (MNF-beta) forms a co-repressor complex with mammalian sin3B. Biochem J. 2000 Jan 15;345 Pt 2:335-43.

Yoder BK, Hou X, Guay-Woodford LM. The polycystic kidney disease proteins, polycystin-1, polycystin-2, polaris, and cystin, are co-localized in renal cilia. J Am Soc Nephrol. 2002 Oct;13(10):2508-16.

Yoshimura S, Egerer J, Fuchs E, Haas AK, Barr FA. Functional dissection of Rab GTPases involved in primary cilium formation. J Cell Biol. 2007 Jul 30;178(3):363-9.

Yu X, Lau D, Ng CP, Roy S. Cilia-driven fluid flow as an epigenetic cue for otolith biomineralization on sensory hair cells of the inner ear. Development. 2011 Feb;138(3):487-94.

Yu X, Ng CP, Habacher H, Roy S Foxj1 transcription factors are master regulators of the motile ciliogenic program. Nat Genet. 2008 Dec;40(12):1445-53.

Zaffran S, Küchler A, Lee HH, Frasch M. biniou (FoxF), a central component in a regulatory network controlling visceral mesoderm development and midgut morphogenesis in Drosophila. Genes Dev. 2001 Nov 1;15(21):2900-15.

Zheng JL, Gao WQ. Overexpression of Math1 induces robust production of extra hair cells in postnatal rat inner ears. Nat Neurosci. 2000 Jun;3(6):580-6.

Zhu MX. Multiple roles of calmodulin and other Ca(2+)-binding proteins in the functional regulation of TRP channels. Pflugers Arch. 2005 Oct;451(1):105-15.

Zlatic M, Landgraf M, Bate M. Genetic specification of axonal arbors: atonal regulates robo3 to position terminal branches in the Drosophila nervous system. Neuron. 2003 Jan 9;37(1):41-51.

Zlatic M, Li F, Strigini M, Grueber W, Bate M. Positional cues in the Drosophila nerve cord: semaphorins pattern the dorso-ventral axis. PLoS Biol. 2009 Jun 16;7(6):e1000135.

zur Lage P, Jan YN, Jarman AP Requirement for EGF receptor signalling in neural recruitment during formation of Drosophila chordotonal sense organ clusters. Current Biology 1997 7, 166–175.

zur Lage P, Jarman AP. Antagonism of EGFR and notch signalling in the reiterative recruitment of Drosophila adult chordotonal sense organ precursors. Development. 1999 Jun;126(14):3149-57.

zur Lage P. I, Powell L. M, Prentice D. R, McLaughlin P, Jarman A. P. EGF receptor signaling triggers recruitment of Drosophila sense organ precursors by stimulating proneural gene autoregulation. Dev Cell. 2004 7(5): 687-96.

zur Lage P. I, Prentice D. R, Holohan E. E, Jarman A. P. The Drosophila proneural gene amos promotes olfactory sensillum formation and suppresses bristle formation. Development. 2003 130: 4683-93

zur Lage PI, Jarman AP. The function and regulation of the bHLH gene, cato, in Drosophila neurogenesis. BMC Dev Biol. 2010 Mar 26;10:34.